

**ROLE OF POLYAMINES
IN THE CAROTID BODY**

**A thesis submitted to Cardiff University for the degree of
PhD**

2008

Sébastien H. Cayzac

**Cardiff School of Biosciences
Cardiff University**

UMI Number: U585170

All rights reserved

INFORMATION TO ALL USERS

The quality of this reproduction is dependent upon the quality of the copy submitted.

In the unlikely event that the author did not send a complete manuscript and there are missing pages, these will be noted. Also, if material had to be removed, a note will indicate the deletion.



UMI U585170

Published by ProQuest LLC 2013. Copyright in the Dissertation held by the Author.
Microform Edition © ProQuest LLC.


All rights reserved. This work is protected against
unauthorized copying under Title 17, United States Code.



ProQuest LLC
789 East Eisenhower Parkway
P.O. Box 1346
Ann Arbor, MI 48106-1346


DECLARATION

This work has not been accepted in substance for any degree and is not concurrently submitted in candidature for any degree.

Signed.......... (candidate) Date...16-02-09


STATEMENT 1

This thesis is being submitted in partial fulfilment of the requirements for the degree of.....P.h.D.....

Signed.......... (candidate) Date...16-02-09.


STATEMENT 2

This thesis is the result of my own independent work/investigation, except where otherwise stated. Other sources are acknowledged by footnotes giving explicit references.

Signed.......... (candidate) Date...16-02-09.

STATEMENT 3

I hereby give consent for my thesis, if accepted, to be available for photocopying and for inter-library loan, and for the title and summary to be made available to outside organisations.

Signed.......... (candidate) Date...16-02-09

STATEMENT 4

I hereby give consent for my thesis, if accepted, to be available for photocopying and for interlibrary loans after expiry of a bar on access approved by the Graduate Development Committee.

Signed..... (candidate) Date.....

ABSTRACT

Polyamines are small organic molecules which modulate many physiological processes. Here, an inhibitory effect of spermine on rat carotid body chemoreception is reported. Spermine inhibits catecholamine release, from isolated carotid bodies, induced either by high K^+ or by hypoxia. This inhibitory effect could be mediated by: the activation of the Ca^{2+} sensing receptor (CaR) or the inhibition of the voltage-dependent Ca^{2+} channels. Measurements of intracellular Ca^{2+} in dissociated type 1 cells, demonstrated that spermine inhibits Ca^{2+} influx evoked by either high K^+ or hypoxia, but did not affect the resting intracellular Ca^{2+} levels. Then, the expression of the voltage-dependent Ca^{2+} channels and CaR were assessed by reverse-transcription polymerase chain reaction and immunochemistry in the carotid body. $Ca_v1.2$ and $Ca_v2.2$ were found to be especially expressed in type 1 cells while $Ca_v1.3$, $Ca_v1.4$, $Ca_v2.1$, $Ca_v2.3$, $Ca_v3.1$, $Ca_v3.2$ and $Ca_v3.3$ could not be detected. CaR was detected only in the nerve ending. Having declined a role of the CaR in mediating the spermine inhibition of type 1 cell chemoreception, the effect of spermine on $Ca_v1.2$ was investigated using patch-clamp recording of HEK293 cells transiently or stably expressing human $Ca_v1.2$. Spermine inhibits $Ca_v1.2$ using 2 mM Ba^{2+} as a charge carrier but not with 20 mM Ba^{2+} . The inhibition of $Ca_v1.2$ by spermine in type 1 cells was then confirmed by co-application with nifedipine using Ca^{2+} imaging. These experiments demonstrate an inhibitory effect of spermine on $Ca_v1.2$ and potentially $Ca_v2.2$ in rat type 1 cells. In conclusion, spermine inhibits catecholamine release by type 1 cells, via the direct inhibition of $Ca_v1.2$ and possibly $Ca_v2.2$. This mechanism could act as a negative feedback on the type 1 cells and limit neurotransmitter release.

ACKNOWLEDGMENTS

I would like to thank D. Riccardi and P.J. Kemp for welcoming me to their laboratory and for their continuous support, encouragement and enthusiasm.

I'd like to express my sincerest thanks to all our collaborators from the University of Valladolid, especially, A. Rocher, C. Gonzalez and A. Obeso who taught me the carotid body dissociation and whom participated actively in the project.

I am also grateful to P. Kumar for his technical support and comments.

Thanks to all the guys in the laboratory, especially for their patience whilst teaching me English, and to S. Brazier for his precious help in molecular biology.

Finally, I would like to thank B. Allard for helping me to find this PhD and to my wife, Isil, for her patience and support.

DEDICATION

To all the researchers who do Science in an altruist way.

LIST OF ABBREVIATIONS.....	1
LIST OF FIGURES	3
LIST OF TABLES	5
CHAPTER 1	6
1.1 RESPIRATION.....	8
1.1.1 Respiration and chemoreceptors	8
1.1.2 Response to hypoxia	10
1.2 CHEMORECEPTION BY CAROTID BODY	12
1.2.1 Anatomy of the carotid body	12
1.2.3 O ₂ sensitive ion channels in the carotid body	15
<i>1.2.3.1 BK_{Ca} channel and heme oxygenase-2</i>	15
<i>1.2.3.2 TASK-like channels</i>	16
<i>1.2.3.3 Kv3 and Kv4 channels</i>	18
<i>1.2.3.4 HERG channel</i>	19
1.2.4 Other O ₂ sensors	20
<i>1.2.4.1 NADPH oxidase</i>	20
<i>1.2.4.2 Mitochondria</i>	21
<i>1.2.4.3 GSH/GSSG</i>	22
<i>1.2.4.4 AMP kinase</i>	23
1.2.5 CO ₂ /pH sensing.....	26
1.2.6 Glucose sensing	28

1.2.7 Expression of O ₂ -sensitive ion channels in rat carotid body	28
1.3 NEUROTRANSMITTERS RELEASED BY TYPE 1 CELLS	31
1.3.1 Catecholamines	31
<i>1.3.1.1 Effect of catecholamines on nerve endings</i>	32
<i>1.3.1.2 Effect of catecholamines on type 1 cells</i>	32
1.3.2 Acetylcholine (ACh)	33
<i>1.3.2.1 Effect of ACh on nerve endings</i>	33
<i>1.3.2.2 Effect of ACh on type 1 cells</i>	34
1.3.3 ATP	34
<i>1.3.3.1 Effect of ATP on nerve endings</i>	35
<i>1.3.3.2 Effect of ATP on carotid body type 1 and 2 cells</i>	36
1.3.4 Adenosine	37
1.3.5 Histamine	38
1.3.6 Gamma-aminobutyric acid	38
1.4 EFFECT OF CHRONIC HYPOXIA ON CAROTID BODY	41
1.4.1 Effect of chronic intermittent hypoxia	41
1.4.2 Effect of chronic sustained hypoxia	42
<i>1.4.2.1 Morphological changes of the carotid body</i>	42
<i>1.4.2.2 Electrical changes in the type 1 cell</i>	43
<i>1.4.2.3 Change in neurotransmitter release</i>	44
1.4.3 Role of HIF-1 α , -2 α and -3 α in chronic and sustained hypoxia	44
1.5 POLYAMINES	46
1.5.1 Synthesis of polyamines	46

1.5.2 Regulation of polyamine levels	47
1.5.3 Polyamines in the carotid body	48
1.6 THE EXTRACELLULAR CALCIUM-SENSING RECEPTOR	50
1.6.1 Structure of the extracellular calcium-sensing receptor (CaR).....	50
1.6.2 Allosteric modulators of the CaR	52
1.6.3 Signal transduction pathways of the CaR	54
1.6.4 Role of CaR in the regulation of secretion.....	54
1.6.5 Ion channel regulation by the CaR.....	56
1.7 CALCIUM CHANNELS.....	59
1.7.1 Channels mediating Ca ²⁺ current	59
1.7.2 Structure and family of voltage-dependent Ca ²⁺ channels.....	59
1.7.3 Expression and role of voltage-dependent Ca ²⁺ channels.....	60
1.7.4 Ion channels mediating Ca ²⁺ influx in rat type 1 cells.....	61
1.8 OBJECTIVES	64
 CHAPTER 2	 66
2.1 INTRODUCTION	67
2.2 MATERIALS AND METHODS.....	69
2.2.1 Surgery and carotid body isolation	69
2.2.2 Labelling of catecholamine stores and release of [³ H]catecholamine	69
2.2.2.1 Labelling of the catecholamine stores.....	69
2.2.2.2 [³ H]catecholamine release experiments	70
2.2.2.3 Quantification of [³ H]catecholamine release	71

2.2.3 Carotid body dissociation	72
2.2.4 Calcium imaging on dissociated carotid body cells.....	73
2.2.5 Tyrosine hydroxylase immunostaining.....	76
2.2.6 CaR-HEK293 cells culture	77
2.2.7 Calcium imaging on CaR-HEK293 cells.....	77
2.3 RESULTS	79
2.3.1 Spermine inhibition of catecholamine release induced either by hypoxia or high K ⁺ from isolated carotid body	79
2.3.2 Dose-response curve to neomycin in CaR-HEK293 cells	81
2.3.3 Comparative effect of R-568 and S-568 on CaR-HEK293 cells	83
2.3.3 Comparative effect of R-568 and S-568 on CaR-HEK293 cells	83
2.3.4 Absence of an effect of neomycin and R-568 on carotid body catecholamine release	84
2.3.5 Control of the quality of the dissociated carotid body cell preparations	88
2.3.6 Identification of cell types recorded	88
2.3.7 Effect of Cd ²⁺ on Ca ²⁺ influx induced by high K ⁺ in carotid body type 1 cells	88
2.3.8 Effect of spermine, neomycin and R-568 on [Ca ²⁺] _i increase induced by high K ⁺ on dissociated carotid body cells.....	89
2.3.9 Effect of spermine on [Ca ²⁺] _i increase induced by hypoxia on dissociated carotid body cells	97
2.3.10 Effect of Ca ²⁺ -free solution on the increase in [Ca ²⁺] _i induced by high K ⁺ and neomycin in type 1 and non-type 1 cells.....	101
2.4 DISCUSSION	103

2.5 CONCLUSION.....	109
CHAPTER 3	111
3.1 INTRODUCTION	112
3.2 MATERIALS AND METHODS.....	114
3.2.1 Reverse transcription and polymerase chain reaction (RT-PCR).....	114
3.2.1.1 <i>Total RNA extraction from carotid body, brain and eye</i>	114
3.2.1.2 <i>Reverse transcription</i>	115
3.2.1.3 <i>Polymerase chain reaction</i>	116
3.2.1.4 <i>Sequencing of the PCR products</i>	117
3.2.2 Immunohistochemistry on rat carotid body sections	119
3.2.2.1 <i>Fixation and tissue preparation</i>	120
3.2.2.2 <i>Immunohistochemistry</i>	120
3.3 RESULTS	123
3.3.1 Positive control for tyrosine hydroxylase and β -actin	123
3.3.2 Identification of L-type Ca^{2+} channel expressions in carotid body tissue	123
3.3.2.1 <i>RT-PCR of L-type Ca^{2+} channels</i>	123
3.3.2.2 <i>Immunostaining of $Ca_v1.2$ and $Ca_v1.3$ Ca^{2+} channels</i>	128
3.3.3 Identification of N, P/Q and R-type Ca^{2+} channel expressions in carotid body tissue	132
3.3.3.1 <i>RT-PCR of N, P/Q and R-type Ca^{2+} channels</i>	132
3.3.3.2 <i>Immunostaining of N, P/Q and R-type Ca^{2+} channels</i>	132
3.3.4 Identification of T-type Ca^{2+} channels expression in carotid body tissue	140
3.3.5 Identification of CaR expression in carotid body tissue	140

3.4 DISCUSSION	144
3.5 CONCLUSION.....	148
CHAPTER 4	150
4.1 INTRODUCTION	151
4.2 MATERIALS AND METHODS.....	153
4.2.1 Wild-type HEK293 and Ca _v 1.2-HEK293 Cells Culture.....	153
4.2.2 Transfection of HEK293 cells with Ca _v 1.2 plasmid.....	154
4.2.2.1 Transformation of <i>E.coli</i> with Cav1.2 plasmid.....	154
4.2.2.2 Purification of the Ca _v 1.2 plasmid.....	155
4.2.2.3 Transfection of HEK293 cells with Ca _v 1.2 plasmid	156
4.2.3 Electrophysiological recordings.....	156
4.2.4 Calcium imaging on Ca _v 1.2-HEK293 cells	159
4.2.5 Effect of spermine and of nifedipine on Ca ²⁺ influx in type 1 cells	159
4.3 RESULTS	160
4.3.1 Absence of effect of spermine and R-568 on I _{Ca_v1.2} recorded in 20 mM Ba ²⁺	
.....	160
4.3.2 Effect of Ba ²⁺ concentration on I _{Ca_v1.2}	162
4.3.3 Effect of addition of 0.5 mM extracellular Ca ²⁺ on I _{Ca_v1.2} recorded in 2 mM	
Ba ²⁺	162
4.3.4 Inhibitory effect of spermine and absence of effect of R-568 on I _{Ca_v1.2}	
recorded in the presence of 2 mM Ba ²⁺	165
4.3.5 Effect of CaR modulators, spermine, R-568 and neomycin, on I _{Ca_v1.2} , as	
assessed by Ca ²⁺ _i imaging	165

4.3.6 Effect of co-application of spermine and nifedipine on Ca ²⁺ influx in type 1 cells	169
4.3.6.1 <i>Effect of nifedipine on Ca²⁺ influx</i>	169
4.3.6.2 <i>Effect of co-application of nifedipine and spermine on Ca²⁺ influx</i>	169
4.4 DISCUSSION	173
4.5 CONCLUSION	178
DISCUSSION AND PERSPECTIVES	179
REFERENCES	184

LIST OF ABBREVIATIONS

ACh	acetylcholine
ACTH	adreno corticotropic hormone
ASIC	acid sensing ion channel
$[Ca^{2+}]_i$	intracellular concentration in Ca^{2+}
ADP	adenosine diphosphate
ATP	adenosine triphosphate
BK_{Ca}	large conductance voltage and Ca^{2+} -activated K^+ channel
Bp	base pair
cAMP	cyclic adenosine monophosphate
CaR	extracellular Ca^{2+} sensing receptor
cDNA	complementary DNA
CSN	carotid sinus nerve
EC_{50}	half maximal activation
EGTA	ethylene glycol tetraacetic acid
GABA	gamma-aminobutyric acid
GPCR	G protein coupled receptor
GSH and GSSG	reduced and oxidised form of the cytosolic glutathione
HEK293	human embryonic kidney 293
HIF	hypoxia inducible factor
HO-2	heme oxygenase-2
HVA	high voltage activated
IC_{50}	half maximal inhibition
IP	injected intraperitoneally

IP ₃	inositol -triphosphate
LVA	low voltage activated
mRNA	messenger RNA
NADPH	nicotinamide adenine dinucleotide phosphate
NOS	nitric oxide synthase
Nox	NADPH oxidase
PBS	phosphate-buffered saline
pO ₂	partial pressure in O ₂
pCO ₂	partial pressure in CO ₂
PCR	polymerase chain reaction
PG	petrosal ganglion
ROS	reactive oxygen species
RT-PCR	reverse transcriptase polymerase chain reaction
TRPC	transient receptor potential channel

LIST OF FIGURES

Figure 1.2: Anatomy of the complex carotid bifurcation/carotid body	13
Figure 1.3: Sensitivity of the carotid body to pO ₂ , pCO ₂ and pH.....	14
Figure 1.4: Schematic representation of α subunit of BK _{Ca} channel	15
Figure 1.5: Schematic representation of TASK channel	16
Figure 1.6: Schematic representation of α subunit of Kv channel.....	18
Figure 1.7: Schematic representation of the proposed O ₂ sensing mechanisms in carotid body type 1 cells	25
Figure 1.8: Effect of 20 % CO ₂ on type 1 [Ca ²⁺] _i	26
Figure 1.9: Rat type 1 cells express BK _{Ca} channel.....	29
Figure 1.10: Rat type 1 cells express TASK channels.....	30
Figure 1.11: Schematic representation of carotid body and the effect of neurotransmitters in rat.	40
Figure 1.12: Scheme of polyamine synthesis.	46
Figure 1.13: Predicted structure of the CaR.....	51
Figure 1.14: Structure of the calcimimetics R-568 and S-568,.....	53
Figure 1.15: Summary of the intracellular pathways activated by the CaR.	55
Figure 1.16: Schematic representation of the voltage-dependent Ca ²⁺ channel subunits....	60
Figure 1.17: Schematic representation of carotid body illustrating the working hypotheses	65
Figure 2.1: Inhibitory effect of spermine on ³ H-CA secretion induced either by hypoxia or high K ⁺ in isolated carotid body	80
Figure 2.2: Dose-response curve to neomycin in CaR-HEK293 cells.....	82
Figure 2.3: Effect of R-568 and S-568 on the increase in [Ca ²⁺] _i in CaR-HEK293 cells....	85
Figure 2.4: Dose-response curves to R-568 and S-568 in CaR-HEK293 cells.	86
Figure 2.5: Absence of effect of neomycin and R-568 on ³ H-CA secretion induced by hypoxia in isolated carotid body	87
Figure 2.6: Evolution of 340/380 ratio, in carotid body dissociated cells, during the time in culture	91
Figure 2.7: Tyrosine hydroxylase immunostaining on cells previously used for Ca ²⁺ imaging	91

Figure 2.8: Effect of Cd^{2+} on Ca^{2+} influx, induced by 15 mM K^+ , in type 1 cells.	92
Figure 2.9: Effect of 200 μM spermine on $[\text{Ca}^{2+}]_i$ in dissociated carotid body cells.	93
Figure 2.10: Dose-response curve to spermine in carotid body type 1 cells	94
Figure 2.11: Effect of 300 μM neomycin on $[\text{Ca}^{2+}]_i$ in dissociated carotid body cells	95
Figure 2.12: Effect of 100 nM R-568 on $[\text{Ca}^{2+}]_i$ in dissociated carotid body cells	96
Figure 2.13: Effect of high K^+ , hypoxia and spermine on $[\text{Ca}^{2+}]_i$ in type 1 cells	98
Figure 2.14: Comparison of the inhibitory effect of spermine on Ca^{2+} influx induced either by hypoxia or high K^+	99
Figure 2.15: Effect of spermine on pO_2 chemosensitivity.	100
Figure 2.16: Effect of removal of extracellular Ca^{2+} on increase in $[\text{Ca}^{2+}]_i$ induced by high K^+ in dissociated carotid body cells.	102
Figure 3.1: Positive controls for the reverse-transcription from isolated rat carotid body mRNA	125
Figure 3.2: Expression of $\text{Ca}_v1.2$ but not $\text{Ca}_v1.3$ and $\text{Ca}_v1.4$ mRNAs in carotid body.	126
Figure 3.3: Alignment of the sequence of $\text{Ca}_v1.2$ product amplified by RT-PCR in the carotid body with the $\text{Ca}_v1.2$ sequence from the Gene Bank.	127
Figure 3.4: View of a carotid body/superior cervical ganglion region immunostained for $\text{Ca}_v1.2$ and tyrosine hydroxylase.....	129
Figure 3.5: Expression of $\text{Ca}_v1.2$ protein in type 1 cells.	130
Figure 3.6: Absence of immunoreactivity for $\text{Ca}_v1.3$ protein in type 1 cells	131
Figure 3.7: Expression of $\text{Ca}_v2.2$ mRNA in carotid body.	134
Figure 3.8: Alignment of the sequence of $\text{Ca}_v2.2$ product amplified by RT-PCR in the carotid body with the $\text{Ca}_v2.2$ sequence from the Gene Bank.	135
Figure 3.9: Absence of expression of $\text{Ca}_v2.1$ and $\text{Ca}_v2.3$ mRNAs in carotid body.....	136
Figure 3.10: Expression of $\text{Ca}_v2.2$ protein in carotid body type 1 cells.	137
Figure 3.11: Absence of immunoreactivity for $\text{Ca}_v2.1$ protein in type 1 cells.	138
Figure 3.12: Absence of immunoreactivity for $\text{Ca}_v2.3$ protein in type 1 cells.	139
Figure 3.13: Absence of expression of T-type Ca^{2+} channel mRNAs in carotid body.....	142
Figure 3.14: CaR protein was not expressed in carotid body type 1 cells but was present in nerve endings	143

Figure 4.1: CaR activators, spermine and R-568, have no effect on $I_{Ca_{v1.2}}$ carried by 20 mM external Ba^{2+} .	161
Figure 4.2: Effect of extracellular Ba^{2+} concentration on $I_{Ca_{v1.2}}$.	163
Figure 4.3: Effect of addition of 0.5 mM extracellular Ca^{2+} on $I_{Ca_{v1.2}}$ recorded in the presence of 2 mM external Ba^{2+} .	164
Figure 4.4: Inhibitory effect of spermine on $I_{Ca_{v1.2}}$ recorded in presence of 2 mM external Ba^{2+} .	166
Figure 4.5: Absence of effect of R-568 on $I_{Ca_{v1.2}}$ recorded in the presence of 2 mM external Ba^{2+} .	167
Figure 4.6: Effect of neomycin, R-568 and spermine on $I_{Ca_{v1.2}}$ recorded by Ca^{2+} imaging in 1.2 mM external Ca^{2+} .	168
Figure 4.7: Inhibitory effect of nifedipine on Ca^{2+} influx in type 1 cells.	170
Figure 4.8: Effect of co-application of nifedipine and spermine on Ca^{2+} influx induced by high K^+ in type 1 cells.	171
Figure 4.9: Schematic representation of carotid body illustrating the expression of CaR and voltage-dependent Ca^{2+} channel and the inhibitory effect of spermine on type 1 cells.....	181

LIST OF TABLES

Table 1.1: Nomenclature, localization and antagonist of voltage-dependent Ca^{2+} channels	62
Table 3.1: Primers used for the amplification of CaR, voltage-dependent Ca^{2+} channels, β -actin and tyrosine hydroxylase transcripts by RT-PCR.	118

CHAPTER 1

GENERAL INTRODUCTION

Introduction

This study focuses on the effect of spermine on the carotid body function, based on hypothesis of a co-secretion of spermine with neurotransmitters by type 1 cells, similarly to neurons. It tests the hypothesis of an activation of the CaR and/or an inhibition of voltage-dependent Ca^{2+} channels by spermine in type 1 cell. The introduction aims to review the literature on these topics. The part 1.1 deals with the regulation of respiration, showing the role of the carotid bodies in the intact respiratory system. The part 1.2 describes the molecular, cytoplasmic and membrane mechanisms involved in pO_2 , pCO_2 and pH sensing in the carotid body type 1 cells. The activation of type 1 cell by such stimuli leads to the excitation of the petrosal nerve endings via synaptic transmission. This particular point is discussed in the part 1.3 with the description of the neurotransmitters released and their post- and pre-synaptic effects. The section 1.4 concerns the modifications observed in the carotid body in response to chronic sustained or intermittent hypoxia during which the polyamine levels are likely to increase. The metabolism and the physiological roles of polyamines are also examined in the section 1.5. Finally, the parts 1.6 and 1.7 review the literature about the two putative targets of spermine in type 1 cell tested in this study, the CaR and the voltage-dependent Ca^{2+} channels.

1.1 RESPIRATION

1.1.1 Respiration and chemoreceptors

During the life of any mammal the circulatory and respiratory system need to be tuned to match the oxygen demand of the organism. These adaptations of the circulatory and respiratory systems appear in response to variation in the organism's oxygen (O_2) consumption or to a decrease in O_2 availability in the air. To be compatible with the homeostasis of the organism, the partial pressure of oxygen (pO_2) and the partial pressure of carbon dioxide (pCO_2) in the blood must be maintained within narrow optimal levels (Gonzalez *et al.*, 1994). For instance, in the systemic arterial circulation, pO_2 should be around 95 mmHg and pCO_2 around 40 mmHg (Ganong, 1997). This gas homeostasis is maintained by the balance between the cellular consumption of O_2 , the production of CO_2 and gas exchanges in the lung. To match the needs of the organism the respiratory and circulatory systems are able to adapt quickly to any changes in pO_2/pCO_2 in the air/blood.

Changes in pO_2 and pCO_2 are detected in the blood by chemoreceptors: carotid bodies, aortic bodies and central chemoreceptors in the brainstem, and in the air by the neuroepithelial bodies (Ganong, 1997; Ward, 2008). The aortic and carotid bodies are the main chemoreceptors detecting the blood pO_2 , indeed following their denervation the response to a drop in blood pO_2 is almost completely blocked. The remaining response is due to the pO_2 sensitivity of the brainstem. In contrast the pCO_2 and pH sensing takes place in the carotid bodies and the central chemoreceptors. The function of the carotid bodies is the sens these parameters in the blood whereas the central chemosenreceptors detect their

Introduction

level in the brain fluid (Kawai *et al.*, 1996; Duprat *et al.*, 1997; Lahiri & Forster, 2003). In the carotid body, the detection of pCO₂ and pO₂ act in synergy (Pepper *et al.*, 1995; Kumar & Bin-Jaliah, 2007). The information sent by all of these chemoreceptors is integrated in the brain respiratory centres at the level of the nucleus of the solitary tract which then modulates ventilation. The nucleus of the solitary tract is an important centre of integration comprising neurons receiving input from the cardiac, respiratory and gastric system (Paton & Kasparov, 2000).

Three main centres are involved in the control of the respiration (Fig. 1.1). The first, the pontine respiratory group, receives input from the lung baroreceptors and modulates the lung volume and the switch between inspiration and expiration. The second group, the dorsal respiratory group, which lies next to the nucleus of the tract solitarius, receives input from the chemo- and mechanoreceptors. It acts as a relay influencing the respiration by effecting the two other groups and the spinal cord (Benarroch, 2007). The third group, the ventral respiratory group, situated in ventral medulla, controls the resistance of the airway and contains the pre-Botzinger area regrouping critical neurons responsible for the rhythmicity of the respiration (Feldman & Del Negro, 2006). There is a very strong concentration of pCO₂-chemosensitive neurons in the ventral medullary group, and some others more diffusely spread throughout the brainstem (Nattie, 1999; Benarroch, 2007).

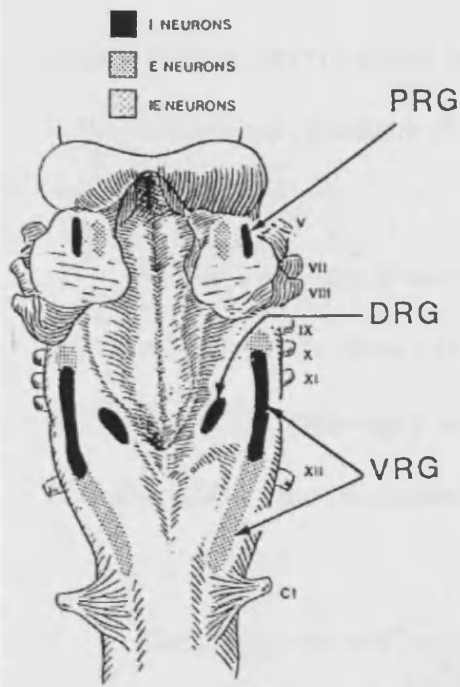


Figure 1.1: Location of the respiratory centres in the brainstem. Schematic dorsal view of the brainstem showing the pontine respiratory (PRG), the dorsal respiratory (DRG) and the ventral respiratory group (VRG) of neurons involved in the regulation of respiration. Each group includes neurons which are active, especially during inspiration (I, black) or expiration (E, dots). From Nattie, 1999.

1.1.2 Response to hypoxia

Decreases in pO_2 in the air or in the arterial blood are classified as acute hypoxia, chronic intermittent hypoxia and sustained hypoxia. They result from pathological situations such as sleep apnoea or chronic obstructive pulmonary disease or during ascent to altitude. Both chronic intermittent and sustained hypoxia lead to pathological situations such as pulmonary or systemic hypertension, respectively (Kemp, 2006).

Hypoxic air or obstruction of the airways induces a situation in which the pulmonary alveolar air becomes hypoxic. As a result, the blood pO_2 decreases and the blood pCO_2 increases. These changes in gas concentration are sensed by the carotid bodies which then stimulate the brainstem respiratory centres and lead to the activation of the sympathetic nervous system (Schultz & Li, 2007). As a result, the heart rate increases producing an increase in blood pressure. In addition, the activation of the sympathetic

Introduction

system and the hypoxic blood induce a systemic vasoconstriction and long lasting changes in the blood vessel resistance (Rouwet *et al.*, 2002; Phillips *et al.*, 2006).

In the lung, the presence of hypoxic air induces a pulmonary vasoconstriction (HPV) which aims to prevent blood reaching unventilated alveoli. This mechanism is under the control of the pulmonary smooth muscle cells, which contract in response to hypoxia (Gurney, 2002). This vasoconstriction induces a pulmonary hypertension (Levitzky, 2008).

Conjointly, the low blood pO_2 triggers the secretion of erythropoietin by the kidney (Levitzky, 2008). This hormone acts on the bone marrow and stimulates an increase in the hematocrit in order to improve the oxygen transport (Levitzky, 2008). The result of this increase in hematocrit is an increase in blood viscosity and pressure, which can lead to cardiac problems (Wagner *et al.*, 2001).

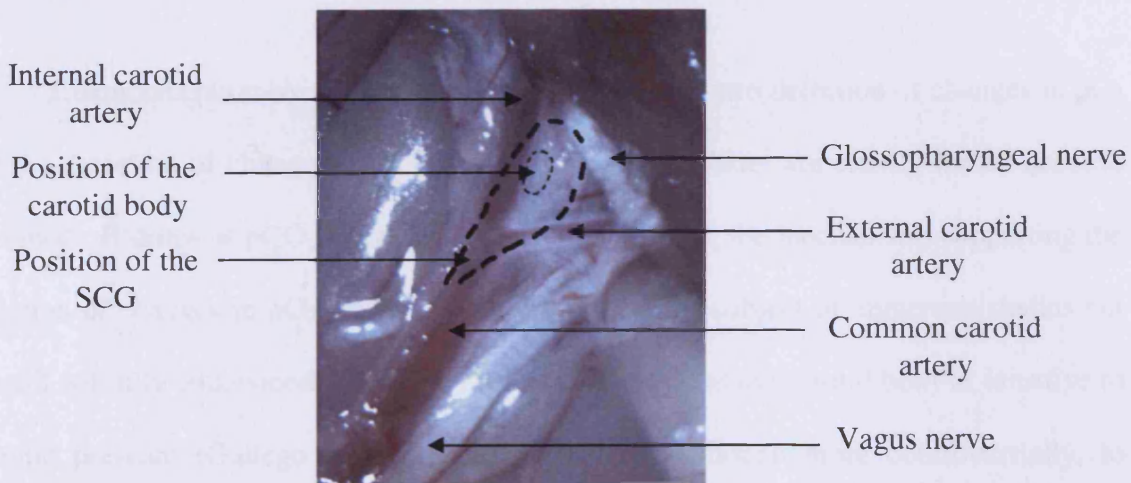
Chronic sustained and intermittent hypoxia trigger several mechanisms, activation of the sympathetic system, pulmonary vasoconstriction and increase in hematocrit. The carotid body plays an important role in the response in mediating the activation of the sympathetic system which then induces hypertension. Better understanding of the functioning of the carotid body and the development of pharmacological tools may help to find a therapeutic cure to prevent pulmonary or systemic hypertension resulting from chronic sustained or intermittent hypoxia.

1.2 CHEMORECEPTION BY CAROTID BODY

1.2.1 Anatomy of the carotid body

The carotid bodies are located between the bifurcation of the carotid artery, in close proximity to the superior cervical ganglion (SCG) (Fig. 1.2). The carotid bodies are innervated by the carotid sinus nerve (CSN) and by the ganglioglomerular nerve. The CSN is afferent and makes contact with: i) type 1 cells (sensing the O_2 , CO_2 and the pH) and ii) the blood vessels inside the carotid bodies (sensing the blood pressure). The somata of the CSN are located in the petrosal ganglion (PG) and project to the nucleus tractus solitarius, one of the brainstem respiratory centres (De Castro & Rubio, 1968). The carotid bodies are supplied with arterial blood by a branch of the external carotid artery which allows them to sense pO_2 , pCO_2 and pH at the aorta level. The organ is vascularised with a network of blood vessels and capillaries, which together occupy one-quarter of the volume of the carotid body (Pallot, 1987). The chemoreceptor type 1 cells (glomus) are located near the capillaries and are organized into clusters (glomeruli) surrounded by glial-like type 2 cells (De Kock, 1951).

A



B

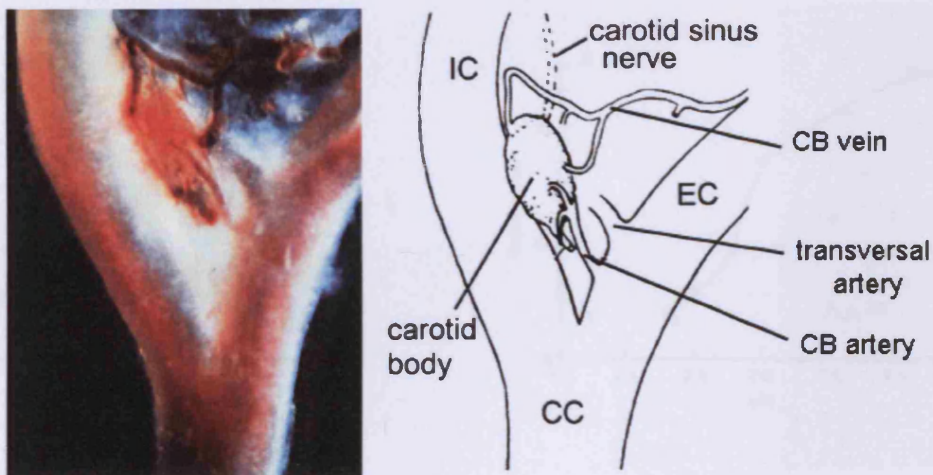


Figure 1.2: Anatomy of the complex carotid bifurcation/carotid body. A) Photo of the carotid bifurcation as it is in the rat prior to its removal for carotid body isolation. The vagus nerve follows the common carotid artery on its external side. The glossopharyngeal nerve passes transversally above the two branches of the carotid artery. The nerve is used as a reference to enable resection of the carotid bifurcation, with the carotid body. The position of the carotid body, which is not visible and among the conjunctive tissue between the two branches of the carotid artery and the position of the superior cervical ganglion (SCG), on the other side of the bifurcation, are drawn in dashed line. B) Photograph and schematic representation of the carotid bifurcation with the carotid body along the internal carotid artery (IC). The carotid body blood supply is provided by small blood vessels emerging form external carotid artery (EC). Common artery, CC. B) Taken from McDonald, 1981.

1.2.2 Chemoreception in type 1 cells, general mechanism

Chemoreception by the type 1 cells can be divided into detection of changes in pO_2 and the detection of changes in pCO_2/pH (Fig. 1.3). The latter are closely linked because the blood pH drops as pCO_2 increases. At the cellular level, the mechanisms supporting the detection of changes in pO_2 , pCO_2 and pH have been the subject of numerous studies but are still not fully understood. Moreover, reports indicate that the carotid body is sensitive to osmotic pressure (Gallego & Belmonte, 1979) and, although more controversially, to glucose (Pardal & Lopez-Barneo, 2002; Zhang *et al.*, 2007).

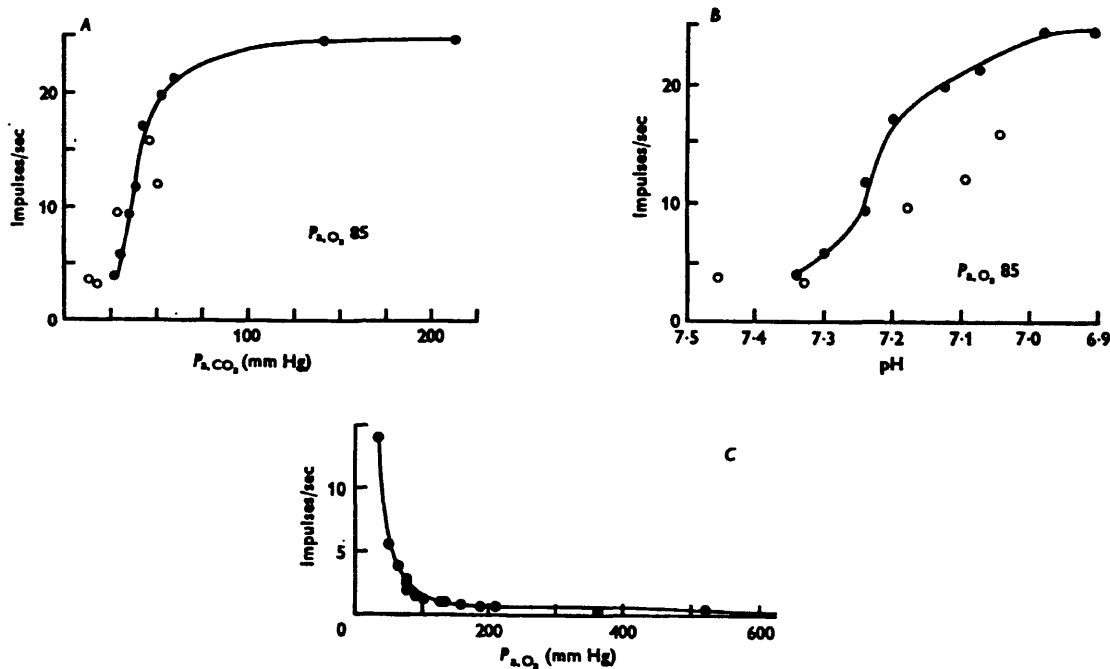


Figure 1.3: Sensitivity of the carotid body to pO_2 , pCO_2 and pH. Recordings of the cat carotid sinus nerve activity plot against the arterial partial pressure in CO₂ (P_aCO_2 , A), the pH (B) and arterial partial pressure in O₂ (P_aO_2 , C) obtained by Biscoe *et al.* in 1970 (Biscoe *et al.*, 1970). The carotid sinus nerve activity is strictly dependent upon the activation of the carotid body by P_aO_2 , P_aCO_2 and pH. The CSN propagates action potential, even at P_aO_2 of 600 mmHg; therefore there is not a threshold for activation of chemosensitivity Biscoe *et al.*, 1970.

It is generally accepted that pO_2 , pCO_2 and pH modulate the activity of a variety of ion channels, such as large-conductance, voltage and Ca^{2+} -activated K^+ channels (BK_{Ca}) (Peers, 1997), TASK-like channels (Buckler, 1997) and acid-sensing ion channels (ASIC) (Tan *et al.*, 2007). The closure of K^+ channels or activation of ASIC leads to depolarization and Ca^{2+} entry via voltage-dependent Ca^{2+} channels. It is the attendant increase in intracellular Ca^{2+} concentration ($[Ca^{2+}]_i$) that induces neurotransmitter release.

1.2.3 O_2 sensitive ion channels in the carotid body

Lopez-Barneo *et al.* was the first group to show involvement of K^+ currents in response to diminution of pO_2 in the rabbit (Lopez-Barneo *et al.*, 1988), giving rise to the membrane hypothesis of O_2 sensing.

1.2.3.1 BK_{Ca} channel and heme oxygenase-2

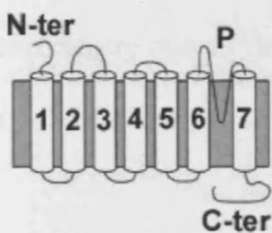


Figure 1.4: Schematic representation of α subunit of BK_{Ca} channel. α subunit of BK_{Ca} possesses 7 transmembrane domains (1 to 7) and a pore (P). The C-terminal part (C-ter) is inside the cell and comprises the Ca^{2+} sensitive segment. Adapted from Lopez-Lopez & Perez-Garcia, 2007.

BK_{Ca} (or maxiK) channels are large-conductance, voltage- and Ca^{2+} -activated K^+ channels. The channels are formed by tetramers of α subunits. The α subunit contains 7 transmembrane domains and comprises the Ca^{2+} -sensitive segment in the C-terminal tail

(Jiang *et al.*, 2001; Patel & Honore, 2001). $[Ca^{2+}]_i$ modulates the activity of the channel, as the intracellular Ca^{2+} concentration increase, the activity of BK_{Ca} increases (Riesco-Fagundo *et al.*, 2001). The regulation of the channel by low pO_2 requires an additional factor identified as heme oxygenase-2 (Williams *et al.*, 2004). Heme oxygenase-2 (HO-2) is a membrane protein, constitutively expressed in carotid body (Prabhakar *et al.*, 1995). HO-2 and BK_{Ca} are closely associated because the channel is still sensitive to pO_2 in excised membrane patches, where a very small part of the cell membrane is taken out from the cell and recorded (Williams *et al.*, 2004). In the presence of O_2 , HO-2 degrades heme in biliverdin and CO, and the later activates BK_{Ca} . CO modulates the channel activity via the C-terminal part with a redox-independent mechanism (Williams *et al.*, 2008). However, studies with mice deficient in HO-2 are contradictory. In such mice, Adachi *et al.* found a decrease of the ventilatory response to hypoxia, supporting the hypothesis that HO-2 is an oxygen sensor (Adachi *et al.*, 2004) whereas Ortega-Saenz *et al.* reported similar responses to hypoxia in control versus knock-out mice (Ortega-Saenz *et al.*, 2006). These divergent conclusions remain unexplained and the role of HO-2 in O_2 sensing requires more investigation. Moreover, McCartney *et al.* have revealed an alternative O_2 sensing mechanism, due to the presence of cysteine-rich motif in alternatively spliced version of BK_{Ca} (McCartney *et al.*, 2005).

1.2.3.2 TASK-like channels

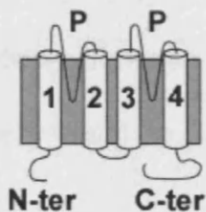


Figure 1.5: Schematic representation of TASK channel. TASK channel is made of 4 transmembrane domains and has 2 pores (P). Adapted from Lopez-Lopez & Perez-Garcia, 2007.

Introduction

TASK-like channels belong to the K2P family, containing two-pore domains (Lotshaw, 2007). TASK channels have 4 transmembrane segments and produce background currents which are insensitive to voltage. The K^+ current is not affected by caesium, tetraethylammonium and 4-aminopyridine and it is blocked by barium, quinine, zinc (Kim *et al.*, 1998; Patel *et al.*, 1999). Moreover, the current is extremely sensitive to pH in the physiological range. At an external pH of 7.3, the channel is half-maximally activated and reaches its maximum activation at pH of 7.7. The sensitivity to pH is physiologically consistent with the sensitivity to O_2 , indeed when the pO_2 decreases, due to the increase of cellular metabolism, the pCO_2 increases and pH decreases (Duprat *et al.*, 1997; Buckler *et al.*, 2000). Nevertheless, in the pathological situations of metabolic acidosis or alkalosis, where the pO_2 and pCO_2 are constant only the changes in pH activate the channel. In the excised patch-clamp configuration, the channel loses its O_2 sensitivity suggesting that the channel response to hypoxia occurs indirectly via a modification of an intracellular component such as auxiliary proteins or pH (Patel & Honore, 2001). When expressed in HEK293 cells, hTASK-1 channel is sensitive to O_2 (Lewis *et al.*, 2001) but when expressed in immortalized adrenomedullary chromaffin cells the channel is insensitive to O_2 , demonstrating that the TASK channel O_2 sensitivity is determined by the cell type (Johnson *et al.*, 2004). The TASK channel O_2 sensitivity is therefore dependent upon specific cytosolic factors. TASK channels have been shown to be modulated by inhibition of mitochondrial function (Ortega-Saenz *et al.*, 2003; Wyatt & Buckler, 2004). The AMP kinase plays an important role as a link between the decrease of the mitochondrial activity and the inhibition of TASK channels (Evans *et al.*, 2005). Therefore the channels would be activated by phosphorylation which is confirmed by the fact that

addition of ATP induces, in excised patch, a rapid increase in channel activity (Williams & Buckler, 2004).

1.2.3.3 Kv3 and Kv4 channels

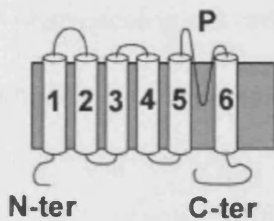


Figure 1.6: Schematic representation of α subunit of Kv channel. The α subunit of Kv channel has 6 transmembrane domains and one pore (P). Adapted from Lopez-Lopez & Perez-Garcia, 2007.

Kv α channels (named KvX.X) have 6 transmembrane domains and are voltage gated channels (Lopez-Lopez & Perez-Garcia, 2007). They are associated with regulatory subunit such as Kv β . Kv channels play a major role in O₂ sensing in the rabbit carotid body. Indeed, negative construct to block expression of Kv4.x suppresses the depolarisation induced by hypoxia. In contrast, the construct blocking Kv1.x has no effect (Perez-Garcia *et al.*, 2000). The expression of Kv4.2 alone in HEK293 cells shows no effect of hypoxia or redox stimulation but co-expression with Kv β 1.2 restores the hypoxia and redox sensitivity of Kv4.X as observed in the rabbit carotid body (Perez-Garcia *et al.*, 1999). The Kv β subunit is therefore the chemosensor and it is constituted of an oxidoreductase enzyme changing the conformation of the complex Kv4.2/Kv β 1.2 depending of its state, either reduced form NADPH or oxidized form NADP⁺ (Pongs *et al.*, 1999). In confirmation of the precedent studies, Sanchez et al have shown the expression of Kv3.1, Kv4.1 and Kv4.3 at the mRNA and protein levels, in the rabbit carotid body (Sanchez *et al.*, 2002). These two channels, Kv3.1 and Kv4.3, produce both a fast

Introduction

inactivated current but only the application of antibody against Kv4.3 inhibits the hypoxic response. Kv3.1 would contribute to speed up the action potential rate in the rabbit carotid body without being the primary O₂ sensor (Lopez-Lopez *et al.*, 2003).

In the rat, Kv current (Kv2) is present but is not sensitive to change in O₂ (Lopez-Lopez & Perez-Garcia, 2007). Finally, mouse type 1 cells express Kv2.2, Kv3.1 and Kv3.2, but pharmacological studies reveal that only Kv3.X are O₂ sensitive and weakly responsible for the O₂ sensing (Lopez-Lopez & Perez-Garcia, 2007).

1.2.3.4 HERG channel

In the rabbit type 1 cells, the K⁺ channel HERG has been shown to be expressed and to participate in the resting membrane potential (Overholt *et al.*, 2000). To date, there is no experiment demonstrating a role of HERG in O₂ sensing in rabbit carotid body nevertheless a strong arguments is in favour of this hypothesis as HERG channels have been shown to be modulated by reactive oxygen species while expressed in *Xenopus* oocytes (Tagliatela *et al.*, 1997).

In parallel to the O₂ sensing membrane theory, other experiments suggest the involvement of NADPH oxidase, mitochondria and AMP kinase whose activity depend directly or indirectly on O₂ availability.

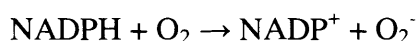
NADPH oxidase and mitochondria produce reactive oxygen species (ROS, i.e. O₂⁻ and OH⁻) during hypoxia (Gonzalez *et al.*, 2007). Then ROS act as second messenger and

modify the redox potential in the cell and interfere with K⁺ channels BK_{Ca} and TASK-like channels (Acker, 1994; Kemp, 2006).

1.2.4 Other O₂ sensors

1.2.4.1 NADPH oxidase

The enzyme is made of several subunits linked to a small GTPase (Rac) (Dinger *et al.*, 2007). There are different isoforms of the catalytic subunit of NADPH oxidase: Nox1-5, Duox1 and Duox2 (Porwol *et al.*, 2001). Only the expression of Nox2 and 4 have been investigated in the carotid body and only Nox4 has been detected in type 1 cells (Gonzalez *et al.*, 2007). In its resting form Nox4 is probably inactive and is switched on by increase in [Ca²⁺]_i via the activation of the protein kinase C (Dinger *et al.*, 2007). The active enzyme catalyses the following reaction:



Then, the O₂⁻ is converted into H₂O₂ due to the action of the superoxide dismutase (Dinger *et al.*, 2007). The H₂O₂ produced acts as a second messenger and modulates the activity of BK_{Ca} and TASK channels. Indeed, data obtained with normal and p47^{phox} (a subunit common to all the Nox isoform) knock-out mice reveal that hypoxia activates ROS production which then opens BK_{Ca} channel (He *et al.*, 2005). Moreover, it has been shown the Nox4 and TASK channels are closely associated, co-localized at the plasma membrane and that Nox4 is responsible for the modulation of TASK channel activity by O₂ (Lee *et*

Introduction

al., 2006). In contrast, the co-expression of Nox2 and TASK channels do not modulate the activity of the channel in hypoxia (Lee *et al.*, 2006). The different interactions between NoxX and TASK channels give a functional meaning to the specific expression of Nox4 in the type 1 cells (Gonzalez *et al.*, 2007).

In conclusion, in normoxia Nox is in its inactive form and gets activated by the rise in $[Ca^{2+}]_i$ induced by hypoxia. Then, Nox produces O_2^- which is converted in H_2O_2 and activates BK_{Ca} and TASK channels which repolarise the type 1 cells. This hypothesis is also supported by the fact that deletion of Nox (by knock-out) does not suppress the carotid body response to O_2 and enhances chemoreceptor sensitivity, demonstrating an inhibitory effect of Nox on the chemoreception (Roy *et al.*, 2000; He *et al.*, 2002).

1.2.4.2 Mitochondria

Very early studies suggested mitochondria as the O_2 sensor. Indeed, application of drugs which inhibit mitochondrial function activates the carotid body (Heymans, 1931). The mitochondria can produce ROS due to the activity of the cytochrome oxidase or the complex I, II and III in the electron transport chain but the amount of ROS which is produced is highly debated. In the first line of thought, hypoxia triggers a decrease in the activity of the cytochrome oxidase and a shift of the redox state within the mitochondria (Mansfield *et al.*, 2005). This increases the production of O_2^- (Chandel & Schumacker, 2000). This phenomenon happens in every cell type but is especially strong in carotid body mitochondria due to the expression of a particular form of cytochrome oxidase with a low affinity for O_2 (Mills & Jobsis, 1972). The second way of ROS production involves the

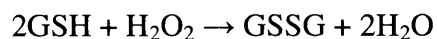
Introduction

complex I, II and III, of the respiratory chain, which convert O_2 molecules into O_2^- , the complex III is thought to produce the most O_2^- (Brunelle *et al.*, 2005; Guzy & Schumacker, 2006). O_2^- is then converted by superoxide dismutase into H_2O_2 , which crosses the mitochondrial membrane (Sauer *et al.*, 2001) and plays a role as a second messenger. Although, these two mechanisms have been identified and mitochondria were shown to play a role in O_2 sensing in pulmonary smooth muscle cells (Waypa *et al.*, 2001) and intact arterioles (Leach *et al.*, 2001), it is still uncertain that they play such a function in the carotid body (Gonzalez *et al.*, 2002; Gonzalez *et al.*, 2007). Indeed, the study of Piruat *et al.* on mice knocked-out for the complex II shows no modification of the type 1 cells response to hypoxia and interestingly a decrease in the activation threshold of K^+ channels (Piruat *et al.*, 2004). This refutes the involvement of complex II in the detection of O_2 . The second study, carried out on rat type 1 cells, demonstrates that inhibition of the electron transport chain by specific blockers inhibits background K^+ channel and induces Ca^{2+} influx, supporting the role of mitochondria in O_2 sensing in the carotid body (Wyatt & Buckler, 2004).

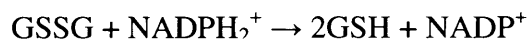
1.2.4.3 GSH/GSSG

In the context of ROS production by mitochondria and Nox, it was thought that cytosolic glutathione, which is a tripeptide (glutamate, cysteine and glycine) would be involved. Indeed, the main role of the glutathione is to act as an antioxidant and protect cells against free radical damage. In normal conditions most of the glutathione present in the cells is in the reduced form, GSH. In the presence of H_2O_2 , the reduced form GSH give a proton and an electron, becomes oxidised and reacts with another oxidised glutathione to give GSSG. This reaction is catalysed by the glutathione peroxidase:

Introduction



The GSSG is normally reduced in GSH by the G reductase (Gonzalez *et al.*, 2007), but in presence of H₂O₂ the GSSG production becomes too high to be converted again in GSH:



Therefore, the production of GSSG and the use of GSH decrease the redox environment in the cell. The increase of the redox environment of the cell modifies channel activities by oxidation of the methionine or cysteine residues present in the proteins. For instance, in BK_{Ca} channels, methionine oxidation increases the channel activity whereas cysteine oxidation decreases it (Tang *et al.*, 2001; Tang *et al.*, 2004; McCartney *et al.*, 2005). The redox sensitivity can be located in the auxiliary subunit, such as Kvβ1.2 which is associated with Kv4.2 (Perez-Garcia *et al.*, 1999). There is no influence of the redox state on TASK channels as demonstrated by the absence of effect of addition of NADH on excised channel activity (Williams & Buckler, 2004).

1.2.4.4 AMP kinase

AMP kinase is an attractive candidate for the O₂ sensor because its activity is dependent upon the energy status of the cell, which decreases in hypoxia. Indeed, as a consequence of O₂ depletion, mitochondrial activity decreases, creating an energetic stress. The lack of energy is translated into an increase in ADP/ATP ratio. To compensate the lack the decrease in ATP production, the ADP is used to produce ATP by the enzyme adenylate kinase with the result that the AMP/ATP ratio rises. This ratio is sensed by the AMP kinase

Introduction

which has been proposed as a sensor for metabolic stress (Hardie *et al.*, 2003). This enzyme is made of one catalytic α subunit and 2 regulatory β and γ subunits. AMP binds to the regulatory subunits and activates the kinase (Scott *et al.*, 2004). In type 1 cells, AMP kinase- α subunit is especially located at the plasma membrane, as demonstrated by immunostaining (Evans *et al.*, 2005). Activation of the AMP kinase results in direct phosphorylation of O₂-sensing K⁺ channels, TASK and BK_{Ca} (Hall & Armstrong, 2000; Wyatt *et al.*, 2007). Once phosphorylated, the channels close leading to a depolarization and activation of voltage-dependent Ca²⁺ channels.

In conclusion, several candidates rise as an O₂ sensor and none of the hypotheses can explain, on its own, all the data collected. It is more likely that the type 1 cells sense the change in pO₂ using multiple mechanisms which is more reliable than the involvement of a single one. The integration of all the mechanisms lead to the closure of K⁺ channels (Fig. 1.7) which depolarises the cell and trigger the neurotransmitter release.

Introduction

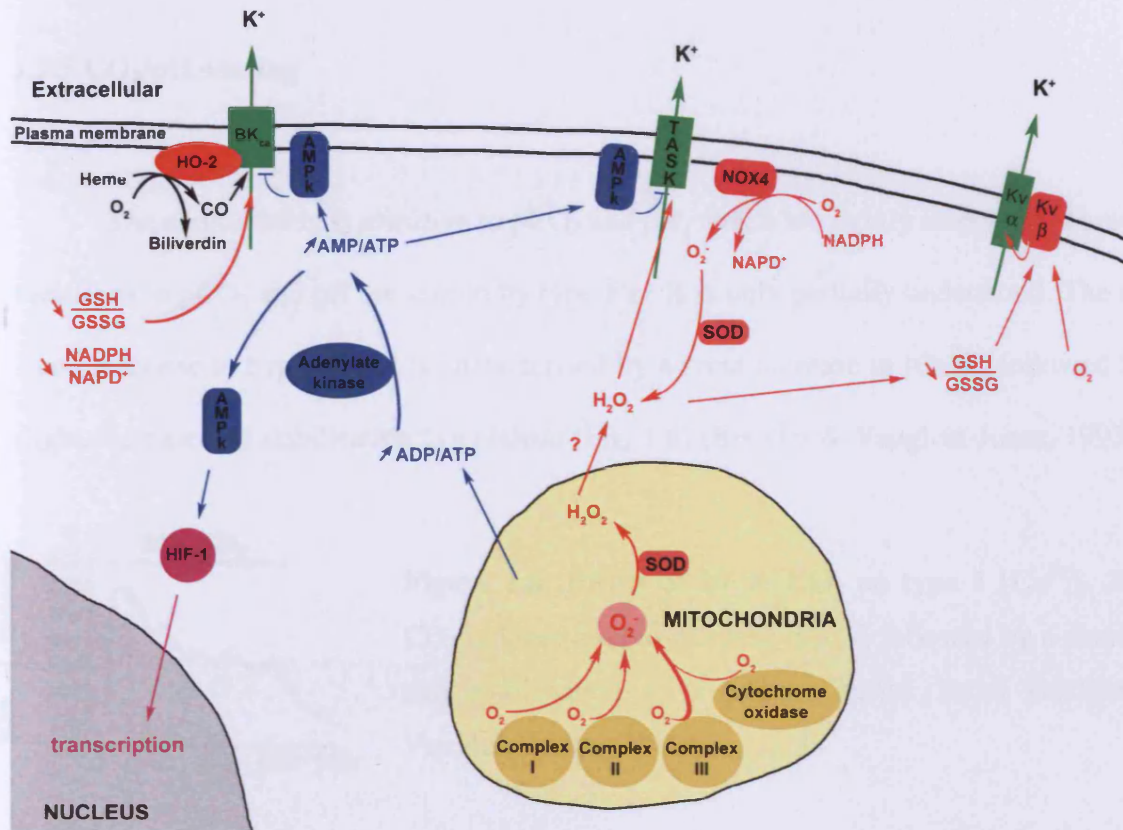


Figure 1.7: Schematic representation of the proposed O₂ sensing mechanisms in carotid body type 1 cells. On the plasma membrane are the K⁺ channels, TASK, BK_{Ca} and K_v. BK_{Ca} is associated with heme oxygenase-2 (HO-2), which produces CO in presence of O₂ and heme. K_{vα} is modulated by pO₂ via the subunit K_{vβ}. Inside the cell, the mitochondria play a role due to energetic stress induced by the lack of O₂, which increases the ratio ADP/ATP, and then AMP/ATP, which activates AMP kinase. The AMP kinase acts as an inhibitor of the K⁺ channels and a regulator of gene transcription via hypoxia inducible factor 1 α (HIF-1α). In addition, the debated role of reactive oxygen species in hypoxia is shown. The mitochondria produce O₂⁻ due to the perturbation of the mitochondrial activity. O₂⁻ is then converted into H₂O₂ by the super oxide dismutase (SOD) and leaves the mitochondria. The NADPH oxidase, such as Nox4, associated with TASK channels, is another source of O₂⁻ production. The presence of H₂O₂ leads to the modification of the redox potential of the cell and alters the GSH/GSSG ratio, which also modulates TASK, BK_{Ca} and K_{vα} (via K_{vβ}) channel activities. Adapted from Lopez-Lopez *et al.*, 2003; Dinger *et al.*, 2007; Gonzalez *et al.*, 2007; Wyatt & Evans, 2007.

1.2.5 CO₂/pH sensing

The carotid body is sensitive to pCO₂ and pH, which are tightly associated. How the variations in pCO₂ and pH are sensed by type 1 cells is only partially understood. The type 1 cell response to hypercapnia is characterised by a rapid increase in [Ca²⁺]_i followed by a slight decrease and stabilisation to a plateau (Fig. 1.8) (Buckler & Vaughan-Jones, 1993).

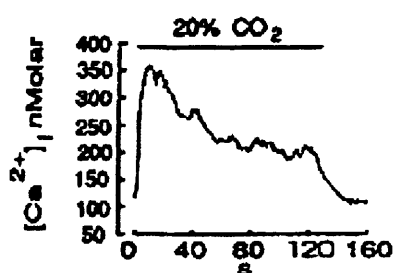
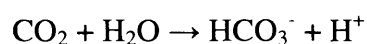


Figure 1.8: Effect of 20 % CO₂ on type 1 [Ca²⁺]_i. 20 % CO₂ induces a rapid increase [Ca²⁺]_i followed by a decrease and stabilisation to a plateau value. From Buckler & Vaughan-Jones, 1994a.

The response is largely dependent upon the pH leading to the hypothesis that the pCO₂ could be sensed via the variations of pH (Buckler *et al.*, 1991; Fitzgerald *et al.*, 2006). Indeed, the augmentation of pCO₂ induces an acidification of the blood and a decrease in intracellular pH due to the activity of the carbonic anhydrase in type 1 cells (Black *et al.*, 1971; Yamamoto *et al.*, 2003; Zhang & Nurse, 2004). This enzyme catalyses the reaction:



The decrease of the intracellular pH modulates ion channel activity (TASK channels) and induces neurotransmitter release (Stea *et al.*, 1991; Stea & Nurse, 1991; Buckler & Vaughan-Jones, 1993; Duprat *et al.*, 1997). The carbonic anhydrase has been shown to be responsible for the first rapid increase in [Ca²⁺]_i as it disappears when inhibitors of the enzyme are used (Buckler *et al.*, 1991). In contrast, the second phase is very sensitive to the

Introduction

extracellular pH and is nonexistent in isohydric hypercapnia (increase in $p\text{CO}_2$ at pH 7.4) (Buckler & Vaughan-Jones, 1993). The carotid body sensitivity to the extracellular pH is due to the expression of recently discovered ion channels sensitive to extracellular pH, the acid sensing ion channels (ASIC). They are especially permeable to Na^+ and are activated by a decrease in extracellular pH (Tan *et al.*, 2007). The pH_{50} of the channel is 6.3 and ASIC are partially open at pH 7. Rat carotid body expresses ASIC1 and 2. Moreover, carotid body cells express other proteins sensitive to pH such as: TASK channels (Buckler *et al.*, 2000); inwardly rectified K^+ (K_{ir}) channels CO_2 and pH sensitive (Yamamoto *et al.*, 2008) and pH sensitive Cl^- currents (Petheo *et al.*, 2001). In conclusion, activation of ASIC and of Cl^- channels in association with the closure of TASK-1 and of K_{ir} channels during acidosis lead to type 1 cells depolarisation and neurotransmitter release.

There is a multiplicative effect of the detection of $p\text{CO}_2$ and $p\text{O}_2$ in the carotid body. Indeed, at a low constant $p\text{O}_2$, the increase in $p\text{CO}_2$ leads to a greater activation of the type 1 cells (Pepper *et al.*, 1995). This interaction is also true for the response to $p\text{CO}_2$ which is enhanced by low $p\text{O}_2$ (Pepper *et al.*, 1995). The molecular mechanisms leading to the interactions between $p\text{CO}_2$ and $p\text{O}_2$ sensing are not elucidated. Experiments conducted on newborn animals shown that there is a post natal increase in the interaction between the stimuli which could explain the postnatal increase in sensitivity to $p\text{CO}_2$ and $p\text{O}_2$ (Pepper *et al.*, 1995; Calder *et al.*, 1997).

1.2.6 Glucose sensing

The sensitivity of the carotid body to low glucose was first demonstrated by Alvarez-Buylla showing that infusion of glucose in the carotid decreases the carotid body activity and raises its threshold to hypoxia (Alvarez-Buylla & de Alvarez-Buylla, 1988). Later on, several studies reported evidence for a sensitivity of the carotid body to hypoglycaemia, such as release of ATP and acetylcholine in hypoglycemia or activation of petrosal neurons by type 1 cells in co-culture (Pardal & Lopez-Barneo, 2002; Garcia-Fernandez *et al.*, 2003; Zhang *et al.*, 2007). The glucose response involves TASK channels (Duprat *et al.*, 1997) and is mediated by Ca^{2+} influx which induces neurotransmitter release. However, other groups were not able to reproduce this result making the carotid body glucose sensitivity very controversial (Bin-Jaliah *et al.*, 2004; Conde *et al.*, 2007; Kumar, 2007).

Type 1 cells are responsive to a large spectrum of stimuli pO_2 , pCO_2/pH , extracellular osmolarity, glucose. Activation by these stimuli appears to converge toward a single effect which is the depolarisation of the type 1 cells. This depolarisation activates voltage-dependent Ca^{2+} channels and/or voltage activated Na^+ channels.

1.2.7 Expression of O_2 -sensitive ion channels in rat carotid body

In rat type 1 cells, the presence of BK_{Ca} channel has been certified by electrophysiological recordings. Indeed, blockade of the Ca^{2+} influx with the use of Cd^{2+} inhibits the K^+ current induced by depolarisation steps (Fig. 1.9) (Peers, 1990a). The shoulder on the K^+ current observed near 20 mV, in control conditions, is due to the

Introduction

activation of the voltage-dependent Ca^{2+} channels. Moreover, the BK_{Ca} is activated at resting membrane potential and inhibited by hypoxia (Fig. 1.9) (Peers, 1990b; Ganfornina & Lopez-Barneo, 1992; Wyatt & Peers, 1995; Riesco-Fagundo *et al.*, 2001; Buttigieg & Nurse, 2004). The application of iberiotoxin, a specific blocker of BK_{Ca} channel corroborates the expression of this channel in rat type 1 cells (Peers & Carpenter, 1998; Pardal *et al.*, 2000).

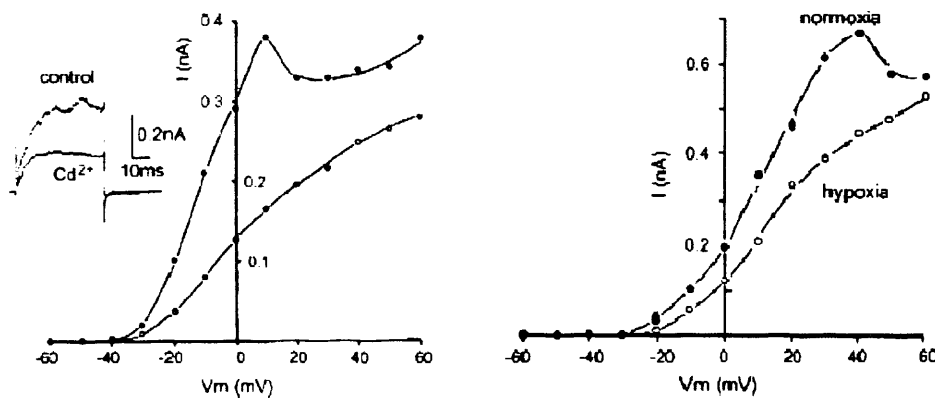


Figure 1.9: Rat type 1 cells express BK_{Ca} channel. A) K^+ current, recorded with 10 mV step from a holding potential of -70 mV in control condition (closed circle) and in presence of Cd^{2+} (open circle). The current is inhibited by suppression of the Ca^{2+} influx, from (Peers, 1990a). B) Current voltage relationship in control (closed circle) and hypoxia (open circle). Hypoxia inhibits the K^+ current, from Peers, 1990b. These two characteristics, Ca^{2+} activation and hypoxic inhibition demonstrate the presence of BK_{Ca} in rat type 1 cells.

In addition, TASK channels play an important role in rat type 1 cells in mediating the response to hypoxia. Experiments conducted in presence of BK_{Ca} channel blockers (tetraethylammonium chloride) reveal the presence of a second K^+ current oxygen sensitive, TASK, in the rat type 1 cells (Fig. 1.10) (Buckler, 1997; Buckler *et al.*, 2000).

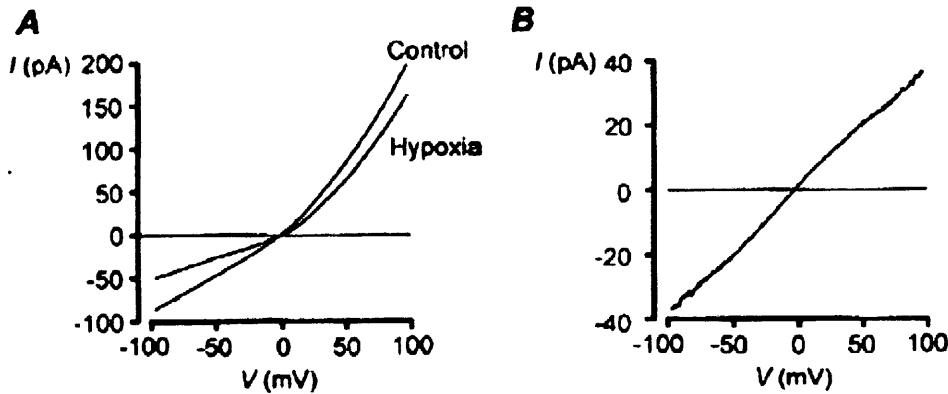


Figure 1.10: Rat type 1 cells express TASK channels. A) Voltage current relationship recorded in 140 mM extracellular K^+ and extracellular Ca^{2+} -free solution with TEA. The current is recorded in control and hypoxic conditions, hypoxia reduces the membrane conductance. B) Trace of the oxygen sensitive component of the K^+ current recorded in A obtained by subtraction of the traces under control and hypoxic conditions. From Buckler *et al.*, 2000.

Rat type 1 cells have been shown to express TASK-1, TASK-2, TASK-3 and TRAAK channels by immunochemistry and *in situ* hybridization (TASK-1) (Yamamoto *et al.*, 2002);(Buckler *et al.*, 2000) or RT-PCR (Nurse & Fearon, 2002; Kim *et al.*, 2006). In the rat, Kv current (Kv2) is present but is not sensitive to change in pO_2 (Lopez-Lopez & Perez-Garcia, 2007).

To conclude, in rat type 1 cells, intracellular or membrane mechanisms have been reported for the chemosensitivity to O_2 , CO_2 and pH. The intracellular mechanisms could be regulated by the intracellular concentration of polyamine which is very likely to increase in chronic hypoxia (see section 1.5), however it is not investigated in this study. In addition, the membrane mechanisms involving K^+ channels could be inhibited by extracellular spermine secreted by type 1 cells, a hypothesis which is tested in chapter 2.

1.3 NEUROTRANSMITTERS RELEASED BY TYPE 1 CELLS

A great variety of neurotransmitters have been identified in type 1 cells including catecholamines (dopamine and adrenaline), ATP, ADP, acetylcholine, GABA, histamine, serotonin and some neuropeptides such as opioid-like peptide, substance P, cholecystinin, galanin, neurotensin, calcitonin and atrial natriuretic peptide (Gonzalez *et al.*, 1994; Koerner *et al.*, 2004). Most of the neurotransmitters released act both on the PG nerve endings and on type 1 cells, where they modulate further the type 1 cells chemosensitivity.

1.3.1 Catecholamines

The presence of catecholamines in the carotid body has been assessed by immunohistochemistry of enzymes responsible for their synthesis, of the neurotransmitters themselves, and by functional studies (Gonzalez *et al.*, 1994). Tyrosine hydroxylase, the first enzyme involved in the synthesis of catecholamines, is expressed in type 1 cells (Karasawa *et al.*, 1982) and is now currently used as an immunostaining marker of type 1 cells. Dopamine and adrenaline are the two more abundant catecholamines in the carotid body, and are secreted in response to hypoxia and acidosis in rat (Vicario *et al.*, 2000b); (Donnelly, 1993; Gauda *et al.*, 1996), cat (Rigual *et al.*, 1991; Chen *et al.*, 1997) and rabbit (Gomez-Nino *et al.*, 1990; Gonzalez *et al.*, 1994).

Introduction

1.3.1.1 Effect of catecholamines on nerve endings

In the rat, cat and rabbit, the PG neurons, express dopamine receptors D1 and D2 (Gauda *et al.*, 1996; Bairam *et al.*, 1998). D1 and D2 receptors are coupled to G_s and G_i, respectively, and their activation results in an activation/inhibition of adenylate cyclase activity. Many experiments have shown that catecholamines are secreted following type 1 cell activation (Gonzalez *et al.*, 1994) but their roles as excitatory neurotransmitters is uncertain. For instance, experiments conducted in cat reveal that dopamine itself can not induce action potentials in PG neurons (Donnelly, 1996; Iturriaga & Alcayaga, 2004). Moreover, in co-cultures of rat type 1 cells and PG neurons, blockade of dopamine receptors have no effect on PG neuronal activity induced by hypoxia (Zhong *et al.*, 1997). The absence of a direct link between catecholamines release and PG neuronal activity leads to the conclusion that catecholamines modulate the responses of PG neurons induced by other neurotransmitters rather than stimulating them directly (Iturriaga & Alcayaga, 2004; Nurse, 2005). This hypothesis is supported by the observation that in dopamine D2 receptor knock-out mice, the ventilatory response to hypoxia is still present but reduced (Prieto-Lloret *et al.*, 2007).

1.3.1.2 Effect of catecholamines on type 1 cells

Rat type 1 cells express D2 receptors (Czyzyk-Krzeska *et al.*, 1992b; Gauda *et al.*, 1996; Gauda *et al.*, 2000) which, when activated, inhibit the Ca²⁺ influx induced by hypoxia (Benot & Lopez-Barneo, 1990; e Silva & Lewis, 1995; Jiang & Eyzaguirre, 2004; Carroll *et al.*, 2005). Therefore, dopamine acts as a negative feedback signal by blocking Ca²⁺ currents and reducing the sensitivity of the carotid body to hypoxia. Mice lacking the

D2 receptor secrete more catecholamines than the wild type, supporting the existence of such a negative feedback in carotid body type 1 cells (Prieto-Lloret *et al.*, 2007).

1.3.2 Acetylcholine (ACh)

ACh was proposed to be an excitatory neurotransmitter very early on in the study of carotid body (Von Euler, 1939). Type 1 cells have been shown to express the molecular machinery needed to synthesise, breakdown (Nurse & Fearon, 2002) and secrete ACh (via the ACh vesicular transporter) (Nurse & Zhang, 1999).

1.3.2.1 Effect of ACh on nerve endings

The nicotinic ACh receptors has been observed in rat PG neurons. The functional evidence for the existence of such a receptor came originally from patch-clamp studies in the somata of cultured PG neurons where ACh exerts an excitatory influence (Zhong & Nurse, 1997). This hypothesis is largely supported by other experiments using co-culture of type 1 cells and PG neurons (Zhong *et al.*, 1997; Zhang *et al.*, 2000) or intact carotid body-nerve preparation (Kholwadwala & Donnelly, 1992). Here, hypoxia induces a depolarisation of PG neurons. This can be mimicked by administration of ACh and is partially inhibited by the nicotinic receptor antagonists hexamethonium and mecamlamine. The partial inhibition obtained with nicotinic receptor blockers indicates that ACh is not the only neurotransmitter involved in excitation of PG neurons (Fitzgerald, 2000).

Introduction

1.3.2.2 Effect of ACh on type 1 cells

Anatomical studies using radioiodinated α -bungarotoxin, a specific ligand of the $\alpha 7$ subunit of the nicotinic receptors have revealed the $\alpha 7$ subunit expression in carotid type 1 cells (Chen *et al.*, 1981). Moreover, the action of ACh on type 1 cells, which induces a rise in $[Ca^{2+}]_i$, can be partially inhibited by nicotinic or muscarinic antagonists, suggesting the presence of the two receptors (Dasso *et al.*, 1997; Jiang & Eyzaguirre, 2004). Functionally, muscarinic receptors induce a rapid increase in $[Ca^{2+}]_i$ followed by a plateau phase. Experiments conducted in absence of extracellular Ca^{2+} show that the response depends on release of Ca^{2+} from the intracellular stores followed by Ca^{2+} influx (Dasso *et al.*, 1997). Furthermore, electrophysiological data in neonatal rat type 1 cells confirm the presence of nicotinic receptors in these cells and show that nicotinic agonists induce inward Ca^{2+} and Na^+ currents (Wyatt & Peers, 1993). In conclusion, ACh is thought to be involved in a positive feedback at the type 1 cells, as it increases $[Ca^{2+}]_i$ (Conde & Monteiro, 2006a).

1.3.3 ATP

ATP is believed to be an excitatory neurotransmitter at the carotid body type 1 cells. Indeed, studies carried out in cat (Obeso *et al.*, 1985), rat (Conde & Monteiro, 2006b) and rabbit (Verna *et al.*, 1990) show that a high amount of ATP is present in type 1 cells (Bock, 1980) and that this decreases after exposure to hypoxia. Using a bioluminescence assay to detect ATP, Buttigieg and Nurse have provided direct evidence that ATP is released during hypoxia by rat isolated carotid body, carotid body slice and type 1 cell (Buttigieg & Nurse, 2004). These observations have been confirmed by a second study in which the authors measured the amount of ATP released using an enzymatic probe combined with

Introduction

amperometry (Masson *et al.*, 2008). ATP was found to be released in response to high K^+ , normoxic hypercapnia and hypoxia. In addition, the cat carotid body possesses a high amount of ectonucleotidase which is a strong indication of extracellular ATP release (Starlinger, 1982).

1.3.3.1 Effect of ATP on nerve endings

Numerous experiments *in situ*, made mostly in cat, show that application of ATP induces a dose-dependent increase in action potential frequency in the CSN (McQueen & Ribeiro, 1986; Iturriaga & Alcayaga, 2004; Reyes *et al.*, 2007; Zapata, 2007). These results have been reproduced *in vitro* with a co-culture of rat type 1 cells and PG neurons. In this preparation, ATP and its analogue α,β -MeATP induce a fast and dose-dependent inward current in PG neurons (Zhang *et al.*, 2000). The kinetics of the response suggests that rat PG neurons express P2X₂/P2X₃ heteromultimers. Moreover, immunostaining (Zhang *et al.*, 2000; Rong *et al.*, 2003) and RT-PCR (Prasad *et al.*, 2001) performed on rat PG neurons confirm the expression of P2X₂ and P2X₃. The involvement of ATP as an excitatory neurotransmitter is confirmed by the use of its antagonists suramin or PPADS (pyridoxal-5'-phosphate-6-azophenyl-2',4'-disulphonic acid), which partially inhibit the response to hypoxia and to isohydric hypercapnia in mice (Rong *et al.*, 2003), cat (Reyes *et al.*, 2007) and in rat co-cultures of type 1 cells and PG neurons (Zhang *et al.*, 2000; Zhang & Nurse, 2004).

Mice deficient in P2X₂ receptors show a markedly attenuated ventilatory response to hypoxia, but not to hypercapnia (Rong *et al.*, 2003). In contrast, P2X₃-deficient mice show no difference in hypoxia and hypercapnia responses compared to the wild type (Rong

Introduction

et al., 2003). The double knock-out for P2X₂ and P2X₃ is highly lethal. In P2X₂ knock-out mice, the respiratory response to hypoxia is strongly attenuated; this suggests that P2X₂ is the receptor for ATP in hypoxia. The inhibitory effect of the deletion of P2X₂ on carotid body hypercapnia chemoreception is not visible in the knock-out mice. This can be explained by the fact that the CO₂ sensors in the brain sense hypercapnia and compensate the disfunctioning of the carotid body. In co-culture application of suramin and hexamethonium, antagonist of P2X and nicotinic receptor, respectively, blocks almost totally the activity of PG neurons, indicating that ACh and ATP are the two principal excitatory neurotransmitters in rat carotid body (Zhang *et al.*, 2000).

The ATP receptors, P2X₂, P2X₃, P2X₄ and P2X₇ have also been reported to be expressed in nitric oxide synthase (NOS) positive fibers present in the carotid body. These NOS positive fibers belong to neurons located along the glossopharyngeal nerve. Such neurons play a role as negative modulator of the type 1 cells via the release of nitric oxide. When the type 1 cells are activated they release ATP which induces the release of nitric oxide by the NOS positive fibers and inhibits the chemoreception (Campanucci *et al.*, 2006).

1.3.3.2 Effect of ATP on carotid body type 1 and 2 cells

The effect of ATP on carotid body type 1 and 2 cells were studied by Xu and al. (Xu *et al.*, 2003; Xu *et al.*, 2005). In type 1 cells, ATP inhibits the [Ca²⁺]_i increase induced by hypoxia. This inhibition is not linked to activation of TASK or to that of BK_{Ca} channels. Patch-clamp experiments reveal that ATP induces an increase in input resistance, due to the inhibition of voltage-dependent Ca²⁺ channels. Combined pharmacological and

Introduction

immunohistochemistry studies yielded to the conclusion that type 1 cells express P2Y₁ (Xu *et al.*, 2005). In type 2 cells, ATP triggers a release of Ca²⁺ from the internal stores, via P2Y₂. In conclusion, ATP exerts a negative feedback to the type 1 cells since it inhibits Ca²⁺ influx and serves as a paracrine signal between type 1 and type 2 cells in rat carotid body.

1.3.4 Adenosine

Adenosine is another molecule which is believed to play a role in carotid body chemotransduction. During hypoxia, the amount of adenosine in the synaptic cleft increases significantly due to a release from type 1 cells, through activation of the equilibrative adenosine transporters, and degradation of ATP by ectonucleotidase (Conde & Monteiro, 2004). Application of adenosine is known to increase CSN firing rate in both cat (Runold *et al.*, 1990) and rat (Monteiro & Ribeiro, 1987). This effect has been reported to be mediated by the adenosine 2A receptors present on the nerve ending (Conde *et al.*, 2006b). Adenosine A1 receptors have also been shown to be expressed in PG neurons by *in situ* hybridization but their physiological role is unknown (Gauda *et al.*, 2000). On type 1 cells, which express adenosine 2A and 2B receptors (Conde *et al.*, 2006b; Xu *et al.*, 2006), the action of adenosine was reported to be excitatory. Excitation mediated by the closure of TASK channels which underlines the effect of hypoxia (Xu *et al.*, 2006). In contrast, Kobayashi *et al.* have observed, in type 1 cells, an inhibition of voltage-dependent Ca²⁺ channels induced by adenosine and therefore a reduction of the effect of hypoxia (Kobayashi *et al.*, 2000).

1.3.5 Histamine

Following the observations that systemic injection of histamine H1 and H3 receptor agonists increases the burst frequency of respiratory neurons in mice (Dutschmann *et al.*, 2003), the putative role of histamine in the carotid body has been investigated. RT-PCR and immunohistochemistry studies show that histidine decarboxylase, the main enzyme responsible for histamine synthesis, is expressed in type 1 cells (Koerner *et al.*, 2004). Moreover, the mRNA for histaminergic receptors, H1, H2, H3 and H4, have been amplified in carotid body although only H1 and H3 can be localized by immunohistochemistry in type 1 cells, and nerve endings (Koerner *et al.*, 2004; Lazarov *et al.*, 2006). In contrast, the only study available on the effect of histamine application in carotid body reveals an increase in cAMP, which suggests the involvement of H2-type receptors (Mir *et al.*, 1983). Furthermore, application of H1 and H3 agonists in carotid body induces a small increase in phrenic nerve activity (Lazarov *et al.*, 2006). In conclusion, as H3 is an autoreceptor which has the ability to modulate release of histamine and of other neurotransmitters, and as histamine has a little effect on nerve activity, histamine probably acts as a modulator of type 1 cells secretion and nerve endings activity rather than being involved as primary excitatory neurotransmitter.

1.3.6 Gamma-aminobutyric acid

Gamma-aminobutyric acid (GABA) and the enzyme glutamate decarboxylase are expressed in mouse type 1 cells as shown by immunostaining (Oomori *et al.*, 1994). In the rat carotid body, the activation of the GABA_B receptors, present on type 1 cells, leads to activation of the G_i protein which inhibits the protein kinase A and activates TASK channels (Fearon *et al.*, 2003). The activation of TASK channels tends to hyperpolarise the

Introduction

type 1 cells and acts as an inhibitory influence on chemoreception. Thus, GABA participates in a negative feedback on the chemoreception.

In summary, the activation of type 1 cells by its natural stimuli, hypoxia, hypercapnia or pH, induce a release of two principal excitatory neurotransmitters, ACh, ATP. In addition, other neurotransmitters are secreted such as catecholamines, adenosine, histamine which modulates both the effects of the principal neurotransmitters on PG nerve endings and on the type 1 cells themselves, stimulating or inhibiting their chemosensitivity (Fig. 1.11). The affinities of the neurotransmitters with their pre- and post-synaptic receptors could be affected by the spermine released in the synaptical cleft. However, these putative interactions are not investigated in this study.

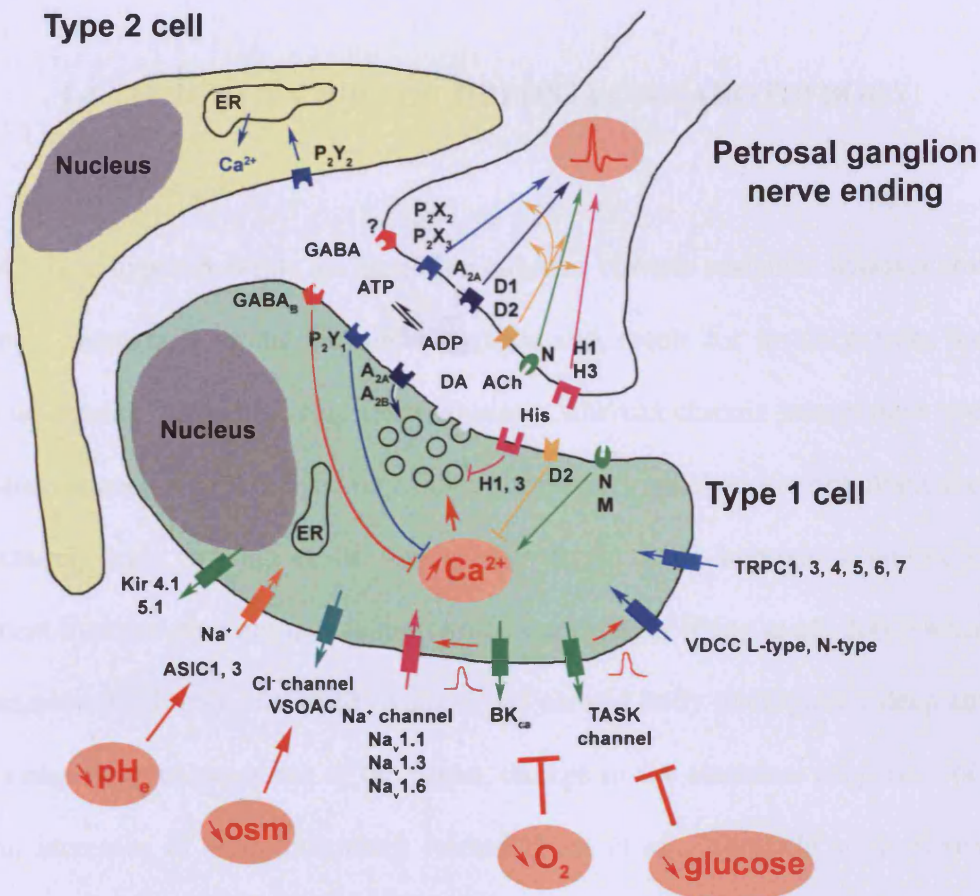


Figure 1.11: Schematic representation of carotid body and the effect of neurotransmitters in rat. The type 1 cell, in green, is the chemosensitive cell of the carotid body and possesses specific mechanisms for sensing pO₂, pCO₂, extracellular pH, osmolarity and glucose. It expresses K⁺ channels sensitive to pO₂, (BK_{Ca} and TASK-like), acid sensing ion channels (ASIC1 and 3) sensing changes in extracellular pH (pH_e) and Cl⁻ channels (VSOAC) sensing changes in osmolarity (osm). In addition, type 1 cells express inward rectifier K⁺ channels (Kir 4.1 and 5.1) and the transient receptor potential channels (TRPC1 and 3-7). Depending on the type of stimulus, the activation of ASIC or Cl⁻ channels or the closure of BK_{Ca} and TASK-like channels, induces a depolarisation, which activates both Na⁺ channels (Na_v 1.1, 1.3 and 1.6) and voltage-dependent Ca²⁺ channels (VDCC). This leads to an increase in [Ca²⁺]_i, which triggers the release of the neurotransmitters ATP, ADP, dopamine (DA), acetylcholine (ACh), GABA and histamine (His). ADP present in the synaptic cleft comes from a release by type 1 cells and the degradation of ATP into ADP. The neurotransmitters activate their specific receptors and mediate the action indicated by the arrows. Nicotinic receptor (N), muscarinic receptor (M), ADP receptors A_{2A} and A_{2B}, ATP receptors P₂X₂, P₂X₃, P₂Y₁ and P₂Y₂, histaminergic receptors H₁ and H₂, dopamine receptor D₁ and D₂ and endoplasmic reticulum (ER). From the references cited in the text and Carpenter & Peers, 1997; Caceres *et al.*, 2007.

1.4 EFFECT OF CHRONIC HYPOXIA ON CAROTID BODY

Chronic hypoxic events are classified either as chronic sustained hypoxia or chronic intermittent hypoxia. Chronic sustained hypoxia can result for instance from ascent in altitude or chronic obstructive respiratory disease, whereas chronic intermittent hypoxia is due to sleep apnoea. Chronic hypoxia can induce physiological and morphological changes in the carotid body, leading to its sensitisation to an acute hypoxic stimulus. Chronic intermittent hypoxia does not induce morphological changes (Peng *et al.*, 2003) whereas, as a consequence of chronic sustained hypoxia, the carotid body undergoes a deep structural change comprising enlargement of the organ, change in the electrical properties of type 1 cells and increases in neurotransmitter release (Lam *et al.*, 2008). In some severe case, chronic sustained hypoxia induces carotid body tumour (Knight *et al.*, 2006). Both forms of chronic hypoxia are important for human health but this section mainly reviews the modifications induced by chronic sustained hypoxia, as it produces the strongest adaptive effects on the carotid body.

1.4.1 Effect of chronic intermittent hypoxia

Chronic intermittent hypoxia induces a sensitisation of the chemosensitivity in the carotid body (Pawar *et al.*, 2008) and a long-term facilitation which corresponds to a lasting increase in baseline activity after a stimulus (Olson *et al.*, 2001; Peng *et al.*, 2003; Peng & Prabhakar, 2004). In contrast, in chronic sustained hypoxia, the carotid body becomes more sensitive but without long-term facilitation (Olson *et al.*, 2001) and increase of size (Pawar *et al.*, 2008). The long-term facilitation is triggered by the increase in

Introduction

reactive oxygen species (Peng *et al.*, 2003). This long-term facilitation has very important clinical implication as it leads to a constant stimulation of the sympathetic nervous system activity. The latter activates the heart and increases the blood vessel resistance leading to a systemic hypertension (Lai *et al.*, 2006).

1.4.2 Effect of chronic sustained hypoxia

1.4.2.1 Morphological changes of the carotid body

Under chronic sustained hypoxia, the carotid body undergoes morphological changes, including enlargement of the organ, hyperplasia of type 1 cells, and neovascularisation. In chronic sustained hypoxia, the carotid body grows several fold, with an increase in the number and size of type 1 cells (McGregor *et al.*, 1984). The origin of the new type 1 cells is controversial, it is not yet clear if the new type 1 cells come from the division of pre-existent ones (Wang *et al.*, 2008) or from the differentiation of the type 2 cells (Pardal *et al.*, 2007). In addition to the increase in type 1 cell number, the glomerular organisation is altered. The cluster size decreases, which increases the contact areas between the cells and blood vessels. Coincident with this cluster modification, the vascularisation increases in the carotid body (Gonzalez *et al.*, 1994) due to the activation of vascular endothelial growth factor (VEGF) regulated by HIF (Prabhakar & Jacono, 2005). In contrast to the type 1 cells, the type 2 cells become more numerous without change of size.

Introduction

1.4.2.2 Electrical changes in the type 1 cell

In chronic sustained hypoxia, the type 1 cells become more excitable as a result of the modification of ion channel expression. Experimentally, as chronic hypoxia induces an increase in type 1 cell volume, the amplitude of the currents recorded by patch-clamp appears greater (Hempleman, 1996). Therefore, the comparative evolution of ion channel expression is made by comparing the density of the currents rather than their amplitudes (Hempleman, 1996; Carpenter *et al.*, 1998). The oxygen sensing K^+ channels, BK_{Ca} do not seem to be involved in this sensitisation which, appears to be largely due to a decrease in expression of Ca^{2+} -insensitive voltage gated K^+ currents (Carpenter *et al.*, 1998) facilitating the depolarisation of the cell. In addition, Nox4, which is associated to TASK channels, is up regulated by chronic hypoxia which may provide a greater sensitivity of TASK channels to hypoxia (Gonzalez *et al.*, 2007). More conflicting results are available for the voltage-dependent Ca^{2+} channels, Hempleman reported an increase of a non L-type channel expression (Hempleman, 1996) whereas Carpentier *et al.* showed no modification of the voltage-dependent Ca^{2+} channels (Carpenter *et al.*, 1998). Finally, Na^+ channels appear to be up regulated as a consequence of chronic hypoxia in rat carotid body (Stea *et al.*, 1992; Hempleman, 1995; Caceres *et al.*, 2007).

These adaptive changes to chronic sustained hypoxia make the type 1 cells more excitable as a consequence of the suppression of hyperpolarising K^+ currents and the increase in depolarising Na^+ currents. Moreover, the neurotransmitter release might be strengthened by a larger voltage-dependent Ca^{2+} influx during hypoxia.

Introduction

1.4.2.3 Change in neurotransmitter release

In chronic sustained hypoxia, the neurotransmitter metabolism is altered. Indeed, tyrosine hydroxylase gene expression is up regulated (Czyzyk-Krzeska *et al.*, 1992a) and the catecholamine turnover is increased (Gonzalez-Guerrero *et al.*, 1993). In addition, new neurotransmitters have been shown to be recruited such as endothelin 1 (Prabhakar & Jacono, 2005). Endothelin 1 is the principal neurotransmitters explaining the sensitisation of the carotid body in response to chronic sustained hypoxia. Chronic sustained hypoxia induces an increase in expression of endothelin 1 and its receptor ET_A in type 1 cells. Endothelin 1 potentiates the response to hypoxia as the activation of the receptor ET_A leads to an increase in Ca²⁺ influx via an increase in cyclic AMP (Chen *et al.*, 2000; Chen *et al.*, 2002).

1.4.3 Role of HIF-1 α , -2 α and -3 α in chronic and sustained hypoxia

HIF-1 α , -2 α and -3 α have been shown to be involved in the regulation of gene transcription in response to chronic hypoxia, for instance of tyrosine hydroxylase (Norris & Millhorn, 1995; Lam *et al.*, 2008). HIF-1 α , -2 α and -3 α are constantly synthesised by the cells and are degraded keeping the level of HIF low. Hypoxia, via AMP kinase activation and production of reactive oxygen species (Leff, 2003; Guzy & Schumacker, 2006; Wyatt & Evans, 2007), prevents proteasomal degradation of HIF-1 α , -2 α and -3 α which, then, translocate to the nucleus where they activate gene transcription by binding to specific promoter sequences (Tanimoto *et al.*, 2000). The responses to chronic intermittent and sustained hypoxia involve different subtypes of HIF. Indeed, chronic intermittent hypoxia induces an increase in HIF-2 α and -3 α whereas chronic sustained hypoxia induces an

Introduction

increase in all the HIF subtypes, HIF-1 α , -2 α and -3 α (Semenza, 2004; Lam *et al.*, 2006). These data are supported by the fact that rat carotid body constitutively express HIF-2 α and -3 α (Lam *et al.*, 2006). These specific HIF subtypes regulation are correlated with the expression profile of the targeted genes involved in the carotid body response to hypoxia. HIF-2 α and -3 α trigger the expression of endothelin-1 and tyrosine hydroxylase and HIF-1 α induces the expression of the vascular endothelial growth factor (Lam *et al.*, 2008). In addition, Peng *et al.*, using mice partially deficient for HIF-1 α , found an important role of HIF-1 α for mediation by the carotid body of the systemic response to chronic intermittent hypoxia (Peng *et al.*, 2006). Indeed, in knocked-out mice for HIF-1 α , the characteristic responses induced by chronic intermittent hypoxia, long term facilitation, increase in blood pressure and increased hypoxic ventilatory response are non-existent or attenuated.

1.5 POLYAMINES

The polyamines spermine, spermidine and putrescine are low molecular weight organic molecules which are positively charged at physiological pH. Polyamines are involved in many physiological and pathological processes such as cell growth, differentiation, responses to hypoxia, modulation of ions channels (from inside and outside the cell) and modulation of mitochondrial function (Lapidus & Sokolove, 1993).

1.5.1 Synthesis of polyamines

Polyamines are produced in every cell type by the conversion of ornithine into putrescine by ornithine decarboxylase in the mitochondria, followed by the actions of

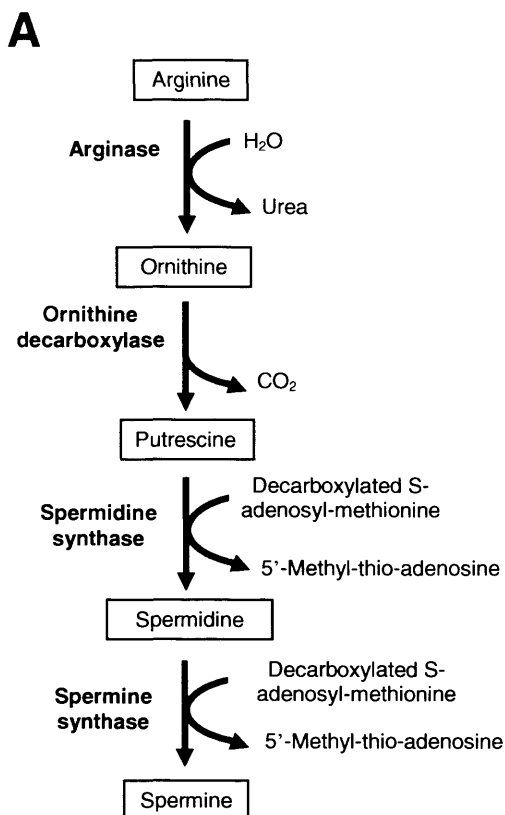
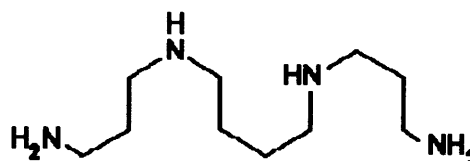


Figure 1.12: Scheme of polyamine synthesis.

A) Polyamines, putrescine, spermidine and spermine are synthesised from arginine adapted from Heby, 1986. B) Structure of the spermine, adapted from Seiler *et al.*, 1996.

B



Introduction

spermidine and spermine synthase to produce, consecutively, spermidine and spermine (Fig. 1.12). The ornithine decarboxylase has a short half life of about 5-15 min allowing for rapid control of the cellular level of the enzyme and, therefore, for regulation of the production of polyamines (Heby, 1986). In addition, all cells possess an uptake system for polyamines which is dependent upon the proteoglycan (such as heparan sulphate) expressed on the cell surface (Belting *et al.*, 2003). In complement to endogenous production, polyamines also come from food. Most of the polyamines present in the blood are stored in lymphocytes, granulocytes and erythrocytes, giving an estimated blood concentration of spermine of about 6 μM (Cohen *et al.*, 1976). In contrast, the plasma concentration of spermine is probably below 0.5 μM (Chaisiri *et al.*, 1979). However, the level of polyamines can increase locally, for instance during tumorigenesis and development (Chaisiri *et al.*, 1979). The intracellular concentration of polyamines has been estimated to be about 0.4 mM for spermine and 0.2 mM for spermidine in intestinal smooth muscle (Sward *et al.*, 1994). However, it is likely thought that polyamines are bound to cellular macromolecules such as DNA and RNA, which would decrease the free intracellular concentration to the μM range (Watanabe *et al.*, 1991). Polyamines are also present in synaptic vesicles where their concentrations may be as high as 2 mM (Masuko *et al.*, 2003).

1.5.2 Regulation of polyamine levels

As a consequence of hypoxia, polyamine metabolism and levels have been reported to be increased in the brain (Longo & Packianathan, 1995), lung (Babal *et al.*, 2002) and heart (Tantini *et al.*, 2006). These changes in polyamine levels are only local and it has never been shown that the plasma concentration can be affected by hypoxia. In the brain,

Introduction

where polyamines are normally secreted by neurons (Fage *et al.*, 1992) and astrocytes (Laube & Veh, 1997), the increase in polyamine content, as a consequence of hypoxia, may be neuroprotective (Clarkson *et al.*, 2004). In the lung, polyamines regulate the response of pulmonary vascular smooth muscle cells to hypoxia. Hypoxia induces a decrease in the activity of ornithine decarboxylase and an increase in polyamine uptake (Babal *et al.*, 2002). In the heart, spermine has a protective effect and prevents apoptosis after ischemia (Zhao *et al.*, 2007). The protective effect of spermine in hypoxia is linked, in part, to its oxidant property, since polyamines act as free radical scavengers (Muscari *et al.*, 1995). Moreover, polyamines have the property to alter the chromatin structure and to protect DNA against breakdown by reactive oxygen (Ha *et al.*, 1998).

1.5.3 Polyamines in the carotid body

Very little is known about polyamines in the carotid body and no study has been conducted which investigates their levels during hypoxia. The only data available come from Ganformina *et al.*, who reported a down regulation of the transcription of ornithine decarboxylase in chronic hypoxia (24h at 10 % pO₂) (Ganformina *et al.*, 2005). By analogy to other tissues, it can be hypothesised that such decrease in polyamine synthesis due to the down regulation of ornithine decarboxylase, in chronic hypoxia in carotid body, will induce an increase in polyamine uptake to maintain the intracellular level of polyamines (Seiler *et al.*, 1996; Babal *et al.*, 2002). Moreover, spermine could be involved in the remodelling of the carotid body during chronic hypoxia since spermine regulates cell growth and differentiation (Heby, 1986). Furthermore, as spermine is co-packaged with neurotransmitters in vesicles of neurons and is excreted with them (Fage *et al.*, 1992; Masuko *et al.*, 2003), spermine levels within the type 1 cell vicinity may increase during

Introduction

carotid body stimulation. Extracellular spermine inhibits voltage-dependent Ca^{2+} channels (Chen *et al.*, 2007), TASK channels (Musset *et al.*, 2006) and activates the CaR (Quinn *et al.*, 1997) and, therefore, could play a role in carotid body chemoreception.

1.6 THE EXTRACELLULAR CALCIUM-SENSING RECEPTOR

1.6.1 Structure of the extracellular calcium-sensing receptor (CaR)

The CaR, originally cloned from bovine parathyroid gland (Brown *et al.*, 1993), belongs to the G protein coupled receptor super family (GPCR). The amino acid sequence of CaR is well conserved across species, with the sequences for human, rat and rabbit receptor being more than 90 % identical to that of bovine CaR (Bai, 2004).

As with other GPCRs, the CaR has three major structural domains: a large extracellular amino (N)-terminal domain (612 amino acids); a central core containing 7-transmembrane domains and a hydrophilic intracellular domain (fig. 1.13). The extracellular domain possesses 11 N-linked glycosylation sites and is responsible, with the TM7 (Hu *et al.*, 2005), for the interaction with extracellular Ca^{2+} . The extracellular domain forms a so-called Venus flytrap in which the Ca^{2+} interacts directly with 5 residues (S¹⁷⁰, D¹⁹⁰, Q¹⁹³, S²⁹⁶ and E²⁹⁷) and 3 others (Y²¹⁸, F²⁷⁰ and S¹⁴⁷) coordinate the interaction (Silve *et al.*, 2005; Hu & Spiegel, 2007). When Ca^{2+} interacts with the CaR, it stabilizes the Venus flytrap in the closed configuration (Hu & Spiegel, 2007).

To be functional, the CaR has to be present in a homodimeric form (Bai *et al.*, 1998) or heterodimeric form with the type B gamma aminobutyric acid receptor (Chang *et al.*, 2007; Cheng *et al.*, 2007). In the homodimeric form, the two CaR molecules are held together via both covalent (disulphide link) and non-covalent interactions (Bai *et al.*, 1998).

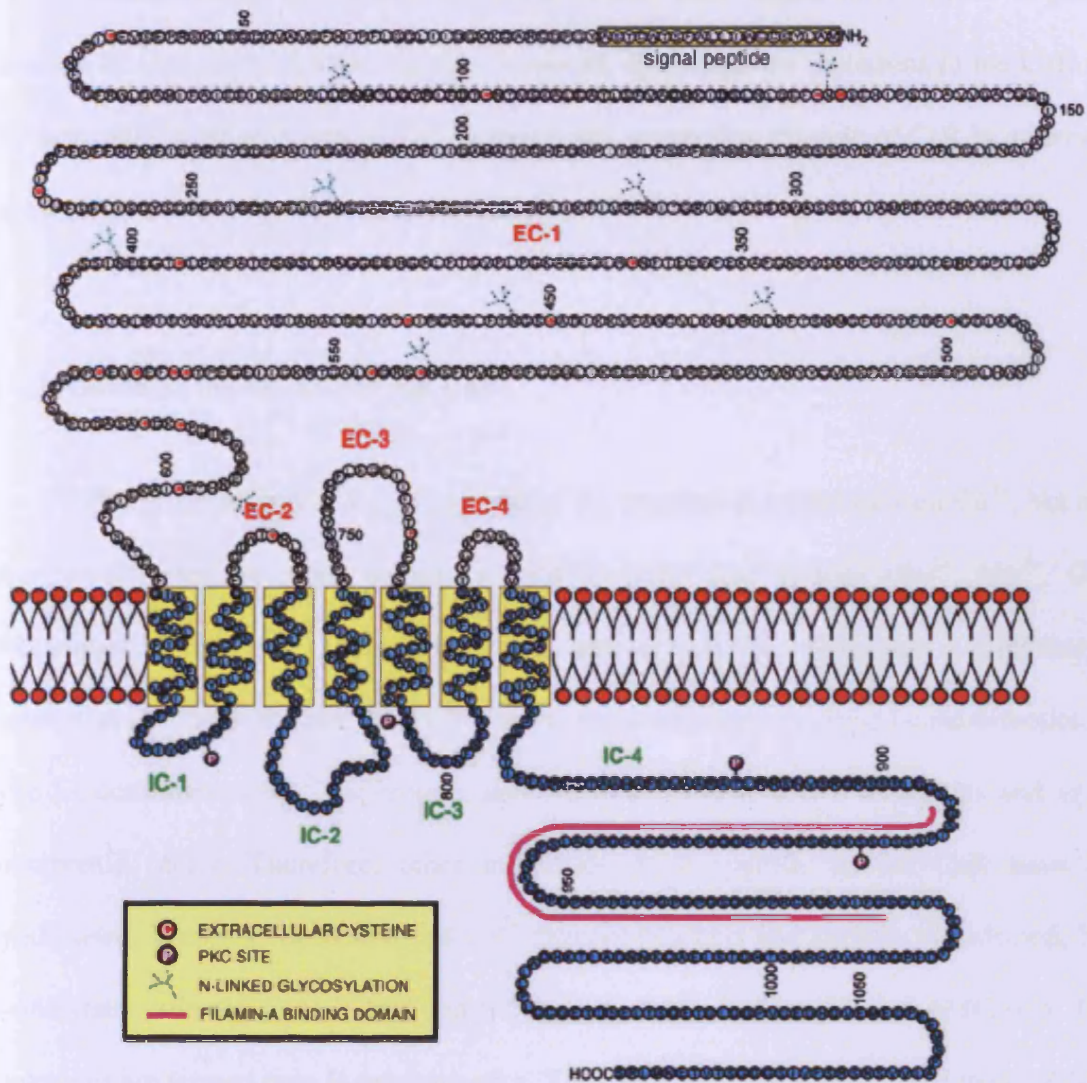


Figure 1.13: Predicted structure of the CaR. EC-1 N-terminal extracellular domain; EC-2-4, extracellular loops 2-4; IC-1-3, intracellular loops; IC-4, C-terminal tail. P indicates the putative consensus sites for protein kinase C (PKC) phosphorylation. Yellow boxes enclose the seven transmembrane regions. From Chang *et al.*, 2004.

Introduction

Genetic studies on inherited mutations in CaR gene, which induce a loss- or gain- of function of CaR, and a knock-out murine model, show that the mutations in the CaR gene are associated with problems in Ca²⁺ homeostasis, supporting the role of CaR in mineral ion metabolism due to impaired hormonal secretion (Thakker, 2004).

1.6.2 Allosteric modulators of the CaR

The principal physiological agonist of the receptor is serum ionised Ca²⁺, but it can also be activated by other molecules such as polyvalent cations (Ba²⁺, Mg²⁺, Gd³⁺), polyamines (spermine, spermidine) and aminoglycoside antibiotics (streptomycin, neomycin) (Urena & Frazao, 2003). Together, these are known as type I calcimimetics. The type I calcimimetics (Ca²⁺, spermine, neomycin) are non selective molecules and so lack therapeutic utility. Therefore, other molecules more specific to the CaR have been synthesised. These are derivatives of Ca²⁺ channel blockers and include NPS-R-568, NPS-S-568 (later referred to as R-568 and S-568, Fig. 1.14), NPS-1377 and AMG-073. These molecules are termed type II calcimimetics. They modulate the activation of the CaR by the class I calcimimetics by increasing the affinity of the CaR for its natural ligands. Thus, the class II calcimimetics act like allosteric modulators as they do not activate the receptor in the absence of extracellular Ca²⁺ and bind to the CaR in a different place from the class I calcimimetics (Petrel *et al.*, 2004).

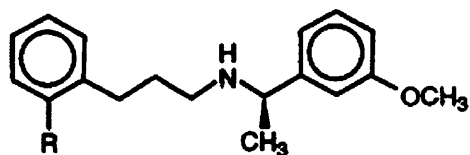


Figure 1.14: Structure of the calcimimetics R-568 and S-568, from Nemeth, 2004

R = H: NPS 467
R = Cl: NPS 568

Class II calcimimetics are derived from fendilines and other drugs which block voltage-dependent Ca^{2+} channels and were shown to have non-specific effect at high concentrations, > 100 nM (Nemeth, 2004). Nevertheless, when used at the appropriate concentrations (< 100 nM), they constitute a good tool for investigating the activity of the CaR. R-568 and S-568 have a stereoselective effect on the CaR, with R-568 being 100 times more potent than the S enantiomer (Nemeth *et al.*, 1996). This stereoselectivity is important as it allows investigators to distinguish between specific and non-specific effects on the CaR. Indeed, the blocking effects of 568 compounds on ion channels (voltage-dependent Ca^{2+} channels, NMDA) are not stereoselective (Nemeth, 2004) and of relatively low affinity.

The activity of the CaR can also be modulated by extracellular pH by modifying the charge on acidic and basic amino acids present in the CaR. In alkaline conditions, the receptor is more sensitive to its agonists, making the CaR a potential pH sensor (Quinn *et al.*, 2004). In addition to the actions on the receptor, the pH can affect protonation of certain agonist such as polyamines (Heby, 1986).

Similarly to pH, ionic strength modulates the CaR activity by modulating electrostatic interactions between the receptor and its agonists. As the ionic strength decreases, the CaR becomes more sensitive to its agonists (Quinn *et al.*, 1998).

1.6.3 Signal transduction pathways of the CaR

The human CaR possesses several putative sites for phosphorylation by protein kinases C and A and activation of the receptor is coupled to the G proteins G_i , G_{q11} and $G_{12/13}$ (Fig. 1.15) (Gomez *et al.*, 1996; Huang & Miller, 2007). Activation of these G proteins induces a decrease in cAMP (G_{ai}) and an activation of phospholipase C (by G_{q11}) to produce inositol tris-phosphate (IP_3) and 1,2 diacylglycerol generation. IP_3 induces release of Ca^{2+} from intracellular Ca^{2+} - IP_3 -sensitive stores. Activation of the protein $G_{12/13}$ stimulates the Rho pathway and induces changes in actin stress fibre assembly (Davies *et al.*, 2006). Furthermore, the receptor can activate cytosolic phospholipase A_2 , phosphatidylinositol 3-kinase and phosphatidylinositol 4 kinase (Ward, 2004). Thus, activation of the receptor leads to the activation of MAP kinases, including p38 MAP kinase, jun amino terminal kinase and extracellular signal regulated protein kinase.

1.6.4 Role of CaR in the regulation of secretion

The CaR was discovered and first studied in the parathyroid glands (Brown *et al.*, 1993) where it regulates the release of parathyroid hormone (PTH), a hormone responsible for the body's Ca^{2+} homeostasis (Nemeth & Scarpa, 1987; Muff *et al.*, 1988). In the parathyroid gland, the CaR plays a role in PTH secretion and gene regulation (Garrett *et al.*, 1995) and its signal transduction pathways are now well known (Randolph & G., 2004). Studies have shown that, in addition to the parathyroid, CaR is also expressed in many cells which are not directly implicated in whole body Ca^{2+} homeostasis. CaR plays a role in regulation of secretion in the thyroid gland (calcitonin and serotonin

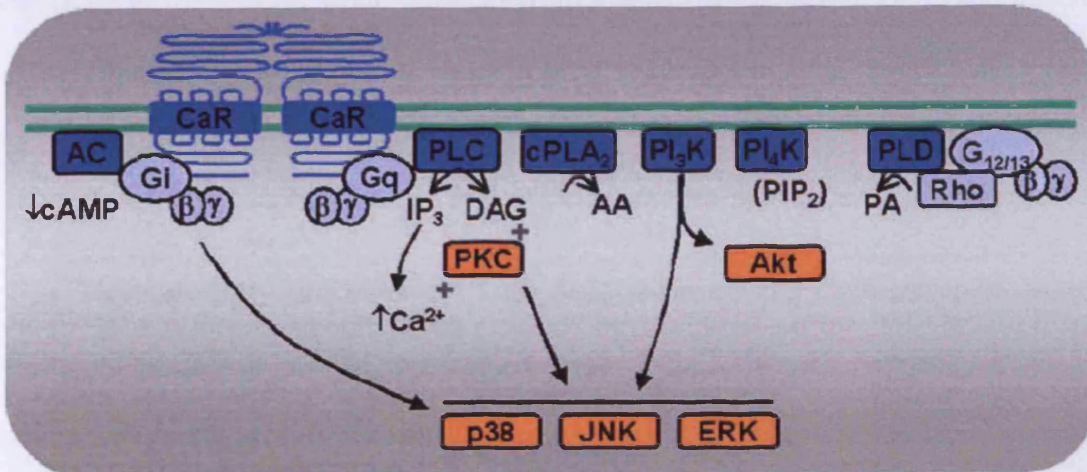


Figure 1.15: Summary of the intracellular pathways activated by the CaR. Activation of the CaR leads to activation of i) G_i which, modulates adenylate cyclase (AC); ii) G_q , which activates phospholipase C (PLC) producing inositol tri-phosphate (IP_3) and 1,2 diacylglycerol (DAG); iii) phospholipase A_2 (cPLA₂), producing arachidonic acid (AA); iv) phosphatidylinositol 3 kinase (PI₃ K) mediating Akt (protein kinase B) activation; vi) protein kinase C (PKC); vii) phosphatidylinositol 4 kinase (PI₄ K) leading to production of phosphatidylinositol 4,5 bisphosphate (PIP₂); viii) MAP kinase including p38 kinase (p38), jun amino-terminal kinase (JNK) and extracellular signal regulated protein kinase (ERK) and ix) $G_{12/13}$ mediated phospholipase D (PLD) activation, leading to phosphatidic acid (PA) production. From Ward, 2004.

(McGehee *et al.*, 1997)), the pituitary gland (adreno corticotropic hormone (ACTH) (Emanuel *et al.*, 1996) and growth hormone (Romoli *et al.*, 1999)), the stomach (gastrin (Ray *et al.*, 1997)) and the pancreas (insulin (Kato *et al.*, 1997)). Except for calcitonin secretion where the activation of the CaR leads to opening of voltage-dependent Ca^{2+} channels, the modulation of hormonal secretion is mediated by mobilization of Ca^{2+} from the internal stores via second messengers. The activation of CaR may induce an increase or a decrease of the secretion in a cell specific manner. In the majority of tissues, an increase in $[Ca^{2+}]_i$ stimulates secretion, as occurs in pituitary (Emanuel *et al.*, 1996; Romoli *et al.*, 1999), thyroid (McGehee *et al.*, 1997), gastric G cells ((Ray *et al.*, 1997) and pancreatic β -

Introduction

cells (Kato *et al.*, 1997)), while in parathyroid glands (Brown *et al.*, 1991) and pancreatic α -cells (Efendic *et al.*, 1982) an increase in $[Ca^{2+}]_i$ leads to an inhibition of tonic secretion. The mechanism of the latter is still not understood.

Most secretory processes (in both neurosecretion and chemoreceptor secretion) involve an increase in $[Ca^{2+}]_i$ via voltage-dependent Ca^{2+} channels (Gonzalez *et al.*, 1994; Catterall *et al.*, 2003). L-type channels are the main contributor and, in some cases, P/Q-type contributes weakly (Rocher *et al.*, 2005). An increase in $[Ca^{2+}]_i$ mediates the secretory stimulus for the release of neurotransmitters in the carotid body (Obeso *et al.*, 1992), ACTH secretion (Hockings *et al.*, 1991; Loechner *et al.*, 1999) and growth hormone from the pituitary (Drouva *et al.*, 1988) and serotonin secretion from the thyroid (McGehee *et al.*, 1997) and neuroepithelial bodies (Fu *et al.*, 2002). In parafollicular cells of the thyroid gland, activation of CaR induces an increase in $[Ca^{2+}]_i$ which evokes release of serotonin and calcitonin (McGehee *et al.*, 1997). In these cells, it appears clearly that activation of CaR is coupled to Ca^{2+} influx since the L-type channel blocker, nimodipine, prevents both the rise in $[Ca^{2+}]_i$ and the secretion induced by CaR (McGehee *et al.*, 1997). McGehee *et al.* have demonstrated that activation of CaR activates protein kinase C which opens a non selective cation channel which depolarises the cells and open L-type Ca^{2+} channels, leading to Ca^{2+} influx and hormone release (McGehee *et al.*, 1997).

1.6.5 Ion channel regulation by the CaR

As described above, the CaR plays an important role in the regulation of secretion in many cell types. By their nature, secretory cells are excitable and the secretory processes depend mostly on changes in transmembrane potential and opening of voltage-dependent

Introduction

Ca²⁺ channels (Randolph & G., 2004; Conde *et al.*, 2006a). The CaR regulates [Ca²⁺]_i and secretion by mobilising Ca²⁺ from the internal stores or/and by altering the Ca²⁺ influx via direct or indirect modulation of ion channels. This paragraph aims at reviewing the modulation of ion channels by the CaR.

The inward rectifier K⁺ channels, Kir4.1 and Kir4.2, have been co-immunoprecipitated with the CaR from rat kidney samples, suggesting a direct interaction between the proteins (Huang *et al.*, 2007). In this organ, Kir4.1 and Kir4.2 are negatively modulated by the activation of CaR. The CaR modulates other channels, listed below, via intracellular transduction pathways:

i) The transient receptor potential channel 1 (TRPC1). TRPC1 has been shown to be alternatively activated by the CaR and inhibited by the rise in [Ca²⁺]_i induced by activation of the CaR (via the protein kinase C) (Rey *et al.*, 2006). This alternative activation and inhibition of TRCP1, induced by activation of CaR, produces [Ca²⁺]_i oscillation.

ii) A Ca²⁺ activated K⁺ channel, present in astrocytes and activated by CaR via p38 MAP kinase (Ye *et al.*, 2004).

iii) A voltage independent cation current in parathyroid cells where the channel is regulated by protein kinase A. In these cells, CaR activation reduces the amount of cAMP, resulting in down regulation of protein kinase A (Chang *et al.*, 1998).

iv) Non selective cation channels have been reported in many cell types to be activated by the CaR. For instance, in thyroid cells, non selective cation channels transiently open via CaR dependent activation of protein kinase C (McGehee *et al.*, 1997) (Liu *et al.*, 2000). In addition, in rat hippocampal neurons and HEK293 cells, the CaR has a direct functional interaction with selective cation channels (Ye *et al.*, 1996a; Ye *et al.*,

Introduction

1996b), whilst breast cancer cells also express selective cation channels which are regulated by CaR via activation of the phospholipase C (El Hiani *et al.*, 2006).

The CaR, by modulating the Ca²⁺ homeostasy via the regulation of ion channels or the release of Ca²⁺ from the intracellular stores, has been shown to modulate secretion in many cell types. In the carotid body, if the CaR is expressed, its activation by spermine could lead to a release of Ca²⁺ from the intracellular stores and modulate neurotransmitter release.

1.7 CALCIUM CHANNELS

1.7.1 Channels mediating Ca^{2+} current

Several channels expressed on the plasma membrane are able to mediate a Ca^{2+} influx, some of them have a specific conductance to Ca^{2+} whereas others are permeable to several cations. These channels can be classified by their opening modality: i) voltage-gated channels: voltage-dependent Ca^{2+} channels ii) ligand-gated channels, such as ATP receptor, P2X receptor (conveying Na^+ , K^+ , Ca^{2+} current); and nicotinic acetylcholine receptor (permeable to Na^+ , Ca^{2+}); iii) acid sensing ion channels (permeable to Na^+ , K^+ , Ca^{2+}); and iv) the channels belonging to the transient receptor potential family which are mostly activated by $\text{G}_{q/11}$ (Alexander *et al.*, 2006).

1.7.2 Structure and family of voltage-dependent Ca^{2+} channels

The voltage-dependent Ca^{2+} channels are a complex association of four or five proteins: one central conducting subunit (α_1) and several auxiliary regulating subunits (α_2 , β , γ , δ ; Fig. 1.16). Ten channels have been identified based on the genetic diversity of the pore-forming subunit α_1 (Doering & Zamponi, 2003). The genetic distinction of the voltage-dependent Ca^{2+} channels gave rise to the old nomenclature $\alpha_1\text{X}$ and the new one $\text{Ca}_v\text{X.X}$ (table 1.1). The α_1 subunit is made of 4 homologous domains constituting 6 transmembrane segments (S1-S6). The S4 segment plays a role as a voltage sensor. The specific selectivity to Ca^{2+} is due to the pore loops between the segment S5 and S6.

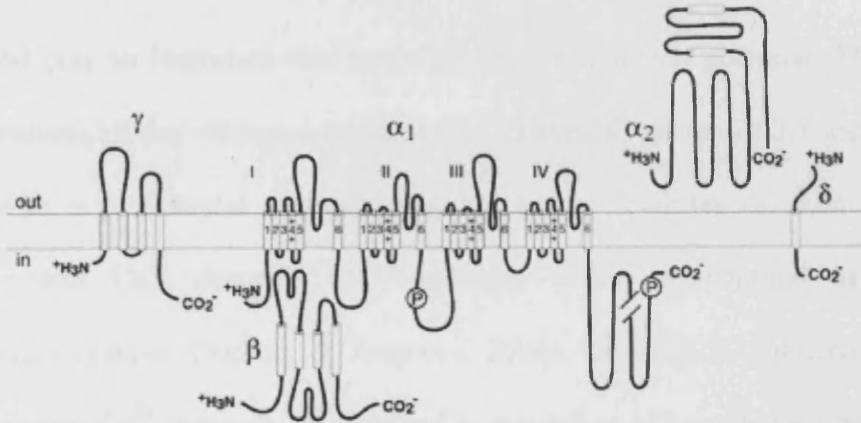


Figure 1.16: Schematic representation of the voltage-dependent Ca^{2+} channel subunits. From Catterall *et al.*, 2003.

According to their electrophysiological and pharmacological properties, voltage-dependent Ca^{2+} channels can be divided in two main groups: high voltage activated (HVA, activated near -50 mV) and low voltage activated (LVA, activated near -70 mV) (Perez-Reyes, 2003). In addition to their different activation potentials, LVA currents deactivate more slowly and at a lower potentials leading to slower tail current (Perez-Reyes, 2003). The HVA group comprises the family L-, N-, P/Q- and R-type channels whereas LVA includes only T-type channels (table 1.1).

1.7.3 Expression and role of voltage-dependent Ca^{2+} channels

Each family is expressed in specific cell types where it plays a particular function. $\text{Ca}_v1.1$ is expressed only in the muscle where it has a crucial role in the excitation contraction coupling (Altafaj *et al.*, 2005). $\text{Ca}_v1.4$ is present exclusively in the retina, in rod and bipolar cells, where its activation triggers neurotransmitter release (Catterall *et al.*, 2003). All the other voltage-dependent Ca^{2+} channels are widely expressed and are found in

Introduction

several cell types. For instance $\text{Ca}_v1.2$, $\text{Ca}_v3.1$ and $\text{Ca}_v3.2$ are expressed in cardiac myocytes and play an important role in the generation of action potential (Maltsev *et al.*, 2006). In neurons, all the voltage-dependent Ca^{2+} channels (except $\text{Ca}_v1.1$ and $\text{Ca}_v1.4$) are expressed with a preferential expression in the soma, dendrites or axon. In neurons, voltage-dependent Ca^{2+} channels are implicated either in neuronal excitability or neurotransmitter release (Doering & Zamponi, 2003). In addition, similarly to neurons, voltage-dependent Ca^{2+} channels are involved in regulation of secretion in endocrine cells. For instance, in adrenal chromaffin cells, $\text{Ca}_v1.2$ and $\text{Ca}_v1.3$ regulate the adrenaline and adrenaline secretion in response to nerve stimulation (Marcantoni *et al.*, 2007). In pituitary gland (Loechner *et al.*, 1999), L- and P/Q-type are responsible for the secretion of ACTH. In the thyroid (McGehee *et al.*, 1997), carotid body (Buckler & Vaughan-Jones, 1994b; Peers *et al.*, 1996; Conde *et al.*, 2006a) and neuroepithelial body (Fu *et al.*, 2002), L-type mediated secretion or neurotransmitter release.

1.7.4 Ion channels mediating Ca^{2+} influx in rat type 1 cells

Many experiments have been performed regarding Ca^{2+} influx in rat type 1 cells and its modulation. In 1993, Fieber et McCleskey were the first to show the involvement of L-type Ca^{2+} channels in carotid body chemoreception (Fieber & McCleskey, 1993) using nifedipine and Bay K 86449 (an antagonist and agonist of L-type Ca^{2+} channels, respectively). Voltage-dependent Ca^{2+} channel types responsible for the Ca^{2+} entry have been fully identified in rabbit carotid body. Here, L- and P/Q-type channels support the response to hypoxia (Rocher *et al.*, 2005). Experiments in rat carotid body

Introduction

Genetic Nomenclature		Localization	Biophysic nomenclature		Specific antagonists
New	Old		Super family	family	
Ca _v 1.1	α1s	Skeletal muscle	High voltage activated	L	Dihydropyridines
Ca _v 1.2	α1c	Cardiac myocytes, endocrine cells, neuronal cells			
Ca _v 1.3	α1d	Endocrine cells, neuronal cells			
Ca _v 1.4	α1f	retina		Not established	
Ca _v 2.1	α1a	Nerve terminal and dendrite		P/Q	ω-agatoxin IVA
Ca _v 2.2	α1b	Nerve terminal and dendrite		N	ω-conotoxin GVIA
Ca _v 2.3	α1e	Neuronal cells		R	SNX482
Ca _v 3.1	α1g	Neuronal cells, cardiac myocytes	Low voltage activated	T	Not established
Ca _v 3.2	α1h	Neuronal cells, cardiac myocytes			
Ca _v 3.3	α1i	Neuronal cells			

Table 1.1: Nomenclature, localization and antagonist of voltage-dependent Ca²⁺ channels. Adapted from Catterall *et al.*, 2003.

show that Ca²⁺ influx might be mediated by L-type and/or N-type, as well as an indeterminate voltage-insensitive Ca²⁺ channels (Urena *et al.*, 1989; Buckler & Vaughan-Jones, 1994c; e Silva & Lewis, 1995; Jiang & Eyzaguirre, 2004). Indeed, in these studies, the use of L-type channel blockers induces only a partial (74 % and 67 %, respectively) inhibition of Ca²⁺ influx (Buckler & Vaughan-Jones, 1994c; e Silva & Lewis, 1995). Moreover, ω-conotoxin, which is a specific antagonist of the N-type channel, reduces the Ca²⁺ influx by 40 % in the adult rat type 1 cells (e Silva & Lewis, 1995) and has an inhibitory effect on some type 1 cells in the neonatal rat (Peers *et al.*, 1996). In contrast, Fieber and McCleskey found no effect of ω-conotoxin in rat type 1 cells (Fieber &

Introduction

McCleskey, 1993). The participation of P/Q-type Ca^{2+} channels can be excluded because ω -agatoxin has no effect on Ca^{2+} influx in type 1 cells induced by hypoxia (Peers *et al.*, 1996). These results support a role for L- and N-type Ca^{2+} channels in the rat type 1 cell hypoxic response. The voltage-insensitive Ca^{2+} currents observed by many authors in patch-clamp recordings (Urena *et al.*, 1989; Buckler & Vaughan-Jones, 1994c; Jiang & Eyzaguirre, 2005) are likely to be member of the TRPC family (Buniel *et al.*, 2003). Using immunohistochemistry, expression of TRPC1 and TRCP3 to 7 in tyrosine hydroxylase positive cells has been described (Buniel *et al.*, 2003). The TRPC are activated by the G protein $\text{G}_{q/11}$ pathway (Buniel *et al.*, 2003), which can be activated in the type 1 cells via, for example, the activation of muscarinic receptors (Alexander *et al.*, 2006). Therefore, TRPC induces an increase in $[\text{Ca}^{2+}]_i$, acting as a positive feed back on the type 1 cells. The presence of TRPC channels can explain the residual current resistant to voltage-dependent Ca^{2+} channels blockers. Until now, no T-type currents have been reported in type 1 cells. The release of Ca^{2+} from internal stores, which might participate in the increase in $[\text{Ca}^{2+}]_i$, does not seem to play any important role. Indeed, all the pharmacological manoeuvres used to prevent the Ca^{2+} release from the stores have had little or no effect on the exocytosis process induced by hypoxia (Vicario *et al.*, 2000a; Conde *et al.*, 2006a).

To conclude, rat type 1 cells express voltage-dependent Ca^{2+} channels which couple the hypoxic induced depolarisation with neurotransmitter release. The nature of the Ca^{2+} channels expressed is not fully characterised, however L- and N-type are likely to be involved. Because voltage-dependent Ca^{2+} channels have been shown to be inhibited by polyamines they may play a role in mediating an inhibitory effect of spermine on type 1 cell chemoreception.

1.8 OBJECTIVES

By analogy with other tissues, several studies suggest the involvement of polyamines in the carotid body physiology. Indeed, polyamines have been shown to be co-secreted with neurotransmitters by neurons in the brain, and this is likely to be the case also in type 1 cells as type 1 cells are derived from neuronal crest and share many properties with neurons (Gonzalez *et al.*, 1994). Moreover, during growth and development, polyamines have an important regulatory role. For instance, in the lung arterial smooth muscle cells, the down regulation of the transcription of the ornithine decarboxylase and the polyamine uptake trigger the morphological changes observed after hypoxia. Similarly, in the carotid body the transcription of ornithine decarboxylase is down regulated during chronic sustained hypoxia. Also, as reported by many groups, the extracellular polyamines, especially spermine, are known to block the voltage-dependent Ca^{2+} channels. The latter play a crucial role in the carotid body chemoreception as they induce the release of neurotransmitters by type 1 cells.

In addition, the CaR, which is strongly activated by spermine, is known to be involved in the regulation of many secretory processes and to modulate many ion channel activities, but its expression in the carotid body has never been investigated.

The aim of this study was to assess the putative role of extracellular spermine as a modulator of the type 1 cell chemoreception and to investigate the role that the Ca^{2+} channels and CaR play in mediating the spermine effect on carotid body function (Fig. 1.17). The first hypothesis is that an activation of the CaR by spermine induces a Ca^{2+}

release from the intracellular stores via IP₃-dependent pathway. This release of Ca²⁺ would induce an increase in neurotransmitter release. The second hypothesis postulates an inhibitory effect of spermine on the voltage-dependent Ca²⁺ channels leading to a reduction of the Ca²⁺ influx and neurotransmitter release.

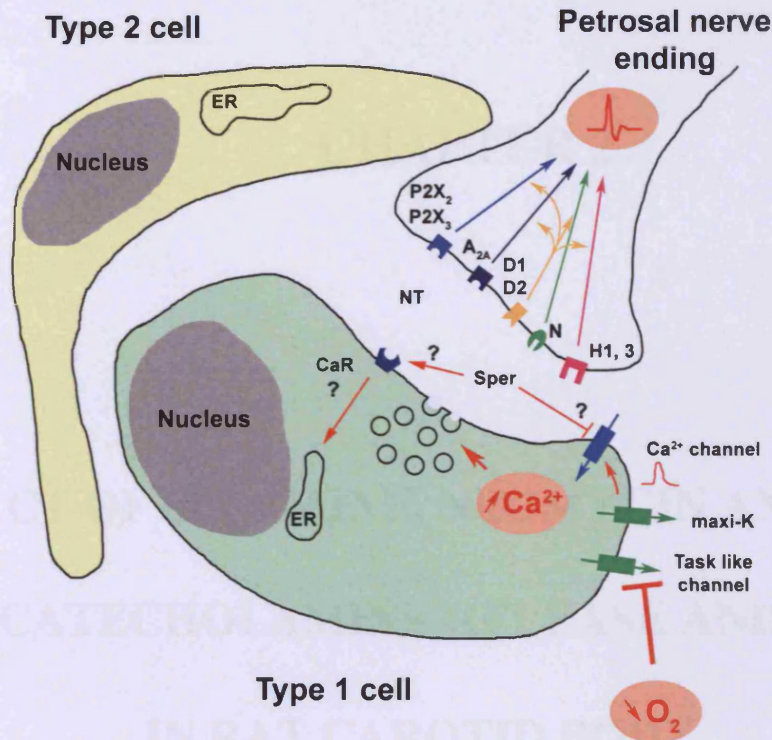


Figure 1.17: Schematic representation of carotid body illustrating the working hypotheses. Type 1 cell possibly co-released spermine (sper) with neurotransmitters (NT). The putative effects of spermine on type 1 cell are investigated following two hypotheses: the activation of CaR and/or the inhibition of voltage-dependent Ca²⁺ channel.

In chapter 2, the effect of both extracellular spermine and activators of CaR on catecholamine release and Ca²⁺ increase induced either by hypoxia or high K⁺ in type 1 cells are characterised. Then, in chapter 3, to identify the molecular mechanisms mediating the inhibitory effect of spermine on chemoreception, the expression of CaR and voltage-dependent Ca²⁺ channels in rat type 1 cells are investigated at the mRNA and protein levels. Finally, in chapter 4, the effect of spermine on Ca_v1.2 current is tested in HEK293 cells expressing Ca_v1.2 and on carotid body type 1 cells.

CHAPTER 2

EFFECT OF SPERMINE, NEOMYCIN AND R-568 ON CATECHOLAMINE RELEASE AND $[Ca^{2+}]_i$ IN RAT CAROTID BODY

2.1 INTRODUCTION

The regulation of respiration depends on the detection of the crucial parameters in the blood: pO_2 , pCO_2 and pH. Diverse organs have the ability to monitor changes in these parameters: the neuroepithelial body, the carotid sinus, the respiratory centre in the brainstem and the carotid body (Ganong, 1997). The mechanisms by which the carotid body senses the blood composition and how the carotid body function is modulated are not yet fully understood.

Polyamines, which are small organic molecules, have been shown to play a crucial role during hypoxia or hypoxia/ischemia in many tissues: lung (Babal *et al.*, 2002), brain (Longo & Packianathan, 1995) or heart (Tantini *et al.*, 2006) where there is a modification of the polyamine metabolism leading to increase in intracellular or extracellular spermine concentration. It is probable that a similar mechanism takes place in other tissues such as carotid body. In addition, the spermine has been shown to be co-secreted with neurotransmitters by neurons (Masuko *et al.*, 2003) which could also to be the case in the carotid body type 1 cells. The first part of my work was to test the effect of spermine on carotid body function. Experiments, carried out in collaboration with C. Gonzalez laboratory (University of Valladolid, Spain), with isolated carotid body revealed that spermine inhibited catecholamine secretion.

Spermine is a well known agonist of the CaR (Riccardi & Maldonado-Perez, 2005) a G protein coupled receptor (Pin *et al.*, 1994). The CaR was discovered in 1993 (Brown *et al.*, 1993), it plays a major role in the regulation of the extracellular Ca^{2+} homeostasis. But

Chapter 2

the recent discoveries that the CaR is expressed in many cell types not involved in extracellular Ca^{2+} homeostasis (Squires, 2000) and its ability to regulate secretory processes for instance, in pituitary gland (Emanuel *et al.*, 1996) and stomach (Ray *et al.*, 1997) leads to the hypothesis that the CaR might play a role in the regulation of secretion in carotid body cells. In addition, the activity of the CaR is modulated by extracellular pH (Quinn *et al.*, 2004) making the CaR a potential candidate for pH-dependent modulation of carotid body secretion.

To test the effect of spermine and the putative involvement of the CaR on carotid body chemoreception, spermine, neomycin (a CaR agonist) and R-568 (an allosteric modulator of the CaR) were tested on catecholamine release from isolated carotid body and on $[\text{Ca}^{2+}]_i$ homeostasis in dissociated carotid body cells. HEK293 cells stably transfected with CaR were used as a positive control and to compare the potency of R-568 and its less active enantiomer, S-568.

2.2 MATERIALS AND METHODS

2.2.1 Surgery and carotid body isolation

Male or female Wistar rats (100-350g) were anesthetized with sodium pentobarbital 60 mg/kg, injected intraperitoneally (IP, Euthatal, Merial, UK), according to the Home Office regulations. After a tracheotomy, the carotid bifurcations were located, removed and placed in a Lucifer chamber with ice-cold Tyrode solution containing (in mM): 143 NaCl, 2 KCl, 2 CaCl₂, 1.1 MgCl₂, 5.5 glucose and 10 HEPES, adjusted to pH 7.4 with NaOH and bubbled with 100 % O₂. The carotid bodies were identified and cleaned of surrounding connective tissue under a dissecting microscope, collected in glass vials containing ice-cold Tyrode's solution. Animals were killed with an intracardiac overdose of pentobarbital (180 mg/kg).

2.2.2 Labelling of catecholamine stores and release of [³H]catecholamine

2.2.2.1 Labelling of the catecholamine stores

The carotid body catecholamine release was quantified using a radioactive 3,5- [³H]tyrosine. Before the experiment, the carotid bodies (12 carotid bodies/experiment) were incubated for 2 h with 30 μM [³H]tyrosine (with specific activities of 48 Ci/mmol), 100 μM of 6-methyl-tetrahydropterine and 1 mM of ascorbic acid; they are cofactors of tyrosine hydroxylase and dopamine-β-hydroxylase, respectively. These reagents were dissolved in HEPES-buffered solution containing (in mM): 140 NaCl, 5 KCl, 2 CaCl₂, 1.1

Chapter 2

MgCl₂, 5 glucose, 10 HEPES, pH 7.4). Afterwards, the [³H]tyrosine which had not been incorporated into catecholamine was washed from the carotid body by rinsing the carotid body in HEPES-buffer for 1 h and changing the solution every 20 min.

2.2.2.2 [³H]catecholamine release experiments

For the release experiments, the carotid bodies were placed individually in 4 ml of bicarbonate-buffered solution containing (in mM): 116 NaCl, 24 NaHCO₃, 5 KCl, 2 CaCl₂, 1.1 MgCl₂, 5 glucose, 10 HEPES, pH 7.4 equilibrated with 20 % O₂, 5 % CO₂, 75 % N₂. The carotid bodies were shaken and kept at 37.5°C. Every 10 min, the bathing solution was collected and replaced by the appropriate solution according to the protocol. The collected solution, containing the secreted [³H]catecholamine, was supplemented with 50 µl of glacial acetic acid (at pH = 3) to prevent the degradation of the neurotransmitters. The solutions used for the protocols were bubbled either with a) 20 % O₂, 5 % CO₂ and 75 % N₂ (normoxia); b) 7 % O₂, 5 % CO₂ and 88 % N₂ (hypoxia) or; c) 20 % O₂, 5 % CO₂ and 75 % N₂ (high K⁺) where NaCl and KCl were changed to 86 and 35 mM, respectively. Except for hypoxia, all the gas mixtures were firstly bubbled in distilled H₂O prior to be bubbled in the experimental solution to prevent evaporation and hence, concentration of the solution. R-568 (Amgen) was initially dissolved in dimethyl sulfoxide (DMSO) at 10 µM as a stock solution and subsequently stored at -20 °C. 500 µM spermine, 100 nM R-568 or 300 µM neomycin were dissolved in the bicarbonate buffered solution and incubated for 20 min prior to the stimulus. Some experiments were performed with two stimulations, a first control stimulation S1 (hypoxia or high K⁺) and a second stimulation (S2) after application of drug in one of the groups. In other experiments, the treatment was applied at the beginning and only one stimulation was performed.

Chapter 2

2.2.2.3 Quantification of [³H]catecholamine release

The [³H]catecholamines present in the collected solution were bound to 100 mg of alumina, 5 ml of 2.5 M tris(hydroxymethyl)aminomethane (Tris) buffer (pH = 8.6) before being shaken for 10 min at room temperature. Afterwards, the alumina was filtered and washed extensively with water and the [³H]catecholamines were eluted using 1 ml of 1 N HCl. 4 ml of scintillant Optiphase Hisafe (PerkinElmer, Massachusetts, USA) were added and the radioactivity was quantified by liquid scintillation counting. Scintillation is based on the principle that the β particles emitted by the radioactive compounds excited aromatic molecules present in the solvent. The excited molecules dissipate their excess of energy by emission of light which is quantified by the counter. This value is reported as counts per min (cpm) which is then converted in disintegration per min (dpm) by correcting the background and the efficiency corresponding to the real level of [³H]catecholamine. The increase in catecholamine secretion was calculated as the quantity secreted above the baseline and expressed as a percentage of the baseline value just before the stimulus was applied. This normalization allowed comparison of the results obtained with different carotid bodies, which might be of different sizes, and that would have quantitatively different amount of catecholamine contents. Data are presented as mean \pm SEM and differences assessed using a two-tailed unpaired Student t-test, as two independent groups of carotid bodies were compared, with the significance achieved at $p < 0.05$.

2.2.3 Carotid body dissociation

Whole isolated carotid bodies (2 – 4 carotid bodies/experiment), extracted as explained above, were used for dissociation of type 1 and type 2 cells. The carotid bodies were incubated in 2 ml of Ca^{2+} - and Mg^{2+} - free Tyrode solution containing collagenase (2.5 mg/ml, Sigma-Aldrich, Gillingham, Dorset, UK) and albumin (6 mg/ml, Sigma-Aldrich), for 15 min at 37°C. The solution was then replaced with a fresh Ca^{2+} - and Mg^{2+} - free Tyrode's solution containing trypsin (1 mg/ml, Sigma-Aldrich) and albumin (6 mg/ml, Sigma-Aldrich) for 20 min at 37°C. Next, the carotid bodies were placed in F-12/Dulbecco's Modified Eagle's Medium (DMEM, Invitrogen, Paisley, UK) supplemented with 10 % foetal calf serum (Invitrogen, Paisley, UK), 1 % (v/v) antibiotic/antimycotic (Invitrogen), 200 mM L-glutamine (Invitrogen) and the carotid bodies were mechanically dissociated by pipetting the solution up and down using a P1000 Gilson pipette (Gilson, Middleton, USA). The isolated cells were then centrifuged at 1,200 g, resuspended in 50 μl of F12/DMEM and seeded onto poly-L-lysine coated coverslips (0.1 mg/ml, Sigma-Aldrich) placed in 12 well plate (5 to 10 μl /coverslip). After letting the cells adhere for 50 min, 500 μl of medium were added to each well. The carotid body cells were used for Ca^{2+} imaging experiments after 16 – 24 h of culture to let the cells recover and allow the type 2 cells to take their characteristic spindle shape (Xu *et al.*, 2005) and therefore, make identification of type 1 cells by eye much easier. The cells were cultured at 37.5 °C in 20 % O_2 , 5 % CO_2 and 75 % N_2 .

2.2.4 Calcium imaging on dissociated carotid body cells

Fura-2 was used for $[Ca^{2+}]_i$ measurement because it is a ratiometric dye. With ratiometric dyes the measurement of $[Ca^{2+}]_i$ is independent of the quantity of the dyes present in the cells, which is a major advantage for prolonged experiment since the dyes can be destroyed. Moreover, ratiometric technique allows suppression of several artefacts (drift along z-axis, autofluorescence of the cells) because both wave lengths (340 and 380 nm) are affected at the same rate (Lohr, 2003).

Carotid body cells were loaded with fura-2 acetoxy methyl ester (4 μ M, Molecular Probes, Eugene, OR, USA) for 40 min in a HEPES-buffered solution containing (in mM): 125 NaCl, 4 KCl, 1 CaCl₂, 1 MgSO₄, 1 NaH₂PO₄, 20 HEPES, 6 glucose (pH 7.4) supplemented with 0.1 % (w/v) bovine serum albumin (Sigma-Aldrich). The cells were then washed for 15 min in HEPES-buffered physiological solution containing (in mM) : 135 NaCl, 5 KCl, 0.5 CaCl₂, 0.5 MgCl₂, 10 glucose and 5 HEPES, pH 7.4, each of the steps were carried out at 37.5°C in 20 % O₂ and 5 % CO₂. The coverslips were mounted in a perfusion chamber (Warner Instruments, Hamden, CT, USA) and continuously superfused with HEPES-buffered physiological solution from a gravity-fed perfusion system at a rate of 1-2 ml/min. The cells were observed under a Nikon Diaphot inverted microscope (Tokyo, Japan) equipped for epifluorescence with quartz optics using a 40x-oil immersion objective. Excitation light was produced by a xenon short arc lamp (Osram GmbH, München, Germany) with the wavelength alternatively selected at 340 and 380 nm with a bandwidth of 10 nm using a CAIRN Optoscan monochromator (Cairn, Kent, UK). Then, the light was reflected on an excitation dichroic mirror 400DCLP (reflecting only the wavelength under 400 nm, Olympus, Watford, UK). The emission light produced by Fura-

Chapter 2

2 at 540 nm passed then through the 400DCLP filter without being affected and reached the emission dichroic filter D510/80m (Olympus), which is a band pass filter at 510 nm, with a bandwidth of 80 nm especially allowing the passage of the light between 470 and 550 nm. The light at 540 nm was detected by a slow-scan CCD camera (Kinetic Imaging Ltd, Nottingham, UK) and images of the two emission intensities for 340 and 380 nm were acquired at 0.2 Hz. All the recordings were done at $22 \pm 1^\circ\text{C}$ (to be in the same condition than the patch-clamp experiments presented later) by heating the solution passing through the perfusion line using a heated stage (Cairn).

The experiments were carried out using the following solutions. HEPES-buffered physiological solution used for the experiment contained (in mM): 115 NaCl, 5 KCl, 0.5 CaCl₂, 0.5 MgCl₂, 5 HEPES and 10 glucose, pH 7.4. For the “high K⁺ solution”, the NaCl was lowered to 105 mM and the KCl increased to 15 mM, pH 7.4. Spermine (300 μM, Sigma-Aldrich), neomycin (200 μM, Sigma-Aldrich) or R-568 (100 nM, Amgen) were diluted on the day of the experiment in the physiological solution or high K⁺ solution as desired. The Ca²⁺ and Mg²⁺ were raised to 1.2 mM in the spermine dose-response curve (to be in physiological condition) and in experiments with R-568 to allow the allosteric modulation of the CaR.

For the experiments involving hypoxic stimulus, the control or spermine solutions were bubbled either with medical air (control) or 100 % N₂ (hypoxia) for 20 min prior to the experiments. The pO₂ in the bath was constantly recorded by a carbon-fibre microelectrode (ProCFE, Continental Laboratory Product, San Diego, USA) normalized to a potential of -600 mV. The reduction of O₂ induced a current which was recorded with a CV2003 BU Headstage (Axon Instruments, Sunnyvale, USA), connected to an Axopatch

Chapter 2

200B voltage-clamp amplifier (Axon Instruments) and digitalized with Digidata 1322A (Axon Instruments). The cells were first exposed to a control high K^+ stimulus (~30s) before being challenged twice by hypoxia (~30s, $pO_2 < 10$ mmHg). 200 μM spermine (Sigma) was then incubated for 3 min and applied in conjunction with hypoxia. After 2 min wash, a last hypoxic challenge was performed.

The analyses of the recordings were carried out off-line. The evolution of fura-2 340/380 ratio (later referred as 340/380 ratio) is expressed either as absolute value or normalized to the increase induced by a high K^+ /hypoxia control stimulation, therefore each cell acted as its own control. The amplitude of the increase in 340/380 ratio is calculated as value above baseline. Data are reported as mean \pm SEM, N = number of rats used, n = number of cells recorded. The concentration-response curves were fitted using the Hill equation:

$$Y = \text{maximum response} / (1 + (X/M1)^{M2})$$

Where $M1 = EC_{50}$ and $M2 =$ Hill coefficient

In the experiments with hypoxia, $[Ca^{2+}]_i$ has been plotted against pO_2 using a single exponential:

$$y = y_b + Ae^{Rx}$$

Where y_b is the baseline value (value at $x \rightarrow \infty$), A give value at $y = 0$ ($y_0 = y_b + A$) and R reflects the sensitivity of the type 1 cell to pO_2 .

Two-tailed, paired Student's t-test or ANOVA with Tukey post-hoc test were used, as appropriate, for statistical analyses with differences considered significant at $p < 0.05$.

2.2.5 Tyrosine hydroxylase immunostaining

The dissociated carotid body cell preparation contained mostly, but not exclusively, type 1 cells and type 2 cells. “Contaminating” cells included vascular smooth muscle cells and fibroblasts. In the Ca^{2+} imaging experiments, high K^+ was used as a stimulus which could, therefore, potentially activate both type 1 and smooth muscle cells, as both of them express voltage-dependent Ca^{2+} channels. To identify positively the cell type from which $[\text{Ca}^{2+}]_i$ measurements were recorded, immunocytochemistry against tyrosine hydroxylase, which is a specific marker of type 1 cell (Caceres *et al.*, 2007), was performed at the end of Ca^{2+} imaging experiment. The following protocol was used (10 min per step, except for fixation, at room temperature): washing with phosphate-buffered saline (PBS, in mM: 0.14 NaCl, 0.84 Na_2HPO_4 and 0.16 $\text{NaH}_2\text{PO}_4 \cdot \text{H}_2\text{O}$, pH 7.4), fixation with 4 % (v/v) paraformaldehyde (5 min), washing with 0.1 % (v/v) Triton x-100 and 5 % seablock in PBS (solution B), incubation with mouse antibody against rat tyrosine hydroxylase (1:500, Sigma-Aldrich) dissolved in solution B, washing with PBS, incubation with secondary antibody (1:500, FITC goat anti-mouse, Molecular Probes, Paisley, UK) dissolved in solution B and washed with PBS. All the manipulations were undertaken carefully to avoid any movement of the preparation. At the end of the protocol, the cells were observed using the same microscope and the same software as the one used for Ca^{2+} imaging.

2.2.6 CaR-HEK293 cells culture

A line expressing the human parathyroid CaR in HEK293 cell, was available in the laboratory. The cells were maintained in MEM (containing Earle's salts and L-glutamine, Invitrogen) supplemented with 10 % (v/v) foetal calf serum (Hyclone, Cramlington, UK), and 1 % (v/v) antibiotic/antimycotic with 200 µg/ml hygromycin B (Sigma) to select the cells containing the plasmid. Cells were grown in 10 ml of medium in 25 ml flask. Every 3-4 days, when 80 % confluency was reached, the cells were dissociated as follow: 2 washes with PBS Ca²⁺- and Mg²⁺-free (Gibco, Invitrogen), 3 min incubation with trypsin 1X in PBS (Gibco) then 7 ml of medium was added and the cells were spun down at 1,200 g for 4 min. Cells were resuspended in 10 ml of fresh medium and cultured at the concentration 1:10 in a new culture flask at 37.5 °C in 20 % O₂, 5 % CO₂ and 75 % N₂.

In preparation for the Ca²⁺ imaging experiments, cells were seeded at a low confluence on 16 mm coverslip placed in 12 well plate and cultured for 24 h prior to the experiment.

2.2.7 Calcium imaging on CaR-HEK293 cells

The CaR-HEK293 cells were processed as explained for the dissociated carotid body cells, with the exception that the loading was done for 20 min with 2 µM of fura-2 AM. The recordings were performed at room temperature and the extracellular Ca²⁺ and Mg²⁺ used were 1.2 mM for the experiment involving R-568 or S-568 and 0.5 mM for the dose-response curve to neomycin. The Ca²⁺ concentration was adjusted to allow a maximum activation of the CaR in the presence of different drugs. As Ca²⁺ and neomycin

Chapter 2

are both class I calcimimetics, then the Ca^{2+} concentration was lowered at 0.5 mM to minimize the competition for the activation of the CaR. In contrast, the R-568 is a class II calcimimetic and requires prior activation of CaR by Ca^{2+} to modulate its activity, therefore a higher Ca^{2+} concentration was used with R-568 (1.2 mM). The S-568 was stored in aliquots as described for the R-568. The CaR agonists were dissolved in the HEPES-buffer physiological solution on the day of the experiment. Each cell was exposed, for 3 min, only to one concentration of one of the CaR allosteric modulator to avoid any problems associated with the refilling of the intracellular stores, which could easily skew the amplitude of the response during the second stimulation. The variations in $[\text{Ca}^{2+}]_i$ following the stimulation were assessed by quantifying three parameters: the amplitude of the $[\text{Ca}^{2+}]_i$ increase, the increase in the number of oscillating cells and increase in the frequency of oscillation, when applicable. The frequency was calculated over a period of 3 min before and during the application of calcimimetic. The amplitude of the response was quantified as the increase in 340/380 ratio above the base line. When the stimulus induced an oscillation in $[\text{Ca}^{2+}]_i$ then the amplitude of the first increase was used. All the data were pooled for each condition and presented as mean \pm SEM, N = number of experiments, n = number of cells recorded.

2.3 RESULTS

2.3.1 Spermine inhibition of catecholamine release induced either by hypoxia or high K^+ from isolated carotid body

In isolated carotid body, a control application of an acute hypoxic challenge (7 % O_2 for 10 min) induced a 3H -CA secretion (Fig. 2.1.A1). In the control group the acute hypoxia triggered a release of 3H -CA of 857 ± 16 dpm/carotid body, $n = 6$ above the baseline secretion. Then, one of the groups was treated with 500 μM spermine. The application of spermine did not affect the baseline secretion of 3H -CA. Indeed, in the control and spermine group, after 20 min of incubation, the run down of the 3H -CA release was similar in both groups, respectively 621 ± 65 to 440 ± 37 dpm/carotid body and 709 ± 76 to 553 ± 70 dpm/carotid body ($n = 6$, Fig. 2.1.A1). Conversely, the 3H -CA secretion induced by 7 % O_2 was inhibited in the spermine group compared to the control group. The ratios between the two stimulations were significantly lower in the spermine group than in the control group with an inhibition of 55 % ($n = 6$, $p < 0.01$, Fig. 2.1.A2). After the stimulation, the basal 3H -CA secretions returned to similar values in the two groups. The effect of 500 μM spermine on high K^+ evoked released was, as well, inhibitory. The secretion, expressed as % of content, in the control group was 17.9 ± 0.9 % and in the treated group 2.3 ± 0.3 %, spermine induced an inhibition of 3H -CA release of 60 %, ($n = 6$, $p < 0.01$, Fig. 2.1.B).

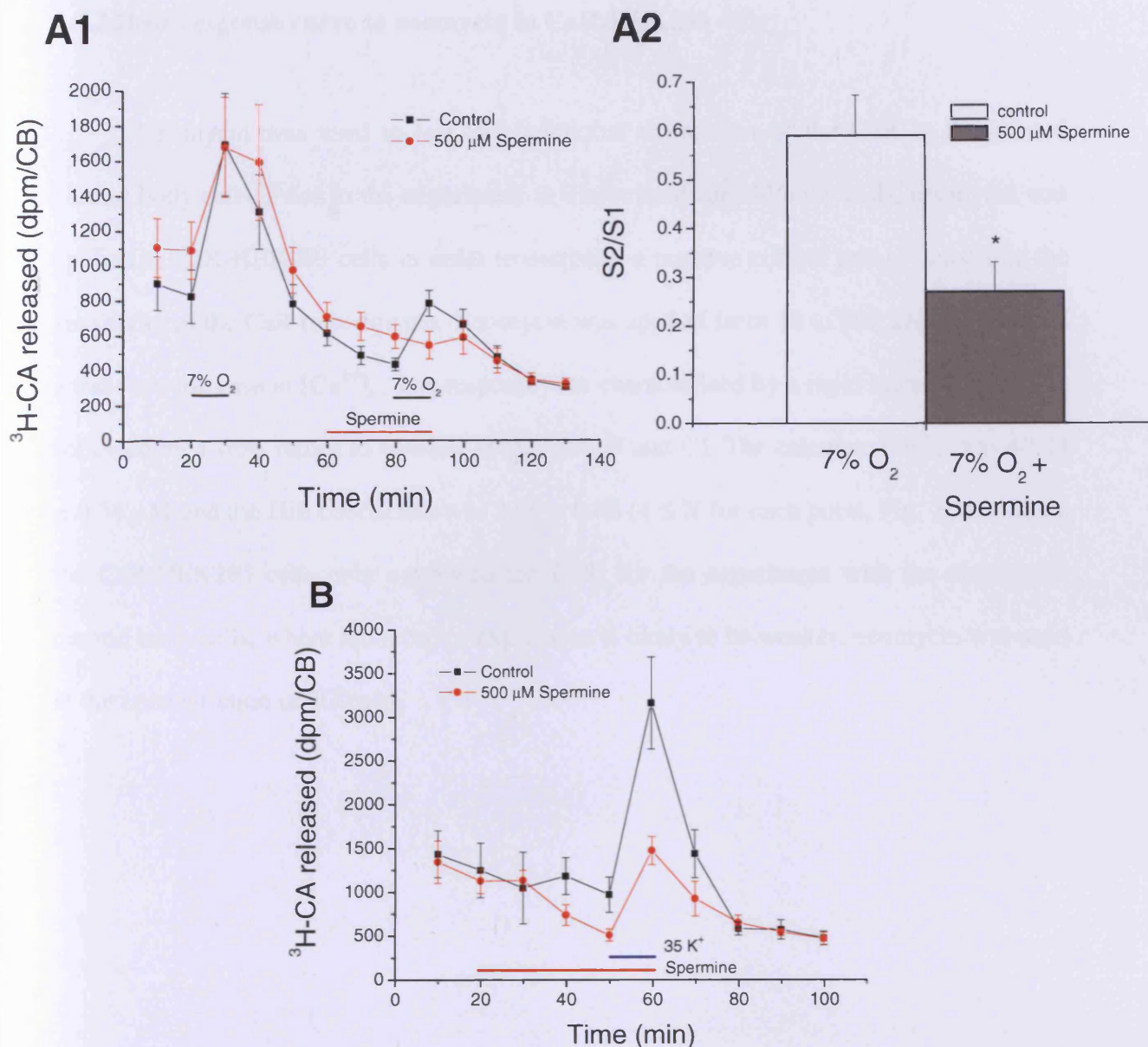


Figure 2.1: Inhibitory effect of spermine on $^3\text{H-CA}$ secretion induced either by hypoxia or high K^+ in isolated carotid body. A1) Hypoxic challenge induced a release of $^3\text{H-CA}$ in rat carotid body (stimulus S1). In the group preincubated with spermine (red) the $^3\text{H-CA}$ release induced by a second hypoxic challenge (S2) was drastically inhibited compared to the control group (black). A2) Histogram presenting the ratio of S2/S1, extracted from data show in A1, in $^3\text{H-CA}$ release between the first and second stimulation in the control (white) and spermine (grey) group. In the treated group, the ratio was inhibited by 55 % ($n = 6$, $p < 0.01$). B) Effect of spermine on catecholamine release induced by high K^+ . In the group preincubated with spermine (red) the catecholamine release was inhibited compared to the control group (black).

2.3.2 Dose-response curve to neomycin in CaR-HEK293 cells

Neomycin was used to test the functional expression of the CaR in dissociated carotid body cells. Prior to the experiment in dissociated carotid body cells, neomycin was applied to CaR-HEK293 cells in order to establish a positive control and to determine the sensitivity of the CaR to neomycin. Neomycin was applied from 10 to 300 μM and induced a transient increase in $[\text{Ca}^{2+}]_i$. The response was characterised by a rapid increase in $[\text{Ca}^{2+}]_i$ followed by a slow return to baseline (Fig. 2.2A, B and C). The calculated EC_{50} was $40.24 \pm 0.54 \mu\text{M}$ and the Hill coefficient was 2.56 ± 0.08 ($4 \leq N$ for each point, Fig. 2.2D). Since the CaR-HEK293 cells over expressed the CaR, for the experiment with the dissociated carotid body cells, where the receptor expression is likely to be weaker, neomycin was used at the concentration of 300 μM .

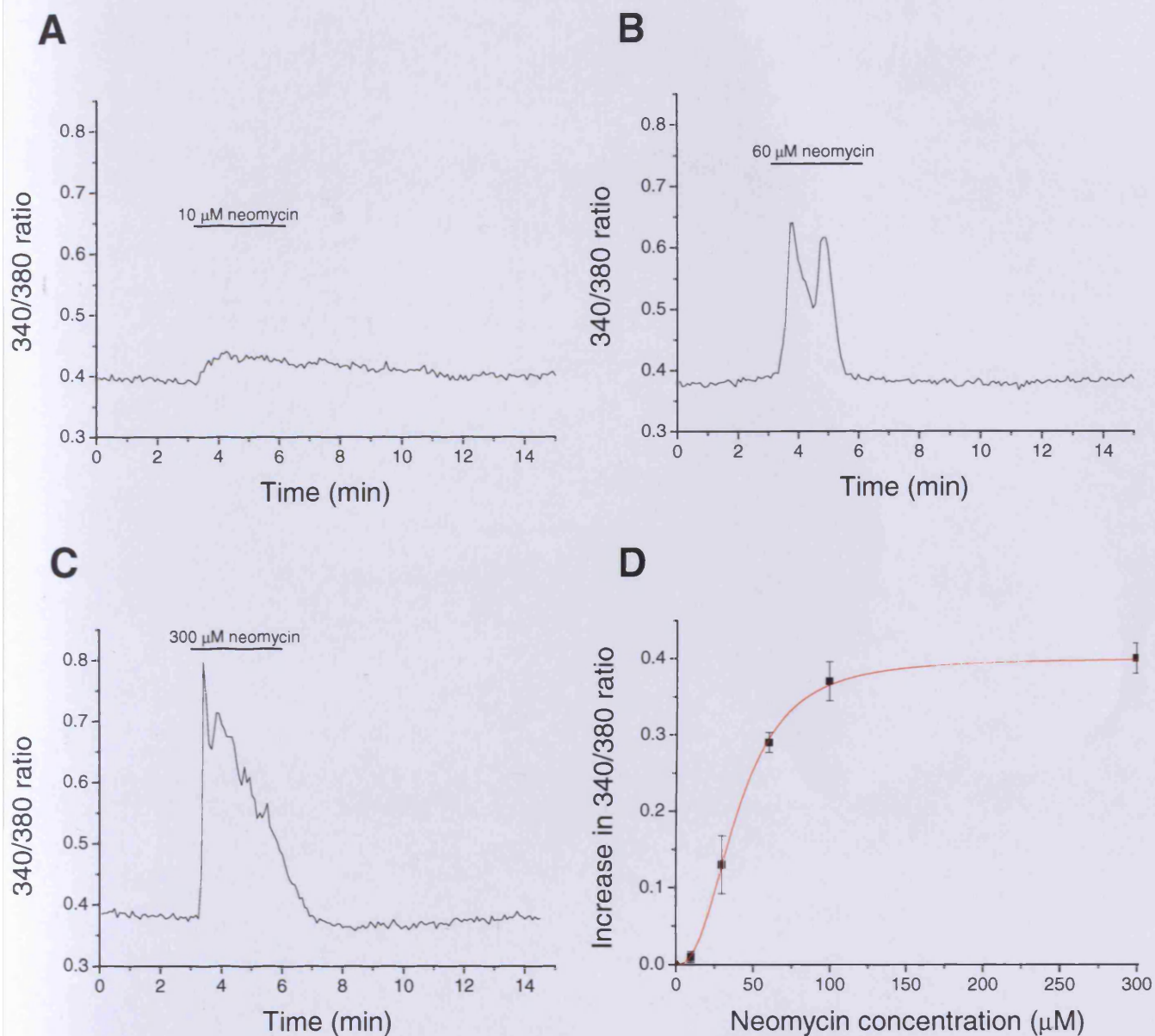


Figure 2.2: Dose-response curve to neomycin in CaR-HEK293 cells. Neomycin from 10 to 300 μM was applied on CaR-HEK293 cells. Typical Ca²⁺ imaging recording of CaR-HEK293 cells exposed to 10, 60 and 300 μM neomycin (A, B and C). D) Dose-response curve, EC₅₀ was calculated as 40.24 ± 0.54 μM with a Hill coefficient at 2.56 ± 0.08 (N ≥ 4 for each point).

2.3.3 Comparative effect of R-568 and S-568 on CaR-HEK293 cells

R-568 and S-568 are enantiomers which have been reported to activate the CaR with different potencies (Nemeth *et al.*, 1998). The use of these two enantiomers allows verifying that the effect observed is due to the activation of the CaR, as a stereoselective effect should be observed, with R-568 being 10-100 fold more potent than S-568.

The aim of this experiment was to determine the concentration at which the stereoselective activation of the CaR was the more visible. R-568 and S-568 were tested at 1, 10 and 100 nM on CaR-HEK293 cells in 1.2 mM extracellular Ca^{2+} (Fig. 2.3). The allosteric modulation of the CaR gave complex patterns of responses which could not be summarized as a strong increase in $[\text{Ca}^{2+}]_i$, like for the activation of the CaR by neomycin. Indeed, the modulation of the CaR had different effect according to the basal activity of the cells and to the concentration of calcimimetic applied. The application of R-568 or S-568 could induce either a single transient increase in $[\text{Ca}^{2+}]_i$ (i.e. Fig. 2.3A1, A2, B1, B2) or oscillations of the $[\text{Ca}^{2+}]_i$, which lasted after the end of the stimulation, depending to the dose and the potency (Fig. 2.3B2, C1 and C2). In case of oscillating cells, a sufficient dose of modulator increased the frequency of oscillations (Fig. 2.3B2 and C2).

To analyse these responses, the amplitude of the increase in 348/380 ratio, the increase in percentage of oscillating cells and the increase in frequency of oscillations were quantified (Fig. 2.4A, B and C). The average percentage of oscillating cell was $15 \pm 3 \%$ and average frequency was $0.22 \pm 0.27 \text{ min}^{-1}$ (all groups together, $N = 28$). It appeared that the R-568 was a more potent allosteric modulator of the CaR than the S-568 only at 10 nM. Indeed, at 10 nM the R-568 had almost its maximum effect and was able to induce an

Chapter 2

absolute increase (maximum peak amplitude) in 348/380 ratio 0.56 ± 0.09 ($n = 45$, $N = 4$), increase the number of oscillating cells 30.19 ± 8.04 % ($n = 61$, $N = 5$) and increase in frequencies, for the oscillating cells, 0.50 ± 0.09 min^{-1} ($n = 45$, $N = 4$), in contrast the S-568 had the similar effect only at 100 nM with an increase 348/380 ratio at 0.68 ± 0.19 ($n = 79$, $N = 5$), increase in number of oscillating cells of 26.68 ± 8.19 % ($n = 63$, $N = 4$) and an increase in frequency of 0.61 ± 0.11 min^{-1} ($n = 63$, $N = 4$). In conclusion, at 10 nM, the stereoselectivity of the R-568 and S-568 was very apparent whereas at 100 nM the effects of the two enantiomers were the same.

2.3.4 Absence of an effect of neomycin and R-568 on carotid body catecholamine release

To test the hypothesis that the CaR was involved in mediating the inhibition induced by spermine, two CaR activators were used: an agonist, neomycin, and a positive allosteric modulator R-568. Application of 300 μM neomycin (Fig. 2.5A) or 100 nM R-568 (Fig. 2.5B1 and B2) did not have any effect on the catecholamine release induced by hypoxia. The inhibitory effect of spermine could not be mimicked by the activation of the CaR, indicating that the CaR is not involved in mediating the spermine effect on carotid body catecholamine release.

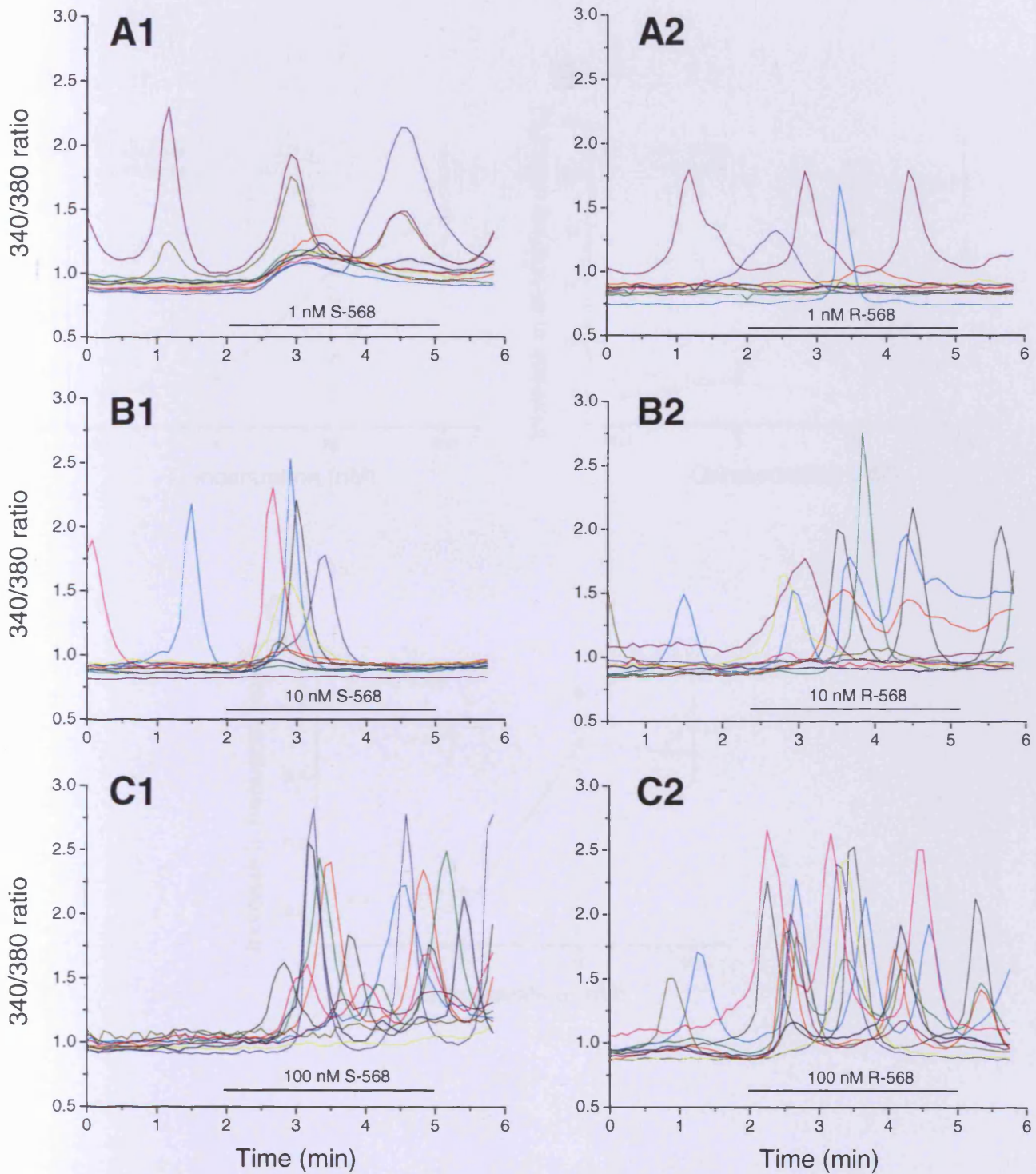


Figure 2.3: Effect of R-568 and S-568 on the increase in $[Ca^{2+}]_i$ in CaR-HEK293 cells. R-568 (right panel) and S-568 (left panel) were applied at 1, 10 and 100 nM for 3 min (A, B and C) on CaR-HEK293 cells. Each graph shows 10 typical cell recordings during the same experiment. The cells responded to the stimulation by either a single increase in $[Ca^{2+}]_i$, as in B1, or in case of a stronger stimulation, by a train of spikes, i.e. C1 and C2.

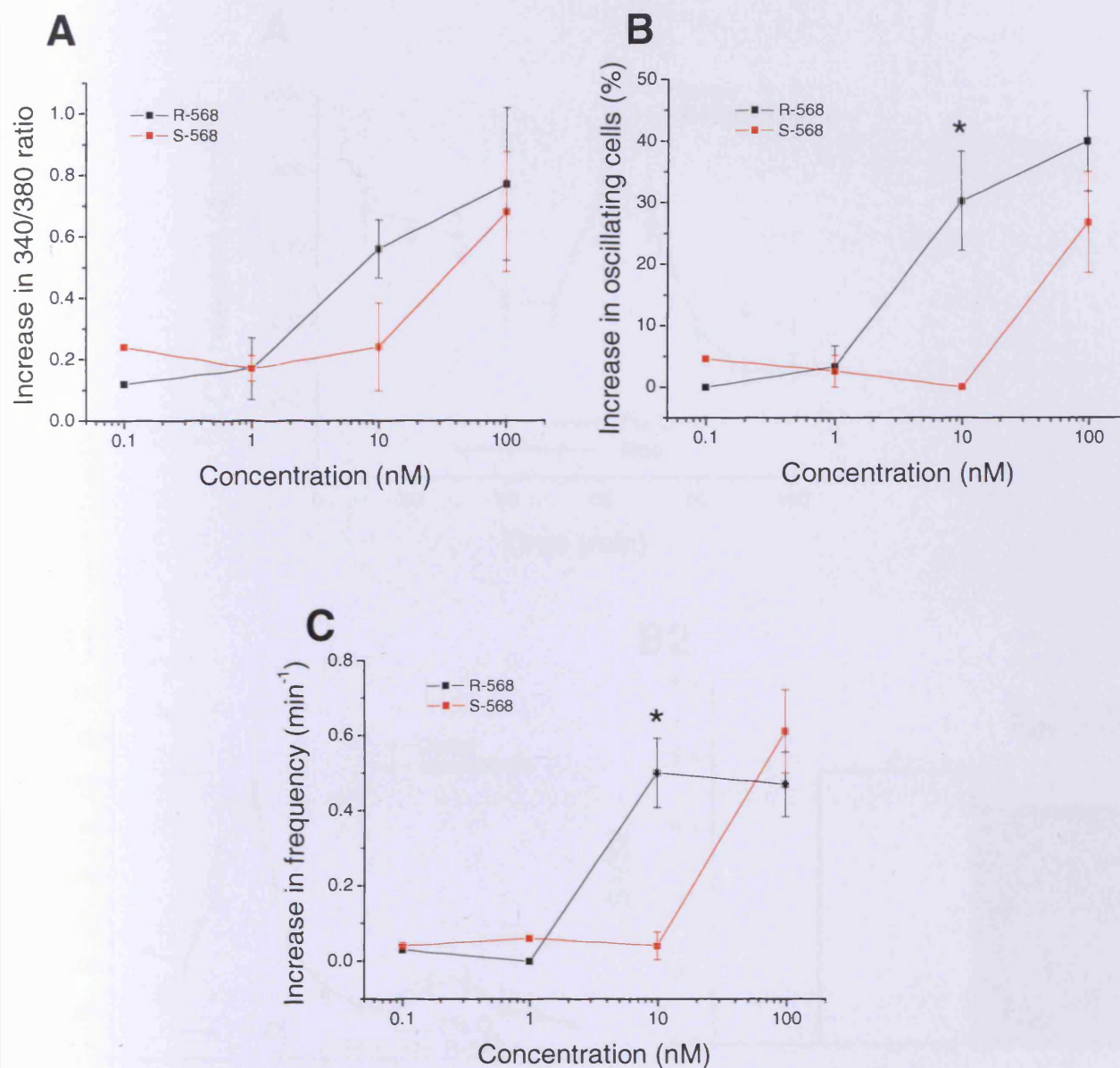


Figure 2.4: Dose-response curves to R-568 and S-568 in CaR-HEK293 cells. Three characteristic parameters of the CaR-HEK293 cell responses were quantified to assess the potency of R-568 and S-568. A) The amplitude of response (increase in 340/380 ratio), B) the percentage of oscillating cells ($p < 0.05$ at 10 nM) and C) the increase in frequency of the oscillations ($p < 0.05$ at 10 nM). R-568 was, for the three parameters analysed, a more potent allosteric modulator of the CaR at the concentration of 10 nM. ($2 < N < 6$ and $24 < n < 82$).

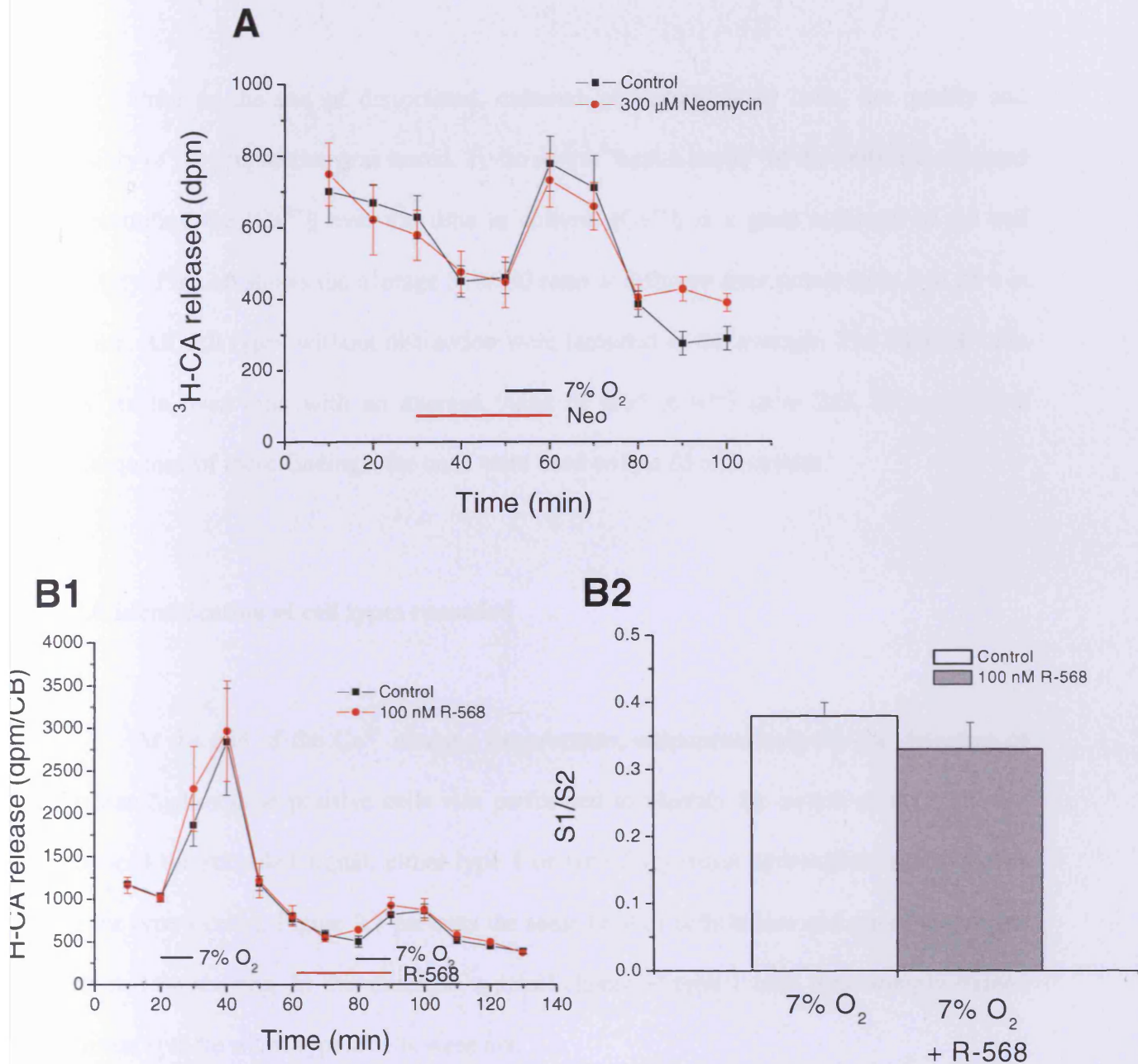


Figure 2.5: Absence of effect of neomycin and R-568 on ³H-CA secretion induced by hypoxia in isolated carotid body. A) In isolated carotid body, the ³H-CA secretion induced by hypoxia was not inhibited by preincubation with 300 μM neomycin (control group in black, neomycin treated group in red, n = 6). B1) Hypoxic challenge induced a release of ³H-CA in rat carotid body (stimulus S1). In the two groups, control (black) and preincubated with R-568 (100 nM, red) the ³H-CA release induced by a second hypoxic challenge (S2) was similar. B2) Histogram presenting the ratio of S2/S1, extracted from data show in B1, in ³H-CA release between the first and second stimulation in the control (white) and R-568 (grey) group (n = 6). 100 nM R-568 had not effect on catecholamine secretion.

2.3.5 Control of the quality of the dissociated carotid body cell preparations

Prior to the use of dissociated, cultured rat carotid body cells, the quality and stability of the preparation was tested. To do so the “health status” of the cells was assessed by recording the $[Ca^{2+}]_i$ over the time in culture. $[Ca^{2+}]_i$ is a good indicator of the cell viability. Fig. 2.6 shows the average 340/380 ratio at different time points from 3 to 25 h in culture. All cell types without distinction were included in the average. The 340/380 ratio was stable over time with an average value of 0.65 ± 0.03 ($n = 222$, $N = 4$). As a consequence of these findings, the cells were used within 25 h in culture.

2.3.6 Identification of cell types recorded

At the end of the Ca^{2+} imaging experiments, immunostaining for the detection of tyrosine hydroxylase positive cells was performed to identify the nature of the cells that produced the recorded signal, either type 1 or type 2 (tyrosine hydroxylase positive cells are the type 1 cells). Figure 2.7 presents the same field of cells before and after the tyrosine hydroxylase staining. In this example, a small cluster of type 1 cells was strongly stained whereas spindle shape type 2 cells were not.

2.3.7 Effect of Cd^{2+} on Ca^{2+} influx induced by high K^+ in carotid body type 1 cells

To determine if the increase in $[Ca^{2+}]_i$ which was induced by high K^+ in type 1 cells was due to Ca^{2+} influx via voltage-dependent Ca^{2+} channels or to Ca^{2+} release from the intracellular stores, Cd^{2+} , a blocker of voltage-dependent Ca^{2+} channels (Peers *et al.*, 1996),

was applied. Application of 200 μM Cd^{2+} on carotid body type 1 cells inhibited the high K^+ induced increase in $[\text{Ca}^{2+}]_i$ by $79.13 \pm 10.23 \%$ ($n = 8$, $N = 1$, Fig. 2.8).

2.3.8 Effect of spermine, neomycin and R-568 on $[\text{Ca}^{2+}]_i$ increase induced by high K^+ on dissociated carotid body cells

As catecholamine secretion is dependent upon Ca^{2+} influx, $[\text{Ca}^{2+}]_i$ imaging was used to investigate whether the inhibitory effect of spermine was associated with an alteration of $[\text{Ca}^{2+}]_i$ homeostasis. Moreover, spermine is an agonist of the CaR and is membrane-impermeable. Therefore, $[\text{Ca}^{2+}]_i$ imaging was used to test the potential role of CaR independently of neurotransmitter release. Indeed, in many cell types, the activation of the CaR involves a Ca^{2+} release from intracellular stores (Pin *et al.*, 1995). The effects of 200 μM spermine, 300 μM neomycin and 100 nM R-568 were tested on baseline $[\text{Ca}^{2+}]_i$ and on the increased in $[\text{Ca}^{2+}]_i$ induced by 15 mM K^+ .

Two main types of cells could be distinguished according to their responses to high K^+ . One type responded with an increase in 340/380 ratio whereas the other one did not. The immunostaining performed at the end of the Ca^{2+} imaging experiments revealed that among 60 cells responding to high K^+ with an increase in $[\text{Ca}^{2+}]_i$, 57 cells were tyrosine hydroxylase-positive. Therefore, the high K^+ -responding cells were considered as type 1 cells. Of the tyrosine hydroxylase-negative cells, 20 cells responded to high K^+ only after pre-incubation with spermine, neomycin or R-568. Finally, 29 tyrosine hydroxylase-negative cells did not respond at all ($N = 6$).

As expected, stimulation of type 1 cells by high K^+ induced a transient increase in the 340/380 ratio. For instance, in the spermine experiment, the average increase was of 0.47 ± 0.09 (Fig. 2.9A and C). The application of spermine (Fig. 2.9A), neomycin (Fig. 2.11A) or R-568 (Fig. 2.12A) did not affect the baseline 340/380 ratio, strongly suggesting that the CaR was not expressed in type 1 cells. However, the incubation with 200 μM spermine reduced the increase in $[Ca^{2+}]_i$ induced by high K^+ , from 0.47 ± 0.09 to 0.32 ± 0.07 ($n = 22$, $N = 5$, $p < 0.01$, Fig. 2.9A and C). The estimated IC_{50} for spermine in type 1 cells was $473.5 \pm 70.3 \mu M$ and the Hill coefficient was 0.84 ± 0.10 ($n \geq 17$, $N \geq 3$ for each point, Fig. 2.10).

Similarly to spermine, incubation with 300 μM neomycin inhibited the increase in $[Ca^{2+}]_i$ induced by high K^+ from 0.35 ± 0.07 to 0.07 ± 0.03 ($n = 11$, $N = 4$, $p < 0.01$, Fig. 2.11A and C). The inhibitory effect of spermine and neomycin were fully reversible as demonstrated by the ability of high K^+ to evoke a response similar to the one obtained by the first control high K^+ stimulation.

In contrast to spermine and neomycin, application of 100 nM R-568 had no effect on the increase in the 340/380 ratio in type 1 cells (Fig. 2.12A and C).

Surprisingly, some cells which did not express voltage-dependent Ca^{2+} channels (as evidenced by the absence of response to high K^+ alone) were able to respond to high K^+ with an increase in $[Ca^{2+}]_i$ only after co-incubation with either spermine (Fig. 2.6B and C), neomycin (Fig. 2.8B and C) or R-568 (Fig. 2.9B and C). These cells were always tyrosine hydroxylase negative.

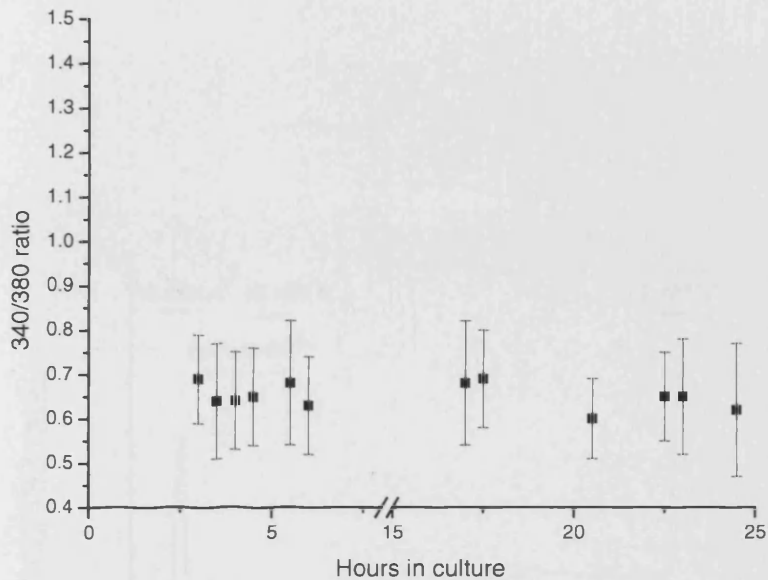


Figure 2.6: Evolution of 340/380 ratio, in carotid body dissociated cells, during the time in culture. After enzymatic digestion isolated cells were plated and kept in culture with F12/DMEM + 10 % foetal calf serum + 1 % antibiotic/antimicotic + 200 mM L-glutamine. The figure shows the basal 340/380 ratio during the time in culture in dissociated carotid body cells. The basal 340/380 ratio did not change during the time in culture between 3 to 24 h, with an average value of 0.65 ± 0.03 ($n = 222$, $N = 4$).

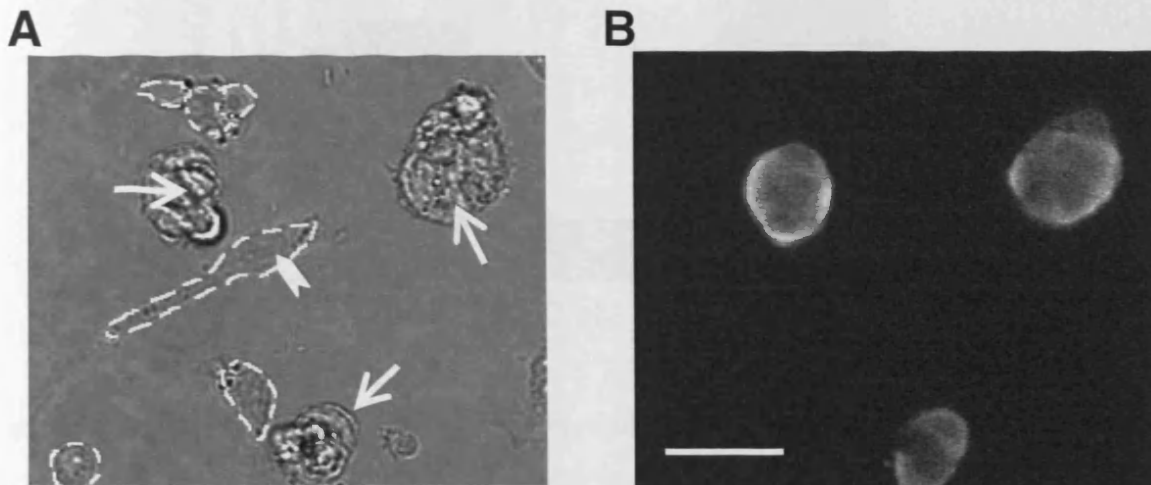


Figure 2.7: Tyrosine hydroxylase immunostaining on cells previously used for Ca^{2+} imaging. A) Light field view containing the recorded cells. B) View of the same field, using FITC fluorescence after the tyrosine hydroxylase staining. The tyrosine hydroxylase staining revealed the presence of three clusters of type 1 cell (arrow). A characteristic type 2 cell, which had a spindle shape and was tyrosine hydroxylase negative, was in the middle of the field (indicated by the arrow end). Scale bar = 10 μ m.

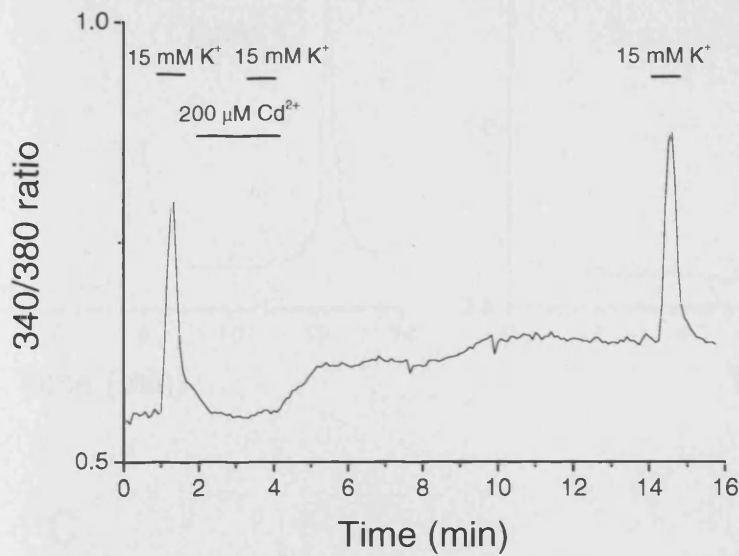
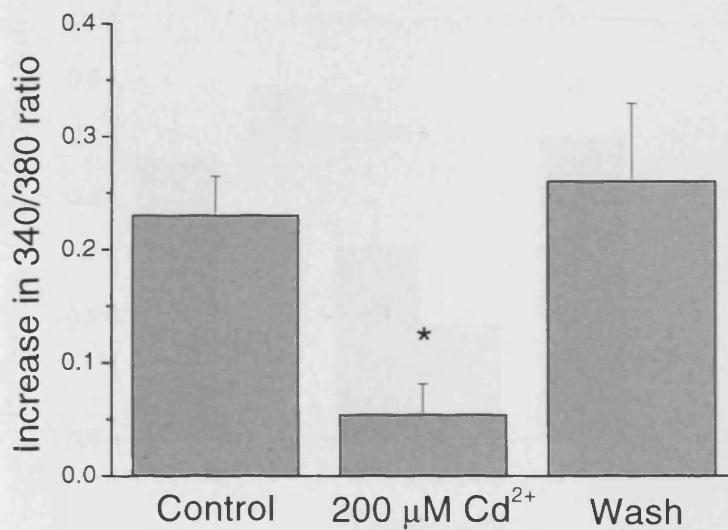
A**B**

Figure 2.8: Effect of Cd²⁺ on Ca²⁺ influx, induced by 15 mM K⁺, in type 1 cells. A) Typical recording of the 340/380 ratio from a type 1 cell. Application of 200 μM Cd²⁺ almost totally suppressed the [Ca²⁺]_i increase induced by high K⁺. The effect of Cd²⁺ was fully reversible. B) Average data, for each cells, of the effect of Cd²⁺ on K⁺ dependent increase in [Ca²⁺]_i (p < 0.01, n = 8, N = 1).

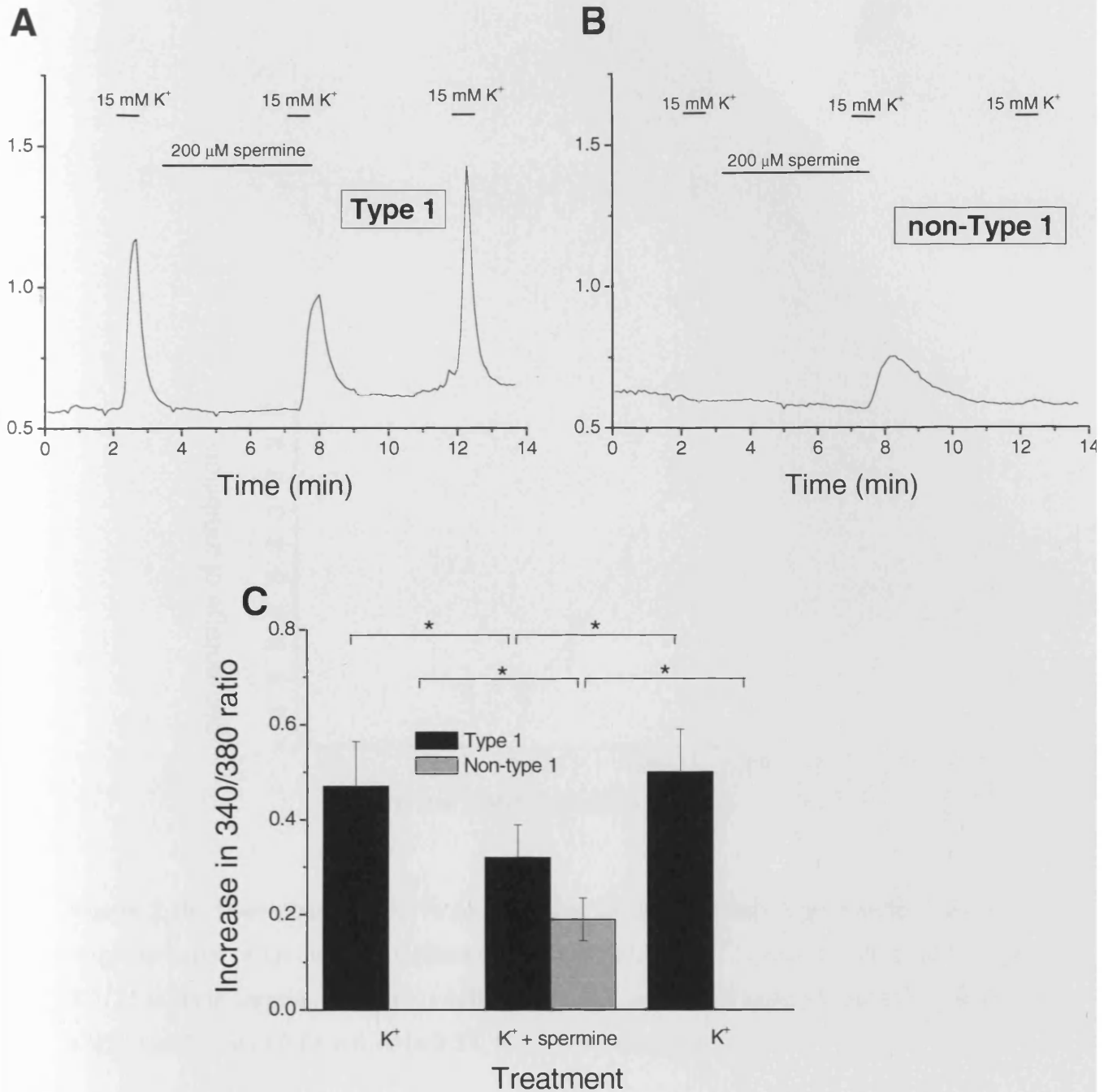


Figure 2.9: Effect of 200 μM spermine on $[\text{Ca}^{2+}]_i$ in dissociated carotid body cells. A) Typical Ca^{2+} imaging recording of a type 1 cell. High K^+ (15 mM) induced an increase in $[\text{Ca}^{2+}]_i$ which was partially inhibited by co-incubation with 200 μM spermine. The spermine effect was reversible, as shown by the full recovery during the 3rd high K^+ stimulation. B) Typical recording of a non-type 1 cell where the cell responded to high K^+ only after co-incubation with 200 μM spermine. C) Bar graph showing the average increase in 340/380 ratio for type 1 ($n = 22$, $N = 3$, $p < 0.01$) and non-type 1 cells ($n = 7$, $N = 2$, $p < 0.01$).

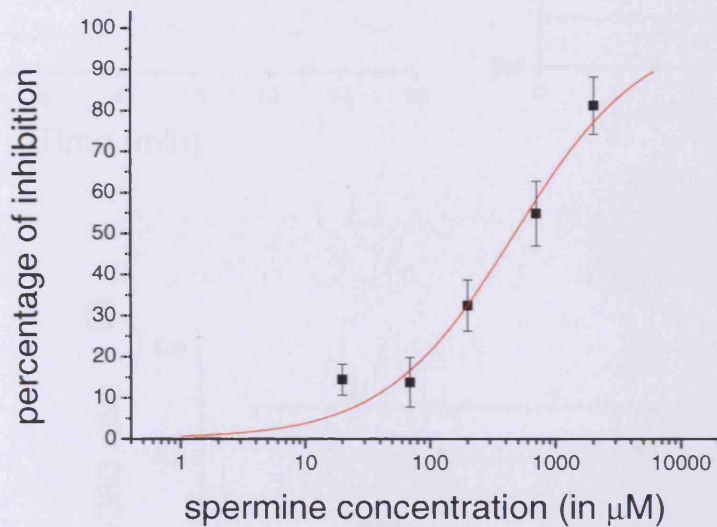


Figure 2.10: Dose-response curve to spermine in carotid body type 1 cells. The dose-response curve of the inhibitory effect of spermine on the $[Ca^{2+}]_i$ increase induced by high K^+ (15 mM) in carotid body type 1 cells gave a IC_{50} calculated at $473.52 \pm 70.27 \mu M$ with a Hill coefficient of 0.84 ± 0.10 ($n \geq 17$, $N \geq 3$ for each point).

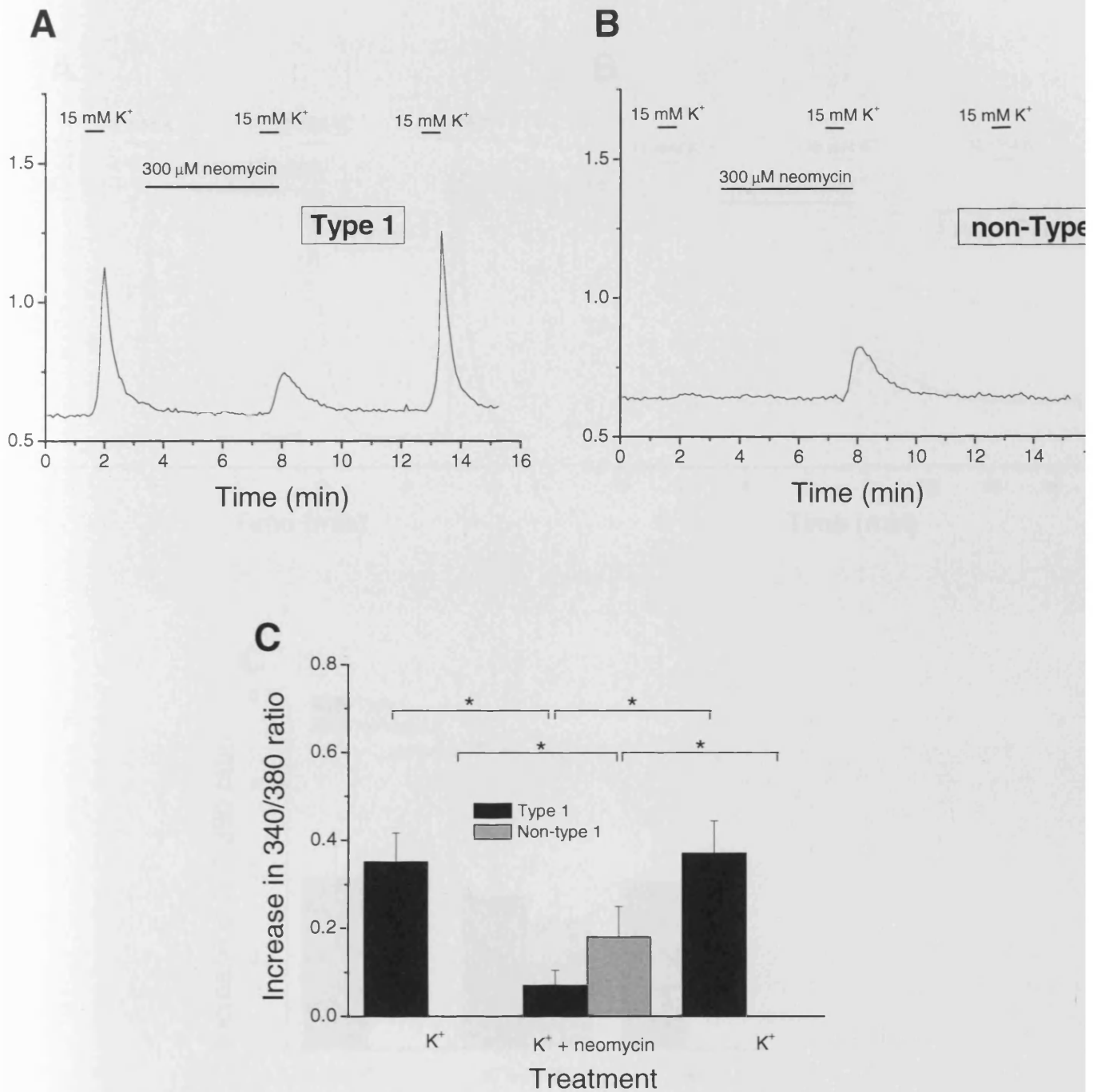


Figure 2.11: Effect of 300 μM neomycin on $[Ca^{2+}]_i$ in dissociated carotid body cells. A) Typical Ca^{2+} imaging recording of a type 1 cell. High K^+ (15 mM) induced an increase in $[Ca^{2+}]_i$ which was inhibited by co-incubation with 300 μM neomycin. The neomycin effect was reversible, as shown by the full recovery during the 3rd high K^+ stimulation. B) Typical recording of a non-type 1 cell where the cell responded to high K^+ only after co-incubation with 300 μM neomycin. C) Bar graph showing the average increase in 340/380 ratio for type 1 ($n = 10$, $N = 4$, $p < 0.01$) and non-type 1 cells ($n = 30$, $N = 4$, $p < 0.01$).

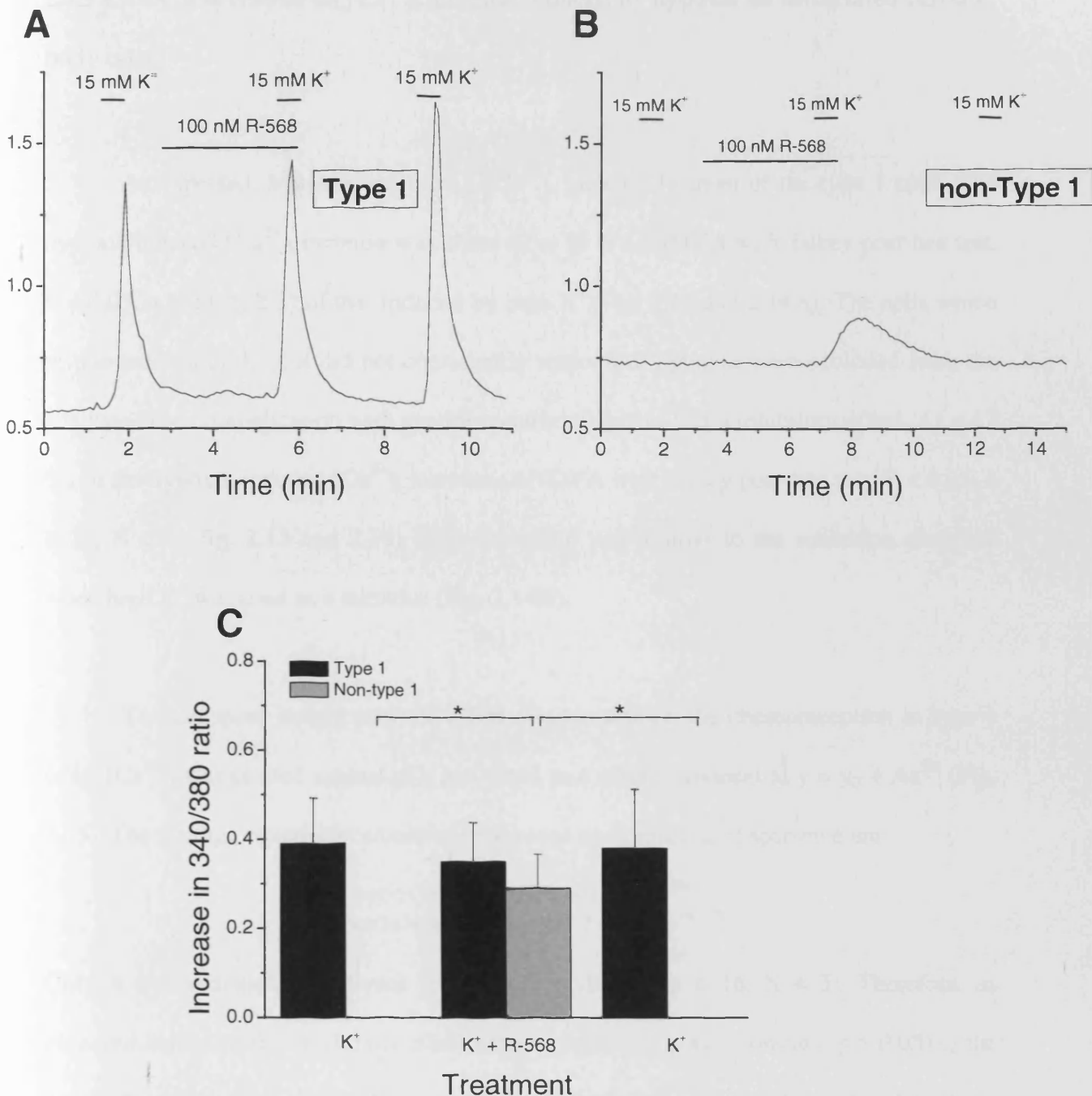


Figure 2.12: Effect of 100 nM R-568 on $[Ca^{2+}]_i$ in dissociated carotid body cells. A) Typical Ca^{2+} imaging recording of a type 1 cell. High K^+ (15 mM) induced an increase in $[Ca^{2+}]_i$ which was not affected by co-incubation with 100 nM R-568. B) Typical recording of a non-type 1 cell where the cell responded to high K^+ only after co-incubation with 100 nM R-568. C) Bar graph showing the average increase in 340/380 ratio for type 1 ($n = 19$, $N = 4$) and non-type 1 cells ($n = 35$, $N = 5$, $p < 0.01$).

2.3.9 Effect of spermine on $[Ca^{2+}]_i$ increase induced by hypoxia on dissociated carotid body cells

As expected, hypoxia triggered a $[Ca^{2+}]_i$ increase in most of the type 1 cells. The hypoxia-induced $[Ca^{2+}]_i$ increase was about 62 ± 15 % (ANOVA with Tukey post-hoc test, $P < 0.05$, $n \geq 23$, $N \geq 3$) of that induced by high K^+ (Fig. 2.13 and 2.14A). The cells which responded to high K^+ but did not consistently respond to hypoxia were excluded from the analyses. The co-application with spermine during hypoxia had an inhibitory effect, 41 ± 12 %, on the hypoxia-induced $[Ca^{2+}]_i$ increase (ANOVA with Tukey post-hoc test, $P < 0.05$, $n \geq 23$, $N \geq 3$, Fig. 2.13 and 2.14). This inhibition was similar to the inhibition observed when high K^+ was used as a stimulus (Fig. 2.14B).

To gain more insight into the effect of spermine on the chemoreception in type 1 cells, $[Ca^{2+}]_i$ was plotted against pO_2 and fitted to a single exponential $y = y_0 + Ae^{Rx}$ (Fig. 2.15). The average equations calculated in absence and presence of spermine are:

$$\begin{aligned} \text{hypoxia: } & y = 0.72 + 0.56e^{-0.08x} \\ \text{hypoxia + sper: } & y = 0.72 + 0.18e^{-0.07x} \end{aligned}$$

Only A was statistically different in the two conditions ($n = 16$, $N = 3$). Therefore, as observed before, spermine did not affect the baseline $[Ca^{2+}]_i$ (y_b is constant, $p > 0.05$) or the sensitivity of the type 1 cells (R is constant, $p > 0.05$) but modified the peak value of the ratio (A decrease with application of spermine, $p < 0.05$).

During the experiments, the temperature oscillated within a 2.77°C range. Since temperature is likely to influence the type 1 chemosensitivity (via the pH), the effect of the changes in temperature on 340/380 ratio was investigated. The average linear

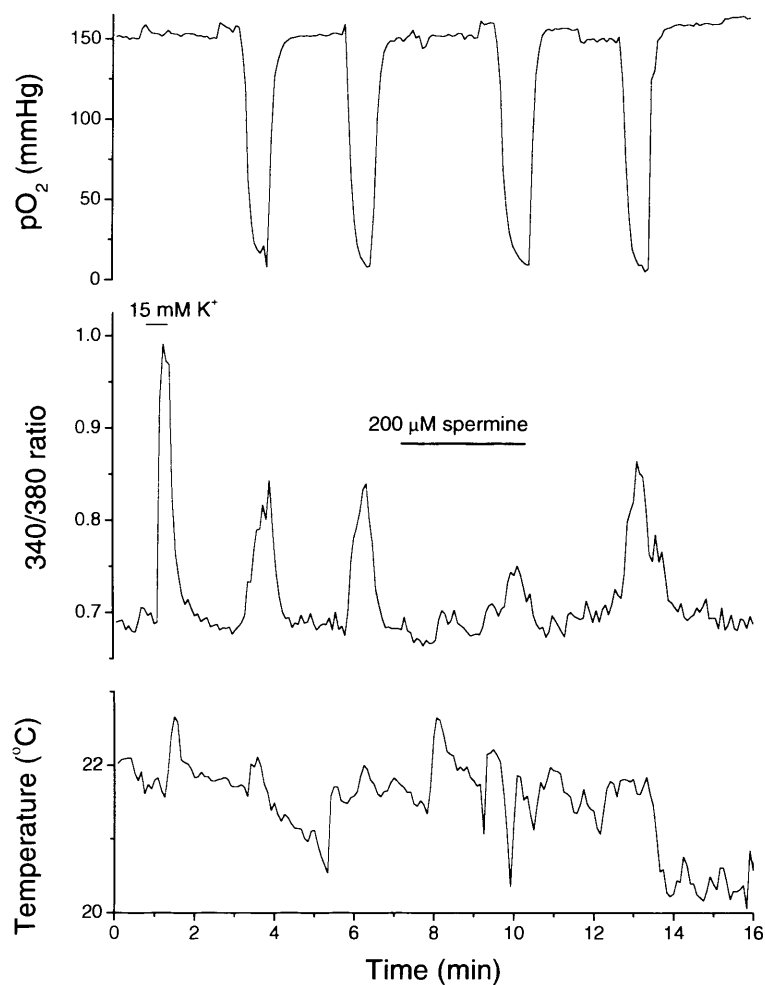


Figure 2.13: Effect of high K⁺, hypoxia and spermine on [Ca²⁺]_i in type 1 cells. Recordings of the pO₂ (top), the 340/380 ratio (middle) and the temperature (bottom). 15 mM K⁺ and hypoxia (pO₂ < 10 mmHg) induced a Ca²⁺ influx in type 1 cell. The application of 200 μM spermine reduced the hypoxia-mediated Ca²⁺ influx.

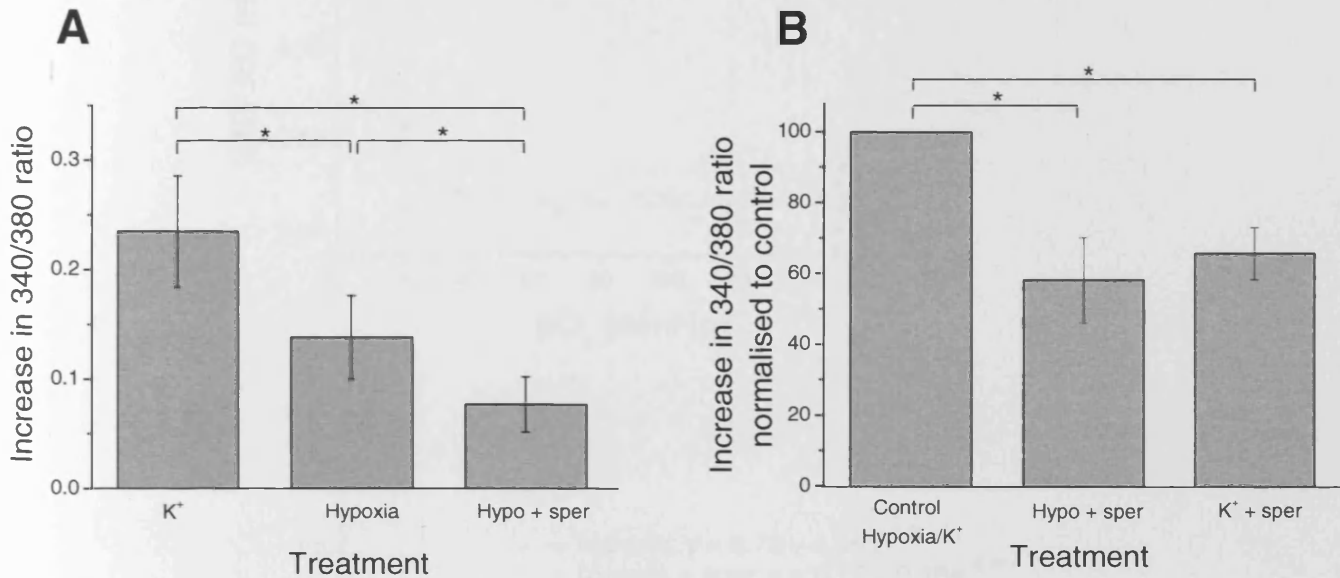


Figure 2.14: Comparison of the inhibitory effect of spermine on Ca²⁺ influx induced either by hypoxia or high K⁺. A) Bar graph showing the average increase in 340/380 ratio induced either by high K⁺, hypoxia or hypoxia + 200 μ M spermine. Hypoxia triggered a Ca²⁺ influx about 62 ± 15 % of the one induced by high K⁺, furthermore, application of 200 μ M spermine reduced the hypoxia-mediated Ca²⁺ influx by 41 ± 12 %. All the conditions were statically different (ANOVA with Tukey test, $P < 0.05$, $n \geq 23$, $N \geq 3$). B) Comparison of the inhibitory effect of 200 μ M spermine on Ca²⁺ influx induced either by high K⁺ (38 ± 7 %, $p < 0.01$, $n = 36$, $N = 4$) or hypoxia (41 ± 12 %, $p < 0.01$, $n \geq 23$, $N \geq 3$). The inhibition induced by spermine was not statistically different between the two conditions.

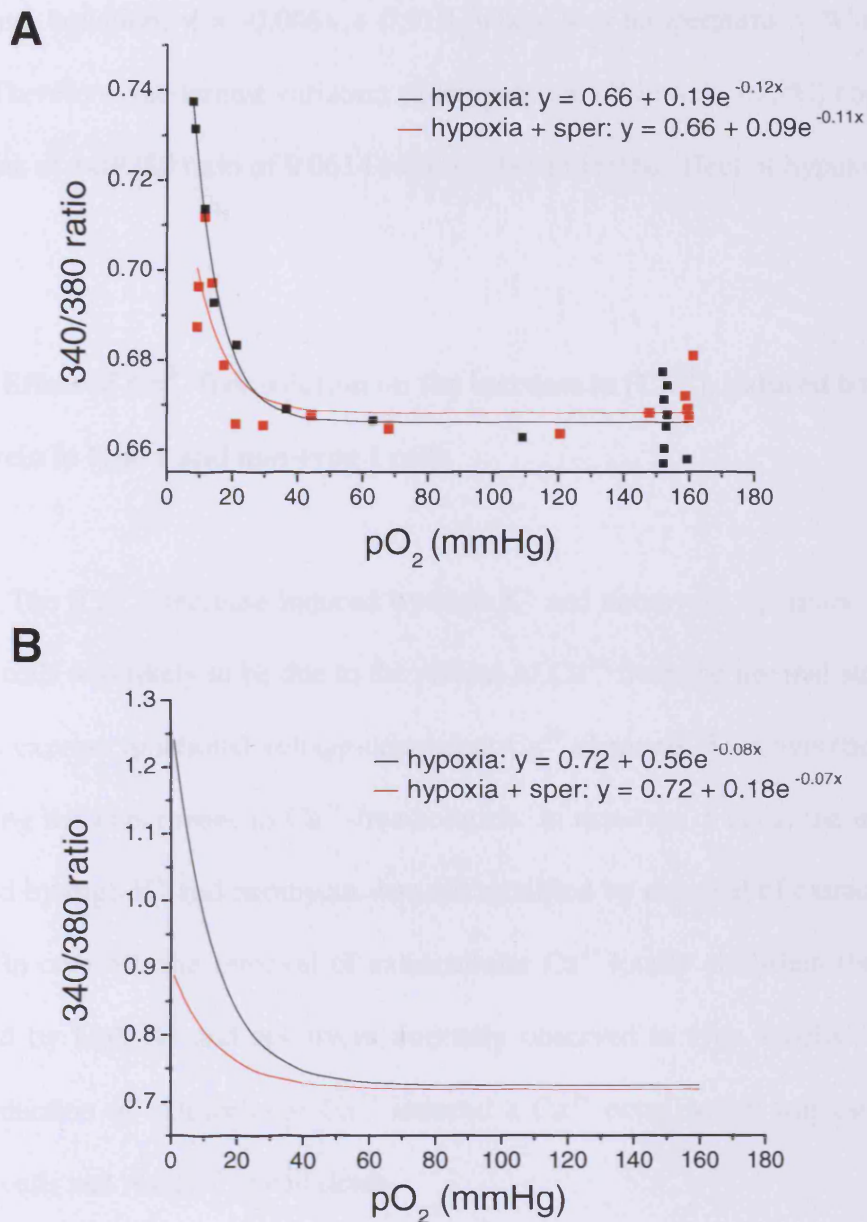


Figure 2.15: Effect of spermine on pO₂ chemosensitivity. A) shows a typical example of the $[Ca^{2+}]_i$ plotted against pO₂, for one cell, in absence (black line) and presence of 200 μ M spermine (red line). The increase in $[Ca^{2+}]_i$ was fitted to a single exponential ($y = y_b + Ae^{Rx}$). Spermine induced a decrease in parameter A only which corresponds to a decrease of the maximum response of type 1 cell without change in sensitivity to pO₂. B) Graph presenting the average calculated curves for $[Ca^{2+}]_i$ in response to change in pO₂ in presence and absence of spermine. The calculated equations are show in the inset, only the parameter A was statistically different between the two conditions ($n = 16$, $N = 3$).

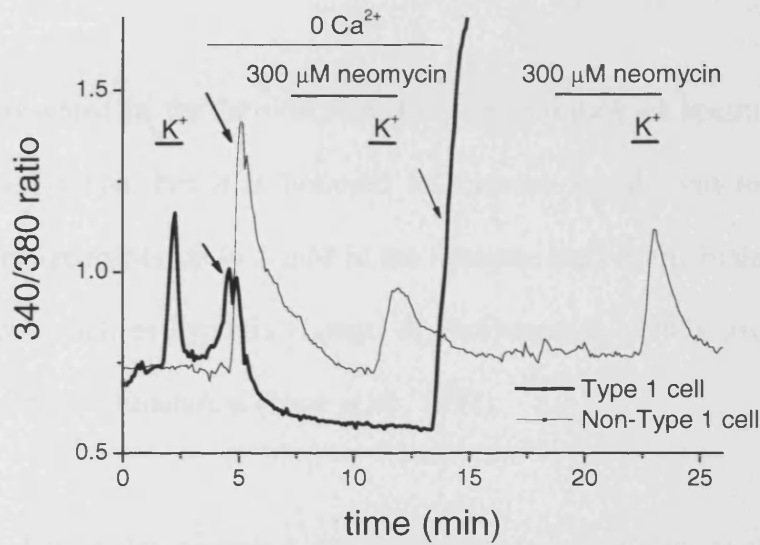
Chapter 2

correlation between the temperature and the 340/380 ratio ($n = 19$, $N = 3$), give the following equation: $y = -0.008x + 0.919$, where $y =$ temperature in $^{\circ}\text{C}$ and $x =$ 340/380 ratio. Therefore, the largest variation of temperature observed (3.75°C) could only induce a variation of 340/380 ratio of 0.0614 which is far under the effect of hypoxia (0.14).

2.3.10 Effect of Ca^{2+} -free solution on the increase in $[\text{Ca}^{2+}]_i$ induced by high K^+ and neomycin in type 1 and non-type 1 cells

The $[\text{Ca}^{2+}]_i$ increase induced by high K^+ and neomycin, spermine or R-568 in non-type 1 cells was likely to be due to the release of Ca^{2+} from the internal stores as these cells did not express functional voltage-dependent Ca^{2+} channels. This hypothesis was tested by repeating the experiment in Ca^{2+} -free solution. In non-type 1 cells, the increase in $[\text{Ca}^{2+}]_i$ induced by high K^+ and neomycin was not modified by removal of extracellular Ca^{2+} (Fig. 2.16). In contrast, the removal of extracellular Ca^{2+} totally abolished the $[\text{Ca}^{2+}]_i$ increase induced by high K^+ and neomycin normally observed in type 1 cells. The removal and reintroduction of extracellular Ca^{2+} induced a Ca^{2+} entry which was especially strong in type 1 cells and resulted in cell death.

A



B

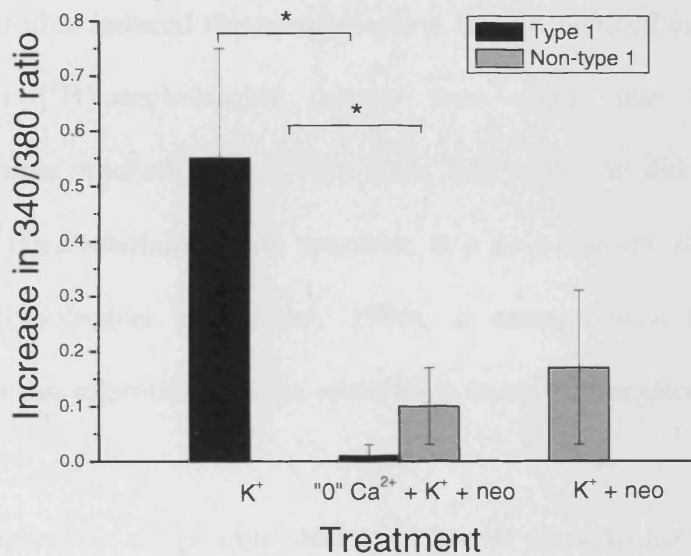


Figure 2.16: Effect of removal of extracellular Ca^{2+} on increase in $[\text{Ca}^{2+}]_i$ induced by high K^+ in dissociated carotid body cells. A) Typical recordings of a type 1 cell (thick trace) and non-type 1 cell (thin trace). Removal of extracellular Ca^{2+} totally inhibited the increase in $[\text{Ca}^{2+}]_i$ observed in type 1 cell but not in non-type 1 cell. Arrows indicate Ca^{2+} entry due to the removal and reintroduction of extracellular Ca^{2+} . B) Average data, type 1 cells ($n = 15$, $N = 1$, t-test $p < 0.01$) and non-type 1 cells ($n = 7$, $N = 1$, t-test $p < 0.01$).

2.4 DISCUSSION

As presented in the introduction, the concentration of spermine in the plasma is within the μM range, but it is believed to increase locally and to reach much higher concentrations (probably up to 1 mM in the synaptic cleft in the brain) under the effect of specific stimuli such as hypoxia (Longo & Packianathan, 1995), growth (Chaisiri *et al.*, 1979) and neuronal stimulation (Fage *et al.*, 1992).

Here, I have demonstrated, for the first time, an inhibitory effect of spermine on catecholamine secretion in rat carotid body. Indeed, the pre-incubation of isolated carotid body with spermine reduced the catecholamine release induced either by 7 % O_2 or high K^+ . Although [^3H]catecholamine release runs down due to the diminution in [^3H]catecholamine stocked, it was very clear that spermine did not affect the baseline secretion of [^3H]catecholamine. As spermine is a poly-cationic molecule with 4 positive charges at physiological pH (Heby, 1986), it cannot cross the plasma membrane, suggesting that this inhibition was the result of an extracellular interaction.

The application of spermine during a hypoxic stimulus leads to an inhibition of the catecholamine secretion. This inhibition could be the result of: spermine-mediated inhibition of oxygen sensing mechanism or; downstream to these mechanisms. The oxygen sensing mechanisms which could be affected by extracellular molecules are the K^+ channels, TASK (Buckler, 1997) and BK_{Ca} (Wyatt & Peers, 1995), especially TASK channels, on which extracellular spermine is known to have an inhibitory effect (Musset *et al.*, 2006). However, this did not seem to be the case here because, in conjunction with

Chapter 2

hypoxia, spermine would have potentiated the closure of TASK channels, and therefore increased the depolarisation and the catecholamine release. The quantitatively similar results obtained using high K^+ as a stimulus rule out the possible interaction of spermine with the oxygen sensing mechanism and as a consequence, spermine has an inhibitory effect downstream to the hypoxic induced depolarisation.

Spermine is a well known agonist of the CaR (Brown *et al.*, 1993), suggesting that the CaR activation might mediate the spermine-evoked inhibition of the hypoxia and K^+ -dependent inhibition of catecholamine release. Two different classes of CaR activators were used to test the involvement of the CaR: a positive allosteric modulator, R-568, and the CaR agonist, neomycin (an aminoglycoside antibiotic). Neomycin is a class I calcimimetics which is not naturally present in the organism but has a strong affinity for the CaR (Urena & Frazao, 2003). The positive controls performed on CaR-HEK293 cells revealed that the activation of CaR by neomycin and R-568 (or S-568) induced the expected increase in $[Ca^{2+}]_i$. The pattern of responses was different between the two type of activators, with neomycin (class I calcimimetic), inducing a strong increase in $[Ca^{2+}]_i$, and the allosteric modulator R-568 (class II calcimimetic), inducing oscillations, confirming that class I and II calcimimetics activate differently the CaR. These differences in activation pattern reflect the fact that class I and II calcimimetics bind to the CaR at distinct sites (Petrel *et al.*, 2004; Hu *et al.*, 2005). Nevertheless, it cannot be exclude that these difference pattern of responses were, in part, due to different concentration of the class I and II calcimimetics. Moreover, the comparison between the effect of R-568 and S-568 in the nM range pointed out that the R-568 was a more potent agonist than the S-568 only at the concentration of 10 nM for the parameters quantified. Below and above these concentrations, the R-568 and S-568 exhibited no stereoselectivity. The response pattern

Chapter 2

obtained with the R-568 correspond to the one describe by Miedlich and al. using the calcimimetic at 0.1 and 10 μM on HEK293 cells stably transfected with the human CaR. For instance, they observed, using Ca^{2+} imaging, a peak-to-peak interval in $[\text{Ca}^{2+}]_i$ oscillation at 69 ± 26 s with 0.1 μM R-568 and a long lasting effect (> 15 min) of the compound after its removal (Miedlich *et al.*, 2002). The peak-to-peak interval with 0.1 μM calculated in the current study was of 86.9 ± 26.5 s (corresponding to a frequency of $0.69 \pm 0.21 \text{ min}^{-1}$) which was within the same order of magnitude as the previously reported values.

In the isolated carotid body, R-568 and neomycin had no effect on the K^+ and hypoxia-evoked catecholamine release, and therefore, the involvement of CaR in mediating the spermine inhibition of catecholamine release seemed unlikely.

As the CaR did not appear to be involved in the inhibition of the $[\text{Ca}^{2+}]_i$ increase by spermine, it seemed likely that it was mediated by an interaction of spermine with voltage-dependent Ca^{2+} channels. These channels link the depolarisation induced by either low pO_2 or high K^+ to release of neurotransmitters via Ca^{2+} influx (Urena *et al.*, 1989). Ca^{2+} imaging was used as a method by which to investigate the effect of spermine, neomycin and R-568 on $[\text{Ca}^{2+}]_i$ homeostasis in dissociated carotid body cells.

Two control experiments were performed in order to ensure that the quality of the preparation was maintained high throughout the experiments. Firstly, the baseline $[\text{Ca}^{2+}]_i$ was used as an indicator of the viability of the cultured cells. These values were constant for up to 25 h in culture. Secondly, since type 1 cells are well known to express voltage-dependent Ca^{2+} channels, the effect of Cd^{2+} (which blocks up to 80 % of the Ca^{2+} influx through voltage-dependent Ca^{2+} channels), was investigated and the cells which were

Chapter 2

recorded were immunostained for tyrosine hydroxylase reactivity at the end of the experiment. As expected, Cd^{2+} blocked the $[\text{Ca}^{2+}]_i$ induced by high K^+ and out of 60 cells expressing voltage-dependent Ca^{2+} channels, 57 were tyrosine hydroxylase positive. These cells were thus identified as type 1. According to their responses to high K^+ and spermine/neomycin/R-568, some tyrosine hydroxylase negative cells were identified, and these cells are referred as non-type 1 cells.

My experiments show that, in type 1 cells, the effect of spermine on $[\text{Ca}^{2+}]_i$ is characterized by an inhibition of the Ca^{2+} influx induced by high K^+ or hypoxia without altering the baseline $[\text{Ca}^{2+}]_i$ value. Therefore, spermine would inhibit catecholamine release by inhibiting the increase in $[\text{Ca}^{2+}]_i$ and the subsequent exocytotic process. The estimated IC_{50} is $\sim 500 \mu\text{M}$ for the inhibitory effect of spermine on $[\text{Ca}^{2+}]_i$ increase induced by high K^+ . Interestingly, this value was in the same range as that observed to inhibit guinea-pig muscle contraction, i.e. $600 \mu\text{M}$ (Kim *et al.*, 2007) suggesting the involvement of a similar mechanism in both tissues (see chapter 4). Moreover, application of spermine did not modify the sensitivity of the type 1 cells to pO_2 but decreased the amplitude of the response induced by a drop in pO_2 . These last data confirmed the fact that spermine did not interact with the pO_2 sensing mechanisms.

R-568 and neomycin had different effects on $[\text{Ca}^{2+}]_i$. Indeed, neomycin did not affect the baseline $[\text{Ca}^{2+}]_i$ but was able to inhibit the Ca^{2+} influx evoked by depolarization. Similarly to spermine, neomycin has been reported to be a non-specific blocker of voltage-dependent Ca^{2+} channels (Parsons *et al.*, 1992; Duarte *et al.*, 1993) (see chapter 4). The experiments performed in the absence of extracellular Ca^{2+} showed that the increase in $[\text{Ca}^{2+}]_i$ observed in presence of neomycin and high K^+ in type 1 cells is only due to a Ca^{2+}

Chapter 2

influx, without any involvement of the intracellular Ca^{2+} stores. The putative release of Ca^{2+} from the internal stores has already been studied by other scientists showing no effect of depletion or blockage of the stores on neurotransmitter release by type 1 cells (Conde *et al.*, 2006a). In type 1 cells, the intracellular Ca^{2+} stores are of very small size and do not play a physiological role, so this point was not investigated furthermore. The R-568 had influence on neither the baseline ratio nor the Ca^{2+} influx induced by high K^+ .

The fact that neomycin reduced the Ca^{2+} influx in Ca^{2+} imaging experiments but not in the catecholamine release experiments could be explained by the different concentrations of extracellular Ca^{2+} used. Indeed, the inhibitory effect of neomycin is dependent on a permissive extracellular Ca^{2+} concentration, as demonstrated by Parsons *et al.* (Parsons *et al.*, 1992). The neomycin concentration has been kept constant in the two types of experiments, whereas the extracellular Ca^{2+} was five fold less in the dissociated cell experiments than in the isolated carotid body experiments. This decrease in extracellular Ca^{2+} could account for the differences in neomycin response in the two types of experiments. After having elucidated the inhibitory mechanism induced by spermine and neomycin, it appears that it would have been more appropriate to use a lower, and therefore permissive Ca^{2+} concentration (such as 0.5 mM) in the isolated carotid body experiment to reveal the inhibitory effect of neomycin.

In non-type 1 cells, the application of spermine, neomycin and R-568 alone had no effect under baseline conditions. Nevertheless, in some cells, the application of these compounds in association with high K^+ induced an increase in $[\text{Ca}^{2+}]_i$. The $[\text{Ca}^{2+}]_i$ increase induced by neomycin and high K^+ was strictly independent of the extracellular Ca^{2+} and, therefore, came from the internal stores. These data suggested the activation of intracellular

Chapter 2

pathway. This Ca^{2+} release from the internal store dependent on depolarisation and on spermine, neomycin or R-568 has never been reported before. Interestingly, under depolarisation, some GPCR, muscarinic receptor, mGLUR1 or purinergic P2Y1, show the equivalent of gating current suggesting the induction of configurational change (Ben-Chaim *et al.*, 2006; Stanfield, 2006). This configurational change has been shown to modify the affinity of such receptor for their agonist (Martinez-Pinna *et al.*, 2004). Nevertheless, none of them present an agonist affinity strictly dependent on depolarisation as it is the case here. The modulation of the affinity of GPCR for their agonist by depolarisation lead to the hypothesis that, due to depolarisation, spermine, neomycin or R-568 may activate a GPCR, different for CaR, and induce Ca^{2+} release from the internal store in non-type 1 cell.

2.5 CONCLUSION

The experiments using whole isolated carotid bodies for quantification of catecholamine release have shown an inhibitory effect of spermine on the catecholamine secretion evoked either by hypoxia and high K^+ . The data lead to the conclusion that the spermine inhibited the catecholamine release downstream to the oxygen sensing mechanisms. As spermine inhibits the neurotransmitter release, it appears clearly that the CaR is not involved in stimulating the neurotransmitter release, refuting the first tested hypothesis of a Ca^{2+} release from the intracellular stores. In addition, the putative role of the CaR in mediating the spermine inhibition has been tested using an alternative agonist of the CaR, neomycin and an allosteric modulator, R-568. The application of these two compounds did not mimic the spermine inhibition observed during hypoxia or high K^+ stimulation, suggesting that the CaR is not involved in mediating the spermine inhibition. The reproduction of the experiments with knock out mice for CaR would allow to rule out completely the involvement of the CaR in mediating spermine inhibition of Ca^{2+} influx in type 1 cells.

Then, the recording of the $[Ca^{2+}]_i$ in type 1 cells demonstrated that spermine inhibits the Ca^{2+} influx induced by high K^+ . Moreover, the experiments revealed the property of another cell type, tyrosine hydroxylase negative cells, which reacted to co-application of high K^+ and spermine, neomycin or R-568 by a release of Ca^{2+} from the internal stores.

The spermine inhibition of catecholamine release was therefore due to the inhibition of the Ca^{2+} influx, which couples the depolarization to neurotransmitter release. Nevertheless, it is still unknown if the spermine inhibited directly or indirectly the voltage-

Chapter 2

dependent Ca^{2+} channels. The voltage-dependent Ca^{2+} channels expressed in rat type 1 cells will then be identified (Chapter 3). The knowledge of the expression of voltage-dependent Ca^{2+} channel will allow the specific testing of the effects of spermine on the channels expressed in type 1 cell. It will also confirm or refute the hypothesis of an inhibitory effect of spermine on voltage-dependent Ca^{2+} channel in type 1 cells (Chapter 4).

CHAPTER 3

IDENTIFICATION OF EXPRESSION OF VOLTAGE-DEPENDENT Ca^{2+} CHANNELS

AND

Ca^{2+} -SENSING RECEPTOR IN RAT CAROTID BODY

3.1 INTRODUCTION

Changes in O₂, CO₂ and pH levels lead to the release of the neurotransmitters, dopamine, ACh, adrenaline and ATP from carotid body type 1 cells (Gonzalez *et al.*, 1994). The three main classes of ion channels believed to be involved in this process are: voltage-gated K⁺ channels, BK_{Ca} channels (pO₂ and pCO₂ sensing); background K⁺ channels (TASK-like, pO₂ and pH sensing); and ASIC (pH sensing). Ion channel modulations by these stimuli induce membrane depolarization by a decrease in K⁺ conductance (BK_{Ca} and TASK-like) or an increase in Na⁺ conductance (ASIC). The induced depolarization activates voltage-dependent Ca²⁺ channels, which in turn results in Ca²⁺-dependent neurotransmitter release.

In rat carotid body, previous studies have shown the expression of L- and N-type channels (Buckler & Vaughan-Jones, 1994c; Jiang & Eyzaguirre, 2004), whereas P/Q-type are probably not expressed (as ω-agatoxin has no effect on Ca²⁺ influx (Peers *et al.*, 1996)). In addition, the existence of T-type channels has never been reported.

To attempt to elucidate the molecular mechanisms mediating the spermine and neomycin inhibition of Ca²⁺ influx induced by high K⁺ or hypoxia in type 1 cells (reported in chapter 2), the molecular identities of the voltage-dependent Ca²⁺ channels expressed in rat type 1 cells was first investigated. This was necessary because most reports have described only functional evidence for the expression of L- and N-type Ca²⁺ channels which does not elucidate the specific genes and gene products underlying the responses.

Chapter 3

Indeed, the L- and T-type families comprise, respectively, four ($Ca_v1.1$, $Ca_v1.2$, $Ca_v1.3$ and $Ca_v1.4$) and three ($Ca_v3.1$, $Ca_v3.2$ and $Ca_v3.3$) genes (Doering & Zamponi, 2003).

The aim of the experiments, which have not yet been published, was to identify, by molecular biology (RT-PCR) and immunohistochemistry, the voltage-dependent Ca^{2+} channel genes and proteins expressed in rat carotid body type 1 cells. Moreover, to gain evidence in support of functional observation, the expression of CaR was investigated.

3.2 MATERIALS AND METHODS

3.2.1 Reverse transcription and polymerase chain reaction (RT-PCR)

3.2.1.1 Total RNA extraction from carotid body, brain and eye

Total RNA was extracted from carotid bodies, brain and eye. Carotid bodies were processed using RNeasy Micro kit (Qiagen, Crawley, U.K.) to extract RNA from small samples. Briefly, carotid bifurcations were removed from three anesthetized rats (with sodium pentobarbital, 60 mg/kg, IP Euthatal, Merial, Essex, U.K.) according to Home Office regulations and placed in cold RNAlater (Sigma, Dorset, U.K.) until the 6 carotid bodies were isolated and cleaned of surrounding tissues. Immediately after their isolation, carotid bodies were homogenized with a pestle in 350 μ l of buffer containing guanidine thiocyanate (buffer RLT) and the solution homogenized through a Qiashredder Spin Column (Qiagen, Crawley, U.K.) at 13,400 g. To the lysate was added 70 % ethanol and the mixture was applied to a silica-gel-membrane to bind the RNA (RNeasy MinElute Spin column, Qiagen) and centrifuged at 11,000 g. The column, containing the RNA, was washed with 350 μ l of buffer RW1 and treated with 30 units of DNase I at room temperature for 15 min. Finally, the column was washed again with 500 μ l buffer RPE and 80 % alcohol before being eluted with nuclease-free water (Ambion, Warrington, U.K.).

Rat eyes (2) and brain (about 100 mg of cortex) isolated from the same rats and kept in RNAlater, were homogenized in Trizol (1 ml, Invitrogen, Paisley, Strathclyde,

Chapter 3

U.K.), following manufacturer's instruction) using a pestle. The samples were incubated at room temperature for 5 min to allow the dissociation of nucleotide complexes. The RNA was extracted by addition of chloroform (Sigma, 0.2 ml, ratio 1:5) followed by 3 min incubation at room temperature. A centrifugation step at 12,000 g (15 min at 4°C), allowed separation of the RNA. Following centrifugation, the upper aqueous phase, containing the RNA, was transferred to a new tube and incubated with 0.5 ml of isopropyl alcohol (Fisher, Loughborough, U.K.) for 10 min at room temperature in order to precipitate the RNA. RNA was then pelleted by centrifugation at 12,000 g for 10 min at 4°C, washed with 75 % alcohol and dissolved in nuclease-free water (Ambion).

The amount and purity of the RNA obtained were checked with a spectrophotometer (SANYO SP65 UV/VIS, Watford, U.K.). The absorbance produced by the RNA and proteins were calculated at 260 and 280 nm, respectively, (with an absorbance of 1 optic density = 40 µg/ml for the RNA) allowing quantifying the ratio RNA/proteins and the concentration of RNA. Only the preparations with 260/280 ratio \geq 1.7 were used.

3.2.1.2 Reverse transcription

For the RT-PCR reaction, 1 µg of total RNA from the brain and eye or all the total RNA extracted from carotid body was used for the reverse synthesis of single-stranded cDNA using the Superscript III (Invitrogen). The reaction solution contained 1 µg of oligo dT (Promega), 1 µl of dNTP mix at 10 mM (Bioline, London, U.K.) and 1 µg of RNA brought up to a final volume of 13 µl with H₂O. This solution was first heated at 65°C for 5 min to allow the association of the oligo dT with the poly A tails of the RNA. Then, 4 µl of 5X first-strand buffer (250 mM Tris-HCl, 375 mM KCl and 15 mM MgCl₂, Invitrogen), 1

Chapter 3

μl of 0.1 M DTT (dithiothreitol, Invitrogen), 1 μl of RNase inhibitor (RNasin Plus RNase Inhibitor, 40 u/ μl , Promega, Southampton, U.K.) and 1 μl of Superscript III RT (200 u/ μl , Invitrogen) were added. The reaction mixture was incubated at 50°C for 30 min and the reaction was stopped by incubating the samples at 75°C for 15 min.

3.2.1.3 Polymerase chain reaction

2 μl of reverse-transcribed samples were used for the PCR reactions using the Premix Ex-taq polymerase kit (Lonza, Basel, Switzerland). The Premix Ex-taq polymerase was used with a final reaction volume of 50 μl giving the following concentrations: 25 mM N-tris(hydroxymethyl)methyl-3-aminopropanesulfonic acid (TAPS, pH 9.5 at 25°C), 50 mM KCl, 2 mM MgCl₂, 1 mM 2-mercaptoethanol and 200 μM of each dNTP (dATP, dGTP, dCTP, dTTP). 35 cycles were performed, consisting of: denaturation at 95°C for 1 min, annealing temperature adjusted according to primers (see Table 3.1) for 1 min and extension at 72°C for 1 min. The primers, the genes targeted and the size of their amplicons are listed in table 3.1. Primers were used at the final concentration of 4 μM . All primers, except for the positive controls tyrosine hydroxylase and β -actin, were intron-spanning and were tested on tissues known to express the specific mRNAs as positive control. The primers were designed against conserved parts of the cDNA, avoiding regions subject to splicing. The PCR conditions were optimised with positive control tissues in which each channel is known to be abundantly expressed, the eye for Ca_v1.1 and in the brain for all other channels. PCR products were visualized by ethidium bromide staining on 2 % agarose gel and their sizes evaluated by comparison with DNA ladder (hyperladder IV, Bioline). All products obtained from the carotid body amplification were sequenced. Negative controls consisted of samples in which the reverse transcriptase was omitted for

the first strand synthesis and blank refers to samples in which the cDNA template was replaced with H₂O. The expression of housekeeping genes, β -actin, and of the carotid body marker, tyrosine hydroxylase, were detected as positive control to attest the presence of viable cDNA after the reverse-transcription.

3.2.1.4 Sequencing of the PCR products

The PCR products were extracted from the agarose gel according to the protocol using a QIAquick gel extraction kit (Qiagen). Briefly, the agarose was cut around the amplified product and dissolved in QG buffer (300 μ l/100mg of agarose gel) containing guanidine thiocyanate and bringing the pH below 7.5 to allow binding the DNA to the column (low pH and high salt condition). The solution was incubated for 10 min at 50°C and vortexed every 2 to 3 min. Then, the solution was applied to a QIAquick column (silica membrane) and centrifuged for 1 min at 17, 900 g. The column was washed from any trace of agarose twice by adding 0.5 ml of QG buffer followed by a centrifugation step (1 min at 17, 900 g) and then by adding 0.75 ml of PE buffer with a centrifugation for 1 min at 17, 900 g. The residual ethanol present in the PE buffer was evaporated by 1 min of centrifugation after the solution has been removed. The DNA was eluted (in low salt) with 50 μ l nuclease-free water (Ambion, Warrington, UK) by 1 min centrifugation at 17, 900 g.

Chapter 3

Gene bank	mRNA	Primer sequences 5'-3'	CG %	Tm/°C	Amplicon size, bp
AF110178	CaR	F ₁ : ACCTGCTTACCCGGAAGAGGGCTTT	56	56.0	582
		R ₁ : GCACAAAGGCGGTCAGGAAAATGCC	56		
		F ₂ : CTGCTTTGAGTGTGTGGAGT	50	62.5	759
		R ₂ : GAAGATGAGCATGCTGAAGG	50		
NM012517	Ca _v 1.2 (L-type)	F : GGAGCCCGAGATGCCTGTG	68	58.3	433
		R : AACGTTGATCGCGCTGGACTGAA	52		
NM017298	Ca _v 1.3 (L-type)	F : CTGCCCGTGCCCTCTTCTGTTTAT	54	56.5	512
		R : GAGGAGGGGGACCATGGCTTTTAT	54		
DQ393415	Ca _v 1.4 (L-type)	F : CCGCCGGGCAGTCAAGT	71	58.5	531
		R : TGGGGGAAGGTATCAAAGGTG	52		
NM012918	Ca _v 2.1 (P/Q-type)	F : GACACGGCCTTACTTCCACTCTT	52	58.0	576
		R : GCTGCCTCTTCCTCTTCTGTTC	55		
NM147141	Ca _v 2.2 (N-type)	F : CCCGTGCGGACCGACTCATT	74	59.3	504
		R : CCTTGGCTGGGCTTCTACCT	67		
NM019294	Ca _v 2.3 (R-type)	F : TACAATACCAATGATGCCTTA	38	55.0	696
		R : GACCCCAAATCAAAGCAGT	44		
NM031601	Ca _v 3.1 (T-type)	F : GCGGCGGTGAGGAGAAGCGACTAC	67	61.0	425
		R : GGGGTTGATGGGCAGCGACAGATT	58		
AF290213	Ca _v 3.2 (T-type)	F : TCGGCGCCGGGAGGAGAAAC	70	61.6	420
		R : ATGCGGATGATGGTGGGATTGATG	50		
AF290214	Ca _v 3.3 (T-type)	F : GCGACCGCGGGGAGGACGAG	80	61.7	485
		R : AGGACCCGGAGGACCCCAAGAATC	67		
NM031144	β-actin	F : TCCTAGCACCATGAAGATC	47	54.0	190
		R : AAACGCAGCTCAGTAACAG	47		
NM012740	Tyrosine hydroxylase	F : CCCAGCGCCCCCTCGCCACAGC	74	60.0	234
		R : GCATTCCCATCCCTCTCCTCAA	62		

Table 3.1: Primers used for the amplification of CaR, voltage-dependent Ca²⁺ channels, β-actin and tyrosine hydroxylase transcripts by RT-PCR. From left to right, columns show the Gene Bank accession number, the mRNA targeted, the primer sequence form 5' to 3', the percentage in GC, the annealing temperature and the length of the amplicon in BP. All the primers were intron-spanning excepted for tyrosine hydroxylase and β-actin.

Chapter 3

The PCR products were then ligated in the pGEM®-T vector (Promega) by preparing the following solution: 5 µl of T4 DNA ligation buffer, 1 µl of pGEM®-T vector, 3.5 µl of PCR products, 1 µl of T4 ligase. The solution was incubated for 1 h at room temperature and stopped by at step at 4°C.

Bacteria (α -select, Bioline) were then transformed with the plasmid containing the PCR products. 50 µl of bacteria were incubated with 10 ng of plasmid for 30 min on ice, then a heat shock was applied (42°C during 50 s) and the bacteria were placed back on ice for 2 min. The bacteria were then growth in super optimal broth with catabolite repression (SOC) medium containing (in mM): 2 % Trypton Peptone, 0.5 % yeast extract, 10 NaCl, 2.5 KCl, 10 MgCl₂, 10 MgSO₄, 20 glucose for 1 h. Afterwards, the bacteria were spread on a pre-warmed LB agar (Sigma) plate supplemented with 100 µg/ml ampicillin (Sigma) and incubated for 12 h at 37.5°C. Then, three colonies, for each insert, were sent for sequencing

3.2.2 Immunohistochemistry on rat carotid body sections

The detection of specific gene expression in the carotid body by RT-PCR demonstrated that the Ca_v1.2 and Ca_v2.2 were expressed but did not provide information on the cell types expressing them. Therefore, immunostaining against the proteins encoded by the mRNA detected by RT-PCR were performed to determine the cell types expressing them and/or to confirm the PCR results at the protein level.

Chapter 3

3.2.2.1 Fixation and tissue preparation

According to the Home Office regulations, adult Wistar rats (250-300 g) were deeply anaesthetized with Euthatal (Merial) 60 mg/kg, IP. After the opening of the thoracic cavity, the rats were firstly transcidentally perfused through the left ventricle with 50 ml of a solution containing 10 unit/ml of heparin in PBS (containing, in mM: 0.14 NaCl, 0.84 Na₂HPO₄ and 0.16 NaHPO₄H₂O, pH 7.4) at a speed of 8 ml/min using a peristaltic pump (Watson Marlow 101U, Birmingham, U.K.) to flush the blood. A second perfusion was then performed with 75-100 ml of ice-cold fixative solution consisting of 4 % paraformaldehyde in PBS (pH 7.4) for 4-5 min at a flow-rate of 20 ml/min. At the end of the perfusion, the carotid bifurcation and brain were removed and placed in 30 % sucrose solution in PBS at 4 °C for 24 h. The carotid bifurcation/cervical superior ganglion was cleaned of surrounding tissue and fat before freezing and subsequent embedding in OCT compound (Tissue-Tek, Sakura Finetek, Torrance, USA). 4 µm sections were cut with a cryostat (OTF5000 Bright, Huntingdon, U.K.) at -25 °C and placed on Superfrost-plus slides (VWR International, Lutterworth, U.K.). During the cutting process, the carotid bodies were visualised using eosin-Y coloration, which stains the cytoplasm, collagen and muscle fibres. The sections were kept at -80 °C until use.

3.2.2.2 Immunohistochemistry

For immunohistochemistry, the sections were processed as follows: 5 min rehydration in PBS, 5 min in 1 % SDS in PBS to permeabilise the sections, 2 x 5 min wash in PBS and 1 h in solution A containing: 5 % Seablock (Eastcoast, Stratech Scientific, Soham, U.K.) in PBS, to prevent non-specific binding of the primary antibody.

Chapter 3

Then, the primary antibodies were incubated at the appropriate dilution overnight at 4 °C: tyrosine hydroxylase (1/1000, Sigma), Ca_v1.2 (1/200, Alomone, Buckingham, U.K.), Ca_v1.3 (1/200, Sigma), Ca_v2.1 (1/200 Alomone), Ca_v2.2 (1/100, Alomone), Ca_v2.3 (1/200, Santa Cruz, Heidelberg, Germany) and CaR (1/200, USbiological, Massachusetts, USA). All antibodies were diluted in solution A. After incubation with the primary antibodies, the slides were washed 3 x 5 min in PBS. The secondary antibodies (FITC-conjugated goat anti-mouse, Molecular Probes, Invitrogen, and TRITC-conjugated goat anti-rabbit, Molecular Probes) were diluted 1/1000 in solution A, the slides were incubated for 1 h at room temperature and then washed 3 x 5 min with PBS before mounting.

Negative controls were made by omitting the primary antibodies or by pre-incubating the primary antibodies with an excess of the antigenic peptide using the following protocol. The primary antibody was incubated overnight at 4 °C, at the concentration used for the staining, with the antigenic peptide at a ratio $1/2 w_{\text{antibody}}/w_{\text{peptide}}$ diluted in solution A. The antibodies linked to the peptide were then spun down at 15,000 g for 15 min and the supernatant was used as a primary antibody solution.

As the positive stainings obtained were specifically localised in type 1 cells or in nerve endings, it was assumed that the staining was not due to non-selective immunoglobulin binding and no control was done using non-selective rabbit/mouse immunoglobulin.

The slides were mounted onto glass coverslips using Vectashield (Vector, Orton, U.K.) mounting medium and observed within the next 24 h.

Chapter 3

Observations were carried out with a Leica DM6000B confocal upright microscope linked to a laser scan head (Leica, Bucks, U.K.). The laser scanning system, TCS SP2 AOBS, comprised one diode, one argon and two helium neon lasers allowing respectively the excitation of DAPI (405 nm), Alexa-488 and FITC (488 nm), Alexa-546 and TRITC (543 nm). Each dye was excited separately and sequentially to avoid interference. The entire setup was controlled with a Pentium PC running Leica Confocal Software (Version 2.61). Images were acquired and analysed using the same software. Pictures were taken with a 60x-oil immersion objective. Each picture is the average value of 6 pictures of the same place. The z-scans were done by performing a scan every 0.7 μm with the pictures for the different antibodies taken sequentially for each stack, starting by the weaker staining (usually FITC) and finishing with DAPI staining.

3.3 RESULTS

3.3.1 Positive control for tyrosine hydroxylase and β -actin

To assess the quality of the reverse-transcription, the presence of a housekeeping gene was detected. This was β -actin in the brain, eye and carotid body. In addition, a marker of type 1 cells, tyrosine hydroxylase, was also amplified from the carotid body mRNA. Figure 3.1 shows a typical example of tyrosine hydroxylase amplification, with an amplicon size of 234 bp (A), whereas figure 3.1B presents a β -actin amplification from the carotid body and eye, with bands at 190 bp, as expected. These products confirm the presence of bona fide tyrosine hydroxylase and carotid body transcripts in carotid body cDNA preparation.

3.3.2 Identification of L-type Ca^{2+} channel expressions in carotid body tissue

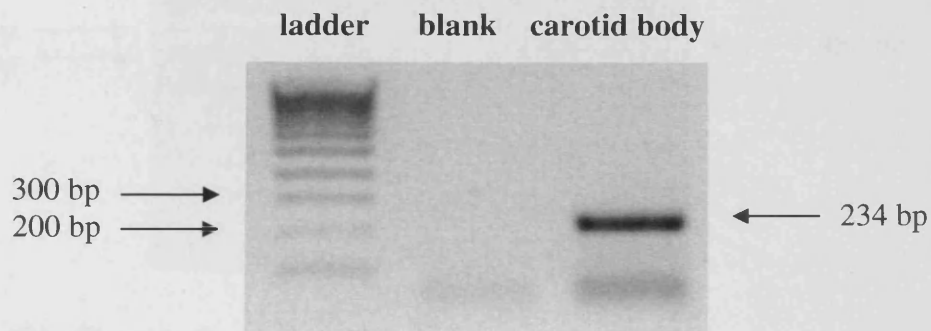
3.3.2.1 RT-PCR of L-type Ca^{2+} channels

The L-type Ca^{2+} channel family comprises four genes: $\text{Ca}_v1.1$, $\text{Ca}_v1.2$, $\text{Ca}_v1.3$ and $\text{Ca}_v1.4$. $\text{Ca}_v1.1$ is located only in the transverse tubules of skeletal muscle and is coupled to ryanodine receptors (Altafaj *et al.*, 2005), where it plays a role in excitation contraction coupling. Moreover, it has never been found to be expressed in another cell type, therefore no attempt was made to amplify $\text{Ca}_v1.1$ from carotid body. $\text{Ca}_v1.4$ is generally thought to be especially expressed in the retina (Soong *et al.*, 1993). Nevertheless, McRory *et al.* have reported its expression in other tissues such as adrenal gland, bone marrow, spinal cord,

Chapter 3

muscle and spleen (McRory *et al.*, 2004); so its expression in the carotid body was assessed. Ca_v1.2 and Ca_v1.3 are widely expressed in many cell types, including endocrine glands (Catterall *et al.*, 2003) and are, therefore, very likely to be expressed in carotid body type 1 cells. The PCR results showed that Ca_v1.2 was detectable in carotid body with a sequenced amplicon of 433 bp (Fig. 3.2A). In contrast, Ca_v1.3 (Fig. 3.2B) and Ca_v1.4 (Fig. 3.2C) could not be amplified while the positive controls, brain and eye, gave amplicons at the expected size of 512 and 531 bp, respectively. The sequencing of the PCR products obtained in the carotid body for Ca_v1.2 showed 100 % homology with the sequence targeted in the Ca_v1.2 rat mRNA obtained from Gene Bank (Fig. 3.3).

A) Tyrosine hydroxylase



B) β -actin

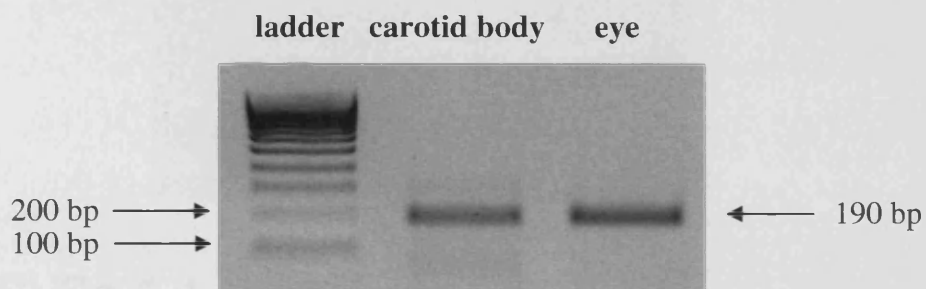


Figure 3.1: Positive controls for the reverse-transcription from isolated rat carotid body mRNA. Typical examples of control PCRs run for amplification of tyrosine hydroxylase in carotid body (A), an enzyme marker of type 1 cells; and of β -actin, a house keeping gene (B). The amplicons were of the expected size for both tyrosine hydroxylase (234 bp) and for β -actin (190 bp). The ladder shows one band every 100 bp.

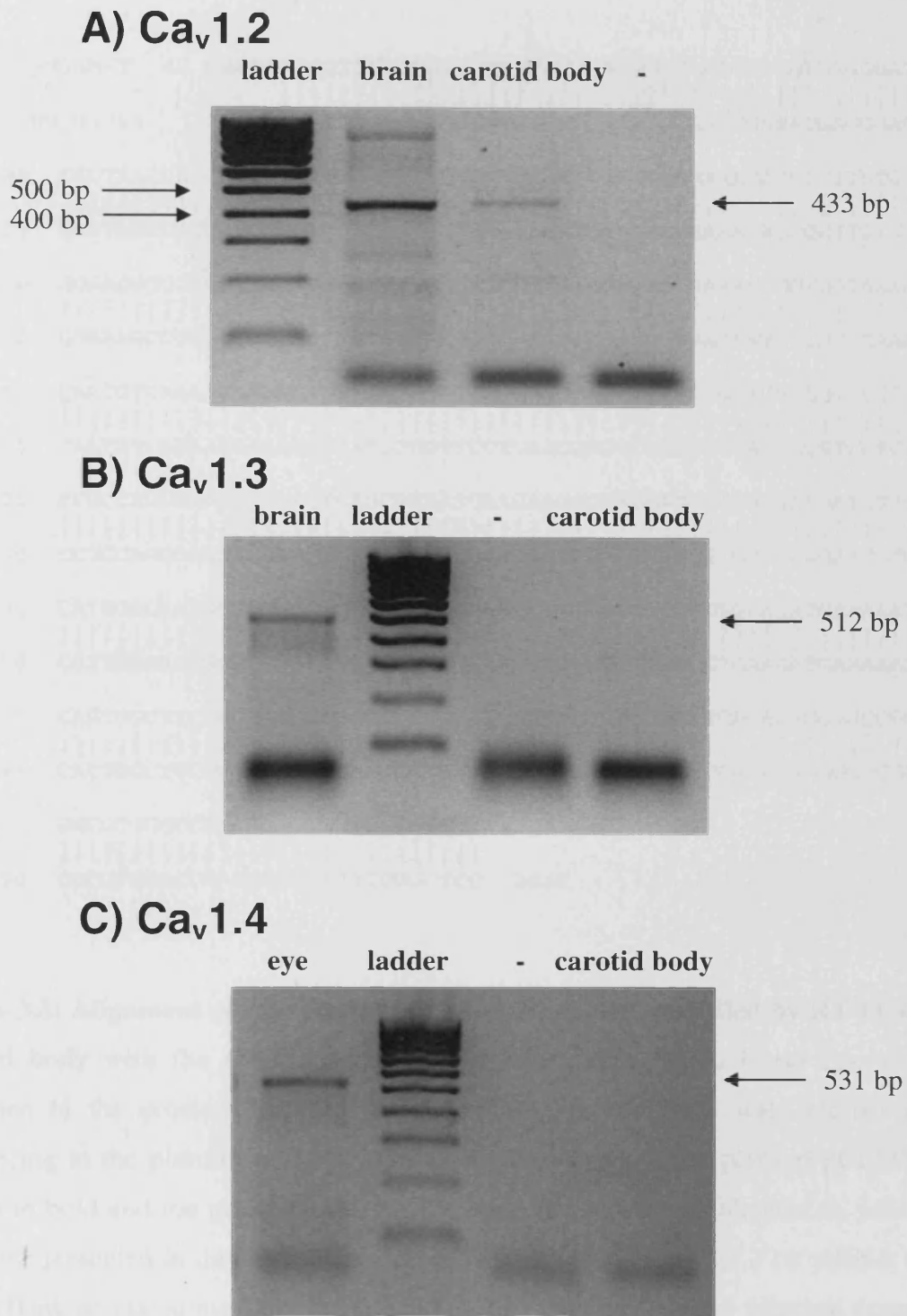


Figure 3.2: Expression of $Ca_v1.2$ but not $Ca_v1.3$ and $Ca_v1.4$ mRNAs in carotid body. $Ca_v1.2$ was amplified from the carotid body and the brain with an amplicon of the expected size of 433 bp (A). In contrast, $Ca_v1.3$ and $Ca_v1.4$ could not be detected in the carotid body while it was expressed in brain or eye samples, at 512 and 531 bp respectively (B and C). $Ca_v1.2$ is, therefore, the only L-type Ca^{2+} channel expressed in carotid body. (-) consists of total mRNA extraction sample in which the reverse transcriptase has been omitted. The ladder shows one band every 100 bp.

```

pGEM-T 40 GNATTAACGTTGATCGCGCTGGNACTGAATGCCAAAGGAGATGAGGGACA
          |||
NM_012517 3254 AACGTTGATCGCGCTGG-ACTGAATGCCAAAGGAGATGAGGGACA

90  CGCTAACCACCAGCAGGTCCAGGATATTGAAGTAATTTTCGGCAGAAAGAGCCCTTGTGCA
    |||
3210 CGCTAACCACCAGCAGGTCCAGGATATTGAAGTAATTTTCGGCAGAAAGAGCCCTTGTGCA

150  GGAAAGCCCCGTAAGCAGTCATCTTTAGAGCAATTTCAATGGTGAAAATGGTGGTAAAAA
    |||
3150  GGAAAGCCCCGTAAGCAGTCATCTTTAGAGCAATTTCAATGGTGAAAATGGTGGTAAAAA

210  CAATGTCAAAAATAAAAACAGAATGTGGTTCCTGAAGGAGGTGTGCTGGACGGGGTCCTCAG
    |||
3090  CAATGTCAAAAATAAAAACAGAATGTGGTTCCTGAAGGAGGTGTGCTGGACGGGGTCCTCAG

270  CCGCCAGGGAGATGCTACTGAGCAGAATGAAGAAGAGGATGAGGTTGGTGAAGATCGTGT
    |||
3030  CCGCCAGGGAGATGCTACTGAGCAGAATGAAGAAGAGGATGAGGTTGGTGAAGATCGTGT

330  CATTGACAATGCGGTGGCACTGCAGGCGGAACCTGTTGTTTGGGCTGAAGATGAAAAATG
    |||
2970  CATTGACAATGCGGTGGCACTGCAGGCGGAACCTGTTGTTTGGGCTGAAGATGAAAAATG

390  CACTGGCTTCCGGCATGGGGACTGCCTTTTCCTTAAGGTGCAGCTCAGACAGGGGCCGGG
    |||
2910  CACTGGCTTCCGGCATGGGGACTGCCTTTTCCTTAAGGTGCAGCTCAGACAGGGGCCGGG

450  GGCGTGGGCCCACAGGCATCTCGGGCTCCAATCA 483
    |||
2850  GGCGTGGGCCCACAGGCATCTCGGGCTCC 2822

```

Figure 3.3: Alignment of the sequence of Ca_v1.2 product amplified by RT-PCR in the carotid body with the Ca_v1.2 sequence from the Gene Bank. Upper line shows the sequence of the product amplified by RT-PCR. The amplicon was inserted prior to sequencing in the plasmid pGEM®-T. The adjacent parts of the plasmid pGEM®-T are shown in bold and the primers used for the amplification are highlighted in yellow. The sequence presented in the lower line corresponds to part of the Ca_v1.2 rat mRNA targeted (Gene Bank accession number NM_012517). The two sequences are identical excepted for one sequencing mistake located in the primer. The amplified product has the expected length of 433 bases.

3.3.2.2 Immunostaining of $Ca_v1.2$ and $Ca_v1.3$ Ca^{2+} channels

To confirm the presence of protein and investigate cellular localisation of the L-type Ca^{2+} channels, immunostaining against tyrosine hydroxylase, $Ca_v1.2$ and $Ca_v1.3$ was performed. Figure 3.4 shows a view of the carotid body/superior cervical ganglion region and figure 3.5 presents tyrosine hydroxylase and $Ca_v1.2$ immunostaining in rat carotid body. Tyrosine hydroxylase immunostaining allowed identification the type 1 cells which are organised in clusters (Fig. 3.4C and 3.5B). $Ca_v1.2$ was expressed in superior cervical ganglion and in the carotid body (Fig. 3.4B, D and 3.5A, C). In the carotid body, tyrosine hydroxylase and $Ca_v1.2$ immunoreactivity co-localised, demonstrating that type 1 cells express $Ca_v1.2$. In addition, $Ca_v1.2$ was found to be expressed in the nerve (N, Fig.3.4B, D and 3.5A, C). The negative control for $Ca_v1.2$, carried out by omission of the primary antibody, demonstrated that no staining was detected (Fig. 3.5D).

The carotid body did not demonstrate any immunoreactivity for $Ca_v1.3$, as revealed by the figure 3.6. The positive control, on brain tissue (Fig. 3.6E), showed the expression of $Ca_v1.3$ in specific areas of cortical neurons, probably corresponding to the synapses, where $Ca_v1.3$ is known to be expressed (Ludwig *et al.*, 1997).

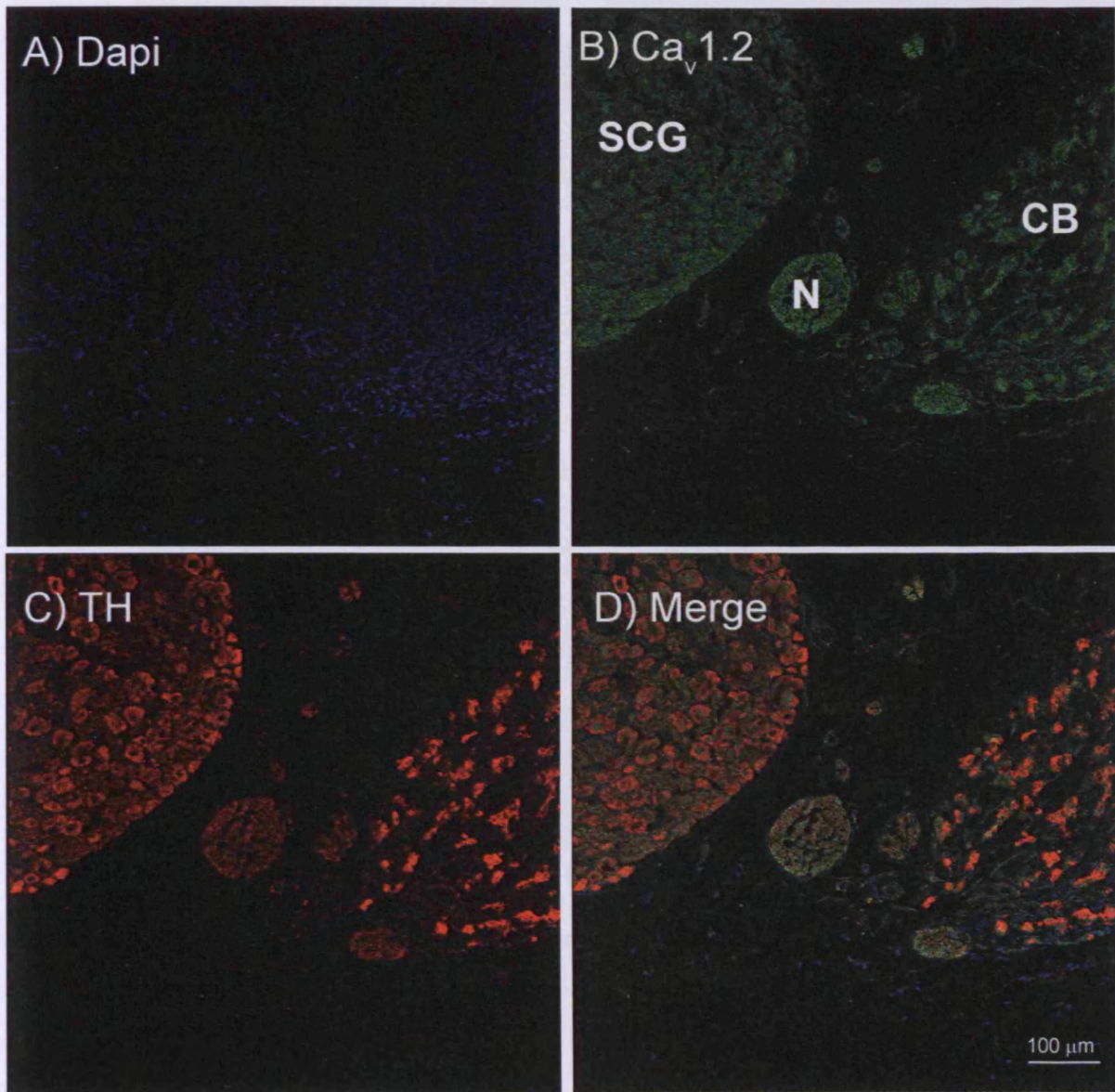


Figure 3.4: View of a carotid body/superior cervical ganglion region immunostained for Ca_v1.2 and tyrosine hydroxylase. A) Nuclei are stained with DAPI in blue. B) Ca_v1.2 immunoreactivity is green (FITC-conjugated secondary antibody). C) Tyrosine hydroxylase (TH) is red (TRITC-conjugated secondary antibody). D) Merged image of A, B and C. Ca_v1.2 was present in nerve (N), type 1 cells in carotid body and superior cervical ganglion (SCG). Scale bar = 100 μm and applies to all panels.

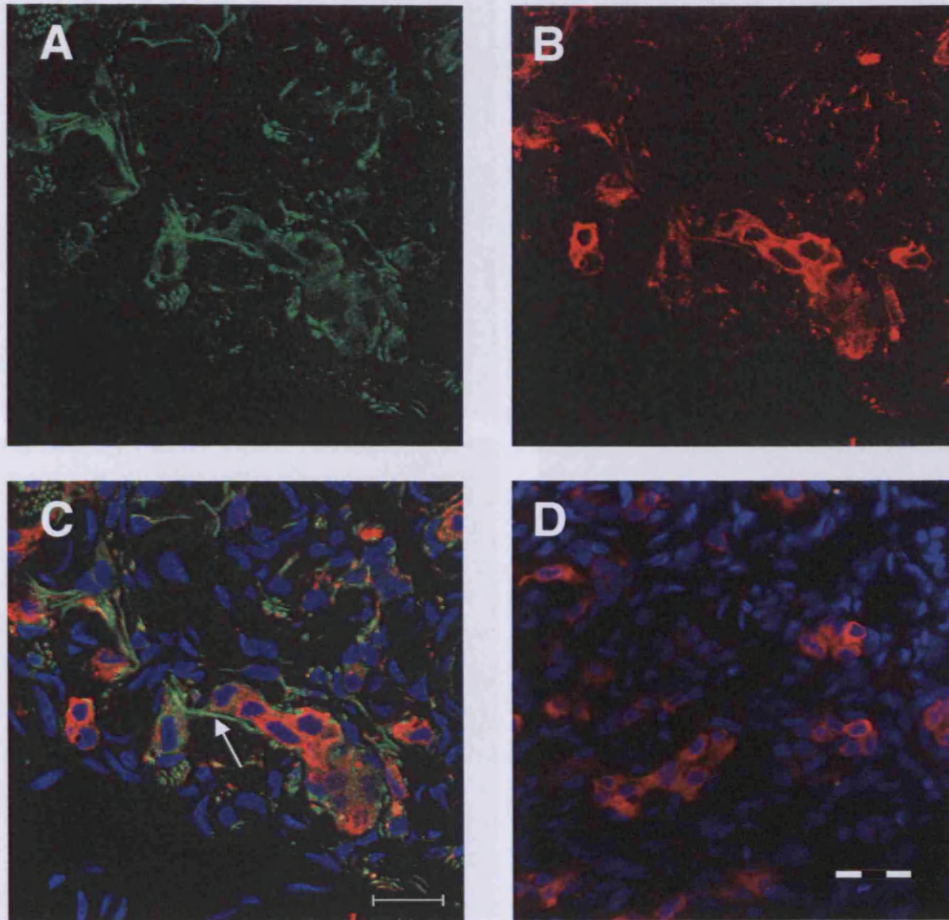


Figure 3.5: Expression of Ca_v1.2 protein in type 1 cells. A) Ca_v1.2 is green (FITC-conjugated secondary antibody). B) Tyrosine hydroxylase is red (TRITC-conjugated secondary antibody). C) Merged image of A and B. The nuclei are stained in blue with DAPI. Ca_v1.2 and tyrosine hydroxylase co-localize within the same cells, indicating that Ca_v1.2 is expressed in type 1 cells. Ca_v1.2 is also expressed in the nerve as shown by the arrow. D) The negative control, consisting of omission of primary antibody for Ca_v1.2, shows no immunoreactivity. Scale bar = 20 μm for A, B and C and 50 μm for D.

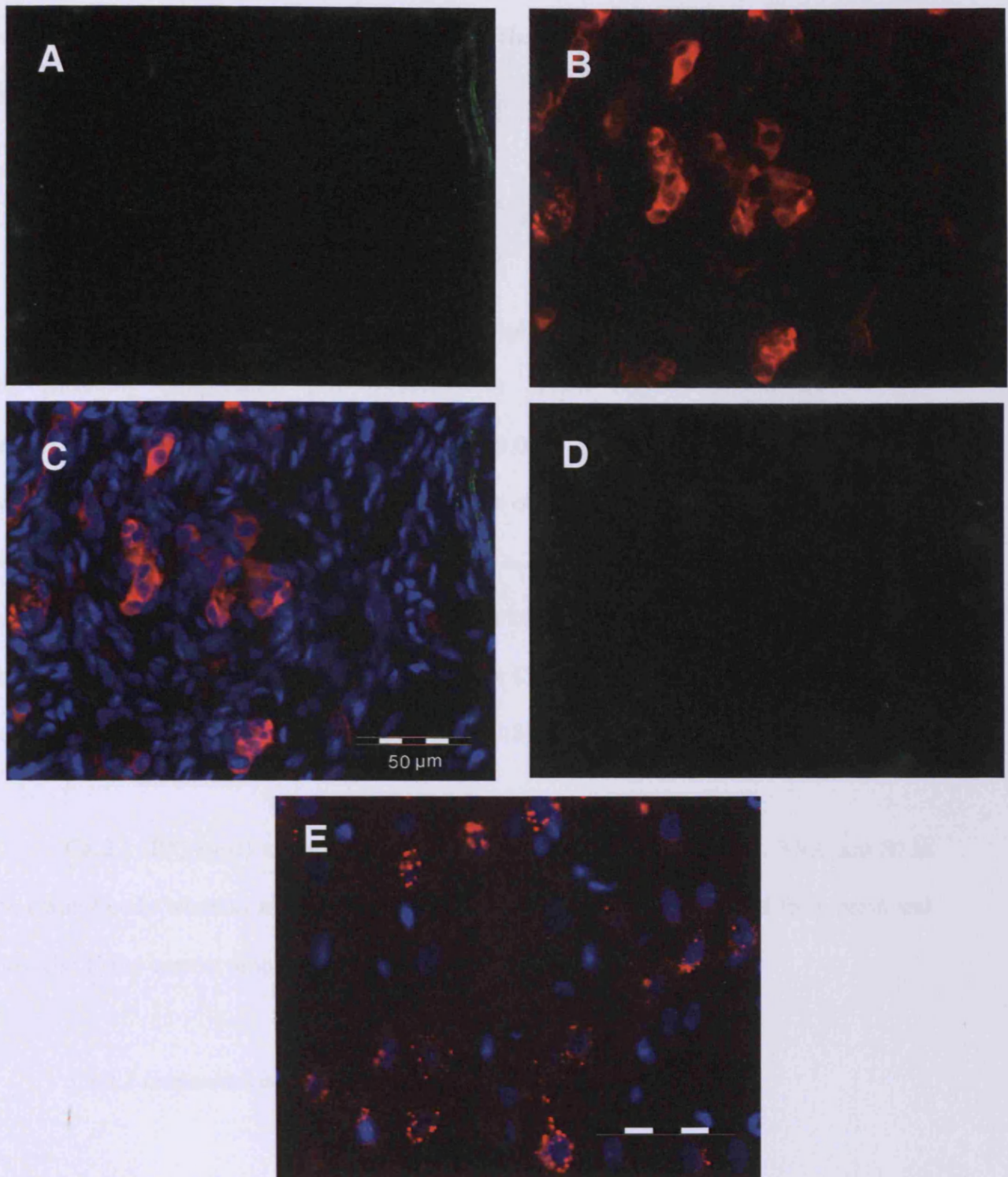


Figure 3.6: Absence of immunoreactivity for Ca_v1.3 protein in type 1 cells. A) Exemplar carotid body section stained for Ca_v1.3 in green (FITC-conjugated secondary antibody). Carotid body did not have any immunoreactivity for Ca_v1.3. B) Tyrosine hydroxylase staining is red (TIRTC-conjugated secondary antibody). C) Merged image of A and B with DAPI in blue. D) Negative control made by omission of the primary antibody. E) Positive control shows Ca_v1.3 immunostaining, in red, made in rat cortex. Scale bars = 50 μm.

3.3.3 Identification of N, P/Q and R-type Ca^{2+} channel expressions in carotid body tissue

3.3.3.1 RT-PCR of N, P/Q and R-type Ca^{2+} channels

Figure 3.7A shows a typical example of optimisation of the PCR conditions, where the annealing temperature was modified to obtain optimal amplification. Three temperatures were tested: 55.0 °C, 57.2 °C and 59.0 °C. The optimal annealing temperature was estimated at 57.2 °C but the best results were obtained at 59.0 °C, a temperature which was then used for subsequent PCR reactions. $Ca_v2.2$ (N-type) could be amplified in the carotid body and in the brain at the predicted size of 504 bp (Fig. 3.7B). The sequencing of the PCR product obtained in the carotid body for $Ca_v2.2$ shows 100 % homology with the sequence targeted in the $Ca_v2.2$ rat mRNA (Fig. 3.8).

$Ca_v2.1$ (P/Q-type) and $Ca_v2.3$ (R-type) could not be detected (Fig. 3.9A and B) in the carotid body whereas transcripts for these channels could be amplified from brain and gave rise to the correct amplicon sizes 576 and 696 bp, respectively.

3.3.3.2 Immunostaining of N, P/Q and R-type Ca^{2+} channels

Figure 3.10 shows the immunoreactivity for $Ca_v2.2$ in rat carotid body. The same cells which were immunoreactive for tyrosine hydroxylase (Fig. 3.10B, C) also exhibited $Ca_v2.2$ immunostaining, (Fig. 3.10A, C) leading to the conclusion that type 1 cells express $Ca_v2.2$. The negative control, made by pre-incubation of the primary antibody with the blocking peptide presented no immunoreactivity (Fig. 3.10D).

Chapter 3

In contrast, the carotid body did not show any immunoreactivity for Ca_v2.1 (Fig. 3.11) or Ca_v2.3 (Fig. 3.12). The use of brain tissue as a positive control confirmed the sensitivity of the antibodies against Ca_v2.1 and Ca_v2.3. Brain highly expresses these two channels and therefore exhibited a high background fluorescence (Doering & Zamponi, 2003).

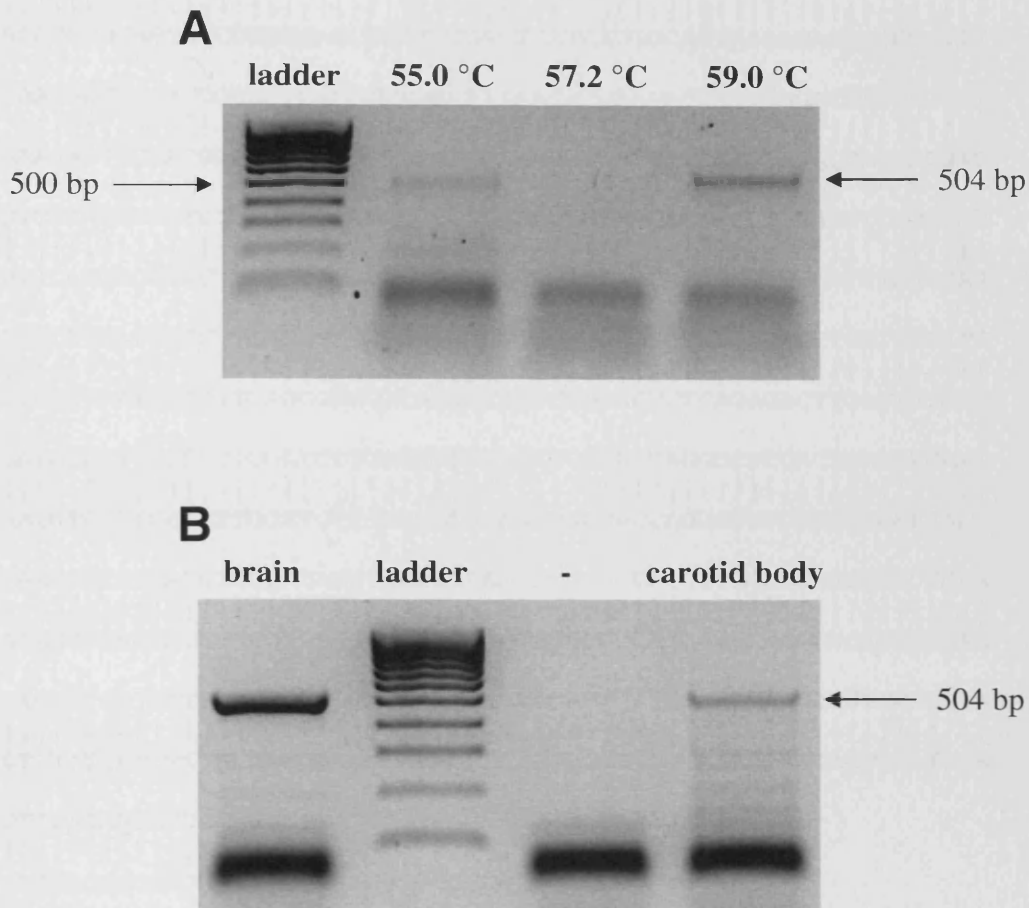


Figure 3.7: Expression of $Ca_v2.2$ mRNA in carotid body. A) Typical example of optimization of the annealing temperature showed here with $Ca_v2.2$. Three different temperatures were tested 55.0 °C, 57.2 °C and 59.0 °C. 59.0 °C gave the best result and was then used for the amplification of $Ca_v2.2$ from carotid body mRNA shown in (B). $Ca_v2.2$ was amplified from brain, as a positive control, and in carotid body at the predicted size of 504 bp, confirmed by sequencing.


```

pMGEM-T 34 GGATTCCTTGGCTGGGCTTCTACCTCTTCCTTCTCATAATCCAAATACTG
          |||
NM_147141 4099 CCTTGGCTGGGCTTCTACCTCTTCCTTCTCATAATCCAAATACTG

84  ACCCCTGCAGTCCCGCTCCAGCTCCTTGGACTCATCAGTGCAGTAAAAGAAGTCCCTTT
4054 |||
     ACCCCTGCAGTCCCGCTCCAGCTCCTTGGACTCATCAGTGCAGTAAAAGAAGTCCCTTT

144  GAAGAGTTGGACGGCGATGACGGCAAATATAAACATGAAGAGCATGTAGACGATCAGGAT
3994 |||
     GAAGAGTTGGACGGCGATGACGGCAAATATAAACATGAAGAGCATGTAGACGATCAGGAT

204  GTTCAAGACATTCTTCAGAGAGTTACCCACACAGTCAAACACAGCCTTGAGTTTAGGCAG
3934 |||
     GTTCAAGACATTCTTCAGAGAGTTACCCACACAGTCAAACACAGCCTTGAGTTTAGGCAG

264  CCGCTTGATGGTCTTGAGGGGCCGAGGACTCGCAGGACTCTCAGAGACTTGATGGTATT
3874 |||
     CCGCTTGATGGTCTTGAGGGGCCGAGGACTCGCAGGACTCTCAGAGACTTGATGGTATT

324  GATGCTTTCCCTTTGGATCCTGAGAAATGCAAATGCCACCAGGGCTCCACTGACAACAAT
3814 |||
     GATGCTTTCCCTTTGGATCCTGAGAAATGCAAATGCCACCAGGGCTCCACTGACAACAAT

384  GAAGTCCAGAATGTTCCACAGGTCCCGGAAGTAGGCCCCAGGGTGCAGCAGCAGGCCCAA
3754 |||
     GAAGTCCAGAATGTTCCACAGGTCCCGGAAGTAGGCCCCAGGGTGCAGCAGCAGGCCCAA

444  GTCTATCATCTTTATGACCATCTCAAAGGTGAAGACTCCTGTAAAGATGTAGTCCATGTA
3694 |||
     GTCTATCATCTTTATGACCATCTCAAAGGTGAAGACTCCTGTAAAGATGTAGTCCATGTA

504  CTTCAGAGCATTGTTCCGGAAATGAGTCGGTCCGCACGGGAATCA 548
          |||
3634 CTTCAGAGCATTGTTCCGGAATGAGTCGGTCCGCACGGG 3595

```

Figure 3.8: Alignment of the sequence of Ca_v2.2 product amplified by RT-PCR in the carotid body with the Ca_v2.2 sequence from the Gene Bank. Upper line shows the sequence of the product amplified by RT-PCR. The amplicon was inserted prior to sequencing in the plasmid pGEM®-T. The adjacent parts of the plasmid pGEM®-T are shown in bold and the primers used for the amplification are highlighted in yellow. The sequence presented in the lower line corresponds to the part of the Ca_v2.2 rat mRNA targeted (Gene Bank accession number NM_147141). The two sequences are identical and the amplified product had the expected length of 504 bases.

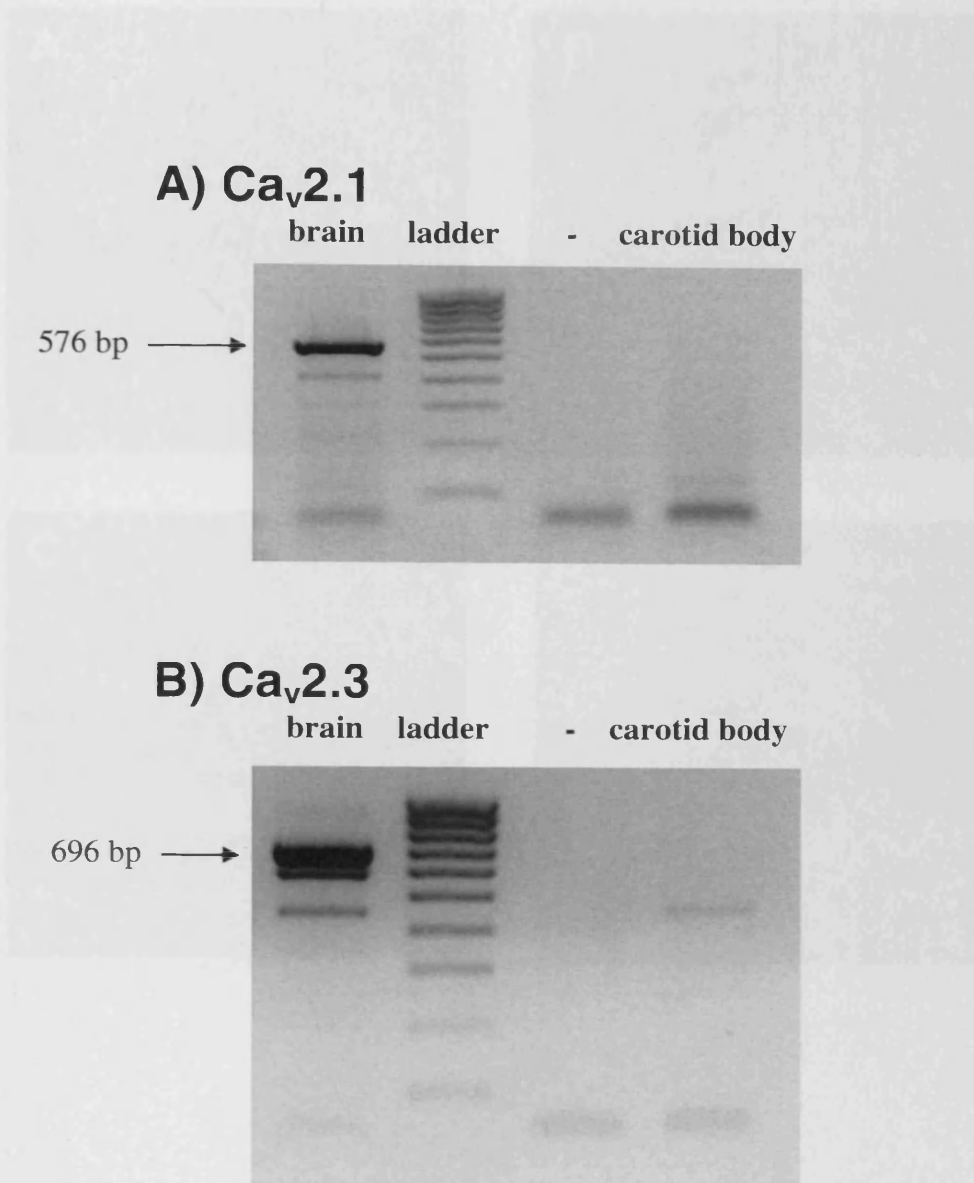


Figure 3.9: Absence of expression of Ca_v2.1 and Ca_v2.3 mRNAs in carotid body. A) Ca_v2.1 mRNA could not be amplified in the carotid body sample while the positive control gave the appropriate amplicon at the size of 576 bp. B) Ca_v2.3 mRNA could not be detected in the carotid body. The RT-PCR carried out on brain mRNA (positive control) produced an amplicon at the expected size at 696 bp and probably amplified a splice-variant at a slightly lower weight near 600 bp. A non-specific band appeared around 450 bp in the brain and carotid body. The sequencing of this amplified transcripts revealed that this band corresponded to the amplification of adenosine phosphorylase transferase indicating a non specific product.

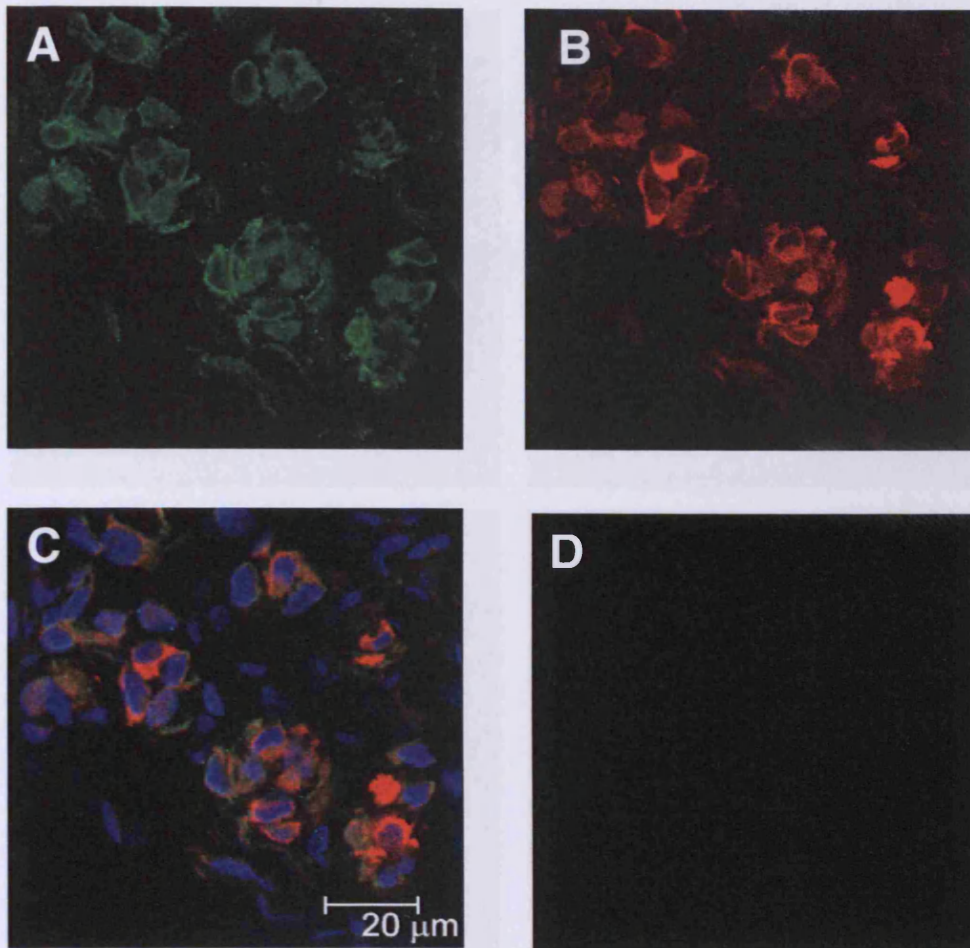


Figure 3.10: Expression of Ca_v2.2 protein in carotid body type 1 cells. Typical immunostaining to detect Ca_v2.2 in green (FITC-conjugated secondary antibody). B) Tyrosine hydroxylase is red (TRITC-conjugated secondary antibody). C) Merged image of A, B with the nuclei stained in blue with DAPI. Tyrosine hydroxylase positive cells also exhibited Ca_v2.2 immunoreactivity demonstrating that type 1 cells express Ca_v2.2. D) is a negative control made by pre-incubation of the primary antibody with the blocking peptide. Scale bar = 20 μm.

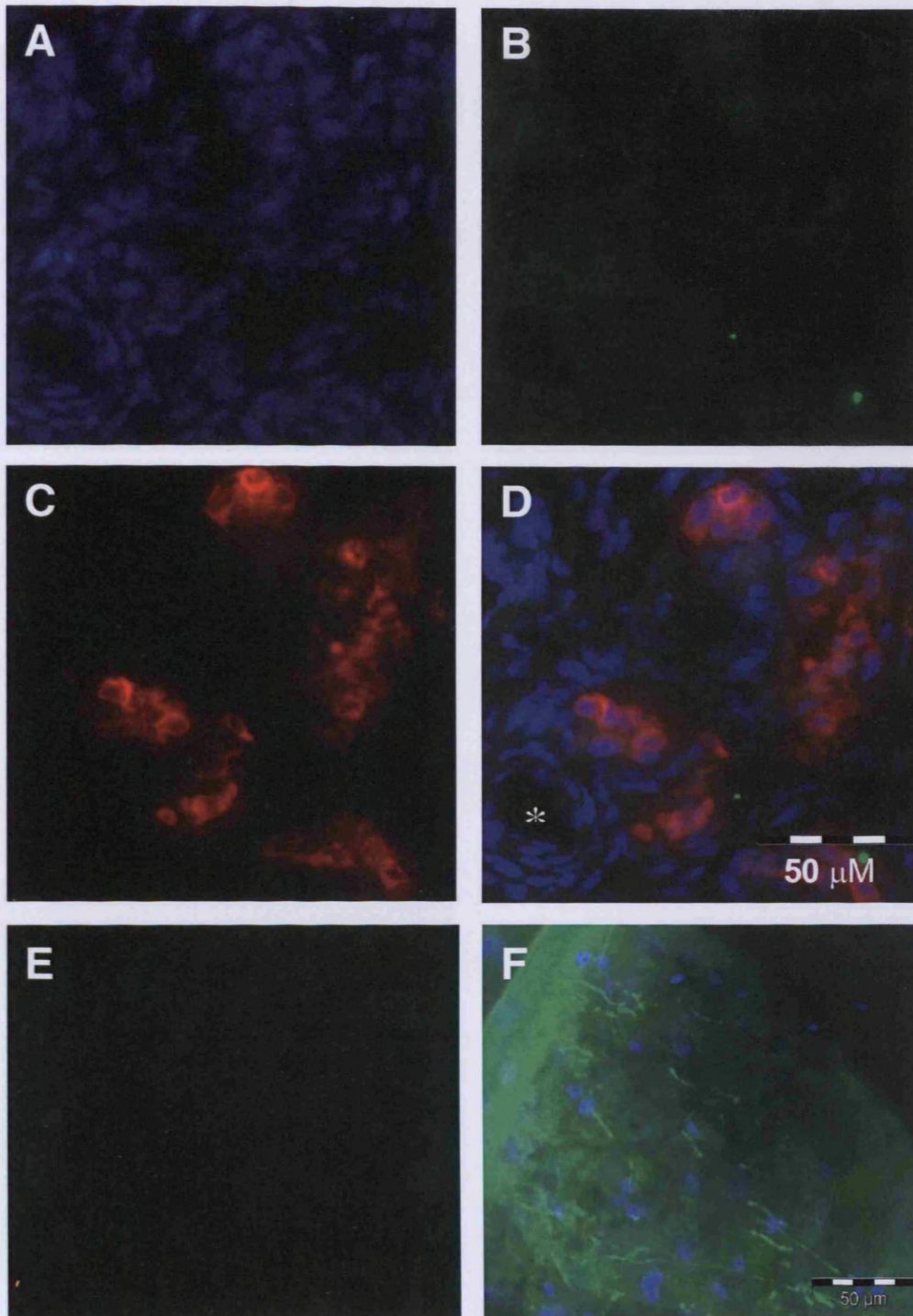


Figure 3.11: Absence of immunoreactivity for $Ca_v2.1$ protein in type 1 cells. A) DAPI staining is blue. B) $Ca_v2.1$ immunoreactivity is green (FITC-conjugated secondary antibody). C) Tyrosine hydroxylase is red (TRITC-conjugated secondary antibody). D) Merged image of A, B and C. Carotid body did not present any immunoreactivity for $Ca_v2.1$. The asterisk (*) marks a blood vessel cut transversally. A negative control (omission of the primary antibody) in the carotid body is shown in (E) and a positive control was made using a brain slice (F). F) Presents a typical staining with numerous nerves positive to $Ca_v2.1$ in green. Scale bars = 50 μm .

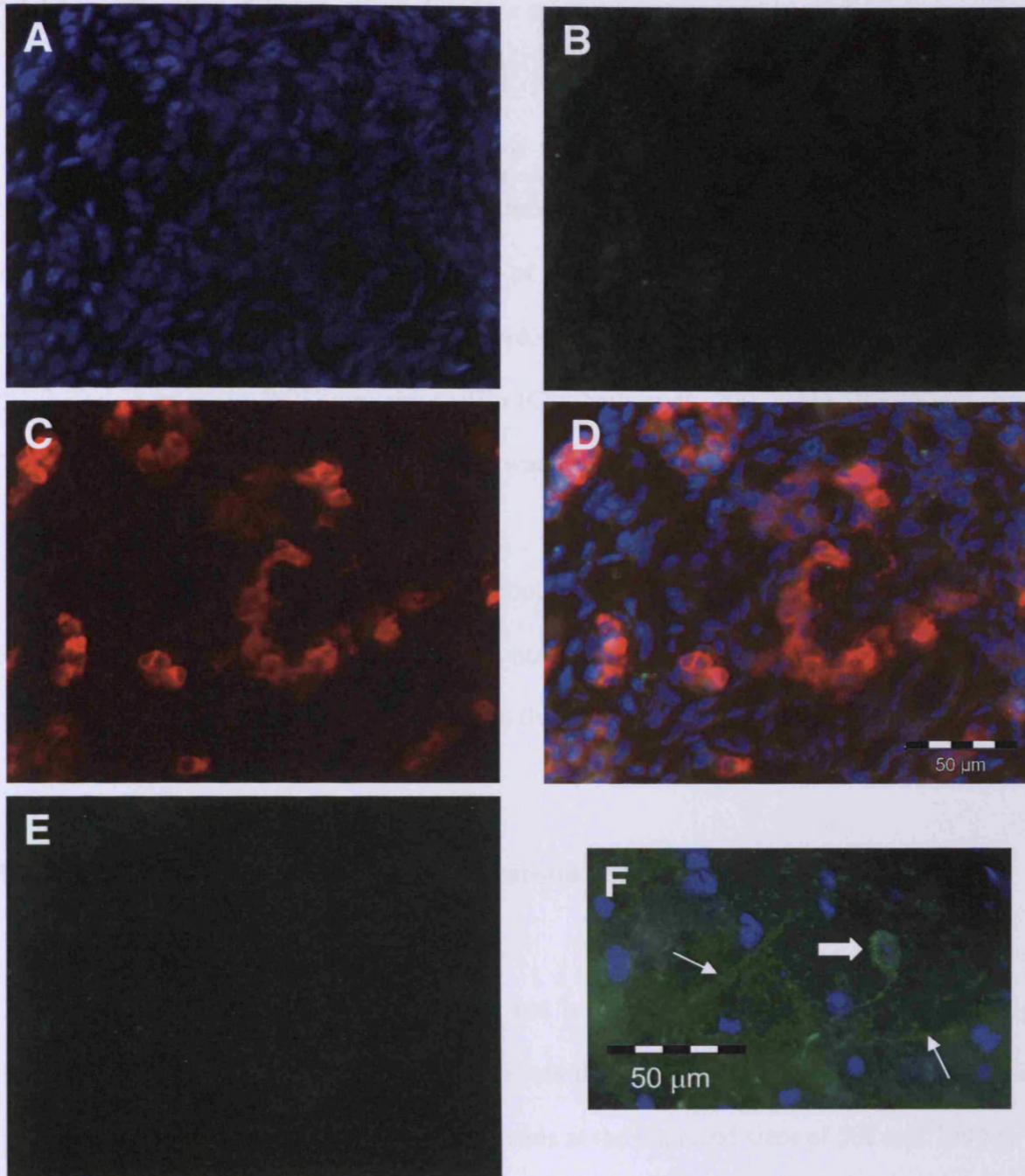


Figure 3.12: Absence of immunoreactivity for $Ca_v2.3$ protein in type 1 cells. A) DAPI staining is blue. B) $Ca_v2.3$ is green (FITC-conjugated secondary antibody). C) Tyrosine hydroxylase is red (TRITC-conjugated secondary antibody). D) Merge imaged of A, B and C. Carotid body did not present any immunoreactivity for $Ca_v2.3$. A negative control (omission of the primary antibody) in the carotid body is shown in (E) and a positive control was made using a brain slice (F). F) shows a typical staining with the soma of a neuron (thick arrow) and some nerves (thin arrow) positive to $Ca_v2.3$ in green. Scale bars = 50 μm .

3.3.4 Identification of T-type Ca^{2+} channels expression in carotid body tissue

T-type currents are known to regulate many processes taking place in the carotid body in chronic hypoxia such as neurosecretion, differentiation, growth and proliferation, leading to the hypothesis of an involvement of T-type currents in these processes in type 1 cells. In addition, in response to chronic hypoxia, T-type ($\text{Ca}_v3.1$) current is up regulated in PC12 (Del Toro *et al.*, 2003) and chromaffin (Carabelli *et al.*, 2007) cells. Because of these findings, the expression of the T-type genes was investigated in rat carotid body.

$\text{Ca}_v3.1$, $\text{Ca}_v3.2$ and $\text{Ca}_v3.3$ mRNAs could not be amplified in the carotid body (Fig. 3.13A, B and C) whereas the positive control (brain) produced the amplicons at the expected sizes of 425, 420 and 480 bp, respectively.

3.3.5 Identification of CaR expression in carotid body tissue

Using RT-PCR, CaR mRNA could not be amplified from rat carotid body (Fig. 3.14A). Indeed, with two different set of primers the CaR was not amplified in the carotid body, yet the positive controls yielded amplicons at the expected sizes of 582 and 759 bp.

Immunostaining for tyrosine hydroxylase and CaR proteins revealed that the CaR was expressed in the nerve endings but not in type 1 cells or type 2 cells (Fig. 3.14B, C and D). The use of confocal imaging clearly shows that the CaR immunostaining follows a line pattern characteristic of nerve terminals. Moreover, a side view of the z-stack, presented on

Chapter 3

the side of the merged image, shows the section of the nerve which appeared like a circle-shape abutting the type 1 cells (Fig. 3.14D).

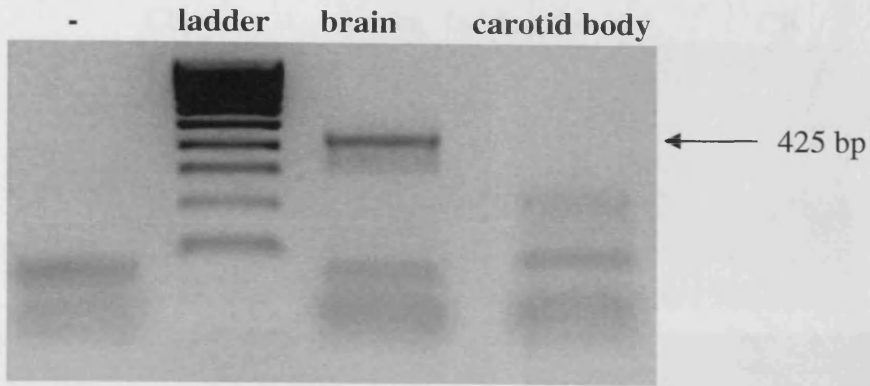
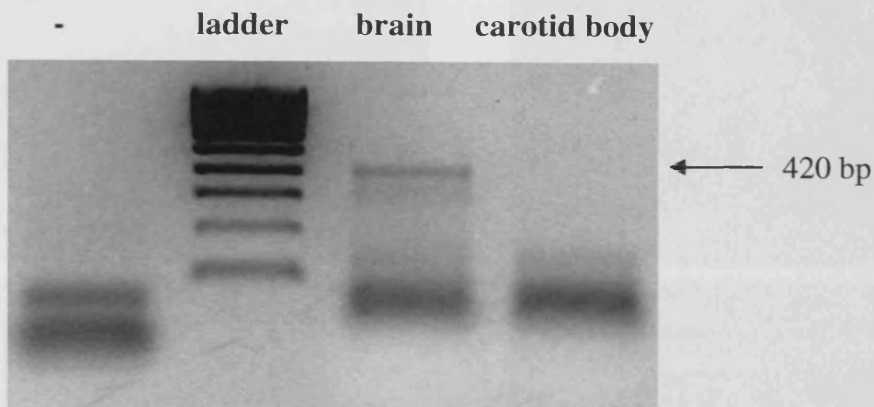
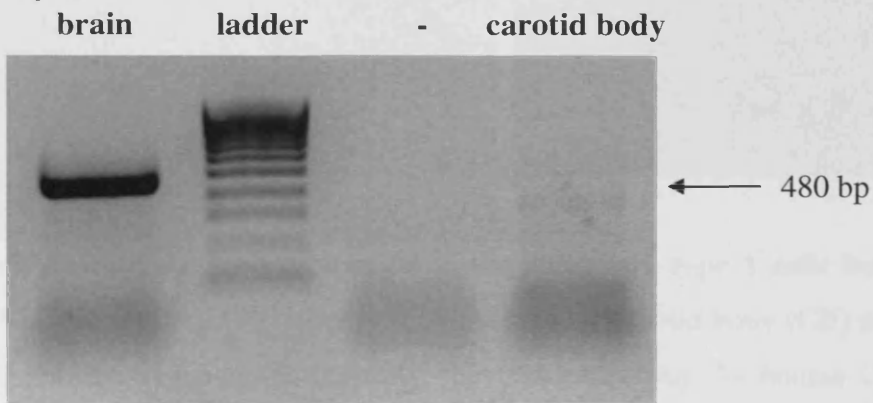
A) Ca_v3.1**B) Ca_v3.2****C) Ca_v3.3**

Figure 3.13: Absence of expression of T-type Ca²⁺ channel mRNAs in carotid body. RT-PCR from carotid body total mRNA for Ca_v3.1 (A), Ca_v3.2 (B) and Ca_v3.3 (C) did not give any products whereas the positive control, brain mRNA, gave amplicons at the predicted sizes, of 425, 420 and 480 bp, respectively.

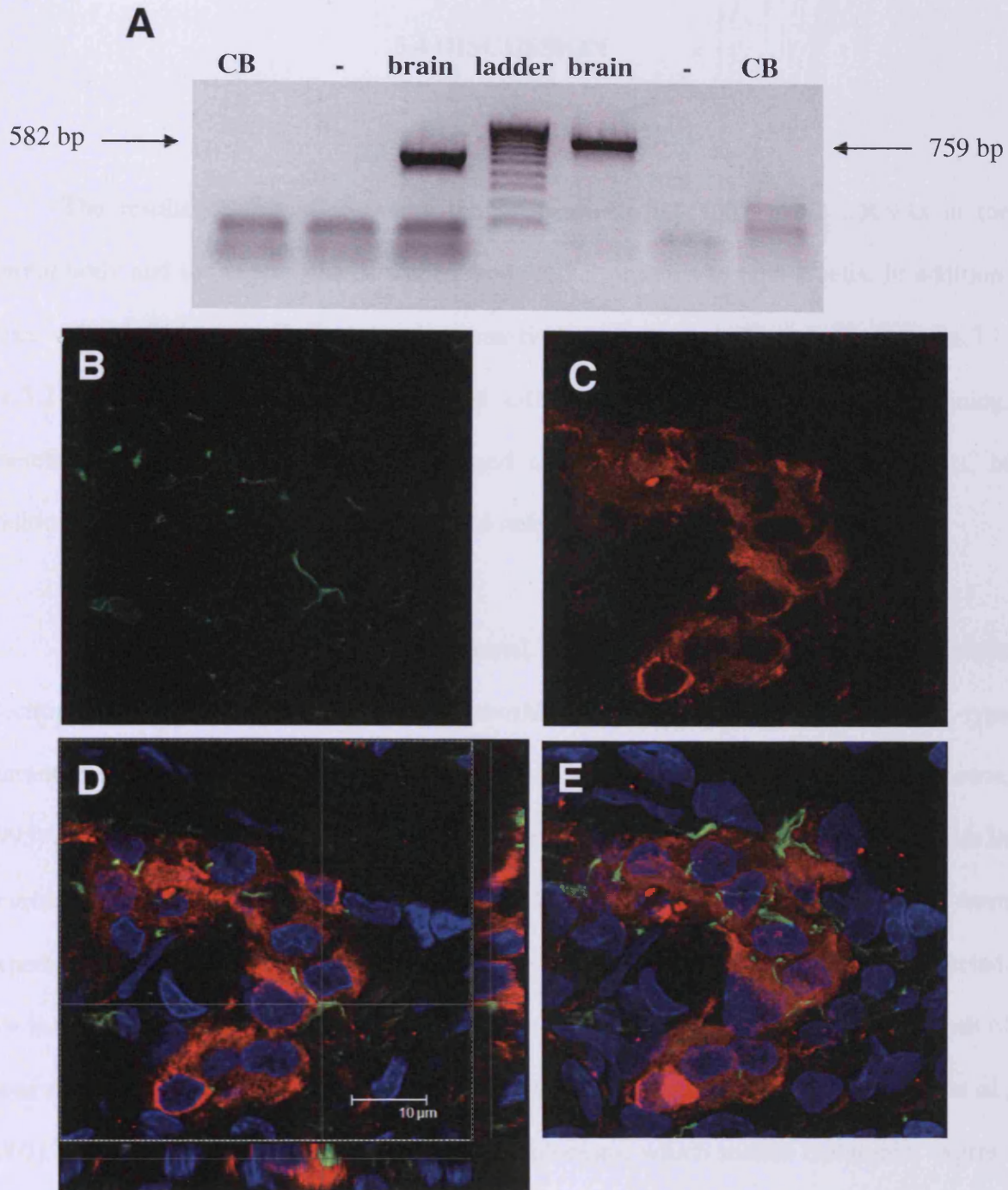


Figure 3.14: CaR protein was not expressed in carotid body type 1 cells but was present in nerve endings. A) CaR could not be amplified by PCR in rat carotid body (CB) using two different sets of primers. Although, the positive controls, plasmid containing the human CaR, produced the right size amplicons at 582 and 759 bp. Double immunostaining in carotid body slice to detect CaR (in green, B) and tyrosine hydroxylase (in red, C) revealed that the CaR was expressed only in the nerve ending, but not in type 1 cells. The merge confocal image (D) also shows the z-stack at the level where the lines cross (DAPI was in blue). E is the sum of the maximum signal from each slice. The CaR staining follows a linear pattern corresponding to the nerve. Scale bar = 10 μm .

3.4 DISCUSSION

The results of this study show the presence $Ca_v1.2$ and $Ca_v2.2$ mRNAs in the carotid body and the expression of $Ca_v1.2$ and $Ca_v2.2$ proteins in type 1 cells. In addition, other voltage-dependent Ca^{2+} channels, namely $Ca_v1.3$, $Ca_v1.4$, $Ca_v2.1$, $Ca_v2.3$, $Ca_v3.1$, $Ca_v3.2$ and $Ca_v3.3$ could not be detected either by RT-PCR or by immunostaining. Therefore, these channels are not expressed or are present at undetectable levels. In addition, the CaR was shown to be expressed only in the nerve ending.

The detection of an L-type Ca^{2+} channel is in agreement with most of the previous electrophysiological data obtained in rat carotid body, showing a central role of L-type current in mediating the Ca^{2+} influx (Buckler & Vaughan-Jones, 1994c; e Silva & Lewis, 1995) and others (see Introduction to this chapter). According to their expression profiles in neurons and neuroendocrine cells (Catterall *et al.*, 2003), both $Ca_v1.2$ and $Ca_v1.3$ were expected to be expressed in type 1 cells; yet only the expression of $Ca_v1.2$ was detected. For instance, in the adrenal gland, chromaffin cells express $Ca_v1.2$ and $Ca_v1.3$ and both of these channels link the catecholamine secretion with the depolarisation (Marcantoni *et al.*, 2007). Or, contrary to the carotid body, rat pinealocytes, which secrete melatonin, express only the subtype $Ca_v1.3$ (Chik *et al.*, 1997). The expression of $Ca_v1.2$ and $Ca_v1.3$ is, therefore, tissue specific. This specificity can be explained by the different electrical and pharmacological properties of $Ca_v1.2$ and $Ca_v1.3$. Indeed, $Ca_v1.3$ is activated at a membrane potential of - 65 mV and $Ca_v1.2$ at - 40 mV (Xu & Lipscombe, 2001) and $Ca_v1.3$ is less sensitive to dihydropyridines than $Ca_v1.2$ (Xu & Lipscombe, 2001). Type 1 cells have a resting membrane potential of - 50 mV (Gonzalez *et al.*, 1994), therefore, it is

Chapter 3

coherent that they express $\text{Ca}_v1.2$ but not $\text{Ca}_v1.3$. Moreover the activation of voltage-dependent Ca^{2+} channels in rat type 1 cells start at - 40 mV (Peers *et al.*, 1996), corresponding to the value found for $\text{Ca}_v1.2$ (Xu & Lipscombe, 2001).

The identification of $\text{Ca}_v2.2$ (N-type) in rat carotid body by RT-PCR and immunostaining corroborates the results obtained by others showing the participation of $\text{Ca}_v2.2$ to the Ca^{2+} influx induced by hypoxia (e Silva & Lewis, 1995; Peers *et al.*, 1996). In addition, $\text{Ca}_v2.1$ (P/Q-type) and $\text{Ca}_v2.3$ (R-type) could not be detected by either RT-PCR or by immunohistochemistry. The absence of expression of $\text{Ca}_v2.1$ gene is in accordance with the lack of effect of ω -agatoxin IVA, a specific blocker of $\text{Ca}_v2.1$, on Ca^{2+} influx in type 1 cells (Peers *et al.*, 1996). To date, no functional data can confirm the absence of expression of $\text{Ca}_v2.3$ in rat carotid body found in this study as the effect of SNX482, the only specific blocker of $\text{Ca}_v2.3$, has never been tested on type 1 cells.

It is interesting to notice that BK_{Ca} can form macromolecular complexes with $\text{Ca}_v1.2$, $\text{Ca}_v2.1$ and $\text{Ca}_v2.2$, as shown by co-immunoprecipitation from solubilised plasma membranes from rat brain (Berkefeld *et al.*, 2006). The formation of this complex would help to supply quickly Ca^{2+} to BK_{Ca} to induce the activation of this latter channel. As all the voltage-dependent Ca^{2+} channels, with the exception of $\text{Ca}_v1.1$ and $\text{Ca}_v1.4$, are expressed in the brain, it is likely that BK_{Ca} only forms macromolecular complexes with the channels found to co-immunoprecipitate: $\text{Ca}_v1.2$, $\text{Ca}_v2.1$ and $\text{Ca}_v2.2$. Since the carotid body expresses $\text{Ca}_v1.2$ and $\text{Ca}_v2.2$, it is possible that this macromolecular complex exists in the carotid body as well.

Chapter 3

The fact that T-type Ca^{2+} channels are up regulated by chronic hypoxia in chromaffin cells ($\text{Ca}_v3.2$) (Carabelli *et al.*, 2007) and in PC12 cells ($\text{Ca}_v3.1$) (Del Toro *et al.*, 2003) has led to the hypothesis that T-type Ca^{2+} channels could be expressed in carotid body type 1 cells. Nevertheless, T-type Ca^{2+} channels were not detectable by RT-PCR. This result is consistent with functional observations which show the lack of T-type currents in type 1 cells. Indeed, Ca^{2+} currents in type 1 cells, begin to be activated at - 40 mV (Peers *et al.*, 1996; Lopez-Lopez *et al.*, 1997) which is above the threshold of activation of T-type currents (Perez-Reyes, 2003). For these reasons, the immunocytochemistry against T-type channels was not carried out. The absence of expression of T-type Ca^{2+} channels in normoxia does not refute the hypothesis that they might be up regulated in chronic hypoxia in the carotid body. According to Hempleman, the amplitude and density of Ca^{2+} currents increases in chronic hypoxia (Hempleman, 1996). This increase is probably due in part to an increase in $\text{Ca}_v1.2$. Indeed, in HEK293 cells stably transfected with $\text{Ca}_v1.2$, the current density and $\text{Ca}_v1.2$ protein expression increased after 24 h of chronic hypoxia (Scragg *et al.*, 2005). Nonetheless, a dihydropyridine-insensitive channel increases its expression after chronic hypoxia, and in chronic hypoxia nifedipine blocks only 43 % of the current (whereas it blocks about 70 % of the current in normoxia (Buckler & Vaughan-Jones, 1994c; e Silva & Lewis, 1995)). These results should be considered carefully as Peers and Carpenter observed only an increase in current amplitude, but not current density, following chronic hypoxia (Peers *et al.*, 1996; Carpenter *et al.*, 1998). This increase in current amplitude but not density is due to the fact that in chronic hypoxia the cells are bigger but, relatively, do not express more channels as the density of the current is constant between normoxia and chronic hypoxia.

Chapter 3

My results also show that the CaR could not be amplified by RT-PCR from rat carotid body but was detected by immunostaining in the nerve ending. These results are in agreement with the absence of effect of CaR agonists, spermine and neomycin, and of the allosteric modulator, R-568, on $[Ca^{2+}]_i$ homeostasis in type 1 and type 2 cells, observed in chapter 2. The fact that the CaR mRNA could not be detected by RT-PCR but the protein was found in the nerve ending can be explained by the fact that the mRNA is synthesised in the soma of the neurons, whereas the protein is synthesised there and then trafficked to the nerve ending. The expression of CaR in the nerve ending corroborates the results of Ruat and al. showing the expression of CaR in other neuronal nerves ending (Ruat *et al.*, 1995).

3.5 CONCLUSION

This study represents the first complete description of the gene expression of voltage-dependent Ca^{2+} channel mRNA and protein in rat carotid body. The results show the expression of $\text{Ca}_v1.2$ and $\text{Ca}_v2.2$ in rat type 1 cells, confirming the conclusions of the electrophysiological data gathered by others. In addition to the data obtained by Buriel *et al.* on transient receptor potential channel (TRPC) expression in rat carotid body (Buniel *et al.*, 2003), a complete picture of the ion channels responsible for the Ca^{2+} influx in type 1 cells can now be produced. Thus, $\text{Ca}_v1.2$ and $\text{Ca}_v2.2$ are the voltage-dependent Ca^{2+} channels mediating the primary Ca^{2+} influx induced by membrane depolarisation and leading to neurotransmitter release. The release of ACh leads to the activation of muscarinic receptor which, via the protein G_q , opens the transient receptor potential channel 1 and 3 to 7 inducing a Ca^{2+} influx.

Regarding the effect of spermine on carotid body, the experiments in chapter 2 revealed an inhibitory effect of this polyamine on catecholamine release due to an inhibition of the Ca^{2+} influx mediated by voltage-dependent Ca^{2+} channels. The molecular identification of the voltage-dependent Ca^{2+} channels expressed in rat carotid body lead to the hypothesis that spermine should inhibit $\text{Ca}_v1.2$ and/or $\text{Ca}_v2.2$. This hypothesis will be assessed in the chapter 4.

The absence of expression of CaR in type 1 and type 2 cells corroborates the absence of effect of CaR modulators on $[\text{Ca}^{2+}]_i$ in type 1 and type 2 cells. Moreover, CaR has been implicated in neuronal development. It modulates axonal and dendritic growth

Chapter 3

(Vizard *et al.*, 2008) and neuronal migration (Chattopadhyay *et al.*, 2007). In accordance with these findings, in the carotid body, the CaR could be involved in the remodelling of the nerve endings in chronic hypoxia as the carotid body increases in size (Gonzalez *et al.*, 1994). Further studies, using normoxic and hypoxic carotid body from wild type versus CaR knock-out mice, are needed to test this hypothesis.

CHAPTER 4

**EFFECT OF SPERMINE, NEOMYCIN AND R-568 ON
VOLTAGE-DEPENDENT Ca^{2+} CHANNELS $\text{Ca}_v1.2$
EXPRESSED IN HEK293 CELLS**

AND

**EFFECT OF CO-APPLICATION OF SPERMINE AND
NIFEDIPINE ON TYPE 1 CELLS**

4.1 INTRODUCTION

In chapter 2, the modulation of catecholamine secretion and $[Ca^{2+}]_i$ homeostasis by spermine, neomycin and by R-568 was investigated. Spermine had an inhibitory effect on both catecholamine secretion and $[Ca^{2+}]_i$ increase induced by high K^+ and neomycin was able to block the Ca^{2+} influx whilst R-568 did not interact with any of this process. The conclusion was that the spermine and neomycin were inhibiting, directly or indirectly, the voltage-dependent Ca^{2+} channels through which the Ca^{2+} entered the type 1 cells.

Electrophysiological data from other groups (Fieber & McCleskey, 1993; Buckler & Vaughan-Jones, 1994c; e Silva & Lewis, 1995) have shown the central role of L-type channels in mediating the $[Ca^{2+}]_i$ increase evoked by hypoxia. Moreover, other channels could be implicated to a lesser extent, such as N-type and/or voltage insensitive calcium channels (Buniel *et al.*, 2003). The molecular analysis, performed in chapter 3, of the expression of voltage-dependent Ca^{2+} channels in rat carotid body supports the functional evidence of L- and N-type (Peers *et al.*, 1996) calcium channels in type 1 cells and have pushed forward the investigation by identifying the genes expressed. Indeed, the experiments showed that L-type channel expressed in carotid body is Cav1.2.

The next experiments aimed to elucidate the mechanism mediating the inhibitory effect of spermine and neomycin on voltage-dependent Ca^{2+} channels expressed in rat carotid body. This inhibition could be either direct or indirect. The fact that L-type calcium channels are responsible for 70-80 % (Buckler & Vaughan-Jones, 1994c; e Silva & Lewis, 1995) of the $[Ca^{2+}]_i$ increase in type 1 cells, and that Cav1.2 is the only L-type Ca^{2+} channel

Chapter 4

gene detectable in rat carotid body, led to the hypothesis that spermine and/or neomycin might inhibit $\text{Ca}_v1.2$. In addition, as calcimimetics are derivatives of Ca^{2+} channel blockers, the effect of R-568 on $\text{Ca}_v1.2$ was investigated. These hypotheses were tested by patch-clamp recording and Ca^{2+} imaging in HEK293 cells transiently and stably transfected with human $\text{Ca}_v1.2$. The alignment of the amino acid sequence of the human (Gene Bank accession number AF465484) and rat (NM012517) $\text{Ca}_v1.2$ channel shows 94 % of identities. The electrical and pharmacological properties of the two channels are very likely similar and the results obtained with the human $\text{Ca}_v1.2$ channel are transferable to the rat channel.

Finally, to test the involvement of $\text{Ca}_v1.2$ in mediating the spermine effect in type 1 cells, spermine and nifedipine were co-applied simultaneously on type 1 cells.

4.2 MATERIALS AND METHODS

4.2.1 Wild-type HEK293 and Ca_v1.2-HEK293 Cells Culture

HEK293 cells were used to study the effect of spermine on Ca_v1.2. Compare to carotid body cells or more generally, to any primary cultured cells, HEK293 cells have the advantage to express specifically and, usually at a high level, the cDNA transfected. The high expression of Ca_v1.2 allows testing the direct effect of spermine on the channel, without any possible interference due to the presence of other molecules which could be expressed in native cells line such as other Ca²⁺ channels or CaR.

Wild-type HEK293 cells were purchased from ATCC (Teddington, UK) and HEK293 cells stably expressing human Ca_v1.2 (Ca_v1.2-HEK293) were kindly donated by Prof C. Peers (Leeds University, UK). All cells were maintained in DMEM containing Earle's salts and L-glutamine (Invitrogen, Paisley, UK) supplemented with 10 % (v/v) foetal calf serum (Hyclone, Cramlington, UK), and 1 % (v/v) antibiotic/antimycotic; with 500 mg/l of G418 (Invitrogen) for Ca_v1.2-HEK293 cells. The G418 is an antibiotic for which the resistance gene was included in the plasmid, therefore only the transfected cells were able to grow. Cells were grown in 10 ml of medium in filter capped T25 culture flasks. Every 3-4 days, when ~80 % confluency was reached, the cells were dissociated as follow: 2 washes with Ca²⁺- and Mg²⁺-free PBS (Gibco, Invitrogen), 3 min incubation with trypsin 1X in PBS (Gibco), 7 ml of medium was then added and the cells were spun down at 1, 200 g for 4 min. Cells were resuspended in 10 ml of fresh medium and cultured at the concentration 1:9 in a new culture flask at 37 °C in 5 % CO₂ and 95 % air.

Chapter 4

In preparation for patch-clamp and Ca^{2+} imaging experiments, cells were seeded at a low density on 16 mm coverslips placed in 12 well plates and cultured for 24 h prior to the experiments to let the cells recover and settle down.

4.2.2 Transfection of HEK293 cells with $\text{Ca}_v1.2$ plasmid

4.2.2.1 Transformation of *E.coli* with *Cav1.2* plasmid

The plasmid containing the human $\text{Ca}_v1.2$ was a gift from Prof C Peers (Leeds University, UK). For the transformation, 50 μl of *E.coli* cells (Bioline, London, UK) with 10 μg of plasmid were placed on ice for 30 min before a heat shock was administered at 42 °C for 50 s. Subsequently, the bacteria were placed on ice for 2 min and then suspended in 150 μl of super optimal broth with catabolite repression (SOC) containing (in mM): 2 % trypton peptone, 0.5 % yeast extract, 10 NaCl, 2.5 KCl, 10 MgCl_2 , 10 MgSO_4 , 20 glucose. The cells were then shaken for 1 h at 37 °C. Afterwards, the bacteria were spread on a pre-warmed LB agar (Sigma) plate supplemented with 100 $\mu\text{g/ml}$ ampicillin (Sigma) and incubated for 12 h at 37.5 °C. The $\text{Ca}_v1.2$ plasmid contains a gene providing the resistance against ampicillin, which allows especially the growth of the bacteria expressing the plasmid. One of the colonies was then picked, dissolved in 1 ml of LB Broth EZMIX medium (20.1 g/l Sigma) with 100 $\mu\text{g/ml}$ ampicillin and incubated at 37.5 °C. 8 h later, the 1 ml of the *E.coli* culture was incubated into 100 ml of LB Broth EZMIX medium (with ampicillin) and incubated one more time overnight before the extraction of the plasmid.

Chapter 4

4.2.2.2 Purification of the *Ca_v1.2* plasmid

To purify the *Ca_v1.2* plasmid from *E. coli*, a Maxiprep kit from Invitrogen was used as follows. The bacteria were pelleted by centrifugation at 8,000 g for 10 min. The supernatant was then removed and the pellet resuspended in 10 ml of buffer containing RNase (buffer R3). The bacteria were then lysed by addition of 10 ml of the lysis buffer (L7). The solution was mixed gently and incubated for 5 min at room temperature. The cellular debris were then precipitated using the precipitation buffer (N3) and spun down at 15,000 g for 10 min. The supernatant was passed through a column to purify the plasmid. The column contained small resin particles associated to an anion exchanger molecule allowing binding of the plasmid. The column was then washed with buffer (W8) and the plasmid eluted with the buffer (E4). To concentrate and wash the DNA, the eluted solution was centrifuged at 15,000 g for 30 min at 4 °C and the supernatant was removed. The resulting DNA pellet was washed with 70 % ethanol and, after evaporation of the ethanol, the DNA was resuspended and kept in nuclease-free water (Ambion, Warrington, UK) at -20 °C.

The amount and purity of the DNA obtained were checked with a spectrophotometer (SANYO SP65 UV/VIS, Watford, UK). The absorbance produced by the DNA and proteins were calculated at 260 and 280 nm, respectively, (with an absorbance of 1 optic density = 50 µg/ml for the DNA) allowing quantification of the ratio DNA/proteins and the concentration of DNA. Only the extractions with a DNA/proteins ratio ≥ 1.7 were used.

Chapter 4

4.2.2.3 Transfection of HEK293 cells with $Ca_v1.2$ plasmid

The transfection was made by nucleofection following the Amaxa protocol for the HEK293 cells (kit V, Amaxa, Cologne, Germany). The nucleofection consists of making transient, holes into the plasma membrane by applying short electric pulses (electroporation). At 70-80 % confluency, the cells to be transfected were gently removed from the flask using trypsin and pelleted by centrifugation. Cells were resuspended in 100 μ l of nucleofector solution with 5 μ g of $Ca_v1.2$ DNA and transfected with an Amaxa Nucleofector II machine. To optimize the protocol and/or visualise the transfected cells, 2 μ g of plasmid of the green fluorescent protein (GFP) were used (provided with the kit). To perform the co-transfection, the two plasmids were incubated together for 20 min at room temperature in the nucleofector solution prior to the transfection. By doing so, the $Ca_v1.2$ and GFP plasmids combined due to their electric charges and therefore transfected conjointly into the cells. Immediately after the transfection, the cells were diluted into 500 μ l of pre-warmed medium and seeded at low density on coverslips. The experiments were performed 24 to 48 h after the transfection. Since the plasmid used for the transient transfection is the same than the one used to create the stable cell line, the transiently and stably transfected cells gave indential results. The data were then pooled and treated without distinction.

4.2.3 Electrophysiological recordings

Electrophysiological recordings were made in the whole-cell configuration of the patch-clamp technique. Currents were recorded with a CV2003 BU Headstage (Axon Instruments, Sunnyvale, USA), connected to an Axopatch 200B voltage-clamp amplifier

Chapter 4

(Axon Instruments), digitised with Digidata 1322A (Axon Instruments) and analysed with Clampfit (Axon Instruments). The bath solutions used for gigaseal formation was a HEPES-buffered physiological saline with the following composition (in mM): 135 NaCl, 5 KCl, 1.2 CaCl₂, 1.2 MgCl₂, 5 HEPES and 10 glucose, pH 7.4. The pipette was made by pulling, in two steps, a glass tube (World Precision Instrument, Stevenage, UK) using a Narishige electrode puller (Narishige, Tokyo, Japan). The pipette solution, sterilized by passing it through a 22 µm filter, contained (in mM): 120 CsCl₂, 20 Tetraethylammonium chloride (TEA-Cl), 2 MgCl₂, 10 EGTA, 10 HEPES, 2 Na-ATP, pH 7.2 with CsOH. After the whole-cell configuration had been achieved in the physiological solution, the cells were perfused with a solution containing 2 or 20 mM Ba²⁺ (in mM): 113 or 95 NaCl respectively, 5 CsCl, 0.6 MgCl₂, 2 or 20 BaCl₂, 5 HEPES, 10 glucose and 20 TEA-Cl, pH 7.4 with NaOH. The solutions contained TEA and CsCl to block K⁺ channels. Spermine, R-568 and nifedipine were dissolved in the Ba²⁺ solution to the desired concentration. The effect of neomycin could not be tested by patch-clamp as neomycin precipitated in presence of Ba²⁺. Cell membrane potential was held at -60 mV. The protocol, applied at 0.1 Hz, consisted of a hyperpolarising step to -100 mV for 50 ms followed by a ramp from -100 mV to +100 mV over 200 ms. After 50 ms a step from -80 mV to +15 mV for 100 ms was applied. The steps at -80 mV were done to reactivate the Ca_v1.2 channels, which are normally inactivated at positive potentials. The final step at +15 mV was carried out to activate rapidly all the Ca_v1.2 channels, as the increase in potential during the ramp could produce some inactivation. Nevertheless, no differences were observed between the peak of the current during the ramp or the +15 mV step. The analyses of the currents were performed with the value obtained during the step. Normalized data were used in preference of current density since the HEK293 cells transfected expressed at different level Ca_v1.2 which would result in high error bar in control condition and also during

Chapter 4

application of spermine. To normalise the data, the reference maximum value (100 %) of the current was obtained by calculating the average of the three maximum values in control condition.

Signals were filtered with a low pass Bessel filter at 2 kHz. The currents were leak-subtracted off-line in all experiments by subtracting the slope, calculated at the beginning of the ramp between -100 to -80 mV.

In the first set of experiments, the effects of the CaR agonists on $\text{Ca}_v1.2$ channels were studied. The CaR agonists were diluted in the 20 mM Ba^{2+} solution and administrated through the perfusion line. The cells were exposed to the drugs: spermine (300 μM) and R-568 (100 nM) for 3 min and then washed away by Ba^{2+} solution. Nifedipine (10 μM , Sigma), a specific blocker of the L-type channels, was used as a control to verify the nature of the current. Each cell was exposed only to one drug.

The second group of experiments aimed to establish the relationship between $[\text{Ba}^{2+}]$ and the amplitude of the $\text{Ca}_v1.2$ current recorded. Four concentrations of Ba^{2+} were used (in mM): 20, 5, 2 and 1. The cells were exposed to 20 mM $[\text{Ba}^{2+}]$ then shifted to 5, 2 or 1 mM until the current stabilized. Experiments in reverse order were also performed to negate time-dependent effects. The relationship between $[\text{Ba}^{2+}]$ and $I_{\text{Ca}v1.2}$ was fitted to a Michaelis-Menten curve defined by the equation:

$$Y = V_{\max} * X / (K_m + X)$$

Where V_{\max} is the maximum response and K_m is the affinity.

Chapter 4

The data are presented as mean \pm SEM. Two-tailed, paired Student t-test was used for statistical analysis with differences considered significant at $p < 0.05$.

4.2.4 Calcium imaging on $\text{Ca}_v1.2$ -HEK293 cells

The $\text{Ca}_v1.2$ -HEK293 cells were prepared for the Ca^{2+} imaging experiments as described for the CaR-HEK293 (see Chapter 2). Spermine, neomycin and R-568 were applied for 2.5 or 3 min in HEPES-buffered physiological solution containing (in mM): 135 NaCl, 5 KCl, 1.2 CaCl_2 , 1.2 MgCl_2 , 10 glucose and 5 HEPES, pH 7.4. The cells were stimulated by a depolarisation induced by high K^+ solution of the same composition than the HEPES-buffered physiological solution where K^+ was increased to 30 mM and NaCl decreased to 110 mM to keep the osmolarity constant. Two-tailed, paired Student t-test was used for statistical analysis with differences considered significant at $p < 0.05$.

4.2.5 Effect of spermine and of nifedipine on Ca^{2+} influx in type 1 cells

The effect of spermine and of nifedipine on Ca^{2+} influx in type 1 cells was assessed by Ca^{2+} imaging. Carotid body preparation and the Ca^{2+} imaging experiments were carried out as explained in Chapter 2. Spermine (Sigma) was used at the 200 μM and the nifedipine (Sigma) at 0.1, 1 and 10 μM . The drugs were applied in the order indicated in the figures and text. N is the number of rats used and n is the number of cells recorded. The data are presented as mean \pm SEM. Analysis was carried out with a paired t-test excepted for the comparison of the pooled data where an ANOVA with Turkey post-doc test was used, significant was achieved at $p < 0.05$.

4.3 RESULTS

4.3.1 Absence of effect of spermine and R-568 on $I_{Ca_v1.2}$ recorded in 20 mM Ba^{2+}

The $Ca_v1.2$ current recorded from $Ca_v1.2$ -HEK293 demonstrated a slow rundown over time in control condition (Fig. 4.1A). Perforated whole-cell patches did not attenuate the rate of this rundown significantly (data not shown). The pre-application of either 300 μ M spermine or 100 nM R-568 did not affect the amplitude of the current recorded in 20 mM Ba^{2+} compared to the control (Fig. 4.1B, C and D). Indeed, in the three conditions, control, spermine and R-568, the rundown was similar (Fig. 4.1D). Considering the effects on Ca^{2+} influx shown in Chapter 2, this was a surprise. This difference could be the result of using different Ba^{2+} concentrations in patch-clamp (20 mM Ba^{2+}) and Ca^{2+} imaging (0.5 and 1.2 mM Ca^{2+} and Mg^{2+}) experiments. Therefore, in the next experiment, the effect of different Ba^{2+} concentrations were tested.

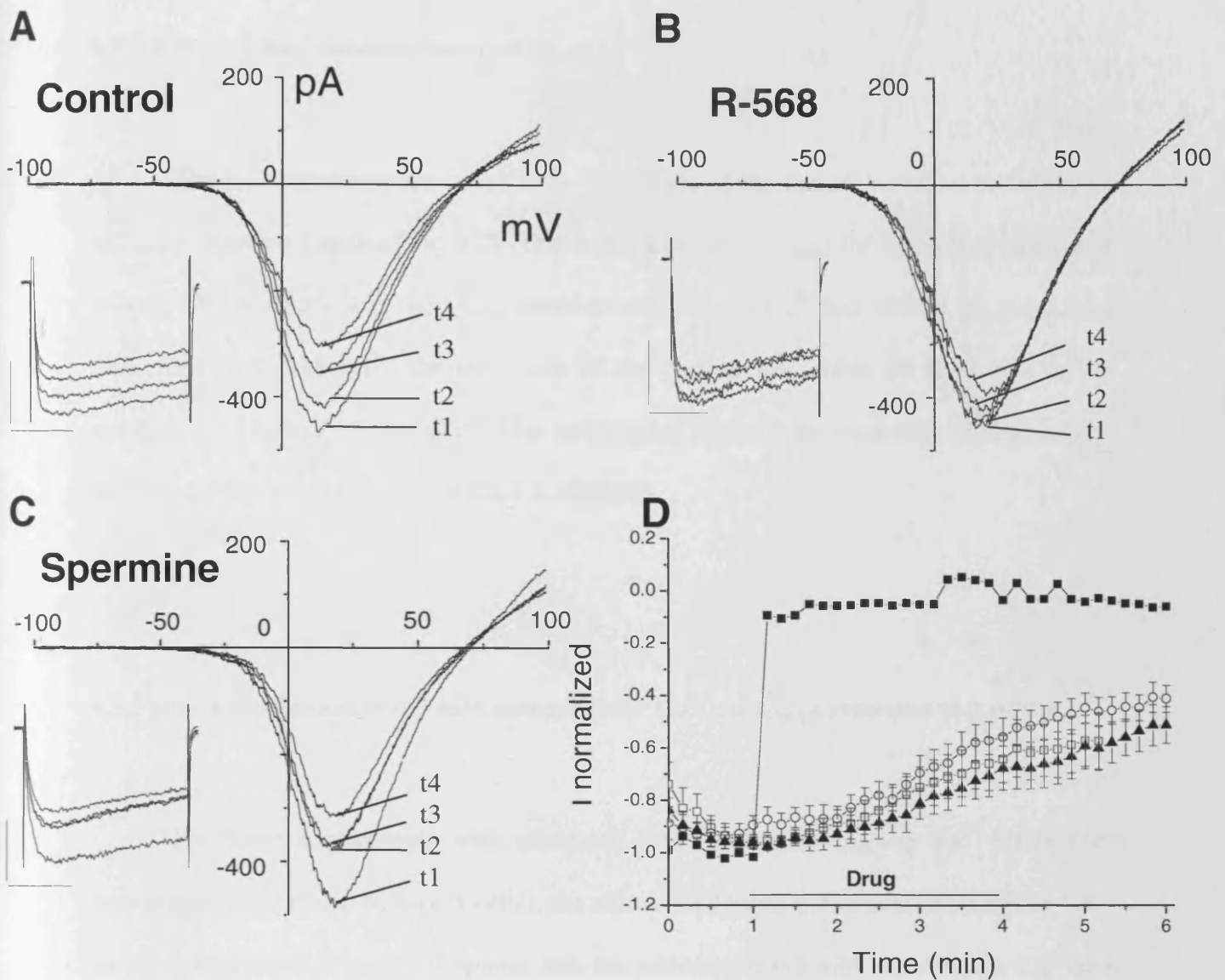


Figure 4.1: CaR activators, spermine and R-568, have no effect on $I_{Ca_v1.2}$ carried by 20 mM external Ba^{2+} . $Ca_v1.2$ expressed in HEK293 is not inhibited by 3 min incubation with the CaR activators: 300 μ M spermine or 100 nM R-568 in 20 mM Ba^{2+} . Typical raw data showing the intensity of the current at $t = 0$ (drug application), $t = 1$, $t = 2$ and $t = 3$ min in control conditions (A) and in cells exposed to 300 μ M spermine (B) or 100 nM R-568 (C). The insets represent the current induced by a +15 mV step. Scale bar, 200 pA and 40 ms. D) Normalized average values: 300 μ M spermine (open square, $n = 5$) or 100 nM R-568 (open circle, $n = 5$), control (closed triangle, $n = 6$). The rundown of the current was similar and comparable in the three conditions. Nifedipine (10 μ M) fully blocked the channel, as expected (closed square).

4.3.2 Effect of Ba²⁺ concentration on I_{Cav1.2}

The Ba²⁺ concentration affected the amplitude of the current recorded according to Michaelis-Menten kinetics (Fig. 4.2). The maximum value (V_{max}) for I_{Cav1.2} was calculated to be at 121.96 ± 8.69 % of the I_{Cav1.2} obtained with 20 mM Ba²⁺ and affinity (K_m) at 4.56 ± 0.86 mM. At 1 mM Ba²⁺, the amplitude of the current was about 30 % of that in the standard condition of 20 mM Ba²⁺. This experiment showed the feasibility of using a low Ba²⁺ for the recording of I_{Cav1.2} in Ca_v1.2-HEK293.

4.3.3 Effect of addition of 0.5 mM extracellular Ca²⁺ on I_{Cav1.2} recorded in 2 mM Ba²⁺

For future experiments with other cell types and involving the Ca²⁺ influx (i.e. neurotransmitter release by type 1 cells), the effect of addition of 0.5 mM extracellular Ca²⁺ on I_{Cav1.2} was tested. Figure 4.3 reveals that the addition of 0.5 mM extracellular Ca²⁺ had an inhibitory effect on I_{Cav1.2}. It inhibited by 87 ± 19 % ($n = 3$) the current compared to 2 mM Ba²⁺ alone.

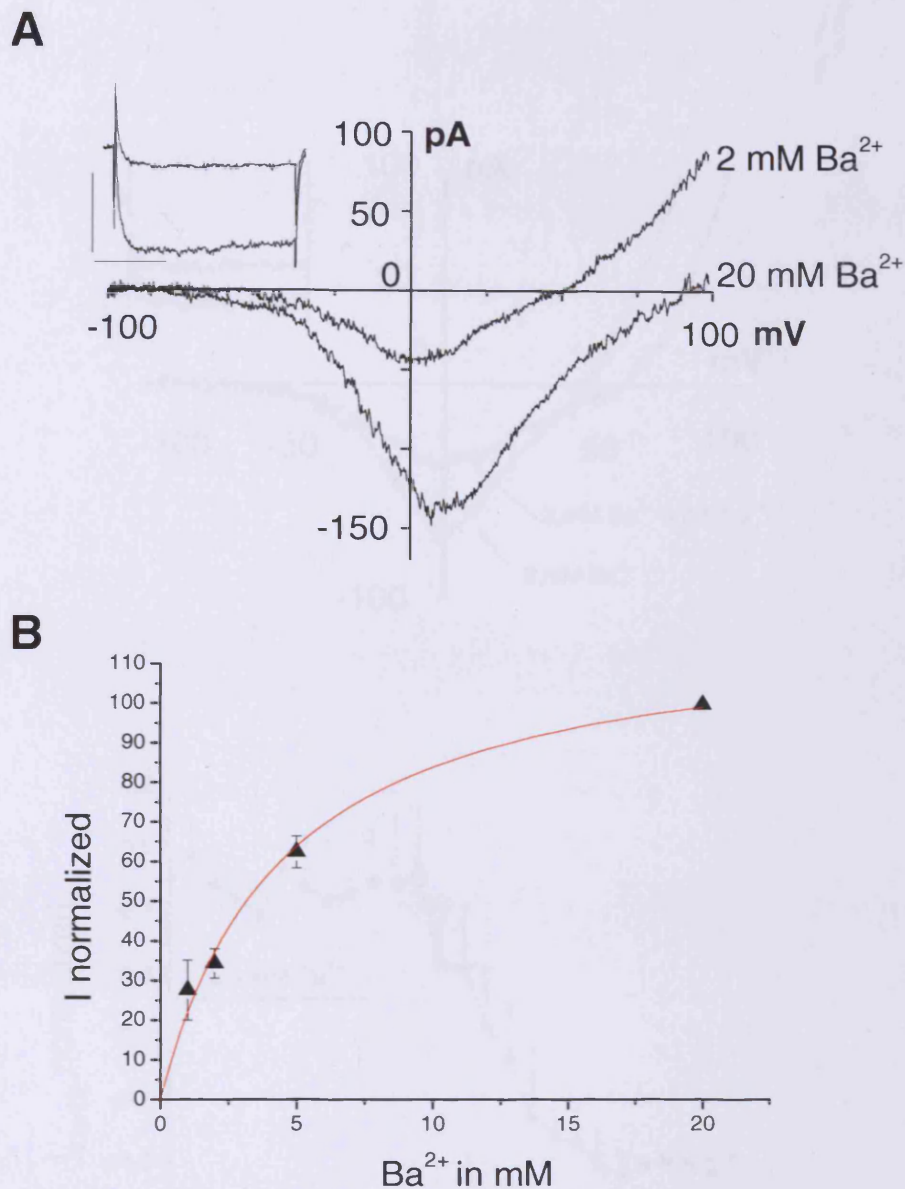
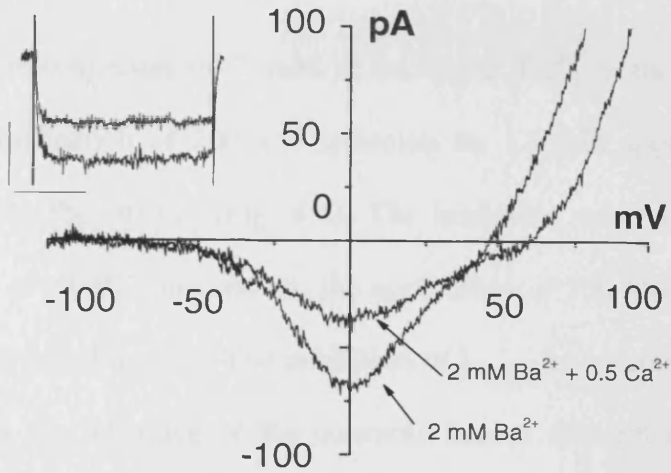


Figure 4.2: Effect of extracellular Ba²⁺ concentration on I_{Cav1.2}. A) Typical examples of I_{Cav1.2} recorded from the same cell in either 2 or 20 mM Ba²⁺. The inset shows the corresponding trace induced by the step at +15 mV. Scale bars are 100 pA and 40 ms. B) Curve presenting the intensity of the current in relation to extracellular Ba²⁺ concentration. The amplitude of the current was normalised to the amplitude of the current recorded with the standard patching solution with 20 mM Ba²⁺. The curve was fitted using Michaelis-Menten equation, $V_{\max} = 121.96 \pm 8.69 \%$ and $K_m = 4.56 \pm 0.86$ mM. At 1 mM Ba²⁺, the amplitude of the current is about 30 % of the intensity obtained in the standard condition with 20 mM Ba²⁺. N = 4 for each points.

A



B

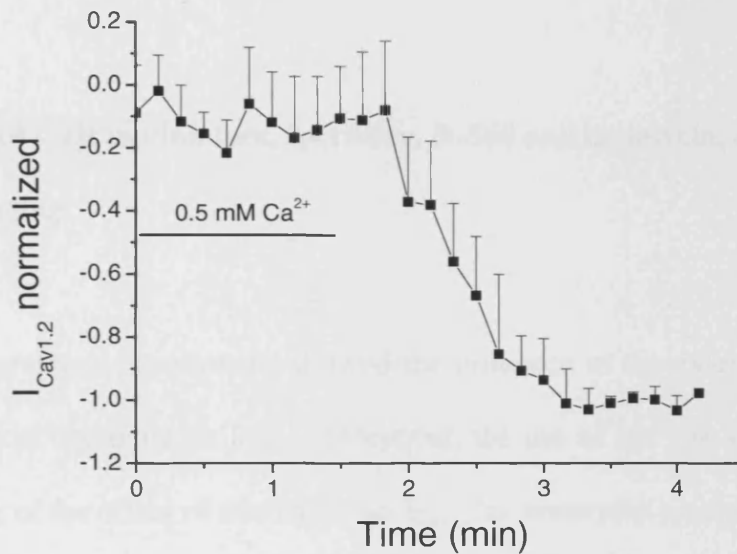


Figure 4.3: Effect of addition of 0.5 mM extracellular Ca²⁺ on $I_{Cav1.2}$ recorded in the presence of 2 mM external Ba²⁺. A) Raw data showing the inhibitory effect of addition of 0.5 mM Ca²⁺ on $I_{Cav1.2}$ recorded in 2 mM Ba²⁺. The insets show the data obtained with the step at +15 mV, scale bars 25 pA and 40 ms. B) Average data of the normalized value of the current at the +15 mV step, 0.5 mM Ca²⁺ has an inhibitory effect on $I_{Cav1.2}$ ($n = 3$, $87 \pm 19\%$).

4.3.4 Inhibitory effect of spermine and absence of effect of R-568 on $I_{Cav1.2}$ recorded in the presence of 2 mM Ba^{2+}

Using a concentration of 2 mM extracellular Ba^{2+} in the recording solution to measure $I_{Cav1.2}$, application of 200 μ M spermine for 1.5 min appeared to have a strong inhibitory effect on the current (Fig. 4.4). The inhibition was 53 ± 3 % and was fully reversible ($n = 3$, $p < 0.01$). In contrast, the application of 100 nM R-568 for 2.5 min did not effect $I_{Cav1.2}$ ($n = 3$, Fig. 4.5). The inhibition of $I_{Cav1.2}$ by spermine in the presence of 2 mM Ba^{2+} showed the influence of the concentration of divalent cation on the effect of spermine. Moreover, this result confirmed the inhibitory effect of spermine on Ca^{2+} influx in type 1 cells.

4.3.5 Effect of CaR modulators, spermine, R-568 and neomycin, on $I_{Cav1.2}$, as assessed by Ca^{2+}_i imaging

The previous experiments showed the influence of the external Ba^{2+} concentration on the effect of spermine on $I_{Cav1.2}$. Moreover, the use of Ba^{2+} as a charge carrier did not allow testing of the effect of neomycin on $I_{Cav1.2}$ as neomycin precipitated in Ba^{2+} solution. Therefore, to avoid these limitations, the effect of spermine, R-568 and neomycin were assessed by Ca^{2+} imaging which allowed experiments to be performed using a physiological solution containing 1.2 mM extracellular Ca^{2+} . In this condition, 200 μ M spermine and 300 μ M neomycin had an inhibitory effect on Ca^{2+} influx through $I_{Cav1.2}$ which was of 76.6 ± 3.6 % ($n = 3$, $p < 0.01$) and 99.1 ± 0.9 % ($n = 3$, $p < 0.05$), respectively. However, 100 nM R-568 did not effect Ca^{2+} influx ($n = 3$, $p > 0.05$).

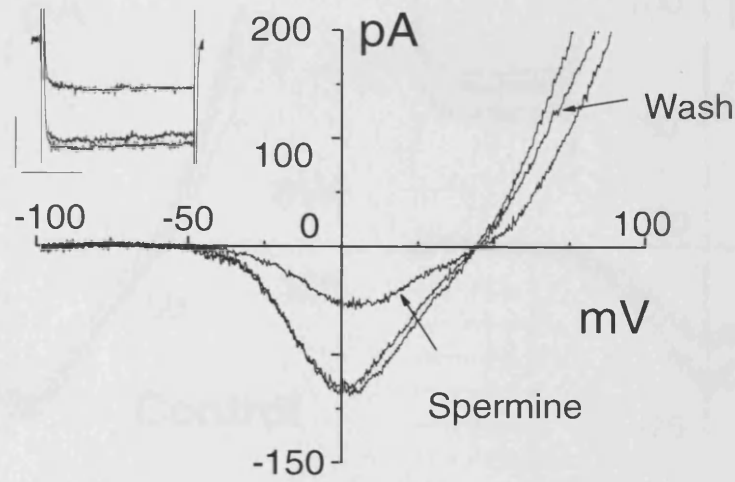
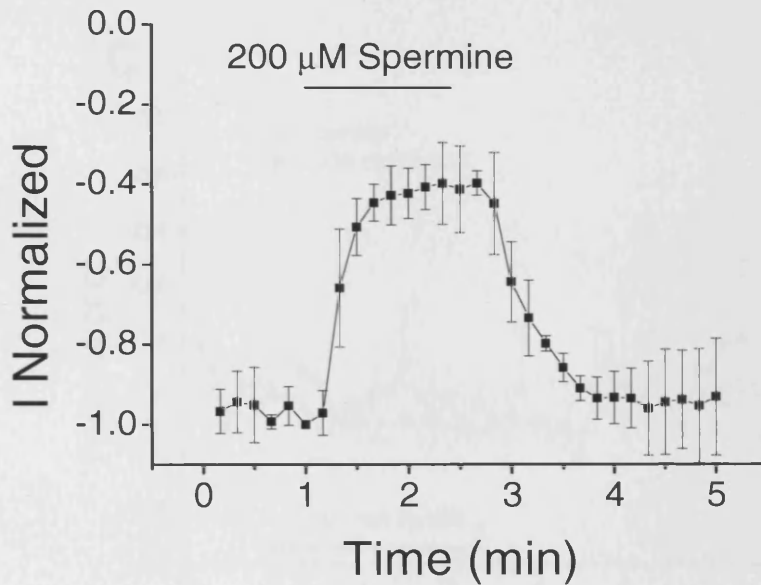
A**B**

Figure 4.4: Inhibitory effect of spermine on $I_{Cav1.2}$ recorded in presence of 2 mM external Ba^{2+} . A) Typical examples of the effect of 200 μM spermine on $I_{Cav1.2}$ recorded in the presence of 2 mM external Ba^{2+} . The effect of spermine was reversible. The inset shows traces obtained at the +15 mV step. Scale bars are 50 pA and 40 ms. B) Average data of the normalized $I_{Cav1.2}$ current over time. The reversible inhibition induced by spermine was $53 \pm 3\%$ of the $I_{Cav1.2}$ control current ($N = 3$, $p < 0.01$).

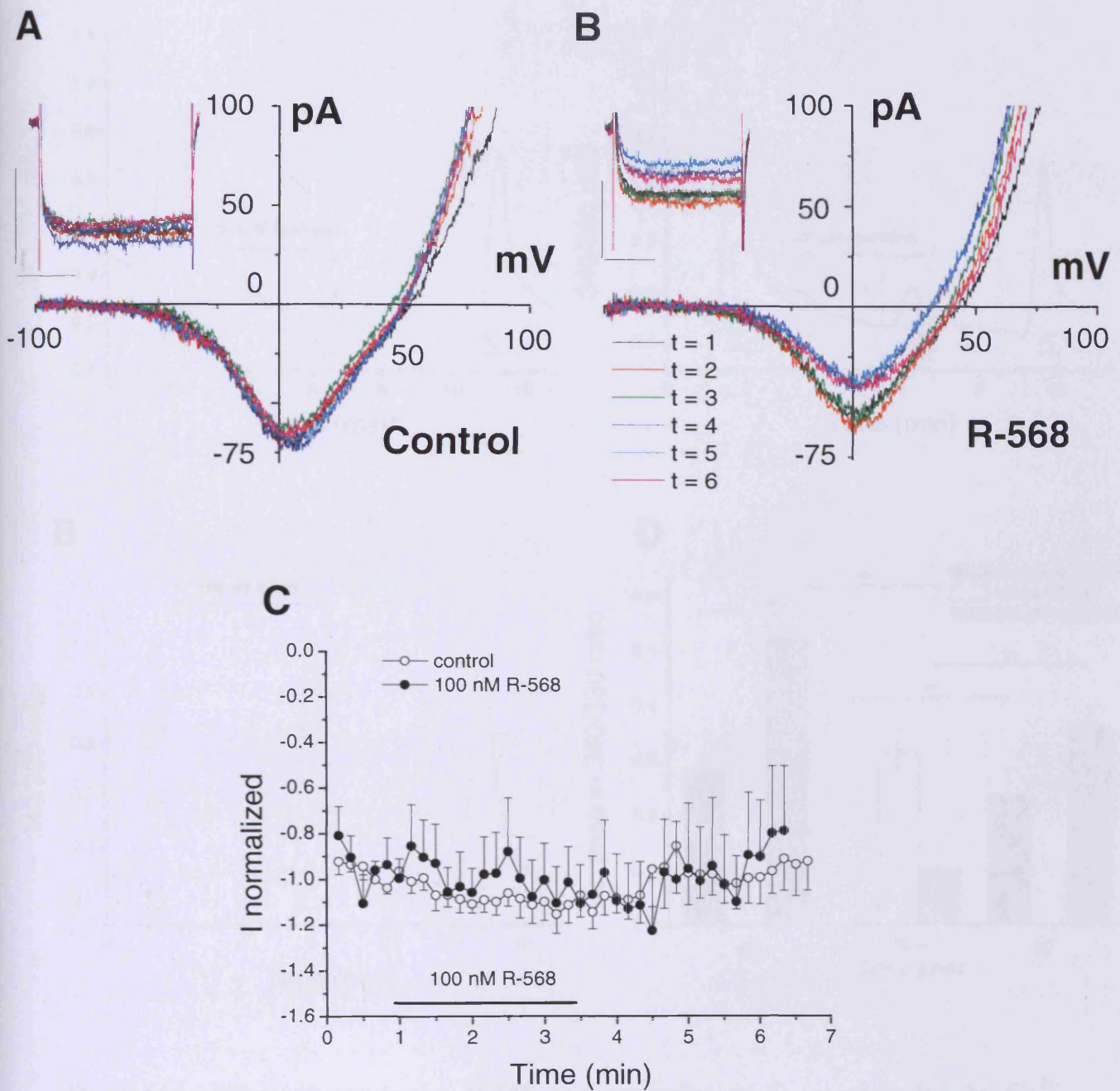


Figure 4.5: Absence of effect of R-568 on $I_{Cav1.2}$ recorded in the presence of 2 mM external Ba^{2+} . Typical recordings made in control solution (A) or with application of 100 nM R-568 for 2.5 min. (B) The drug application was at t = 1. The inset shows the currents induced by a +15 mV step. Scale bars are 50 pA and 40 ms. C) presents the average time-course data and indicates that the rundown of the $I_{Cav1.2}$ currents was the same in the control (open circles, n = 5) and R-568 treated cells (closed circles, n = 6). Application of R-568 is indicated by the black bar.

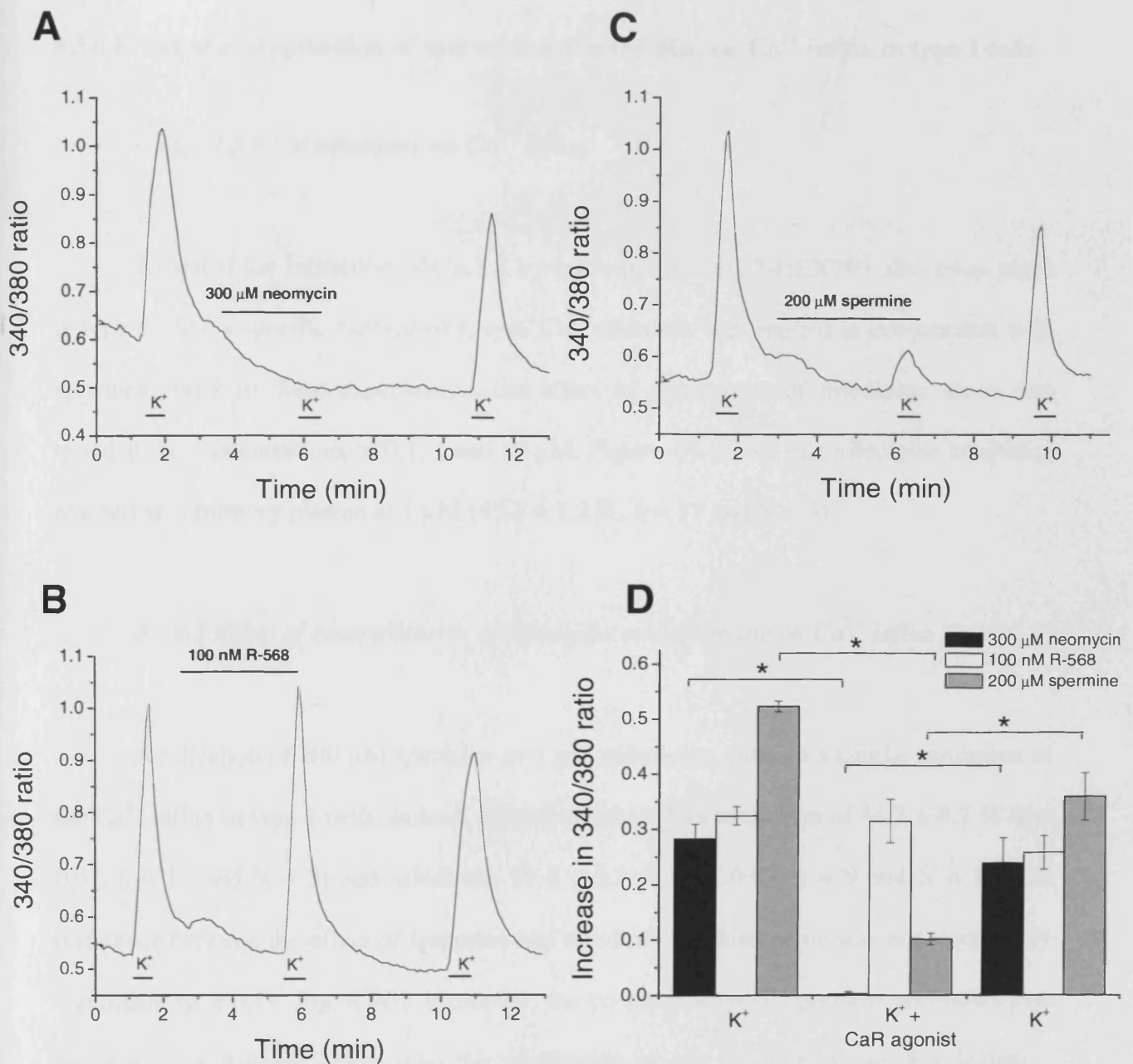


Figure 4.6: Effect of neomycin, R-568 and spermine on $I_{\text{Cav}1.2}$ recorded by Ca^{2+} imaging in 1.2 mM external Ca^{2+} . As expected, high K^+ induced a large Ca^{2+} influx. The co-application with 300 μM neomycin (A, $n = 3$) or 200 μM spermine (C, $n = 3$) inhibited the Ca^{2+} influx induced by high K^+ . The neomycin and spermine effects were reversible, as indicated by the third high K^+ stimulation. In contrast, 100 nM R-568 (B, $n = 3$) had no effect on $I_{\text{Cav}1.2}$. The effect of neomycin ($p < 0.05$) and spermine ($p < 0.01$) were statistically significant (D).

4.3.6 Effect of co-application of spermine and nifedipine on Ca^{2+} influx in type 1 cells

4.3.6.1 Effect of nifedipine on Ca^{2+} influx

To test if the inhibition of $Ca_v1.2$ by spermine in $Ca_v1.2$ -HEK293 also takes place in type 1 cells, a specific blocker of L-type Ca^{2+} channels was applied in conjunction with spermine. Prior to these experiments, the effect of application of nifedipine alone was tested at the concentrations of 0.1, 1 and 10 μ M. Figure 4.7 shows that nifedipine inhibition reached an inhibitory plateau at 1 μ M (45.3 ± 5.2 %, $n = 17$ and $N = 3$).

4.3.6.2 Effect of co-application of nifedipine and spermine on Ca^{2+} influx

Application of 200 μ M spermine or 1 μ M nifedipine induced a similar inhibition of the Ca^{2+} influx in type 1 cells. Indeed, spermine induced an inhibition of 44.3 ± 4.3 % ($p < 0.01$, $n = 18$ and $N = 3$) and nifedipine 39.4 ± 5.5 % ($p < 0.01$, $n = 9$ and $N = 3$). The difference between the effect of spermine and nifedipine applied alone was not statistically significant ($p = 0.14$, Fig. 4.8E). Moreover, the co-application of spermine and nifedipine had always a stronger effect than the application of one of them alone. For instance, spermine induced 44.3 ± 4.3 % of inhibition whereas spermine + nifedipine

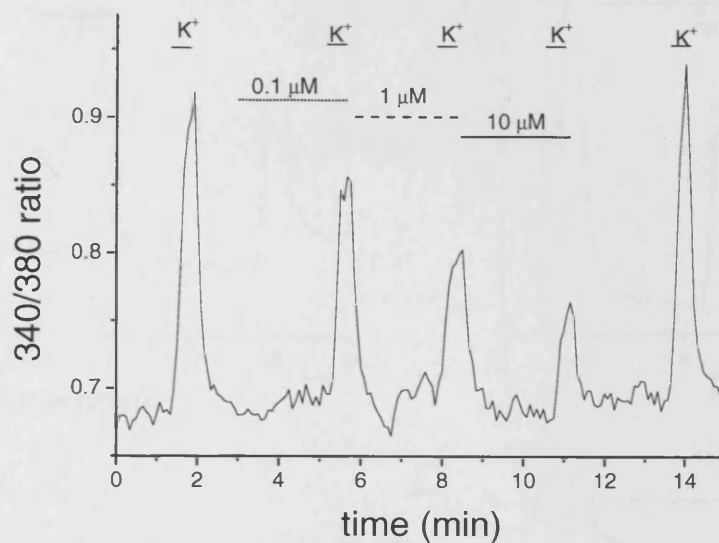
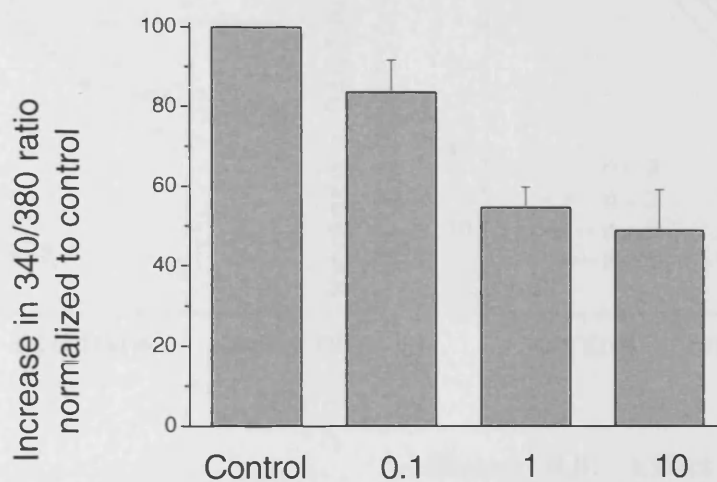
A**B**

Figure 4.7: Inhibitory effect of nifedipine on Ca^{2+} influx in type 1 cells. A) Typical recording showing the effect of increasing concentrations of nifedipine (0.1, 1 and 10 μM) on Ca^{2+} influx induced by high K^+ in type 1 cells. The nifedipine inhibition was reversible. B) Bar graph of the average data showing that at 1 μM nifedipine reached its maximal inhibitory effect ($15 \leq n \leq 17$ and $N = 3$ for each concentration).

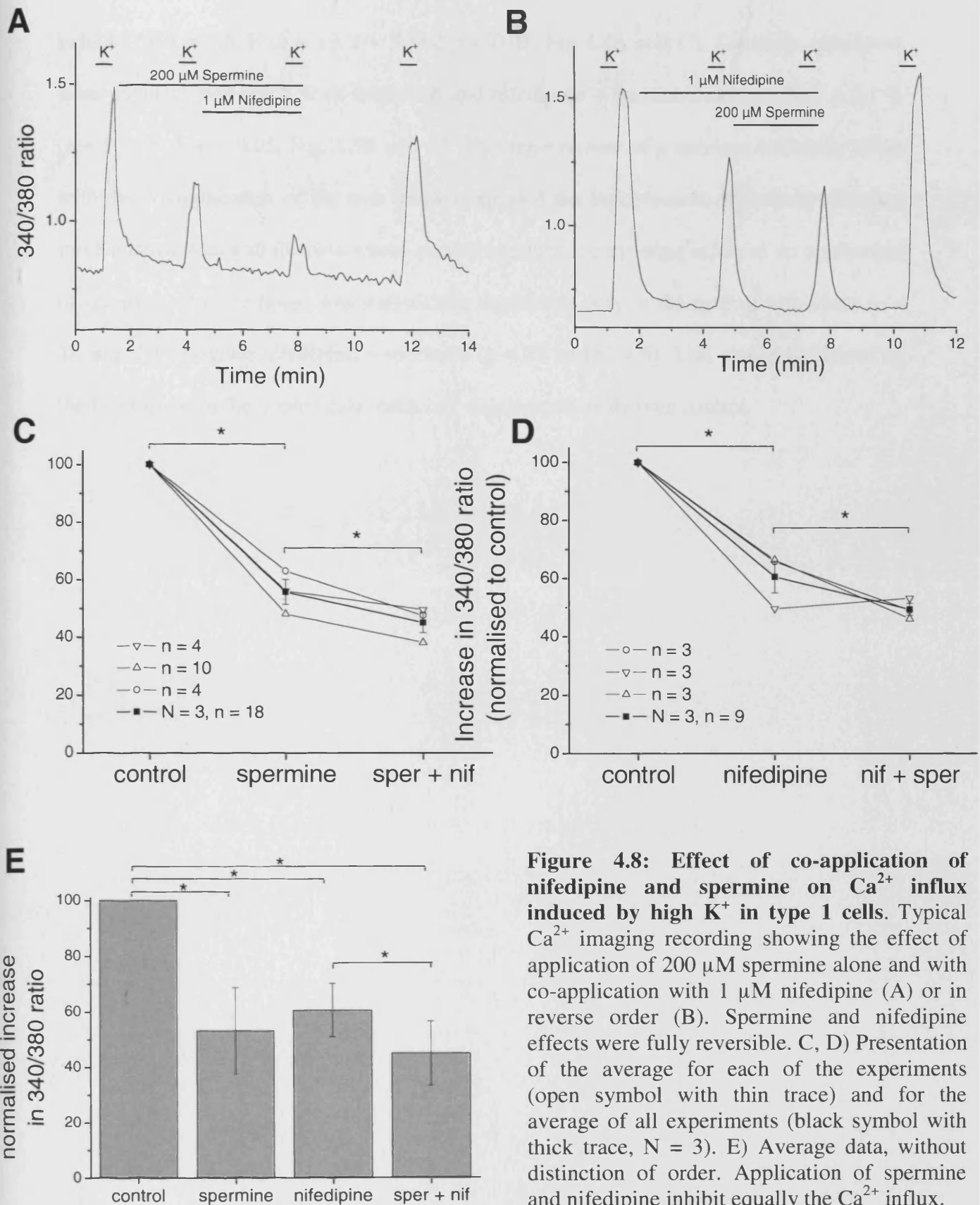


Figure 4.8: Effect of co-application of nifedipine and spermine on Ca^{2+} influx induced by high K^+ in type 1 cells. Typical Ca^{2+} imaging recording showing the effect of application of $200 \mu\text{M}$ spermine alone and with co-application with $1 \mu\text{M}$ nifedipine (A) or in reverse order (B). Spermine and nifedipine effects were fully reversible. C, D) Presentation of the average for each of the experiments (open symbol with thin trace) and for the average of all experiments (black symbol with thick trace, $N = 3$). E) Average data, without distinction of order. Application of spermine and nifedipine inhibit equally the Ca^{2+} influx.

Chapter 4

induced $54.9 \pm 3.5 \%$ ($n = 18$, $N = 3$ and $p < 0.01$, Fig 4.8A and C). Similarly, nifedipine alone induced $39.4 \pm 5.5 \%$ of inhibition and nifedipine + spermine induced $50.6 \pm 2.1 \%$ ($n = 9$, $N = 3$, $p < 0.05$, Fig. 4.8B and C). The achievement of a stronger inhibitory effect with the co-application of the two drugs suggested the involvement of partially different mechanisms. When all the data were pooled together, the synergic effect of co-application of spermine and nifedipine was statistically significant only in the case of nifedipine ($n = 18$ and $N = 6$) versus nifedipine + spermine ($n = 27$ and $N = 6$). This can be explained by the fact that, with the pooled data, each cell does not act as its own control.

4.4 DISCUSSION

As suggested by the Ca^{2+} imaging experiments in carotid body type 1 cells (Chapter 2), spermine and neomycin are able to inhibit voltage-dependent Ca^{2+} influx induced by hypoxia or high K^+ . Nevertheless, these previous experiments did not allow any conclusions as to whether the inhibition is direct or indirect.

Neomycin and spermine belong to two different classes of molecule, an aminoglycoside antibiotic and a polyamine, respectively. Nevertheless, they share the characteristic of being variably protonated and becoming positively charged at physiological pH. Indeed, neomycin possesses 4.4 positive charges (McLarnon & Riccardi, 2002) and spermine has 4 charges (Heby, 1986) at pH 7.4. It is possible that these positive charges confer to neomycin and spermine the ability to block the channel. Whereas R-568 is not positively charged at physiological pH (Nemeth, 2004).

With a standard patch-clamp solution containing 20 mM Ba^{2+} , spermine had no effect on the $\text{Ca}_v1.2$ current, but lowering the Ba^{2+} concentration to 2 mM revealed a dramatic inhibition of the current by spermine. Moreover, the Ca^{2+} imaging experiments showed that neomycin and spermine were strong inhibitors of $\text{Ca}_v1.2$ in physiological solutions (containing no Ba^{2+} and 1.2 mM extracellular Ca^{2+}). R-568 did not have any effect on the $\text{Ca}_v1.2$ current recorded by patch-clamp in either 20 or 2 mM Ba^{2+} or by Ca^{2+} imaging. The results found with patch-clamp in 2 mM Ba^{2+} and Ca^{2+} imaging are in accordance with the data obtained in carotid body type 1 cells showing that spermine and neomycin inhibit voltage-dependent Ca^{2+} channels. For the patch-clamp experiment no recording with Ca^{2+} as a charge carrier was attempted as the amplitude of the current in 2

Chapter 4

mM Ba^{2+} was only about 50-100 pA. Indeed, the use of Ca^{2+} would have decrease the amplitude of the current as Ca^{2+} has a lower permeability through the voltage-dependent Ca^{2+} channel and inhibits the channel. Moreover, the nature of the interaction between spermine and $\text{Ca}_v1.2$ has not been investigated, single channel recording would have been usefull to study the effect of spermine on the conductance and the opening probability of $\text{Ca}_v1.2$.

The inhibition of $\text{Ca}_v1.2$ by spermine and neomycin presented in this study are in agreement with most data obtained by other groups in native cells. For instance, neomycin has been reported to inhibit voltage-dependent Ca^{2+} channels in chromaffin cells (50 to 200 μM) (Duarte *et al.*, 1993), neurons (IC_{50} at 50 μM) (Parsons *et al.*, 1992) (90 to 400 μM) (Keith *et al.*, 1992) and cardiac myocytes (IC_{50} at 90 μM) (Belus & White, 2001). In addition, spermine induces an inhibition of voltage-dependent Ca^{2+} channels in muscle (100 to 1000 μM) (Gomez & Hellstrand, 1995) and (IC_{50} at 800 μM in 10 mM Ba^{2+}) (Kim *et al.*, 2007) and retinal neurons (IC_{50} at 28 μM) (Lasater & Solessio, 2002).

The fact that the inhibitory effect of spermine is dependent upon the permeating cation concentration is suggestive of a competitive process between spermine and cations. The situation is likely to be the same with neomycin as suggested by the experiment of Parson *et al.* in which the inhibitory effect of neomycin on voltage-dependent Ca^{2+} channels in nerve can be suppressed by increasing the Ca^{2+} concentration from 2 to 10 mM (Parsons *et al.*, 1992). The mechanism of the inhibitory effect of spermine and neomycin is probably the same and due to the presence of positive charges on these molecules. Spermine and neomycin might screen the negative charges which are on the plasma membrane and modify the opening of the voltage-dependent Ca^{2+} channels or reduce the

Chapter 4

effectiveness of the Ca^{2+} (Belus & White, 2001). Increasing the cation concentration, in my experiments and in those of Parsons *et al.* (Parsons *et al.*, 1992), may either increase the competition between spermine/neomycin and cations to screen the charge on the plasma membrane or/and increase the driving force which may compensate the decreased opening of the channel. The fact that the inhibitory effect of spermine can be observed only with a low cation (Ba^{2+} or Ca^{2+}) concentration may explain the absence of effect observed by Herman *et al.* on neurons (Herman *et al.*, 1993). Indeed, the Ba^{2+} concentration used in their experiments was 110 mM with a spermine concentration of 1 mM. R-568, which does not possess positive charges, has no effect on the $\text{Ca}_v1.2$, which is consistent with charge-screening hypothesis. Interestingly, and supporting the screening hypothesis, among the three polyamines, spermine is the most potent at inhibiting the voltage-dependent Ca^{2+} channels and is also the most charged polyamine (Nilsson *et al.*, 2002).

Moreover, R-568 does not have any other type of interaction with $\text{Ca}_v1.2$ at the concentration tested. This finding completes and confirms the data of Nemeth *et al.* showing an inhibitory effect of this calcimimetic on L-type Ca^{2+} channels only at concentrations of 500 nM and above (Nemeth, 2004).

The experiments in this chapter carried out on $\text{Ca}_v1.2$ -HEK293 demonstrate a very likely interaction between $\text{Ca}_v1.2$ and spermine or neomycin. Nevertheless, excised patch-clamp experiments would have been more appropriate to test for a direct interaction. In the case of spermine, my data confirm the result of Gomez *et al.* who were the only one to show a direct inhibition of voltage-dependent Ca^{2+} channels by spermine using excised patch-clamp configuration with guinea-pig smooth muscle cells (Gomez & Hellstrand, 1999). In all other studies, it cannot be excluded that spermine/neomycin inhibit the

Chapter 4

voltage-dependent Ca^{2+} channels indirectly by acting on a receptor, like CaR. The idea of modulation of voltage-dependent Ca^{2+} channels by activation of the CaR was my first hypothesis to explain the inhibition of catecholamine release by spermine in isolated carotid body. However, further experiments revealed that the CaR was not expressed in type 1 cells and, therefore, not involved in the inhibitory effect of spermine. Nevertheless, the hypothesis of modulation of the voltage-dependent Ca^{2+} channels by the CaR could explained some of the data obtained by other groups on native cell types which may express the CaR, i.e. neurons (Quinn *et al.*, 1997). Moreover, Parkash has recently shown a co-localisation of CaR and voltage-dependent Ca^{2+} channels in beta-cells supporting the hypothesis of an indirect modulation of the voltage-dependent Ca^{2+} channels by CaR (Parkash, 2008).

The comparative effect of spermine and nifedipine on Ca^{2+} influx in type 1 cells was assessed by Ca^{2+} imaging in preference to patch-clamp. This choice was made on the basis that the inhibitory effect of spermine could only be studied at low cation concentration (2 mM Ba^{2+}), which mediates a weak current, and therefore requires a high expression of $\text{Ca}_v1.2$. The use of Ca^{2+} imaging appears to be a good alternative to avoid this problem.

The application of nifedipine alone induces an inhibition about of 45 % of the Ca^{2+} influx in type 1 cells. This value is slightly less than the 74 % and 67 % obtained by other groups studying the voltage-dependent Ca^{2+} channel by patch-clamp in these cells (Buckler & Vaughan-Jones, 1994c; e Silva & Lewis, 1995). The smaller inhibition found in this study can be explained by the fact that type 1 cells still associated in small cluster have been used rather than totally dissociated cells, as required for patch-clamp experiments.

Chapter 4

This may have reduced the access of nifedipine to the channel and therefore equally reduced the inhibitory effect. However, the experiment corroborates the evidence for expression of L-type Ca^{2+} channels in type 1 cells. The inhibitory effects of applications of either spermine or nifedipine, quantitatively, do not differ. Nevertheless, nifedipine is a specific blocker of the L-type Ca^{2+} channels whereas spermine is not and at the concentration used (200 μM) does block only partially (about 50 %) the $\text{Ca}_v1.2$ current in $\text{Ca}_v1.2\text{-HEK293}$. These points lead to the conclusion that nifedipine blocks almost fully the $\text{Ca}_v1.2$ current while spermine blocks partially $\text{Ca}_v1.2$ current and partially blocks $\text{Ca}_v2.2$ which gives the same total inhibition of the Ca^{2+} influx that the one observed with nifedipine. To furthermore confirm this point, it would have been useful to compare the effect of spermine or nifedipine on $\text{Ca}_v1.2\text{-HEK}$. The comparison of the inhibition induced by spermine and nifedipine alone or following co-application shows that the two drugs together have a mildly additive effect. In addition, their effects are not due to totally distinct mechanisms because the drug co-application gives a smaller inhibition (about 60 %) than the sum of their inhibition alone, which would be near 80 %. These results confirm that spermine blocks partially $\text{Ca}_v1.2$ and possibly $\text{Ca}_v2.2$ in type 1 cells. According to the screening charge hypothesis, the effect of spermine should be unspecific and inhibit $\text{Ca}_v1.2$ and $\text{Ca}_v2.2$. The inhibition of $\text{Ca}_v2.2$ by spermine is in agreement with recent the conclusion of Cino and al. showing an inhibitory effect of 500 μM spermine on $\text{Ca}_v2.2$ in rat dorsal root ganglion neurons (Cino & Formenti, 2008).

4.5 CONCLUSION

The experiments on carotid body and dissociated type 1 cells have revealed an inhibitory effect of spermine and neomycin on neurotransmitters release and on the Ca^{2+} influx induced either by hypoxia or high K^+ . Using molecular techniques, I have demonstrated that carotid body type 1 cells express $\text{Ca}_v1.2$ and $\text{Ca}_v2.2$. In this chapter, the effect of spermine, neomycin and R-568 on $\text{Ca}_v1.2$ was investigated. The electrophysiological experiments show that spermine has an inhibitory effect on $\text{Ca}_v1.2$ depending on the extracellular Ba^{2+} concentrations, with a stronger effect at low Ba^{2+} concentration. Moreover, experiments carried out in physiological conditions, using Ca^{2+} imaging, confirm the inhibitory effect of spermine and neomycin on $\text{Ca}_v1.2$. In addition, the use of HEK293 cells expressing $\text{Ca}_v1.2$ has ruled out the possible interaction of spermine and neomycin with an extracellular receptor and demonstrated a direct inhibition of $\text{Ca}_v1.2$ by these molecules. In type 1 cells, the co-application of spermine and nifedipine has demonstrated that spermine partially inhibits $\text{Ca}_v1.2$ and probably $\text{Ca}_v2.2$. Therefore, the inhibition of the catecholamine release by spermine is due to the direct inhibition, by spermine, of $\text{Ca}_v1.2$ and $\text{Ca}_v2.2$.

DISCUSSION AND PERSPECTIVES

DISCUSSION AND PERSPECTIVES

This study on the carotid body has reported, for the first time, an inhibitory effect of spermine on chemoreception using different approaches. Spermine inhibits catecholamine secretion from isolated carotid body and Ca^{2+} influx in type 1 cells induced either by high K^+ or hypoxia. Then, the molecular mechanisms mediating this inhibition were investigated. The expression of voltage-dependent Ca^{2+} channels in rat type 1 cells was detected. RT-PCR and immunohistochemistry showed the presence of $\text{Ca}_v1.2$ and $\text{Ca}_v2.2$ in type 1 cells. As L-type Ca^{2+} channels are the major way of Ca^{2+} entry in the cytosol, the effect of spermine on $\text{Ca}_v1.2$ was then tested by patch-clamp and Ca^{2+} imaging in $\text{Ca}_v1.2$ -HEK293. These experiments demonstrated an inhibitory effect of spermine only with a low extracellular cation concentration and a direct inhibition of the channel by spermine. The co-application of spermine and nifedipine in type 1 cells showed that spermine inhibits $\text{Ca}_v1.2$ and $\text{Ca}_v2.2$. Therefore the inhibitory effect of spermine on catecholamine secretion is due to an inhibition of $\text{Ca}_v1.2$ and $\text{Ca}_v2.2$, resulting in a smaller $[\text{Ca}^{2+}]_i$ increase and weaker neurotransmitter release (Fig. 4.9) as postulated in the second hypothesis.

The physiological relevance of the spermine inhibition of the carotid body chemoreception depends on the extracellular concentration of spermine. The plasma concentration of spermine is in the μM range which is far below the minimal spermine concentration required to inhibit $\text{Ca}_v1.2$ in rat type 1 cells. Indeed, the IC_{50} for spermine in dissociated type 1 cells is $\sim 500 \mu\text{M}$. The plasma spermine concentration is known to be increased in certain physiological situations (during development (Tabor & Tabor, 1984), due to hormonal variations (Gilad *et al.*, 2002)) as well as pathological situations

(malignant tumour (Casero & Marton, 2007)). In such situations the plasmic spermine concentration increases but not sufficiently to have an effect on carotid body function. So, the plasma concentration of spermine can not inhibit carotid body function.

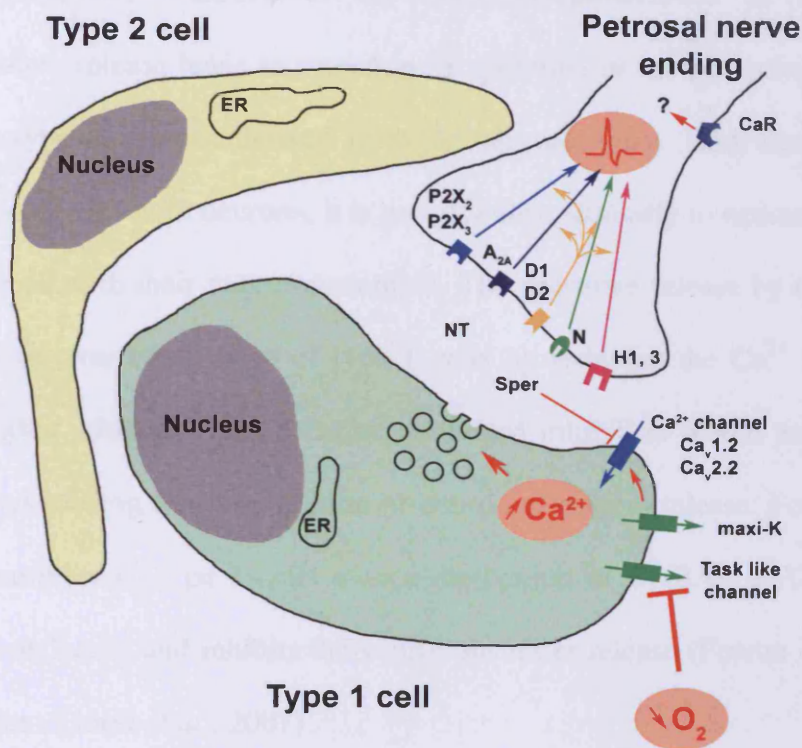


Figure 4.9: Schematic representation of carotid body illustrating the expression of CaR and voltage-dependent Ca²⁺ channel and the inhibitory effect of spermine on type 1 cells. Type 1 cells express the voltage-dependant Ca²⁺ channel subunits Ca_v1.2 and Ca_v2.2 but not the CaR which was found to be expressed in the nerve endings. The spermine (Sper), co-released with neurotransmitters (NT), inhibits the Ca_v1.2 and possibly Ca_v2.2. This inhibition induces a reduction of the Ca²⁺ influx and then of the neurotransmitter release.

In neuronal tissue, independently of the plasma contribution in spermine, the extracellular spermine concentration can be increased, locally, as a result of spermine

Discussion and Perspectives

secretion in the synaptic cleft. It has been shown that neurons and potentially glial cells are able to release spermine in the extracellular medium under high K^+ stimulation (Masuko *et al.*, 2003) or N-methyl-D-aspartate receptor activation (Fage *et al.*, 1992). In neurons, spermine is concentrated, up to 2.8 mM, in intracellular vesicles via a proton gradient-dependent transporter (Masuko *et al.*, 2003). Depolarisation of neurons inducing neurotransmitters release leads to secretion of spermine in the synaptic cleft (Fage *et al.*, 1992). Since type 1 cells are derived from the neuronal crest (Gonzalez *et al.*, 1994) and share many properties with neurons, it is possible that, similarly to neurons, type 1 cells co-release spermine with their neurotransmitters. The spermine release by type 1 cells would then prevent an over stimulation of type 1 cells by reducing the Ca^{2+} influx induced by hypoxia or other stimuli. This spermine mediated inhibition would act in synergy with other pathways leading to the inhibition of neurotransmitters release. For instance, release of neurotransmitters by type 1 cells induces activation of $GABA_B$, P_2Y_1 , or D_2 receptors present on type 1 cells and inhibits the neurotransmitter release (Fearon *et al.*, 2003; Xu *et al.*, 2005; Prieto-Lloret *et al.*, 2007).

Further work is needed to gain better understanding of the role of polyamines in carotid body physiology. Indeed, on one hand, polyamine could be co-secreted with neurotransmitters and, locally, modulate ion channels and on another hand, polyamines could be involved in the regulation of cell division and growth during chronic sustained hypoxia. In the carotid body, as in the lung vascular smooth muscle cells, hypoxia induces a decrease in ornithine decarboxylase gene expression (Babal *et al.*, 2002; Ganfornina *et al.*, 2005) and probably, similarly to the situation in the lung, an increase in polyamine uptake which triggers the morphological changes, such as cell division (Babal *et al.*, 2002).

Discussion and Perspectives

To complete this study further more experiments are needed, especially concerning the spermine metabolism in carotid body. In a very short future, I am planning to quantify the spermine up-take and release by isolated carotid body in normoxia versus hypoxia using [^{14}C]-spermine. By analogy with the situation in lung vascular smooth muscle cells, I would anticipate that the uptake would be higher in hypoxia. Also, the release of spermine, by isolated carotid body induced either by high K^+ or hypoxia, will be quantified to assess the hypothesis of a co-release of spermine and neurotransmitters. In addition, the putative effect of spermine on the receptors expressed on the petrosal nerve endings, specifically for ATP or ACh which are the two main excitatory neurotransmitters, could be tested to have a full picture of the effect of spermine on carotid body chemoreception.

Another interesting approach to the role of spermine in carotid body chemoreception would be to determine the effect of low spermine concentration on type 1 cells. Indeed, it has been recently shown that spermine potentiates $\text{Ca}_v2.2$ when applied in the nM range on rat dorsal root ganglia neurons (Cino & Formenti, 2008). If spermine has a similar effect on $\text{Ca}_v1.2$ and $\text{Ca}_v2.2$ in type 1 cells, spermine would potentiate or inhibit the neurotransmitters release according to its concentration.

REFERENCES

- Acker H. (1994). Mechanisms and meaning of cellular oxygen sensing in the organism. *Respir Physiol* **95**, 1-10.
- Adachi T, Ishikawa K, Hida W, Matsumoto H, Masuda T, Date F, Ogawa K, Takeda K, Furuyama K, Zhang Y, Kitamuro T, Ogawa H, Maruyama Y & Shibahara S. (2004). Hypoxemia and blunted hypoxic ventilatory responses in mice lacking heme oxygenase-2. *Biochem Biophys Res Commun* **320**, 514-522.
- Alexander SP, Mathie A & Peters JA. (2006). Guide to receptors and channels, 2nd edition. *Br J Pharmacol* **147 Suppl 3**, S1-168.
- Altafaj X, Cheng W, Esteve E, Urbani J, Grunwald D, Sabatier JM, Coronado R, De Waard M & Ronjat M. (2005). Maurocalcine and domain A of the II-III loop of the dihydropyridine receptor Cav 1.1 subunit share common binding sites on the skeletal ryanodine receptor. *J Biol Chem* **280**, 4013-4016.
- Alvarez-Buylla R & de Alvarez-Buylla ER. (1988). Carotid sinus receptors participate in glucose homeostasis. *Respir Physiol* **72**, 347-359.
- Babal P, Ruchko M, Ault-Ziel K, Cronenberg L, Olson JW & Gillespie MN. (2002). Regulation of ornithine decarboxylase and polyamine import by hypoxia in pulmonary artery endothelial cells. *Am J Physiol Lung Cell Mol Physiol* **282**, L840-846.
- Bai M. (2004). Structure-function relationship of the extracellular calcium-sensing receptor. *Cell Calcium* **35**, 197-207.
- Bai M, Trivedi S & Brown EM. (1998). Dimerization of the extracellular calcium-sensing receptor (CaR) on the cell surface of CaR-transfected HEK293 cells. *J Biol Chem* **273**, 23605-23610.
- Bairam A, Frenette J, Dauphin C, Carroll JL & Khandjian EW. (1998). Expression of dopamine D1-receptor mRNA in the carotid body of adult rabbits, cats and rats. *Neurosci Res* **31**, 147-154.
- Belting M, Mani K, Jonsson M, Cheng F, Sandgren S, Jonsson S, Ding K, Delcros JG & Fransson LA. (2003). Glypican-1 is a vehicle for polyamine uptake in mammalian cells: a pivotal role for nitrosothiol-derived nitric oxide. *J Biol Chem* **278**, 47181-47189.
- Belus A & White E. (2001). Effects of antibiotics on the contractility and Ca²⁺ transients of rat cardiac myocytes. *Eur J Pharmacol* **412**, 121-126.
- Ben-Chaim Y, Chanda B, Dascal N, Bezanilla F, Parnas I & Parnas H. (2006). Movement of 'gating charge' is coupled to ligand binding in a G-protein-coupled receptor. *Nature* **444**, 106-109.
- Benarroch EE. (2007). Brainstem respiratory control: substrates of respiratory failure of multiple system atrophy. *Mov Disord* **22**, 155-161.
- Benot AR & Lopez-Barneo J. (1990). Feedback Inhibition of Ca²⁺ Currents by Dopamine in Glomus Cells of the Carotid Body. *Eur J Neurosci* **2**, 809-812.
- Berkefeld H, Sailer CA, Bildl W, Rohde V, Thumfart JO, Eble S, Klugbauer N, Reisinger E, Bischofberger J, Oliver D, Knaus HG, Schulte U & Fakler B. (2006). BKCa-Cav channel complexes mediate rapid and localized Ca²⁺-activated K⁺ signaling. *Science* **314**, 615-620.

- Bin-Jaliah I, Maskell PD & Kumar P. (2004). Indirect sensing of insulin-induced hypoglycaemia by the carotid body in the rat. *J Physiol* **556**, 255-266.
- Biscoe TJ, Purves MJ & Sampson SR. (1970). The frequency of nerve impulses in single carotid body chemoreceptor afferent fibres recorded in vivo with intact circulation. *J Physiol* **208**, 121-131.
- Black AM, McCloskey DI & Torrance RW. (1971). The responses of carotid body chemoreceptors in the cat to sudden changes of hypercapnic and hypoxic stimuli. *Respir Physiol* **13**, 36-49.
- Bock P. (1980). Adenine nucleotides in the carotid body. *Cell Tissue Res* **206**, 279-290.
- Brown EM, Gamba G, Riccardi D, Lombardi M, Butters R, Kifor O, Sun A, Hediger MA, Lytton J & Hebert SC. (1993). Cloning and characterization of an extracellular Ca(2+)-sensing receptor from bovine parathyroid. *Nature* **366**, 575-580.
- Brown EM, Katz C, Butters R & Kifor O. (1991). Polyarginine, polylysine, and protamine mimic the effects of high extracellular calcium concentrations on dispersed bovine parathyroid cells. *J Bone Miner Res* **6**, 1217-1225.
- Brunelle JK, Bell EL, Quesada NM, Vercauteren K, Tiranti V, Zeviani M, Scarpulla RC & Chandel NS. (2005). Oxygen sensing requires mitochondrial ROS but not oxidative phosphorylation. *Cell Metab* **1**, 409-414.
- Buckler KJ. (1997). A novel oxygen-sensitive potassium current in rat carotid body type I cells. *J Physiol* **498 (Pt 3)**, 649-662.
- Buckler KJ & Vaughan-Jones RD. (1993). Effects of acidic stimuli on intracellular calcium in isolated type I cells of the neonatal rat carotid body. *Pflugers Arch* **425**, 22-27.
- Buckler KJ & Vaughan-Jones RD. (1994a). Arterial chemoreceptors. *Adv Exp Med Biol* **360**, 41-45.
- Buckler KJ & Vaughan-Jones RD. (1994b). Effects of hypercapnia on membrane potential and intracellular calcium in rat carotid body type I cells. *J Physiol* **478 (Pt 1)**, 157-171.
- Buckler KJ & Vaughan-Jones RD. (1994c). Effects of hypoxia on membrane potential and intracellular calcium in rat neonatal carotid body type I cells. *J Physiol* **476**, 423-428.
- Buckler KJ, Vaughan-Jones RD, Peers C, Lagadic-Gossmann D & Nye PC. (1991). Effects of extracellular pH, PCO₂ and HCO₃⁻ on intracellular pH in isolated type-I cells of the neonatal rat carotid body. *J Physiol* **444**, 703-721.
- Buckler KJ, Williams BA & Honore E. (2000). An oxygen-, acid- and anaesthetic-sensitive TASK-like background potassium channel in rat arterial chemoreceptor cells. *J Physiol* **525 Pt 1**, 135-142.
- Buniel MC, Schilling WP & Kunze DL. (2003). Distribution of transient receptor potential channels in the rat carotid chemosensory pathway. *J Comp Neurol* **464**, 404-413.
- Buttigieg J & Nurse CA. (2004). Detection of hypoxia-evoked ATP release from chemoreceptor cells of the rat carotid body. *Biochem Biophys Res Commun* **322**, 82-87.
- Caceres AI, Obeso A, Gonzalez C & Rocher A. (2007). Molecular identification and functional role of voltage-gated sodium channels in rat carotid body chemoreceptor cells. Regulation of expression by chronic hypoxia in vivo. *J Neurochem* **102**, 231-245.

- Calder NA, Kumar P & Hanson MA. (1997). Development of carotid chemoreceptor dynamic and steady-state sensitivity to CO₂ in the newborn lamb. *J Physiol* **503** (Pt 1), 187-194.
- Campanucci VA, Zhang M, Vollmer C & Nurse CA. (2006). Expression of multiple P2X receptors by glossopharyngeal neurons projecting to rat carotid body O₂-chemoreceptors: role in nitric oxide-mediated efferent inhibition. *J Neurosci* **26**, 9482-9493.
- Carabelli V, Marcantoni A, Comunanza V, de Luca A, Diaz J, Borges R & Carbone E. (2007). Chronic hypoxia up-regulates alpha₁H T-type channels and low-threshold catecholamine secretion in rat chromaffin cells. *J Physiol* **584**, 149-165.
- Carpenter E, Bee D & Peers C. (1998). Ionic currents in carotid body type I cells isolated from normoxic and chronically hypoxic adult rats. *Brain Res* **811**, 79-87.
- Carpenter E & Peers C. (1997). Swelling- and cAMP-activated Cl⁻ currents in isolated rat carotid body type I cells. *J Physiol* **503** (Pt 3), 497-511.
- Carroll JL, Boyle KM, Wasicko MJ & Sterni LM. (2005). Dopamine D2 receptor modulation of carotid body type 1 cell intracellular calcium in developing rats. *Am J Physiol Lung Cell Mol Physiol* **288**, L910-916.
- Casero RA, Jr. & Marton LJ. (2007). Targeting polyamine metabolism and function in cancer and other hyperproliferative diseases. *Nat Rev Drug Discov* **6**, 373-390.
- Catterall WA, Striessnig J, Snutch TP & Perez-Reyes E. (2003). International Union of Pharmacology. XL. Compendium of voltage-gated ion channels: calcium channels. *Pharmacol Rev* **55**, 579-581.
- Chaisiri P, Harper ME & Griffiths K. (1979). Plasma spermine concentrations of patients with benign and malignant tumours of the breast or prostate. *Clin Chim Acta* **92**, 273-282.
- Chandel NS & Schumacker PT. (2000). Cellular oxygen sensing by mitochondria: old questions, new insight. *J Appl Physiol* **88**, 1880-1889.
- Chang W, Chen TH, Pratt S & Shoback D. (1998). Regulation of extracellular calcium-activated cation currents by cAMP in parathyroid cells. *Am J Physiol* **275**, E213-221.
- Chang W, Rodriguez L, Chen TH, Tu C & Shoback D. (2004). Extracellular Ca²⁺-sensing in cartilage. *Journal of musculoskeletal & neuronal interactions* **4**, 410-411.
- Chang W, Tu C, Cheng Z, Rodriguez L, Chen TH, Gassmann M, Bettler B, Margeta M, Jan LY & Shoback D. (2007). Complex formation with the type B gamma-aminobutyric acid receptor affects the expression and signal transduction of the extracellular calcium-sensing receptor: Studies with HEK-293 cells and neurons. *J Biol Chem*.
- Chattopadhyay N, Jeong KH, Yano S, Huang S, Pang JL, Ren X, Terwilliger E, Kaiser UB, Vassilev PM, Pollak MR & Brown EM. (2007). Calcium receptor stimulates chemotaxis and secretion of MCP-1 in GnRH neurons in vitro: potential impact on reduced GnRH neuron population in CaR-null mice. *Am J Physiol Endocrinol Metab* **292**, E523-532.
- Chen I, Mascorro JA & Yates RD. (1981). Autoradiographic localization of alpha-bungarotoxin-binding sites in the carotid body of the rat. *Cell Tissue Res* **219**, 609-618.

- Chen J, Gomez-Nino A, Gonzalez C, Dinger B & Fidone S. (1997). Stimulus-specific mobilization of dopamine and norepinephrine stores in cat carotid body. *J Auton Nerv Syst* **67**, 109-113.
- Chen J, He L, Dinger B & Fidone S. (2000). Cellular mechanisms involved in rabbit carotid body excitation elicited by endothelin peptides. *Respir Physiol* **121**, 13-23.
- Chen W, Harnett MT & Smith SM. (2007). Modulation of neuronal voltage-activated calcium and sodium channels by polyamines and pH. *Channels (Austin)* **1**, 281-290.
- Chen Y, Tipoe GL, Liong E, Leung S, Lam SY, Iwase R, Tjong YW & Fung ML. (2002). Chronic hypoxia enhances endothelin-1-induced intracellular calcium elevation in rat carotid body chemoreceptors and up-regulates ETA receptor expression. *Pflugers Arch* **443**, 565-573.
- Cheng Z, Tu C, Rodriguez L, Chen TH, Dvorak MM, Margeta M, Gassmann M, Bettler B, Shoback D & Chang W. (2007). Type B Gamma-aminobutyric Acid Receptors Modulate the Function of the Extracellular Ca²⁺-sensing Receptor and Cell Differentiation in Murine Growth Plate Chondrocytes. *Endocrinology*.
- Chik CL, Liu QY, Li B, Klein DC, Zylka M, Kim DS, Chin H, Karpinski E & Ho AK. (1997). Alpha 1D L-type Ca(2+)-channel currents: inhibition by a beta-adrenergic agonist and pituitary adenylate cyclase-activating polypeptide (PACAP) in rat pinealocytes. *J Neurochem* **68**, 1078-1087.
- Cino I & Formenti A. (2008). Spermine biphasically affects N-type calcium channel currents in adult dorsal root ganglion neurons of the rat. *Biochim Biophys Acta*.
- Clarkson AN, Liu H, Pearson L, Kapoor M, Harrison JC, Sammut IA, Jackson DM & Appleton I. (2004). Neuroprotective effects of spermine following hypoxic-ischemic-induced brain damage: a mechanistic study. *Faseb J* **18**, 1114-1116.
- Cohen LF, Lundgren DW & Farrell PM. (1976). Distribution of spermidine and spermine in blood from cystic fibrosis patients and control subjects. *Blood* **48**, 469-475.
- Conde SV, Caceres AI, Vicario I, Rocher A, Obeso A & Gonzalez C. (2006a). An overview on the homeostasis of Ca²⁺ in chemoreceptor cells of the rabbit and rat carotid bodies. *Adv Exp Med Biol* **580**, 215-222; discussion 351-219.
- Conde SV & Monteiro EC. (2004). Hypoxia induces adenosine release from the rat carotid body. *J Neurochem* **89**, 1148-1156.
- Conde SV & Monteiro EC. (2006a). Activation of nicotinic ACh receptors with alpha4 subunits induces adenosine release at the rat carotid body. *Br J Pharmacol* **147**, 783-789.
- Conde SV & Monteiro EC. (2006b). Profiles for ATP and adenosine release at the carotid body in response to O₂ concentrations. *Adv Exp Med Biol* **580**, 179-184; discussion 351-179.
- Conde SV, Obeso A & Gonzalez C. (2007). Low glucose effects on rat carotid body chemoreceptor cells secretory responses and action potential frequency in the carotid sinus nerve. *J Physiol*.
- Conde SV, Obeso A, Vicario I, Rigual R, Rocher A & Gonzalez C. (2006b). Caffeine inhibition of rat carotid body chemoreceptors is mediated by A_{2A} and A_{2B} adenosine receptors. *J Neurochem* **98**, 616-628.

- Czyzyk-Krzeska MF, Bayliss DA, Lawson EE & Millhorn DE. (1992a). Regulation of tyrosine hydroxylase gene expression in the rat carotid body by hypoxia. *J Neurochem* **58**, 1538-1546.
- Czyzyk-Krzeska MF, Lawson EE & Millhorn DE. (1992b). Expression of D2 dopamine receptor mRNA in the arterial chemoreceptor afferent pathway. *J Auton Nerv Syst* **41**, 31-39.
- Dasso LL, Buckler KJ & Vaughan-Jones RD. (1997). Muscarinic and nicotinic receptors raise intracellular Ca²⁺ levels in rat carotid body type I cells. *J Physiol* **498** (Pt 2), 327-338.
- Davies SL, Gibbons CE, Vizard T & Ward DT. (2006). Ca²⁺-sensing receptor induces Rho kinase-mediated actin stress fiber assembly and altered cell morphology, but not in response to aromatic amino acids. *Am J Physiol Cell Physiol* **290**, C1543-1551.
- De Castro F & Rubio M. (1968). *The anatomy and innervation of the blood vessels of the carotid body and the role of chemoreceptive reactions in the autoregulation of the blood flow*. Oxford.
- De Kock LL. (1951). Histology of the carotid body. *Nature* **167**, 611-612.
- Del Toro R, Levitsky KL, Lopez-Barneo J & Chiara MD. (2003). Induction of T-type calcium channel gene expression by chronic hypoxia. *J Biol Chem* **278**, 22316-22324.
- Dinger B, He L, Chen J, Liu X, Gonzalez C, Obeso A, Sanders K, Hoidal J, Stensaas L & Fidone S. (2007). The role of NADPH oxidase in carotid body arterial chemoreceptors. *Respir Physiol Neurobiol* **157**, 45-54.
- Doering CJ & Zamponi GW. (2003). Molecular pharmacology of high voltage-activated calcium channels. *J Bioenerg Biomembr* **35**, 491-505.
- Donnelly DF. (1993). Electrochemical detection of catecholamine release from rat carotid body in vitro. *J Appl Physiol* **74**, 2330-2337.
- Donnelly DF. (1996). Chemoreceptor nerve excitation may not be proportional to catecholamine secretion. *J Appl Physiol* **81**, 657-664.
- Drouva SV, Rerat E, Bihoreau C, Laplante E, Rasolonjanahary R, Clauser H & Kordon C. (1988). Dihydropyridine-sensitive calcium channel activity related to prolactin, growth hormone, and luteinizing hormone release from anterior pituitary cells in culture: interactions with somatostatin, dopamine, and estrogens. *Endocrinology* **123**, 2762-2773.
- Duarte CB, Tome AR, Forsberg E, Carvalho CA, Carvalho AP, Santos RM & Rosario LM. (1993). Neomycin blocks dihydropyridine-insensitive Ca²⁺ influx in bovine adrenal chromaffin cells. *Eur J Pharmacol* **244**, 259-267.
- Duprat F, Lesage F, Fink M, Reyes R, Heurteaux C & Lazdunski M. (1997). TASK, a human background K⁺ channel to sense external pH variations near physiological pH. *Embo J* **16**, 5464-5471.
- Dutschmann M, Bischoff AM, Busselberg D & Richter DW. (2003). Histaminergic modulation of the intact respiratory network of adult mice. *Pflugers Arch* **445**, 570-576.
- e Silva MJ & Lewis DL. (1995). L- and N-type Ca²⁺ channels in adult rat carotid body chemoreceptor type I cells. *J Physiol* **489** (Pt 3), 689-699.

- Efendic S, Grill V, Nysten A & Ostensson CG. (1982). Difference in calcium dependency of insulin, glucagon and somatostatin secretion in response to glibenclamide in perfused rat pancreas. *Diabetologia* **22**, 475-479.
- El Hiani Y, Ahidouch A, Roudbaraki M, Guenin S, Brule G & Ouadid-Ahidouch H. (2006). Calcium-sensing receptor stimulation induces nonselective cation channel activation in breast cancer cells. *J Membr Biol* **211**, 127-137.
- Emanuel RL, Adler GK, Kifor O, Quinn SJ, Fuller F, Krapcho K & Brown EM. (1996). Calcium-sensing receptor expression and regulation by extracellular calcium in the AtT-20 pituitary cell line. *Mol Endocrinol* **10**, 555-565.
- Evans AM, Mustard KJ, Wyatt CN, Peers C, Dipp M, Kumar P, Kinnear NP & Hardie DG. (2005). Does AMP-activated protein kinase couple inhibition of mitochondrial oxidative phosphorylation by hypoxia to calcium signaling in O₂-sensing cells? *J Biol Chem* **280**, 41504-41511.
- Fage D, Voltz C, Scatton B & Carter C. (1992). Selective release of spermine and spermidine from the rat striatum by N-methyl-D-aspartate receptor activation in vivo. *J Neurochem* **58**, 2170-2175.
- Fearon IM, Zhang M, Vollmer C & Nurse CA. (2003). GABA mediates autoreceptor feedback inhibition in the rat carotid body via presynaptic GABAB receptors and TASK-1. *J Physiol* **553**, 83-94.
- Feldman JL & Del Negro CA. (2006). Looking for inspiration: new perspectives on respiratory rhythm. *Nat Rev Neurosci* **7**, 232-242.
- Fieber LA & McCleskey EW. (1993). L-type calcium channels in type I cells of the rat carotid body. *J Neurophysiol* **70**, 1378-1384.
- Fitzgerald RS. (2000). Oxygen and carotid body chemotransduction: the cholinergic hypothesis - a brief history and new evaluation. *Respir Physiol* **120**, 89-104.
- Fitzgerald RS, Shirahata M & Chang I. (2006). The impact of PCO₂ and H⁺ on the release of acetylcholine from the cat carotid body. *Neurosci Lett* **397**, 205-209.
- Fu XW, Nurse CA, Wong V & Cutz E. (2002). Hypoxia-induced secretion of serotonin from intact pulmonary neuroepithelial bodies in neonatal rabbit. *J Physiol* **539**, 503-510.
- Gallego R & Belmonte C. (1979). The effects of blood osmolality changes on cat carotid body chemoreceptors in vivo. *Pflugers Arch* **380**, 53-58.
- Ganformina MD & Lopez-Barneo J. (1992). Potassium channel types in arterial chemoreceptor cells and their selective modulation by oxygen. *J Gen Physiol* **100**, 401-426.
- Ganformina MD, Perez-Garcia MT, Gutierrez G, Miguel-Velado E, Lopez-Lopez JR, Marin A, Sanchez D & Gonzalez C. (2005). Comparative gene expression profile of mouse carotid body and adrenal medulla under physiological hypoxia. *J Physiol* **566**, 491-503.
- Ganong RF. (1997). *Review of medical physiology*. Lange.
- Garcia-Fernandez M, Ortega-Saenz P, Pardal R & Lopez-Barneo J. (2003). Glucose sensing cells in the carotid body. *Adv Exp Med Biol* **536**, 47-53.

- Garrett JE, Steffey ME & Nemeth EF. (1995). The calcium receptor agonist NPS R-568 suppresses PTH mRNA levels in cultured bovine parathyroid cells. *J Bone Miner Res* **10**.
- Gauda EB, Bamford O & Gerfen CR. (1996). Developmental expression of tyrosine hydroxylase, D2-dopamine receptor and substance P genes in the carotid body of the rat. *Neuroscience* **75**, 969-977.
- Gauda EB, Northington FJ, Linden J & Rosin DL. (2000). Differential expression of $\alpha(2a)$, A(1)-adenosine and D(2)-dopamine receptor genes in rat peripheral arterial chemoreceptors during postnatal development. *Brain Res* **872**, 1-10.
- Gilad VH, Halperin R, Chen-Levy Z & Gilad GM. (2002). Cyclic changes of plasma spermine concentrations in women. *Life Sci* **72**, 135-141.
- Gomez-Nino A, Dinger B, Gonzalez C & Fidone SJ. (1990). Differential stimulus coupling to dopamine and norepinephrine stores in rabbit carotid body type I cells. *Brain Res* **525**, 160-164.
- Gomez M & Hellstrand P. (1995). Effects of polyamines on voltage-activated calcium channels in guinea-pig intestinal smooth muscle. *Pflugers Arch* **430**, 501-507.
- Gomez M & Hellstrand P. (1999). Endogenous polyamines modulate Ca²⁺ channel activity in guinea-pig intestinal smooth muscle. *Pflugers Arch* **438**, 445-451.
- Gomez J, Joly C, Kuhn R, Knopfel T, Bockaert J & Pin JP. (1996). The second intracellular loop of metabotropic glutamate receptor 1 cooperates with the other intracellular domains to control coupling to G-proteins. *J Biol Chem* **271**, 2199-2205.
- Gonzalez-Guerrero PR, Rigual R & Gonzalez C. (1993). Effects of chronic hypoxia on opioid peptide and catecholamine levels and on the release of dopamine in the rabbit carotid body. *J Neurochem* **60**, 1769-1776.
- Gonzalez C, Agapito MT, Rocher A, Gonzalez-Martin MC, Vega-Agapito V, Gomez-Nino A, Rigual R, Castaneda J & Obeso A. (2007). Chemoreception in the context of the general biology of ROS. *Respir Physiol Neurobiol* **157**, 30-44.
- Gonzalez C, Almaraz L, Obeso A & Rigual R. (1994). Carotid body chemoreceptors: from natural stimuli to sensory discharges. *Physiol Rev* **74**, 829-898.
- Gonzalez C, Sanz-Alfayate G, Agapito MT, Gomez-Nino A, Rocher A & Obeso A. (2002). Significance of ROS in oxygen sensing in cell systems with sensitivity to physiological hypoxia. *Respir Physiol Neurobiol* **132**, 17-41.
- Gurney AM. (2002). Multiple sites of oxygen sensing and their contributions to hypoxic pulmonary vasoconstriction. *Respir Physiol Neurobiol* **132**, 43-53.
- Guzy RD & Schumacker PT. (2006). Oxygen sensing by mitochondria at complex III: the paradox of increased reactive oxygen species during hypoxia. *Exp Physiol* **91**, 807-819.
- Ha HC, Yager JD, Woster PA & Casero RA, Jr. (1998). Structural specificity of polyamines and polyamine analogues in the protection of DNA from strand breaks induced by reactive oxygen species. *Biochem Biophys Res Commun* **244**, 298-303.
- Hall SK & Armstrong DL. (2000). Conditional and unconditional inhibition of calcium-activated potassium channels by reversible protein phosphorylation. *J Biol Chem* **275**, 3749-3754.

- Hardie DG, Scott JW, Pan DA & Hudson ER. (2003). Management of cellular energy by the AMP-activated protein kinase system. *FEBS Lett* **546**, 113-120.
- He L, Chen J, Dinger B, Sanders K, Sundar K, Hoidal J & Fidone S. (2002). Characteristics of carotid body chemosensitivity in NADPH oxidase-deficient mice. *Am J Physiol Cell Physiol* **282**, C27-33.
- He L, Dinger B, Sanders K, Hoidal J, Obeso A, Stensaas L, Fidone S & Gonzalez C. (2005). Effect of p47phox gene deletion on ROS production and oxygen sensing in mouse carotid body chemoreceptor cells. *Am J Physiol Lung Cell Mol Physiol* **289**, L916-924.
- Heby O. (1986). Putrescine, spermidine and spermine. *NIPS* **1**, 3.
- Hempleman SC. (1995). Sodium and potassium current in neonatal rat carotid body cells following chronic in vivo hypoxia. *Brain Res* **699**, 42-50.
- Hempleman SC. (1996). Increased calcium current in carotid body glomus cells following in vivo acclimatization to chronic hypoxia. *J Neurophysiol* **76**, 1880-1886.
- Herman MD, Reuveny E & Narahashi T. (1993). The effect of polyamines on voltage-activated calcium channels in mouse neuroblastoma cells. *J Physiol* **462**, 645-660.
- Heymans C, Bouckaert, J.J., Dautrebande, L. (1931). Sinus carotidien et reflexes respiratoires; sensibilite des sinus carotidiens aux substances chimiques. Action stimulante espiroatoire reflexe du sulfre de sodium, du cyanure de potassium, de la nicotine et de la lobeline. *ARCH INT PHARMACODYN THER* **40**, 54-91.
- Hockings GI, Grice JE, Walters MM & Jackson RV. (1991). L-type calcium channels and CRH-mediated ACTH and cortisol release in humans. *Clin Exp Pharmacol Physiol* **18**, 303-307.
- Hu J, McLarnon SJ, Mora S, Jiang J, Thomas C, Jacobson KA & Spiegel AM. (2005). A region in the seven-transmembrane domain of the human Ca²⁺ receptor critical for response to Ca²⁺. *J Biol Chem* **280**, 5113-5120.
- Hu J & Spiegel AM. (2007). Structure and function of the human calcium-sensing receptor: insights from natural and engineered mutations and allosteric modulators. *J Cell Mol Med* **11**, 908-922.
- Huang C & Miller RT. (2007). The calcium-sensing receptor and its interacting proteins. *J Cell Mol Med* **11**, 923-934.
- Huang C, Sindic A, Hill CE, Hujer KM, Chan KW, Sassen M, Wu Z, Kurachi Y, Nielsen S, Romero MF & Miller RT. (2007). Interaction of the Ca²⁺-sensing receptor with the inwardly rectifying potassium channels Kir4.1 and Kir4.2 results in inhibition of channel function. *Am J Physiol Renal Physiol* **292**, F1073-1081.
- Iturriaga R & Alcayaga J. (2004). Neurotransmission in the carotid body: transmitters and modulators between glomus cells and petrosal ganglion nerve terminals. *Brain Res Brain Res Rev* **47**, 46-53.
- Jiang RG & Eyzaguirre C. (2004). Effects of hypoxia and putative transmitters on [Ca²⁺]_i of rat glomus cells. *Brain Res* **995**, 285-296.

- Jiang RG & Eyzaguirre C. (2005). Calcium channels of cultured rat glomus cells in normoxia and acute hypoxia. *Brain Res* **1031**, 56-66.
- Jiang Y, Pico A, Cadene M, Chait BT & MacKinnon R. (2001). Structure of the RCK domain from the E. coli K⁺ channel and demonstration of its presence in the human BK channel. *Neuron* **29**, 593-601.
- Johnson RP, O'Kelly IM & Fearon IM. (2004). System-specific O₂ sensitivity of the tandem pore domain K⁺ channel TASK-1. *Am J Physiol Cell Physiol* **286**, C391-397.
- Karasawa N, Kondo Y & Nagatsu I. (1982). Immunohistochemical and immunofluorescent localization of catecholamine-synthesizing enzymes in the carotid body of the bat and dog. *Arch Histol Jpn* **45**, 429-435.
- Kato M, Doi R, Imamura M, Furutani M, Hosotani R & Shimada Y. (1997). Calcium-evoked insulin release from insulinoma cells is mediated via calcium-sensing receptor. *Surgery* **122**, 1203-1211.
- Kawai A, Ballantyne D, Muckenhoff K & Scheid P. (1996). Chemosensitive medullary neurons in the brainstem--spinal cord preparation of the neonatal rat. *J Physiol* **492** (Pt 1), 277-292.
- Keith RA, Mangano TJ, DeFeo PA, Horn MB & Salama AI. (1992). Actions of neomycin on neuronal L-, N-, and non-L/non-N-type voltage-sensitive calcium channel responses. *J Mol Neurosci* **3**, 147-154.
- Kemp PJ. (2006). Detecting acute changes in oxygen: will the real sensor please stand up? *Exp Physiol* **91**, 829-834.
- Kholwadwala D & Donnelly DF. (1992). Maturation of carotid chemoreceptor sensitivity to hypoxia: in vitro studies in the newborn rat. *J Physiol* **453**, 461-473.
- Kim D, Fujita A, Horio Y & Kurachi Y. (1998). Cloning and functional expression of a novel cardiac two-pore background K⁺ channel (cTBAK-1). *Circ Res* **82**, 513-518.
- Kim I, Kim JH & Carroll JL. (2006). Postnatal changes in gene expression of subfamilies of TASK K⁺ channels in rat carotid body. *Adv Exp Med Biol* **580**, 43-47; discussion 351-359.
- Kim YC, Sim JH, Kim YH, Kwon SC, Lee SJ, Kim SR, Kim DW, Park SM, Youn SJ, Lee SJ, Xing DG, Xu WX & Kim KW. (2007). Effects of polyamines on contractility of guinea-pig gastric smooth muscle. *J Korean Med Sci* **22**, 48-56.
- Knight TT, Jr., Gonzalez JA, Rary JM & Rush DS. (2006). Current concepts for the surgical management of carotid body tumor. *Am J Surg* **191**, 104-110.
- Kobayashi S, Conforti L & Millhorn DE. (2000). Gene expression and function of adenosine A(2A) receptor in the rat carotid body. *Am J Physiol Lung Cell Mol Physiol* **279**, L273-282.
- Koerner P, Hesslinger C, Schaefermeyer A, Prinz C & Gratzl M. (2004). Evidence for histamine as a transmitter in rat carotid body sensor cells. *J Neurochem* **91**, 493-500.
- Kumar P. (2007). How sweet it is: sensing low glucose in the carotid body. *J Physiol* **578**, 627.
- Kumar P & Bin-Jaliah I. (2007). Adequate stimuli of the carotid body: more than an oxygen sensor? *Respir Physiol Neurobiol* **157**, 12-21.

- Lahiri S & Forster RE, 2nd. (2003). CO₂/H(+) sensing: peripheral and central chemoreception. *Int J Biochem Cell Biol* **35**, 1413-1435.
- Lai CJ, Yang CC, Hsu YY, Lin YN & Kuo TB. (2006). Enhanced sympathetic outflow and decreased baroreflex sensitivity are associated with intermittent hypoxia-induced systemic hypertension in conscious rats. *J Appl Physiol* **100**, 1974-1982.
- Lam SY, Liong EC, Tipoe GL & Fung ML. (2006). Expression of HIF-2 α and HIF-3 α in the rat carotid body in chronic hypoxia. *Adv Exp Med Biol* **580**, 29-36; discussion 351-359.
- Lam SY, Tipoe GL, Liong EC & Fung ML. (2008). Differential expressions and roles of hypoxia-inducible factor-1 α , -2 α and -3 α in the rat carotid body during chronic and intermittent hypoxia. *Histol Histopathol* **23**, 271-280.
- Lapidus RG & Sokolove PM. (1993). Spermine inhibition of the permeability transition of isolated rat liver mitochondria: an investigation of mechanism. *Arch Biochem Biophys* **306**, 246-253.
- Lasater EM & Solessio E. (2002). Regulation of voltage-sensitive Ca²⁺ channels in bipolar cells by divalent cations and polyamines. *Adv Exp Med Biol* **514**, 275-289.
- Laube G & Veh RW. (1997). Astrocytes, not neurons, show most prominent staining for spermidine/spermine-like immunoreactivity in adult rat brain. *Glia* **19**, 171-179.
- Lazarov N, Rozloznik M, Reindl S, Rey-Ares V, Dutschmann M & Gratzl M. (2006). Expression of histamine receptors and effect of histamine in the rat carotid body chemoafferent pathway. *Eur J Neurosci* **24**, 3431-3444.
- Leach RM, Hill HM, Snetkov VA, Robertson TP & Ward JP. (2001). Divergent roles of glycolysis and the mitochondrial electron transport chain in hypoxic pulmonary vasoconstriction of the rat: identity of the hypoxic sensor. *J Physiol* **536**, 211-224.
- Lee YM, Kim BJ, Chun YS, So I, Choi H, Kim MS & Park JW. (2006). NOX4 as an oxygen sensor to regulate TASK-1 activity. *Cell Signal* **18**, 499-507.
- Leff T. (2003). AMP-activated protein kinase regulates gene expression by direct phosphorylation of nuclear proteins. *Biochem Soc Trans* **31**, 224-227.
- Levitzky MG. (2008). Using the pathophysiology of obstructive sleep apnea to teach cardiopulmonary integration. *Adv Physiol Educ* **32**, 196-202.
- Lewis A, Hartness ME, Chapman CG, Fearon IM, Meadows HJ, Peers C & Kemp PJ. (2001). Recombinant hTASK1 is an O(2)-sensitive K(+) channel. *Biochem Biophys Res Commun* **285**, 1290-1294.
- Liu K, Hsiung S, Adlersberg M, Sacktor T, Gershon MD & Tamir H. (2000). Ca(2+)-evoked serotonin secretion by parafollicular cells: roles in signal transduction of phosphatidylinositol 3'-kinase, and the gamma and zeta isoforms of protein kinase C. *J Neurosci* **20**, 1365-1373.
- Loechner KJ, Knox RJ, McLaughlin JT & Dunlap K. (1999). Dexamethasone-mediated inhibition of calcium transients and ACTH release in a pituitary cell line (AtT-20). *Steroids* **64**, 404-412.

- Lohr C. (2003). Monitoring neuronal calcium signalling using a new method for ratiometric confocal calcium imaging. *Cell Calcium* **34**, 295-303.
- Longo LD & Packianathan S. (1995). Acute hypoxia induces elevation of ornithine decarboxylase activity in neonatal rat brain slices. *Reprod Fertil Dev* **7**, 385-389.
- Lopez-Barneo J, Lopez-Lopez JR, Urena J & Gonzalez C. (1988). Chemotransduction in the carotid body: K⁺ current modulated by PO₂ in type I chemoreceptor cells. *Science* **241**, 580-582.
- Lopez-Lopez JR, Gonzalez C & Perez-Garcia MT. (1997). Properties of ionic currents from isolated adult rat carotid body chemoreceptor cells: effect of hypoxia. *J Physiol* **499** (Pt 2), 429-441.
- Lopez-Lopez JR & Perez-Garcia MT. (2007). Oxygen sensitive Kv channels in the carotid body. *Respir Physiol Neurobiol* **157**, 65-74.
- Lopez-Lopez JR, Perez-Garcia MT, Sanz-Alfayate G, Obeso A & Gonzalez C. (2003). Functional identification of K_valpha subunits contributing to the O₂-sensitive K⁺ current in rabbit carotid body chemoreceptor cells. *Adv Exp Med Biol* **536**, 33-39.
- Lotshaw DP. (2007). Biophysical, pharmacological, and functional characteristics of cloned and native mammalian two-pore domain K⁺ channels. *Cell Biochem Biophys* **47**, 209-256.
- Ludwig A, Flockerzi V & Hofmann F. (1997). Regional expression and cellular localization of the alpha1 and beta subunit of high voltage-activated calcium channels in rat brain. *J Neurosci* **17**, 1339-1349.
- Maltsev VA, Vinogradova TM & Lakatta EG. (2006). The emergence of a general theory of the initiation and strength of the heartbeat. *J Pharmacol Sci* **100**, 338-369.
- Mansfield KD, Guzy RD, Pan Y, Young RM, Cash TP, Schumacker PT & Simon MC. (2005). Mitochondrial dysfunction resulting from loss of cytochrome c impairs cellular oxygen sensing and hypoxic HIF- α activation. *Cell Metab* **1**, 393-399.
- Marcantoni A, Baldelli P, Hernandez-Guijo JM, Comunanza V, Carabelli V & Carbone E. (2007). L-type calcium channels in adrenal chromaffin cells: role in pace-making and secretion. *Cell Calcium* **42**, 397-408.
- Martinez-Pinna J, Tolhurst G, Gurung IS, Vandenberg JI & Mahaut-Smith MP. (2004). Sensitivity limits for voltage control of P2Y receptor-evoked Ca²⁺ mobilization in the rat megakaryocyte. *J Physiol* **555**, 61-70.
- Masson JF, Kranz C, Mizaikoff B & Gauda EB. (2008). Amperometric ATP Microbiosensors for the Analysis of Chemosensitivity at Rat Carotid Bodies. *Anal Chem*.
- Masuko T, Kusama-Eguchi K, Sakata K, Kusama T, Chaki S, Okuyama S, Williams K, Kashiwagi K & Igarashi K. (2003). Polyamine transport, accumulation, and release in brain. *J Neurochem* **84**, 610-617.
- McCartney CE, McClafferty H, Huibant JM, Rowan EG, Shipston MJ & Rowe IC. (2005). A cysteine-rich motif confers hypoxia sensitivity to mammalian large conductance voltage- and Ca-activated K (BK) channel alpha-subunits. *Proc Natl Acad Sci U S A* **102**, 17870-17876.

- McDonald DM, ed. (1981). *Peripheral chemoreceptors: Structure-function relationships of the carotid body. In Regulation of Breathing*. New York.
- McGehee DS, Aldersberg M, Liu KP, Hsuing S, Heath MJ & Tamir H. (1997). Mechanism of extracellular Ca²⁺ receptor-stimulated hormone release from sheep thyroid parafollicular cells. *J Physiol* **502** (Pt 1), 31-44.
- McGregor KH, Gil J & Lahiri S. (1984). A morphometric study of the carotid body in chronically hypoxic rats. *J Appl Physiol* **57**, 1430-1438.
- McLarnon SJ & Riccardi D. (2002). Physiological and pharmacological agonists of the extracellular Ca²⁺-sensing receptor. *Eur J Pharmacol* **447**, 271-278.
- McQueen DS & Ribeiro JA. (1986). Pharmacological characterization of the receptor involved in chemoexcitation induced by adenosine. *Br J Pharmacol* **88**, 615-620.
- McRory JE, Hamid J, Doering CJ, Garcia E, Parker R, Hamming K, Chen L, Hildebrand M, Beedle AM, Feldcamp L, Zamponi GW & Snutch TP. (2004). The CACNA1F gene encodes an L-type calcium channel with unique biophysical properties and tissue distribution. *J Neurosci* **24**, 1707-1718.
- Miedlich S, Gama L & Breitwieser GE. (2002). Calcium sensing receptor activation by a calcimimetic suggests a link between cooperativity and intracellular calcium oscillations. *J Biol Chem* **277**, 49691-49699.
- Mills E & Jobsis FF. (1972). Mitochondrial respiratory chain of carotid body and chemoreceptor response to changes in oxygen tension. *J Neurophysiol* **35**, 405-428.
- Mir AK, Pallot DJ & Nahorski SR. (1983). Biogenic amine-stimulated cyclic adenosine-3',5'-monophosphate formation in the rat carotid body. *J Neurochem* **41**, 663-669.
- Monteiro EC & Ribeiro JA. (1987). Ventilatory effects of adenosine mediated by carotid body chemoreceptors in the rat. *Naunyn Schmiedebergs Arch Pharmacol* **335**, 143-148.
- Muff R, Nemeth EF, Haller-Brem S & Fischer JA. (1988). Regulation of hormone secretion and cytosolic Ca²⁺ by extracellular Ca²⁺ in parathyroid cells and C-cells: role of voltage-sensitive Ca²⁺ channels. *Arch Biochem Biophys* **265**, 128-135.
- Muscari C, Guarnieri C, Stefanelli C, Giaccari A & Caldarera CM. (1995). Protective effect of spermine on DNA exposed to oxidative stress. *Mol Cell Biochem* **144**, 125-129.
- Musset B, Meuth SG, Liu GX, Derst C, Wegner S, Pape HC, Budde T, Preisig-Muller R & Daut J. (2006). Effects of divalent cations and spermine on the K⁺ channel TASK-3 and on the outward current in thalamic neurons. *J Physiol* **572**, 639-657.
- Nattie E. (1999). CO₂, brainstem chemoreceptors and breathing. *Prog Neurobiol* **59**, 299-331.
- Nemeth EF. (2004). Calcimimetic and calcilytic drugs: just for parathyroid cells? *Cell Calcium* **35**, 283-289.
- Nemeth EF & Scarpa A. (1987). Rapid mobilization of cellular Ca²⁺ in bovine parathyroid cells evoked by extracellular divalent cations. Evidence for a cell surface calcium receptor. *J Biol Chem* **262**, 5188-5196.

- Nemeth EF, Steffey ME & Fox J. (1996). The parathyroid calcium receptor: a novel therapeutic target for treating hyperparathyroidism. *Pediatric nephrology (Berlin, Germany)* **10**, 275-279.
- Nemeth EF, Steffey ME, Hammerland LG, Hung BC, Van Wagenen BC, DelMar EG & Balandrin MF. (1998). Calcimimetics with potent and selective activity on the parathyroid calcium receptor. *Proc Natl Acad Sci U S A* **95**, 4040-4045.
- Nilsson BO, Gomez MF, Sward K & Hellstrand P. (2002). Regulation of Ca²⁺ channel and phosphatase activities by polyamines in intestinal and vascular smooth muscle--implications for cellular growth and contractility. *Acta Physiol Scand* **176**, 33-41.
- Norris ML & Millhorn DE. (1995). Hypoxia-induced protein binding to O₂-responsive sequences on the tyrosine hydroxylase gene. *J Biol Chem* **270**, 23774-23779.
- Nurse CA. (2005). Neurotransmission and neuromodulation in the chemosensory carotid body. *Auton Neurosci* **120**, 1-9.
- Nurse CA & Fearon IM. (2002). Carotid body chemoreceptors in dissociated cell culture. *Microsc Res Tech* **59**, 249-255.
- Nurse CA & Zhang M. (1999). Acetylcholine contributes to hypoxic chemotransmission in co-cultures of rat type 1 cells and petrosal neurons. *Respir Physiol* **115**, 189-199.
- Obeso A, Almaraz L & Gonzalez C. (1985). Correlation between adenosine triphosphate levels, dopamine release and electrical activity in the carotid body: support for the metabolic hypothesis of chemoreception. *Brain Res* **348**, 64-68.
- Obeso A, Rocher A, Fidone S & Gonzalez C. (1992). The role of dihydropyridine-sensitive Ca²⁺ channels in stimulus-evoked catecholamine release from chemoreceptor cells of the carotid body. *Neuroscience* **47**, 463-472.
- Olson EB, Jr., Bohne CJ, Dwinell MR, Podolsky A, Vidruk EH, Fuller DD, Powell FL & Mitchel GS. (2001). Ventilatory long-term facilitation in unanesthetized rats. *J Appl Physiol* **91**, 709-716.
- Oomori Y, Nakaya K, Tanaka H, Iuchi H, Ishikawa K, Satoh Y & Ono K. (1994). Immunohistochemical and histochemical evidence for the presence of noradrenaline, serotonin and gamma-aminobutyric acid in chief cells of the mouse carotid body. *Cell Tissue Res* **278**, 249-254.
- Ortega-Saenz P, Pardal R, Garcia-Fernandez M & Lopez-Barneo J. (2003). Rotenone selectively occludes sensitivity to hypoxia in rat carotid body glomus cells. *J Physiol* **548**, 789-800.
- Ortega-Saenz P, Pascual A, Gomez-Diaz R & Lopez-Barneo J. (2006). Acute oxygen sensing in heme oxygenase-2 null mice. *J Gen Physiol* **128**, 405-411.
- Overholt JL, Ficker E, Yang T, Shams H, Bright GR & Prabhakar NR. (2000). HERG-Like potassium current regulates the resting membrane potential in glomus cells of the rabbit carotid body. *J Neurophysiol* **83**, 1150-1157.
- Pallot DJ. (1987). The mammalian carotid body. *Adv Anat Embryol Cell Biol* **102**, 1-91.
- Pardal R & Lopez-Barneo J. (2002). Low glucose-sensing cells in the carotid body. *Nat Neurosci* **5**, 197-198.

- Pardal R, Ludewig U, Garcia-Hirschfeld J & Lopez-Barneo J. (2000). Secretory responses of intact glomus cells in thin slices of rat carotid body to hypoxia and tetraethylammonium. *Proc Natl Acad Sci U S A* **97**, 2361-2366.
- Pardal R, Ortega-Saenz P, Duran R & Lopez-Barneo J. (2007). Glia-like stem cells sustain physiologic neurogenesis in the adult mammalian carotid body. *Cell* **131**, 364-377.
- Parkash J. (2008). Inflammatory cytokine signaling in insulin producing beta-cells enhances the colocalization correlation coefficient between L-type voltage-dependent calcium channel and calcium-sensing receptor. *Int J Mol Med* **22**, 155-163.
- Parsons TD, Obaid AL & Salzberg BM. (1992). Aminoglycoside antibiotics block voltage-dependent calcium channels in intact vertebrate nerve terminals. *J Gen Physiol* **99**, 491-504.
- Patel AJ & Honore E. (2001). Molecular physiology of oxygen-sensitive potassium channels. *Eur Respir J* **18**, 221-227.
- Patel AJ, Honore E, Lesage F, Fink M, Romey G & Lazdunski M. (1999). Inhalational anesthetics activate two-pore-domain background K⁺ channels. *Nat Neurosci* **2**, 422-426.
- Paton JF & Kasparov S. (2000). Sensory channel specific modulation in the nucleus of the solitary tract. *J Auton Nerv Syst* **80**, 117-129.
- Pawar A, Peng YJ, Jacono FJ & Prabhakar NR. (2008). Comparative analysis of neonatal and adult rat carotid body responses to chronic intermittent hypoxia. *J Appl Physiol* **104**, 1287-1294.
- Peers C. (1990a). Effect of lowered extracellular pH on Ca²⁺-dependent K⁺ currents in type I cells from the neonatal rat carotid body. *J Physiol* **422**, 381-395.
- Peers C. (1990b). Hypoxic suppression of K⁺ currents in type I carotid body cells: selective effect on the Ca²⁺-activated K⁺ current. *Neurosci Lett* **119**, 253-256.
- Peers C. (1997). Oxygen-sensitive ion channels. *Trends Pharmacol Sci* **18**, 405-408.
- Peers C & Carpenter E. (1998). Inhibition of Ca²⁺-dependent K⁺ channels in rat carotid body type I cells by protein kinase C. *J Physiol* **512** (Pt 3), 743-750.
- Peers C, Carpenter E, Hatton CJ, Wyatt CN & Bee D. (1996). Ca²⁺ channel currents in type I carotid body cells of normoxic and chronically hypoxic neonatal rats. *Brain Res* **739**, 251-257.
- Peng YJ, Overholt JL, Kline D, Kumar GK & Prabhakar NR. (2003). Induction of sensory long-term facilitation in the carotid body by intermittent hypoxia: implications for recurrent apneas. *Proc Natl Acad Sci U S A* **100**, 10073-10078.
- Peng YJ & Prabhakar NR. (2004). Effect of two paradigms of chronic intermittent hypoxia on carotid body sensory activity. *J Appl Physiol* **96**, 1236-1242; discussion 1196.
- Peng YJ, Yuan G, Ramakrishnan D, Sharma SD, Bosch-Marce M, Kumar GK, Semenza GL & Prabhakar NR. (2006). Heterozygous HIF-1 alpha deficiency impairs carotid body-mediated systemic responses and reactive oxygen species generation in mice exposed to intermittent hypoxia. *J Physiol* **577**, 705-716.

- Pepper DR, Landauer RC & Kumar P. (1995). Postnatal development of CO₂-O₂ interaction in the rat carotid body in vitro. *J Physiol* **485** (Pt 2), 531-541.
- Perez-Garcia MT, Lopez-Lopez JR & Gonzalez C. (1999). Kvbeta1.2 subunit coexpression in HEK293 cells confers O₂ sensitivity to kv4.2 but not to Shaker channels. *J Gen Physiol* **113**, 897-907.
- Perez-Garcia MT, Lopez-Lopez JR, Riesco AM, Hoppe UC, Marban E, Gonzalez C & Johns DC. (2000). Viral gene transfer of dominant-negative Kv4 construct suppresses an O₂-sensitive K⁺ current in chemoreceptor cells. *J Neurosci* **20**, 5689-5695.
- Perez-Reyes E. (2003). Molecular physiology of low-voltage-activated t-type calcium channels. *Physiol Rev* **83**, 117-161.
- Petheo GL, Molnar Z, Roka A, Makara JK & Spat A. (2001). A pH-sensitive chloride current in the chemoreceptor cell of rat carotid body. *J Physiol* **535**, 95-106.
- Petrel C, Kessler A, Dauban P, Dodd RH, Rognan D & Ruat M. (2004). Positive and negative allosteric modulators of the Ca²⁺-sensing receptor interact within overlapping but not identical binding sites in the transmembrane domain. *J Biol Chem* **279**, 18990-18997.
- Phillips SA, Olson EB, Lombard JH & Morgan BJ. (2006). Chronic intermittent hypoxia alters NE reactivity and mechanics of skeletal muscle resistance arteries. *J Appl Physiol* **100**, 1117-1123.
- Pin JP, Gomeza J, Joly C & Bockaert J. (1995). The metabotropic glutamate receptors: their second intracellular loop plays a critical role in the G-protein coupling specificity. *Biochem Soc Trans* **23**, 91-96.
- Pin JP, Joly C, Heinemann SF & Bockaert J. (1994). Domains involved in the specificity of G protein activation in phospholipase C-coupled metabotropic glutamate receptors. *Embo J* **13**, 342-348.
- Piruat JI, Pintado CO, Ortega-Saenz P, Roche M & Lopez-Barneo J. (2004). The mitochondrial SDHD gene is required for early embryogenesis, and its partial deficiency results in persistent carotid body glomus cell activation with full responsiveness to hypoxia. *Mol Cell Biol* **24**, 10933-10940.
- Pongs O, Leicher T, Berger M, Roeper J, Bähring R, Wray D, Giese KP, Silva AJ & Storm JF. (1999). Functional and molecular aspects of voltage-gated K⁺ channel beta subunits. *Ann N Y Acad Sci* **868**, 344-355.
- Porwol T, Ehleben W, Brand V & Acker H. (2001). Tissue oxygen sensor function of NADPH oxidase isoforms, an unusual cytochrome aa₃ and reactive oxygen species. *Respir Physiol* **128**, 331-348.
- Prabhakar NR, Dinerman JL, Agani FH & Snyder SH. (1995). Carbon monoxide: a role in carotid body chemoreception. *Proc Natl Acad Sci U S A* **92**, 1994-1997.
- Prabhakar NR & Jacono FJ. (2005). Cellular and molecular mechanisms associated with carotid body adaptations to chronic hypoxia. *High Alt Med Biol* **6**, 112-120.
- Prasad M, Fearon IM, Zhang M, Laing M, Vollmer C & Nurse CA. (2001). Expression of P2X₂ and P2X₃ receptor subunits in rat carotid body afferent neurones: role in chemosensory signalling. *J Physiol* **537**, 667-677.

- Prieto-Lloret J, Donnelly DF, Rico AJ, Moratalla R, Gonzalez C & Rigual RJ. (2007). Hypoxia transduction by carotid body chemoreceptors in mice lacking dopamine D2 receptors. *J Appl Physiol*.
- Quinn SJ, Bai M & Brown EM. (2004). pH Sensing by the calcium-sensing receptor. *J Biol Chem* **279**, 37241-37249.
- Quinn SJ, Kifor O, Trivedi S, Diaz R, Vassilev P & Brown E. (1998). Sodium and ionic strength sensing by the calcium receptor. *J Biol Chem* **273**, 19579-19586.
- Quinn SJ, Ye CP, Diaz R, Kifor O, Bai M, Vassilev P & Brown E. (1997). The Ca²⁺-sensing receptor: a target for polyamines. *Am J Physiol* **273**, C1315-1323.
- Randolph AC & G. WG. (2004). Role of the calcium-sensing receptor in parathyroid gland physiology. *Am j physiol Renal Physiol* **286**, F1005-F1011.
- Ray JM, Squires PE, Curtis SB, Meloche MR & Buchan AM. (1997). Expression of the calcium-sensing receptor on human antral gastrin cells in culture. *J Clin Invest* **99**, 2328-2333.
- Rey O, Young SH, Papazyan R, Shapiro MS & Rozengurt E. (2006). Requirement of the TRPC1 cation channel in the generation of transient Ca²⁺ oscillations by the calcium-sensing receptor. *J Biol Chem* **281**, 38730-38737.
- Reyes EP, Fernandez R, Larrain C & Zapata P. (2007). Effects of combined cholinergic-purinergic block upon cat carotid body chemoreceptors in vitro. *Respir Physiol Neurobiol* **156**, 17-22.
- Riccardi D & Maldonado-Perez D. (2005). The calcium-sensing receptor as a nutrient sensor. *Biochem Soc Trans* **33**, 316-320.
- Riesco-Fagundo AM, Perez-Garcia MT, Gonzalez C & Lopez-Lopez JR. (2001). O₂ modulates large-conductance Ca(2+)-dependent K(+) channels of rat chemoreceptor cells by a membrane-restricted and CO-sensitive mechanism. *Circ Res* **89**, 430-436.
- Rigual R, Lopez-Lopez JR & Gonzalez C. (1991). Release of dopamine and chemoreceptor discharge induced by low pH and high PCO₂ stimulation of the cat carotid body. *J Physiol* **433**, 519-531.
- Rocher A, Geijo-Barrientos E, Caceres AI, Rigual R, Gonzalez C & Almaraz L. (2005). Role of voltage-dependent calcium channels in stimulus-secretion coupling in rabbit carotid body chemoreceptor cells. *J Physiol* **562**, 407-420.
- Romoli R, Lania A, Mantovani G, Corbetta S, Persani L & Spada A. (1999). Expression of calcium-sensing receptor and characterization of intracellular signaling in human pituitary adenomas. *J Clin Endocrinol Metab* **84**, 2848-2853.
- Rong W, Gourine AV, Cockayne DA, Xiang Z, Ford AP, Spyer KM & Burnstock G. (2003). Pivotal role of nucleotide P2X₂ receptor subunit of the ATP-gated ion channel mediating ventilatory responses to hypoxia. *J Neurosci* **23**, 11315-11321.
- Rouwet EV, Tintu AN, Schellings MW, van Bilsen M, Lutgens E, Hofstra L, Slaaf DW, Ramsay G & Le Noble FA. (2002). Hypoxia induces aortic hypertrophic growth, left ventricular dysfunction, and sympathetic hyperinnervation of peripheral arteries in the chick embryo. *Circulation* **105**, 2791-2796.

- Roy A, Rozanov C, Mokashi A, Daudu P, Al-mehdi AB, Shams H & Lahiri S. (2000). Mice lacking in gp91 phox subunit of NAD(P)H oxidase showed glomus cell $[Ca^{2+}]_i$ and respiratory responses to hypoxia. *Brain Res* **872**, 188-193.
- Ruat M, Molliver ME, Snowman AM & Snyder SH. (1995). Calcium sensing receptor: molecular cloning in rat and localization to nerve terminals. *Proc Natl Acad Sci U S A* **92**, 3161-3165.
- Runold M, Cherniack NS & Prabhakar NR. (1990). Effect of adenosine on isolated and superfused cat carotid body activity. *Neurosci Lett* **113**, 111-114.
- Sanchez D, Lopez-Lopez JR, Perez-Garcia MT, Sanz-Alfayate G, Obeso A, Ganformina MD & Gonzalez C. (2002). Molecular identification of K α subunits that contribute to the oxygen-sensitive K $^+$ current of chemoreceptor cells of the rabbit carotid body. *J Physiol* **542**, 369-382.
- Sauer H, Wartenberg M & Hescheler J. (2001). Reactive oxygen species as intracellular messengers during cell growth and differentiation. *Cell Physiol Biochem* **11**, 173-186.
- Schultz HD & Li YL. (2007). Carotid body function in heart failure. *Respir Physiol Neurobiol* **157**, 171-185.
- Scott JW, Hawley SA, Green KA, Anis M, Stewart G, Scullion GA, Norman DG & Hardie DG. (2004). CBS domains form energy-sensing modules whose binding of adenosine ligands is disrupted by disease mutations. *J Clin Invest* **113**, 274-284.
- Scragg JL, Fearon IM, Boyle JP, Ball SG, Varadi G & Peers C. (2005). Alzheimer's amyloid peptides mediate hypoxic up-regulation of L-type Ca $^{2+}$ channels. *Faseb J* **19**, 150-152.
- Seiler N, Delcros JG & Moulinoux JP. (1996). Polyamine transport in mammalian cells. An update. *Int J Biochem Cell Biol* **28**, 843-861.
- Semenza GL. (2004). O $_2$ -regulated gene expression: transcriptional control of cardiorespiratory physiology by HIF-1. *J Appl Physiol* **96**, 1173-1177; discussion 1170-1172.
- Silve C, Petrel C, Leroy C, Bruel H, Mallet E, Rognan D & Ruat M. (2005). Delineating a Ca $^{2+}$ binding pocket within the venus flytrap module of the human calcium-sensing receptor. *J Biol Chem* **280**, 37917-37923.
- Soong TW, Stea A, Hodson CD, Dubel SJ, Vincent SR & Snutch TP. (1993). Structure and functional expression of a member of the low voltage-activated calcium channel family. *Science* **260**, 1133-1136.
- Squires PE. (2000). Non-Ca $^{2+}$ -homeostatic functions of the extracellular Ca $^{2+}$ -sensing receptor (CaR) in endocrine tissues. *J Endocrinol* **165**, 173-177.
- Stanfield P. (2006). Voltage sparks a GPCR. *Nat Cell Biol* **8**, 1323-1325.
- Starlinger H. (1982). ATPases of the cat carotid body and of the neighbouring ganglia. *Z Naturforsch [C]* **37**, 532-539.
- Stea A, Alexander SA & Nurse CA. (1991). Effects of pHi and pHe on membrane currents recorded with the perforated-patch method from cultured chemoreceptors of the rat carotid body. *Brain Res* **567**, 83-90.

- Stea A, Jackson A & Nurse CA. (1992). Hypoxia and N⁶,O^{2'}-dibutyryladenine 3',5'-cyclic monophosphate, but not nerve growth factor, induce Na⁺ channels and hypertrophy in chromaffin-like arterial chemoreceptors. *Proc Natl Acad Sci U S A* **89**, 9469-9473.
- Stea A & Nurse CA. (1991). Contrasting effects of HEPES vs HCO₃⁽⁻⁾-buffered media on whole-cell currents in cultured chemoreceptors of the rat carotid body. *Neurosci Lett* **132**, 239-242.
- Sward K, Nilsson BO & Hellstrand P. (1994). Polyamines increase Ca²⁺ sensitivity in permeabilized smooth muscle of guinea pig ileum. *Am J Physiol* **266**, C1754-1763.
- Tabor CW & Tabor H. (1984). Polyamines. *Annu Rev Biochem* **53**, 749-790.
- Tagliatela M, Castaldo P, Iossa S, Pannaccione A, Fresi A, Ficker E & Annunziato L. (1997). Regulation of the human ether-a-gogo related gene (HERG) K⁺ channels by reactive oxygen species. *Proc Natl Acad Sci U S A* **94**, 11698-11703.
- Tan ZY, Lu Y, Whiteis CA, Benson CJ, Chapleau MW & Abboud FM. (2007). Acid-sensing ion channels contribute to transduction of extracellular acidosis in rat carotid body glomus cells. *Circ Res* **101**, 1009-1019.
- Tang XD, Daggett H, Hanner M, Garcia ML, McManus OB, Brot N, Weissbach H, Heinemann SH & Hoshi T. (2001). Oxidative regulation of large conductance calcium-activated potassium channels. *J Gen Physiol* **117**, 253-274.
- Tang XD, Garcia ML, Heinemann SH & Hoshi T. (2004). Reactive oxygen species impair Slo1 BK channel function by altering cysteine-mediated calcium sensing. *Nat Struct Mol Biol* **11**, 171-178.
- Tanimoto K, Makino Y, Pereira T & Poellinger L. (2000). Mechanism of regulation of the hypoxia-inducible factor-1 alpha by the von Hippel-Lindau tumor suppressor protein. *Embo J* **19**, 4298-4309.
- Tantini B, Fiumana E, Cetrullo S, Pignatti C, Bonavita F, Shantz LM, Giordano E, Muscari C, Flamigni F, Guarnieri C, Stefanelli C & Caldarera CM. (2006). Involvement of polyamines in apoptosis of cardiac myoblasts in a model of simulated ischemia. *J Mol Cell Cardiol* **40**, 775-782.
- Thakker RV. (2004). Diseases associated with the extracellular calcium-sensing receptor. *Cell Calcium* **35**, 275-282.
- Urena J, Lopez-Lopez J, Gonzalez C & Lopez-Barneo J. (1989). Ionic currents in dispersed chemoreceptor cells of the mammalian carotid body. *J Gen Physiol* **93**, 979-999.
- Urena P & Frazao JM. (2003). Calcimimetic agents: review and perspectives. *Kidney Int Suppl*, S91-96.
- Verna A, Talib N, Roumy M & Pradet A. (1990). Effects of metabolic inhibitors and hypoxia on the ATP, ADP and AMP content of the rabbit carotid body in vitro: the metabolic hypothesis in question. *Neurosci Lett* **116**, 156-161.
- Vicario I, Obeso A, Rocher A, Lopez-Lopez JR & Gonzalez C. (2000a). Intracellular Ca⁽²⁺⁾ stores in chemoreceptor cells of the rabbit carotid body: significance for chemoreception. *Am J Physiol Cell Physiol* **279**, C51-61.

- Vicario I, Rigual R, Obeso A & Gonzalez C. (2000b). Characterization of the synthesis and release of catecholamine in the rat carotid body in vitro. *Am J Physiol Cell Physiol* **278**, C490-499.
- Vizard TN, O'Keefe GW, Gutierrez H, Kos CH, Riccardi D & Davies AM. (2008). Regulation of axonal and dendritic growth by the extracellular calcium-sensing receptor. *Nat Neurosci* **11**, 285-291.
- Von Euler GL, Y. Zotterman. (1939). The excitation mechanism of the chemoreceptors of the carotid body. *Scand Arch Physiology* **83**, 20.
- Wagner KF, Katschinski DM, Hasegawa J, Schumacher D, Meller B, Gembruch U, Schramm U, Jelkmann W, Gassmann M & Fandrey J. (2001). Chronic inborn erythrocytosis leads to cardiac dysfunction and premature death in mice overexpressing erythropoietin. *Blood* **97**, 536-542.
- Wang ZY, Olson EB, Jr., Bjorling DE, Mitchell GS & Bisgard GE. (2008). Sustained hypoxia-induced proliferation of carotid body type I cells in rats. *J Appl Physiol* **104**, 803-808.
- Ward DT. (2004). Calcium receptor-mediated intracellular signalling. *Cell Calcium* **35**, 217-228.
- Ward JP. (2008). Oxygen sensors in context. *Biochim Biophys Acta* **1777**, 1-14.
- Watanabe S, Kusama-Eguchi K, Kobayashi H & Igarashi K. (1991). Estimation of polyamine binding to macromolecules and ATP in bovine lymphocytes and rat liver. *J Biol Chem* **266**, 20803-20809.
- Waypa GB, Chandel NS & Schumacker PT. (2001). Model for hypoxic pulmonary vasoconstriction involving mitochondrial oxygen sensing. *Circ Res* **88**, 1259-1266.
- Williams BA & Buckler KJ. (2004). Biophysical properties and metabolic regulation of a TASK-like potassium channel in rat carotid body type 1 cells. *Am J Physiol Lung Cell Mol Physiol* **286**, L221-230.
- Williams SE, Brazier SP, Baban N, Telezhkin V, Muller CT, Riccardi D & Kemp PJ. (2008). A structural motif in the C-terminal tail of slo1 confers carbon monoxide sensitivity to human BK(Ca) channels. *Pflugers Arch*.
- Williams SE, Wootton P, Mason HS, Bould J, Iles DE, Riccardi D, Peers C & Kemp PJ. (2004). Hemoxygenase-2 is an oxygen sensor for a calcium-sensitive potassium channel. *Science* **306**, 2093-2097.
- Wyatt CN & Buckler KJ. (2004). The effect of mitochondrial inhibitors on membrane currents in isolated neonatal rat carotid body type I cells. *J Physiol* **556**, 175-191.
- Wyatt CN & Evans AM. (2007). AMP-activated protein kinase and chemotransduction in the carotid body. *Respir Physiol Neurobiol* **157**, 22-29.
- Wyatt CN, Mustard KJ, Pearson SA, Dallas ML, Atkinson L, Kumar P, Peers C, Hardie DG & Evans AM. (2007). AMP-activated protein kinase mediates carotid body excitation by hypoxia. *J Biol Chem* **282**, 8092-8098.
- Wyatt CN & Peers C. (1993). Nicotinic acetylcholine receptors in isolated type I cells of the neonatal rat carotid body. *Neuroscience* **54**, 275-281.

- Wyatt CN & Peers C. (1995). Ca(2+)-activated K+ channels in isolated type I cells of the neonatal rat carotid body. *J Physiol* **483** (Pt 3), 559-565.
- Xu F, Xu J, Tse FW & Tse A. (2006). Adenosine stimulates depolarization and rise in cytoplasmic [Ca2+] in type I cells of rat carotid bodies. *Am J Physiol Cell Physiol* **290**, C1592-1598.
- Xu J, Tse FW & Tse A. (2003). ATP triggers intracellular Ca2+ release in type II cells of the rat carotid body. *J Physiol* **549**, 739-747.
- Xu J, Xu F, Tse FW & Tse A. (2005). ATP inhibits the hypoxia response in type I cells of rat carotid bodies. *J Neurochem* **92**, 1419-1430.
- Xu W & Lipscombe D. (2001). Neuronal Ca(V)1.3alpha(1) L-type channels activate at relatively hyperpolarized membrane potentials and are incompletely inhibited by dihydropyridines. *J Neurosci* **21**, 5944-5951.
- Yamamoto Y, Fujimura M, Nishita T, Nishijima K, Atoji Y & Suzuki Y. (2003). Immunohistochemical localization of carbonic anhydrase isozymes in the rat carotid body. *J Anat* **202**, 573-577.
- Yamamoto Y, Ishikawa R, Omoe K & Taniguchi K. (2008). Expression of inwardly rectifying K+ channels in the carotid body of rat. *Histol Histopathol* **23**, 799-806.
- Yamamoto Y, Kummer W, Atoji Y & Suzuki Y. (2002). TASK-1, TASK-2, TASK-3 and TRAAK immunoreactivities in the rat carotid body. *Brain Res* **950**, 304-307.
- Ye C, Kanazirska M, Quinn S, Brown EM & Vassilev PM. (1996a). Modulation by polycationic Ca(2+)-sensing receptor agonists of nonselective cation channels in rat hippocampal neurons. *Biochem Biophys Res Commun* **224**, 271-280.
- Ye C, Rogers K, Bai M, Quinn SJ, Brown EM & Vassilev PM. (1996b). Agonists of the Ca(2+)-sensing receptor (CaR) activate nonselective cation channels in HEK293 cells stably transfected with the human CaR. *Biochem Biophys Res Commun* **226**, 572-579.
- Ye CP, Yano S, Tfelt-Hansen J, MacLeod RJ, Ren X, Terwilliger E, Brown EM & Chattopadhyay N. (2004). Regulation of a Ca2+-activated K+ channel by calcium-sensing receptor involves p38 MAP kinase. *J Neurosci Res* **75**, 491-498.
- Zapata P. (2007). Is ATP a suitable co-transmitter in carotid body arterial chemoreceptors? *Respir Physiol Neurobiol* **157**, 106-115.
- Zhang M, Buttigieg J & Nurse CA. (2007). Neurotransmitter mechanisms mediating low-glucose signalling in cocultures and fresh tissue slices of rat carotid body. *J Physiol* **578**, 735-750.
- Zhang M & Nurse CA. (2004). CO2/pH chemosensory signaling in co-cultures of rat carotid body receptors and petrosal neurons: role of ATP and ACh. *J Neurophysiol* **92**, 3433-3445.
- Zhang M, Zhong H, Vollmer C & Nurse CA. (2000). Co-release of ATP and ACh mediates hypoxic signalling at rat carotid body chemoreceptors. *J Physiol* **525 Pt 1**, 143-158.
- Zhao YJ, Xu CQ, Zhang WH, Zhang L, Bian SL, Huang Q, Sun HL, Li QF, Zhang YQ, Tian Y, Wang R, Yang BF & Li WM. (2007). Role of polyamines in myocardial ischemia/reperfusion injury and their interactions with nitric oxide. *Eur J Pharmacol* **562**, 236-246.

Zhong H & Nurse CA. (1997). Nicotinic acetylcholine sensitivity of rat petrosal sensory neurons in dissociated cell culture. *Brain Res* **766**, 153-161.

Zhong H, Zhang M & Nurse CA. (1997). Synapse formation and hypoxic signalling in co-cultures of rat petrosal neurones and carotid body type 1 cells. *J Physiol* **503 (Pt 3)**, 599-612.

